CONTRACT NO. NAS 8-11207

GE NO. 65SD4361

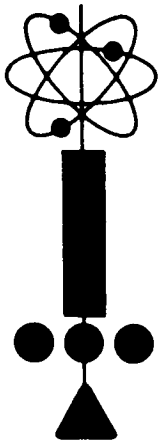

ELECTRICALLY - PROPELLED CARGO VEHICLE FOR SUSTAINED LUNAR SUPPLY OPERATIONS

FINAL REPORT

Prepared for:
GEORGE C. MARSHALL SPACE FLIGHT CENTER
NATIONAL AERONAUTICS AND SPACE ADMINISTRATION
HUNTSVILLE, ALABAMA 35812

28 JUNE 1965

GENERAL ELECTRIC

MISSILE AND SPACE DIVISION

CONTRACT NO. NAS 8-11207

GE NO. 65SD4361

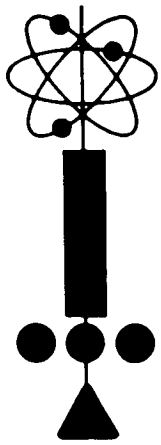

ELECTRICALLY - PROPELLED CARGO VEHICLE FOR SUSTAINED LUNAR SUPPLY OPERATIONS

FINAL REPORT

Prepared for:
GEORGE C. MARSHALL SPACE FLIGHT CENTER
NATIONAL AERONAUTICS AND SPACE ADMINISTRATION
HUNTSVILLE, ALABAMA 35812

28 JUNE 1965

Approved By: _____
J. W. Larson
Program Manager

_____
T. F. Widmer
Manager, Advanced Nuclear Programs

_____
E. Ray
Manager, Advanced Nuclear Systems Engineering

GENERAL ELECTRIC
MISSILE AND SPACE DIVISION
Valley Forge Space Technology Center
P.O. Box 8555 • Philadelphia 1, Penna.

Contributers:

J.W. Larson, Program Manager
H. Brown, Trajectory and Performance Analyses
R.D. Cockfield, Spacecraft Analysis
J.T. Keiser, Spacecraft Analysis

TABLE OF CONTENTS

TABLE OF CONTENTS (Cont'd.)

LIST OF ILLUSTRATIONS

LIST OF ILLUSTRATIONS (Cont'd.)

LIST OF ILLUSTRATIONS (Cont'd.)

LIST OF ILLUSTRATIONS (Cont'd.)

SECTION 1

INTRODUCTION

The General Electric Company has performed a study to determine the applicability and the optimum operating modes of electrically propelled earth-moon shuttle vehicles for logistic support of advanced lunar operations. The results of this study, which was conducted for 13 months under Contract NAS 8-11207 to NASA Marshall Space Flight Center, are presented herein.

The transportation pattern for logistic material support of advanced lunar operations using electrically propelled earth-moon shuttle vehicles consists of the three steps shown in Figure 1-1. (1) Ascent from earth to orbit, (2) transfer from earth orbit to lunar orbit, and (3) descent from orbit to lunar surface. The ascent and descent phases require thrust levels comparable to the vehicle weight, and are achieved by use of chemical rockets. The orbit transfer phase can be accomplished by low thrust electrical propulsion systems as well as by high thrust nuclear and chemical rocket systems. Using electrical propulsion, the trajectory terminal points are approximately circular orbits around the earth and the moon.

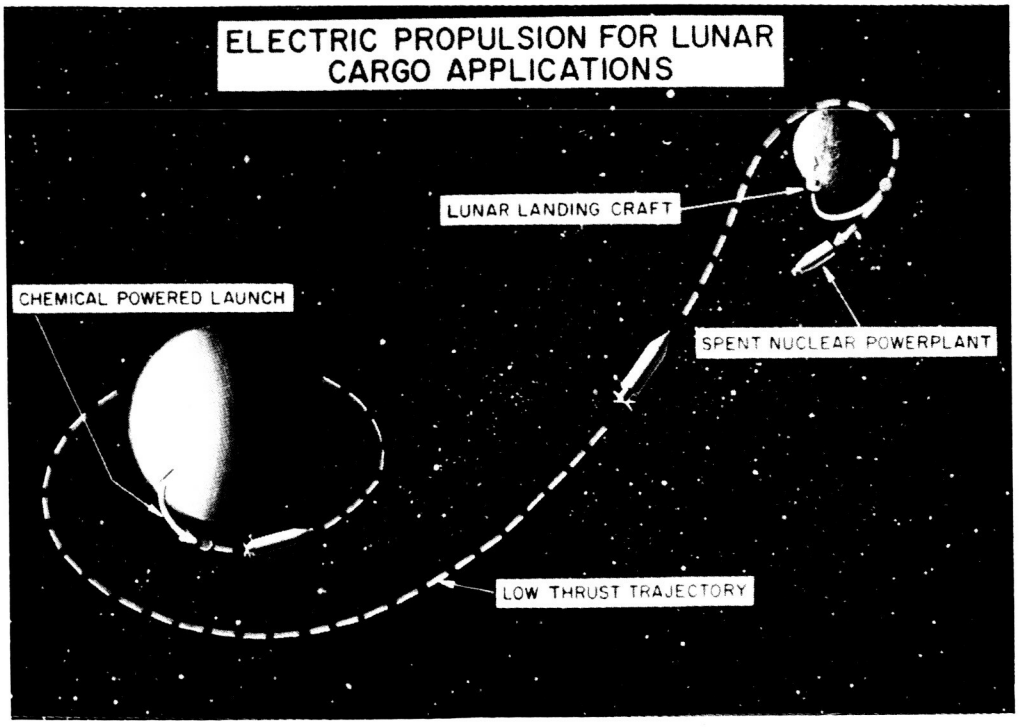

Figure 1-1. Lunar Cargo Transportation Pattern Using Electric Propulsion

The analysis has assumed the existence, in the time period of such operations, of multi-megawatt nuclear electric power sources, such as that based on the SNAP-50 level of technology, and other propulsion systems components, as presently envisioned. The high thrust operations between surfaces and low thrust terminal orbits have been treated only to the extent required for the main theme of this study. The payload capability of the Saturn V has been considered basic; but performance results can be scaled to other size boosters.

The main purpose of the study has been to present the major design choices (e.g., mission profile, trip time, specific impulse) in their proper perspective, defining the consequences of various selections and providing a rational base for system optimization. The initial approach to the study was to develop a generalized analysis of the sustained lunar supply problem based on the use of a reusable, power-limited vehicle or propulsion module. As the study progressed, sufficient variations in operational modes and optimizing criteria were defined that several computer programs were developed, each specialized to investigate a particular topic. The lunar logistic mission requirements were examined to determine the performance requirement for the electrically-propelled vehicle to be competitive with other transportation systems; the physical constraint of trajectory and accompanying propulsion requirement was analyzed; and the state-of-the-art constraints for definition of the spacecraft was investigated. These articles are reported in Sections 3, 4 and 5, respectively. Three parallel computer programs were required to generate the final parametric performance data , presented in Section 6, to accommodate single trip versus multiple trip, and single-powerplant versus multiple-powerplant modes. Recommendations for further work are presented in Section 7. Appendices have been prepared to describe details of the lunar supply system for off-optimum selections, and technical approach for a more refined cost optimization approach for use when more technical information is available on power system development. Conceptual designs are presented for vehicles based on the mission analysis.

The contract study was performed by the Advanced Nuclear Systems Engineering Operation at the GE-MSD in King of Prussia, Pennsylvania. Technical assistance on trajectory analysis and parametric performance computation was provided by the Space Power & Propulsion Systems Operation at Evandale, Ohio.

SECTION 2

SUMMARY

The logistic support requirements for the manned lunar activities following the landings in the Apollo spacecraft system are subject to much debate. A reasonable prediction is that Apollo will be followed by a series of expeditions to various sites by use of vehicles derived from Apollo. It is also likely that one semi-permanent base would be established. In 15 years of post-Apollo activity, the "equivalent" logistic requirement could reach 2000 tons. This quantity could represent a conservative estimate for the subject analysis.

The key element in the lunar logistics requirement is the transport of personnel. In a preliminary analysis, the number of Saturn V boosters required for transport of the men was found to equal approximately the number required for equipment and supplies. Thus, the "equivalent" tonnage, 2000 tons, is 50 percent equipment and 50 percent equivalent tonnage of the personnel.

The electrically propelled space vehicle, such as illustrated in Figure 2-1, makes the orbit transfer in too long a time to participate directly in manned transportation. However, it can transport the lunar landing vehicle from earth to lunar orbit and the men can overtake

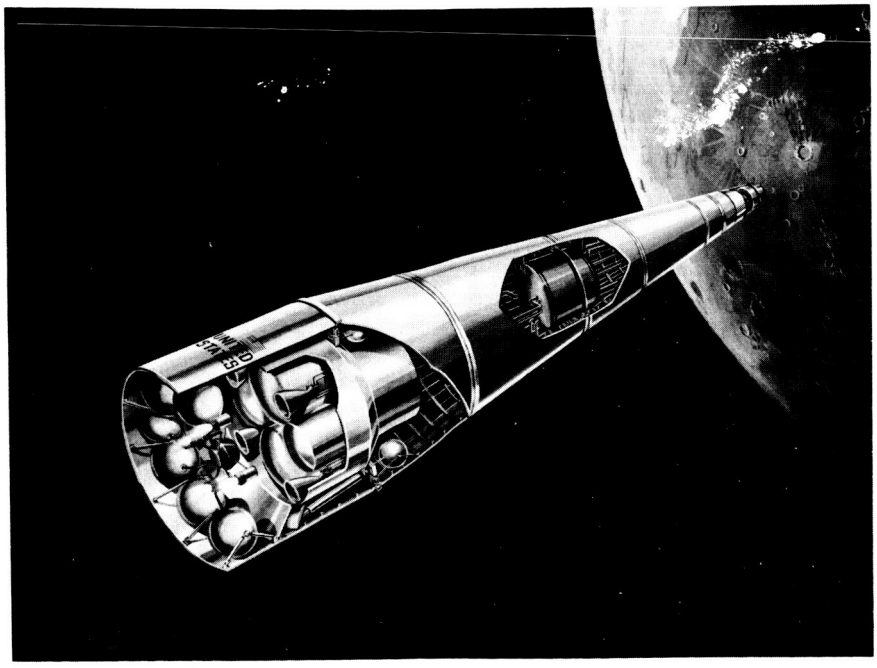

Figure 2-1. Typical Lunar Cargo Vehicle Design

it in lunar orbit by an all-chemical, rocket-propelled vehicle such as Apollo. Using this scheme, ten men plus 15 tons of equipment can be provided for a lunar expedition by the use of two Saturns. Using the all-chemical mode, 4-1/2 Saturns are necessary. As an alternative, a six-man team plus 25 tons of supplies could be transported for a six-month expedition using the "mixed" electrical propulsion and chemical rocket approach.

The nuclear rocket also provides a savings over a chemical rocket transport system. However, its savings is in the range of 28 percent as compared to 43 percent for the electrical propulsion system, at a 2000 ton "equivalent" cargo requirement. At this level of cargo the initial development cost is quickly absorbed, generally after 250 to 500 tons of cargo. The period of lunar expeditions will probably require on the order of 250 tons equivalent cargo, and this will amortize most of the development cost for either nuclear system. Both the development cost and the manufacture cost of the nuclear rocket and electrical propulsion systems affect the relative advantage of these systems over the chemical rocket. Equally important is the cost of the Saturn V, or the cost per unit mass to orbit. These cost factors are important to incorporate in the system optimization.

The mission requirements for the earth-moon transfer are rather reasonable for an electrical propulsion vehicle. The propulsion requirement is defined by a characteristic velocity of 7.8 km/sec. Using a SNAP-50 type of powerplant with Beryllium radiators (specific weight at 10 kg/KWe) and electron bombardment ion engines (70 percent efficiency at 4000 seconds specific impulse), the trip time to transport a 30.8 ton net cargo lunar landing craft is 3280 hours. This represents a sizable cargo increase over the all-chemical Saturn V system (12.7 tons), but is achieved at the expense of greatly increased trip time (100 hours for all-chemical system).

Many operating modes are found to be of interest for the electrical propulsion system. One of the most interesting is the single-trip mode, because it attains most of the economic advantage of using electrical propulsion with the particularly advantageous feature of much shorter life requirements (in the range of 4000 hours). The multiple trip ferry needs at least 10,000 hours and preferably 15,000 hours for a 10 kg/KWe nuclear power supply.

The operating mode comparison most difficult to evaluate is (1) the approach standardizing on a lander size, which requires varying specific impulses (and, thus, separate thrustors) between the different voyages legs, and (2) the approach restricted to a single specific impulse (a single thrustor mounted to the powerplant) whereby different size lunar landers are provided on the initial, middle and terminal voyages. The constant specific impulse approach shows better performance with the cost model used herein, but this subject needs further study.

The multiple powerplant operational mode is an approach that eliminates the constant lander versus constant specific impulse controversy. An additional advantage is the inherent redundancy for improving reliability of cargo delivery.

Another consideration in the multiple-trip analysis is the dumping of spent propellant tanks from the inbound voyages in low earth orbit. The performance penalty has been estimated for carrying these empty tanks out to a high earth orbit or to lunar orbit, and this performance penalty is reasonably small. Thus, this approach can be taken if necessary or desirable.

The multiple-trip ferry did not have any substantial advantage over the single-trip mode. Thus, a reasonable approach is to direct the first generation lunar cargo vehicle development towards the single-trip mode. In this case the power supply life rating need not exceed six months, a more reasonable goal than the 10,000 hours discussed by many investigators. After the power supply is operational, the life rating can be increased by further development. The additional life rating of the power supply can be applied in any or all of four directions. The first is the multiple trip ferry with either single or multiple powerplants; the second is a lunar surface powerplant by retaining the powerplant with the lunar lander for descent from orbit; the third is the propulsion of unmanned probes and/or manned vehicles for interplanetary scientific voyages; and, finally, the fourth is the use as an APU in an orbiting satellite.

The most intriging application for the extended life power supply is the lunar landing to provide surface power. A 1200 KWe power supply could be landed with a 2 π shield plus

16 tons of equipment, forming a complete energy depot for ground operations or plant for manufacture of propellants from lunar resources. The power supply and lander with lunar surface shield is shown in Figure 2-2, along with many other views of the participating vehicles. This subject is also worthy of further investigation.

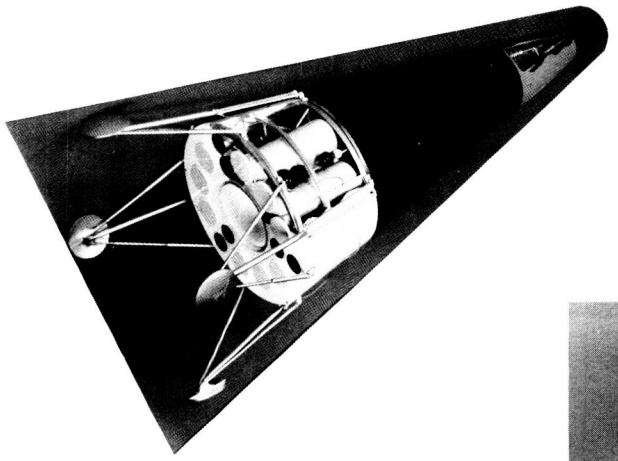

OUTBOUND FLIGHT

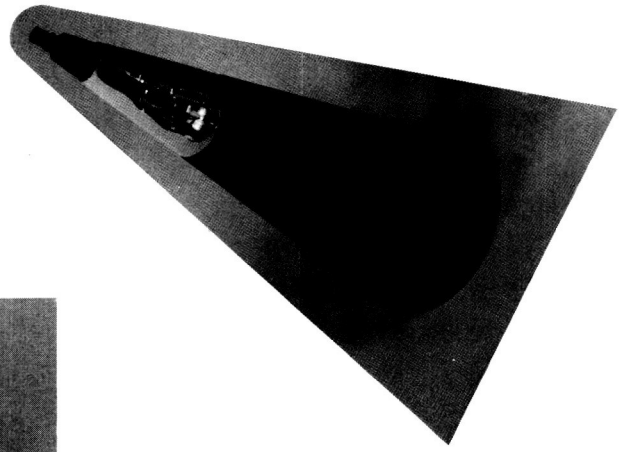

RETURN FLIGHT

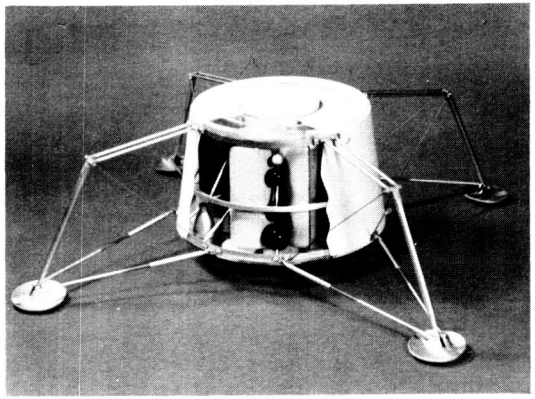

CARGO TRANSPORT

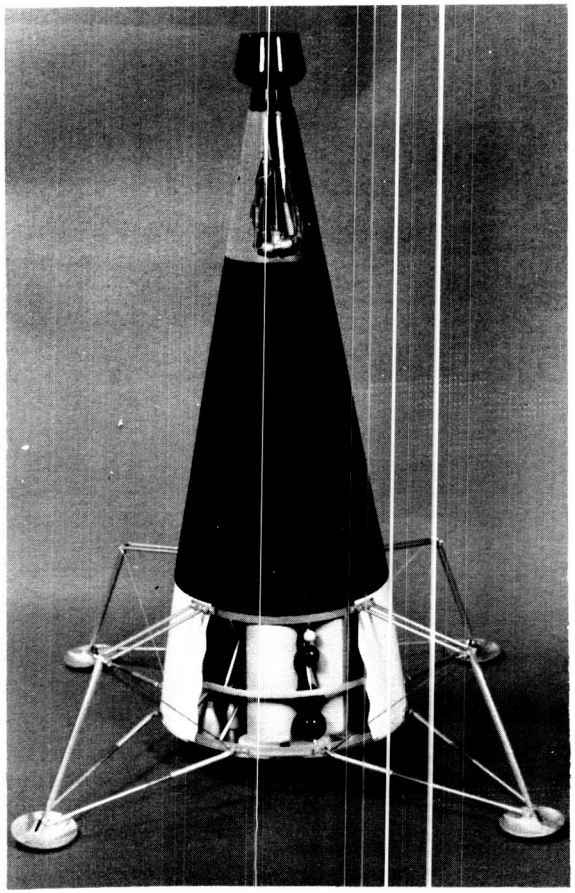

LUNAR SURFACE POWER SUPPLY

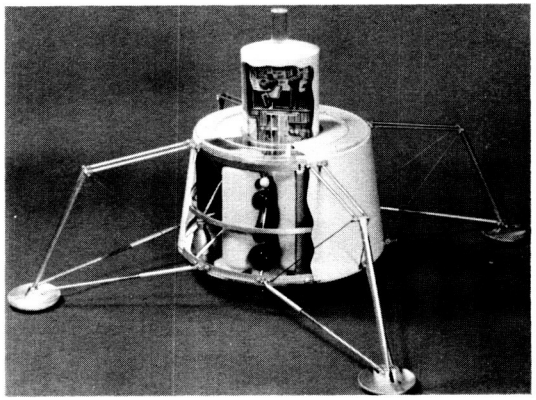

LUNAR SHELTER

Figure 2-2. Application of Nuclear Power Supply to Lunar Operations

SECTION 3
LUNAR LOGISTICS REQUIREMENTS

An understanding of the lunar logistics requirements is the prerequisite for analysis of the transportation system to deliver materials from the earth to the sites of lunar operations. In addition, all contending transportation systems need to be evaluated to determine any advantage for the particular system of interest, which in this study is the electrical propulsion system. Analyses of the mission requirements and competing systems are presented below, which later form the basis for the system optimization criteria.

Manned lunar operations are expected to commence in 1970 with the first manned Apollo landing. The transportation system developed for this goal sets the baseline for subsequent lunar cargo transportation systems and the motivation will be strong for a policy of evolution towards improved performance in terms of increased cargo loads and reduced transportation costs, rather than for revolution towards an entirely new approach.

The Apollo system can be readily converted into a cargo vehicle by elimination of the lunar ascent stage from the LEM (Lunar Excursion Module) and modification of the Apollo spacecraft to unmanned operation. Using this approach, approximately 12.7 metric tons (28,000 lbs) of net cargo can be placed on the lunar surface by one Saturn V launch vehicle. This mass can be adequate for a lunar shelter, a mobile laboratory vehicle, a nuclear reactor power supply, or a variety of other payloads. A space transportation system of this capacity would appear to be quite adequate for a number of small lunar expeditions after Apollo. This should certainly be the case for the first five years, while policies for the long range lunar operations are being conceived, analyzed, re-analyzed, debated, committeed, lobbied, investigated, budgeted, voted and/or approved.

Between 1975 and 1980, the requirement should exist for a substantially lower cost space transportation system with larger capacity payloads. The lunar operations between 1975 and 1980 could likely be limited to a multitude of small expeditions to a variety of lunar sites for time periods between three months and one year. For use in this period the Saturn V logistics capability can be increased by replacement of the S-IV B stage with either a nuclear rocket or an electrical propulsion system.

A number of expeditions are required because the missions are varied and involve different lunar sites. A listing of the sites discussed in the literature are:

(1) Alphonsus Crater
(2) Leibnitz Mountains
(3) Shackleton Mountains
(4) Apennine Mountains
(5) Piazzi Smyth (Mare Imbrium)
(6) Kepler Crater
(7) Copernicus Crater
(8) Bonpland E. Crater
(9) Hyginies Rill
(10) Oceanus Procellarum

These sites vary widely over the lunar surface. Criteria involved in their recommendation involve favorable landing and launch trajectories, good landing site, geologic importance, continuity of sunlight, varied topography, and possibility of water and mineral resources. It appears reasonable to expect a number of these sites to be explored, and the next decade will undoubtedly involve much debate on their order of priority and schedule.

The number of expeditions to be accomplished, the crew size and the length of stay are not presently predictable. Let us assume, for the purpose of this transportation study, the accomplishment of five expeditions over the course of five years after 1975 with a six-man crew and a six-month lunar stay. The crew size assumed allows for two entirely scientific members supported by four operational personnel for piloting, navigation, communications, and maintenance. The staytime assumed is for maximizing acquisition of scientific data within the endurance of the crew, recognizing that certain data communicated to earth for evaluation could feed back to the expedition the requirements for more measurements.

A second type of lunar activity that could commence around 1980 is the establishment of a semi-permanent scientific base. The minimum crew size for the base is estimated at ten men. The more desirable number is probably in the range of 20 to 30 men. Crew

replacement would be required with tours of duty ranging between 6 and 12 months. The decision for undertaking such a task would await the results of the first few lunar expeditions.

Eventually, a permanent lunar base could be developed for the exploration of lunar resources and for military activities. Such a base could require 50 to 100 men, but the need for this activity is very speculative at this time.

Using the above logic a schedule of lunar activities has been assumed and is presented in Figure 3-1. The first five years of lunar operations produce several Apollo landings. During the time period from 1975 to 1990, five lunar expeditions are undertaken and a ten-man semi-permanent base is operated for ten years with a six-month crew replacement cycle. The total personnel involved is 230. Thus, the personnel transportation represents a substantial requirement.

A recent study of lunar exploration systems for Apollo (LESA) by Boeing Company yieided the following estimates of equipment and supplies to support various size bases:

Expedition	No. Men	Staytime, Months	Equipment, Tons
LESA 1	3	3	12.5
LESA 2	6	6	25
LESA 3	12	12	50

These data points have been generalized to form the parametric plot in Figure 3-2, which is assumed for this transportation study as the requirement for the exploration phase of lunar operations.

Estimates of cargo requirements for a semi-permanent base to support a variety of lunar scientific operations vary over the shaded area described in Figure 3-3. This cargo amount applies to a ten-man base and increases proportionally with the number of men. The cumulative cargo over a ten-year, semi-permanent base life ranges between 500 and 900 tons for a ten-man crew. The lower line of the shaded area corresponds to results from

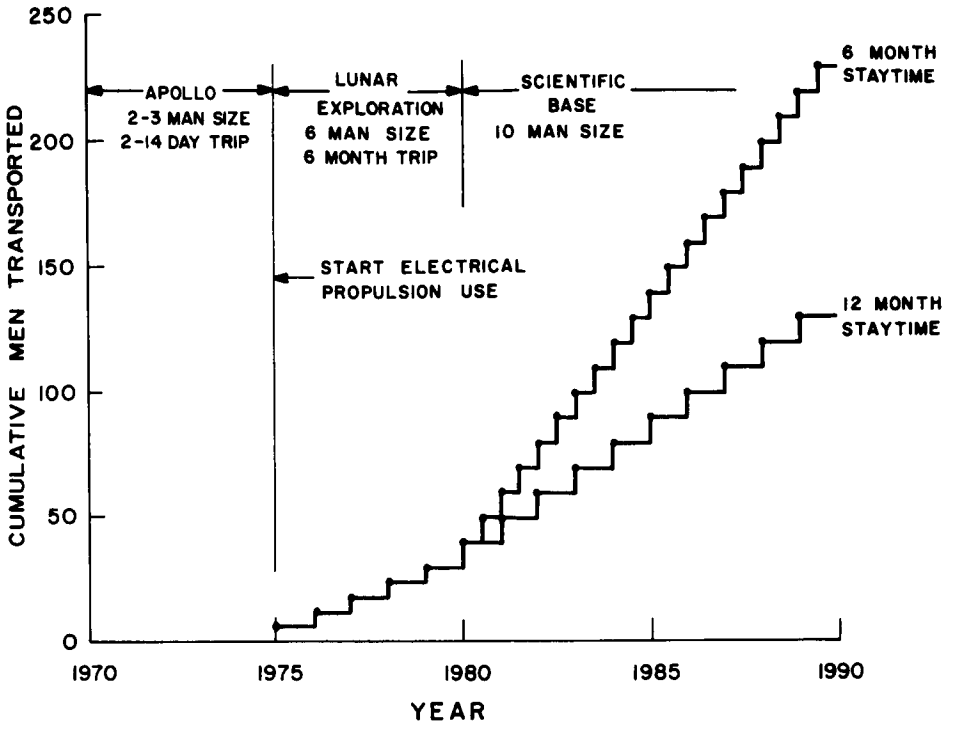

Figure 3-1. Assumed Personnel Schedule for Lunar Operation

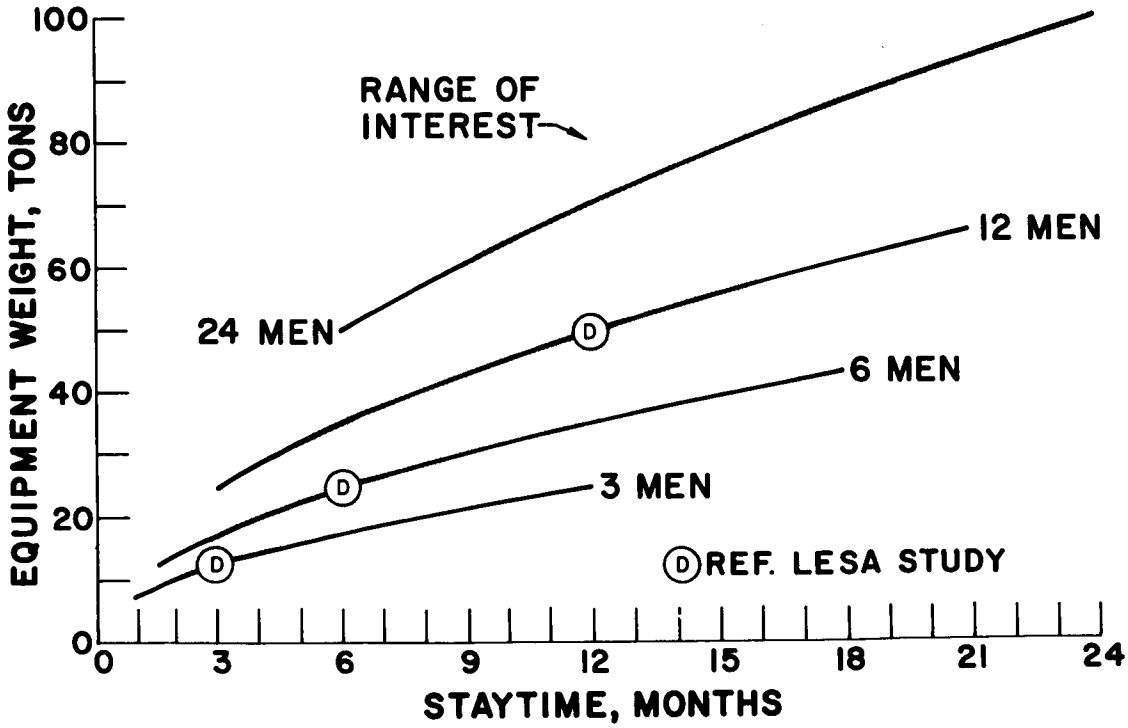

Figure 3-2. Assumed Logistics for Lunar Expedition

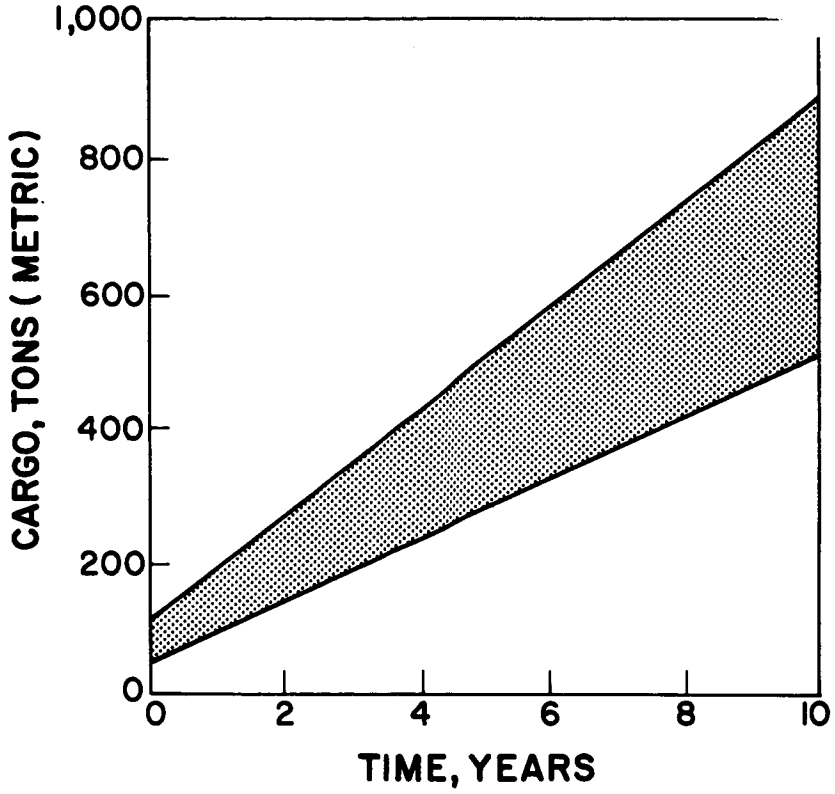

Figure 3-3. Logistic Requirement for Ten-Man Lunar Base

the LESA study by Boeing Company *; and the top line, from the operational analysis study by LTV**. The transportation system could be required to support several bases simultaneously and/or different bases at different periods of time. The spread in cargo requirements shown in Figure 3-3 can be considered the range of uncertainty encompassing many different bases over a decade.

The present Apollo spacecraft provides transportation of three men from earth to lunar orbit and back to earth again. The LEM transports two men from lunar orbit to the lunar surface and back to lunar orbit. These vehicles are approximately 13.5 tons each, at insertion into lunar orbit. An assumed scaling relationship of these vehicles is presented

---

* Initial Concept of Lunar Exploration Systems for Apollo, Boeing Company, Vol. 1, Summary Rpt. prepared under contract no. NASw-792, NASA, Washington, D. C. March, 1964.

** Operations Analysis of Advanced Lunar Transportation Systems, LTV Astronautics Division, Final Progress Report prepared under contract NAS 8-5027, MSFC, Huntsville, Alabama, January, 1964.

in Figure 3-4. The total mass inserted into lunar orbit by the Saturn V booster in the Apollo expedition is 27 tons. It is estimated that the Saturn V capacity can grow to 31.7 tons, and this capacity would allow all three members of the Apollo crew to descend to the lunar surface. As previously mentioned, the Saturn V cargo transporter has a capacity of 12.7 tons delivered to the lunar surface. Thus, each crew member is equivalent to 4.2 tons of cargo, insofar as the transportation system is concerned. From Figure 3-2 a six-man, six-month expedition requires 25 tons of equipment and supplies. The six-man crew adds an equivalent weight of 25.4 tons, resulting in an effective logistics requirement of approximately 50 tons per expedition. Assuming five expeditions of this type, the total cargo requirement for the lunar exploration is 250 tons.

The semi-permanent lunar base can require six-month crew rotation, and, thus, the operation is dependent on scheduled resupply of materials and crew. The equipment and supplies can range between 450 and 880 tons for a ten-year operation, and the crew replacement is equivalent to another 840 tons, assuming a six-month duty time.

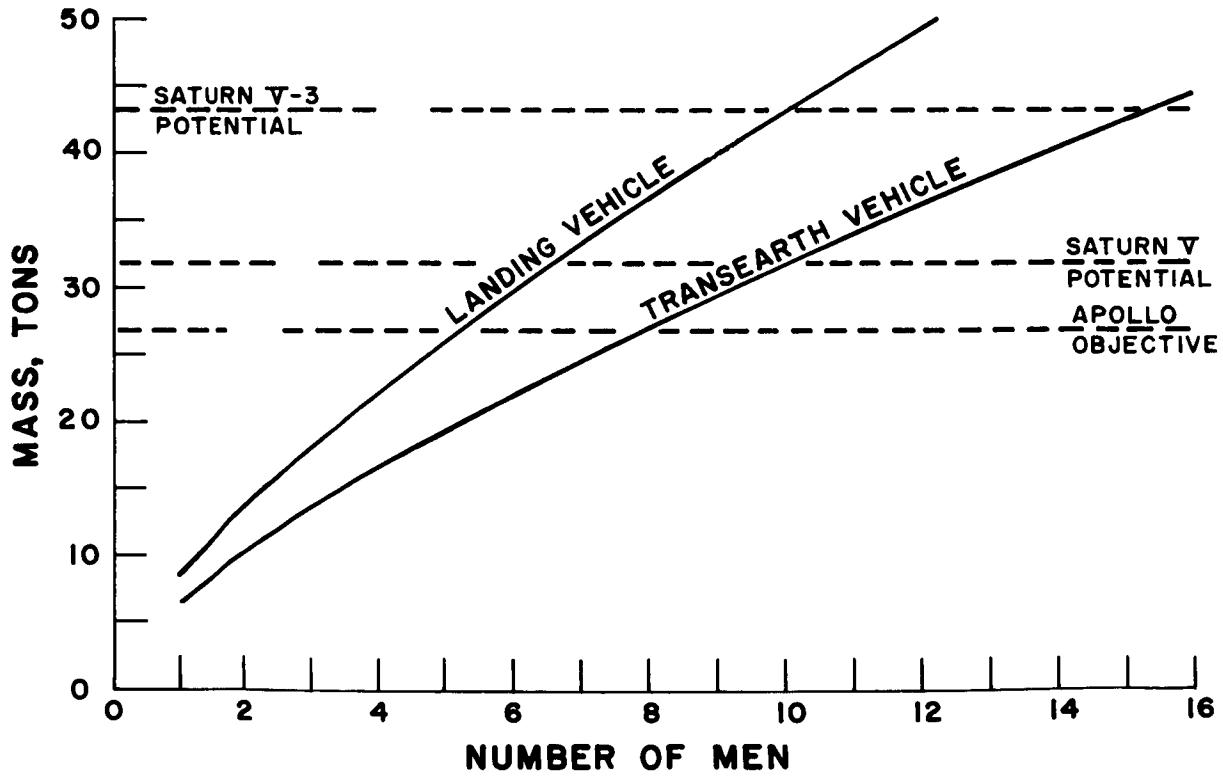

Figure 3-4. Assumed Personnel Transportation Requirements

Using these assumptions the cumulative logistics requirements are presented in Figure 3-5. As shown in Figure 3-5 the logistic requirement for lunar operations can range between 1500 and 2000 tons. Of this quantity, the crew transportation represents a major portion of the task.

The study of electrical propulsion for logistic support of lunar operations has shown that long trip times, on the order of three to six months, are required to provide a sufficient cargo increase to achieve a cost reduction over the chemical rocket system. Because of this long travel time the type of cargo to be transported needs to be restricted. Provisions to transport personnel will be sizably larger for electrical propulsion transportation than for chemical. The ability of electrical propulsion to double the cargo capacity per launch is cancelled if the effective weight per man is doubled. In addition, man hours are lost, which leads to an increase in personnel to accomplish the lunar job. The Van Allen belt and solar radiation add new hazards. Thus, it appears certain that personnel transportation be excluded from consideration in the slow trip vehicle.

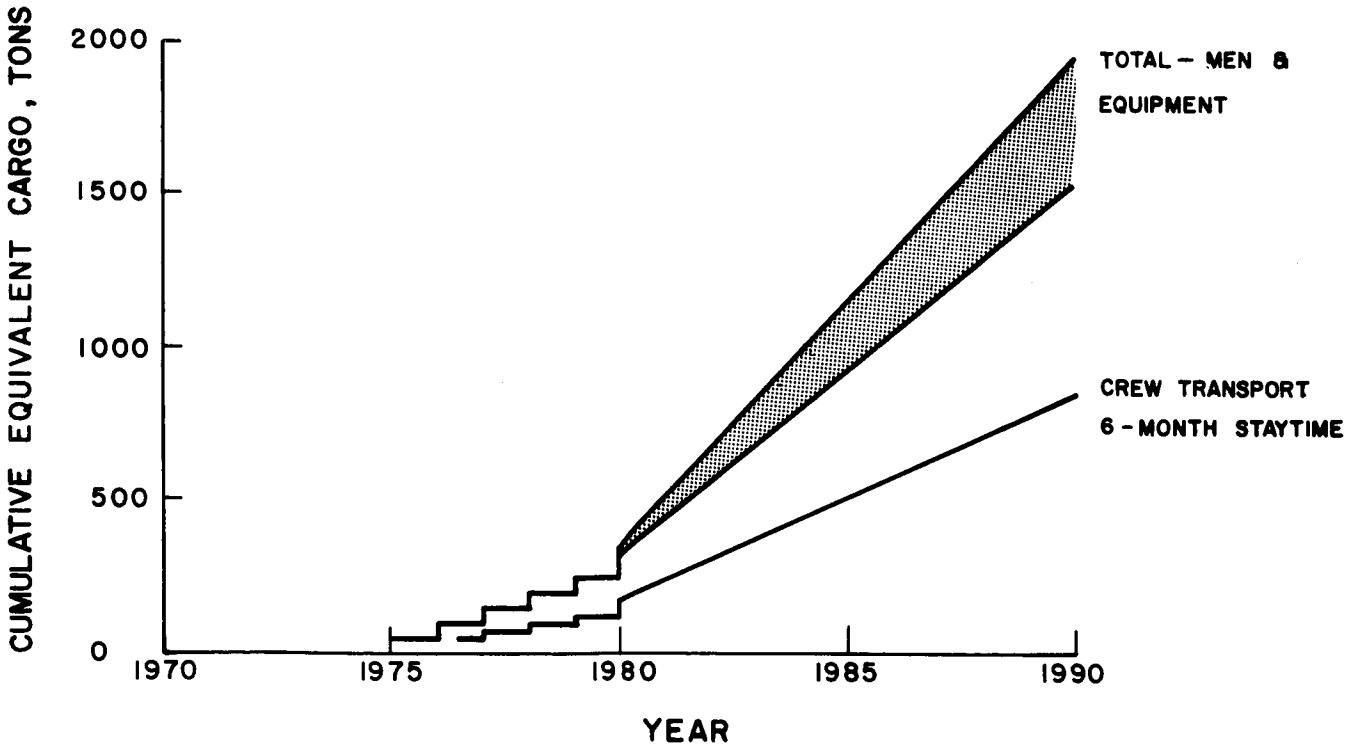

Figure 3-5. Assumed Logistic Requirements

The electrical propulsion system can contribute indirectly to personnel transportation using the approach illustrated in Figure 3-6. The electrically propelled vehicle is used to transport a large lunar landing vehicle from earth orbit to lunar orbit. After this vehicle reaches lunar orbit, a second Saturn V launches a chemical rocket propelled Apollo type system to rendezvous with the electrically propelled vehicle in lunar orbit. The crew transfers to the lunar lander brought over by the electrical propulsion system and descends to the lunar surface.

This approach can be shown to provide a substantial performance advantage over chemical rocket propulsion. The all-chemical Saturn V can insert a 31.7 ton mass into lunar orbit, which corresponds to a ten-man, trans-earth vehicle according to Figure 3-4. Thus, a Saturn V can transport up to ten men from earth to lunar orbit and return. The gross mass of lunar landing vehicle required to land the ten men and return them to lunar orbit is 43 tons. This mass is well within the capacity of a Saturn V system using electrical propulsion for the orbit transfer phase. Using this approach the personnel are transported in a pattern very similar to that followed by Apollo. The added procedure is the initial rendezvous in lunar orbit with the lunar landing craft. At this point the crew can still abort the mission and return to earth, if the lander is not in satisfactory condition. Thus, the risk is fairly comparable to Apollo.

In addition to providing ten men to the lunar base using two Saturn V's, a sizable amount of equipment and supplies can be delivered. The electrical propulsion system can be sized in a reasonable manner to insert a 77-ton mass into lunar orbit. This mass is 34 tons more than that required to transport the ten men, and the resultant net cargo deliverable to the lunar surface is 15 tons. Ten men plus 15 tons is an equivalent cargo of 57 tons (assuming 4.2 tons equivalent per man), which corresponds to the capacity of 4.5 all-chemical Saturn V's. The net booster savings is 2.5, or 55 percent. Therefore, the approach described above for manned transportation is worthy of serious consideration.

A more general criteria can now be developed for optimization of the electrical propulsion system. To factor the cost into the performance estimation, it is first necessary to examine the performance characteristics of competitive lunar cargo delivery systems so that the

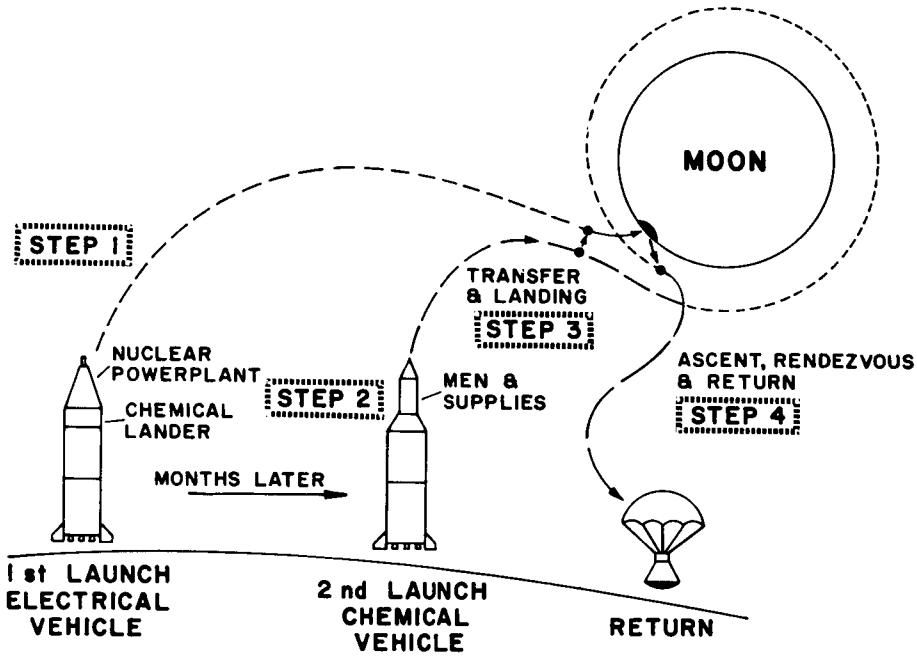

Figure 3-6. Lunar Expedition Strategy

optimizing criteria can properly be applied. Data for an all-chemical Saturn V system are tabulated in Table 3-1. The significant weight item is the orbit transfer stage, which is the difference between net weights placed in earth orbit and in lunar orbit. This weight is shown to be 77.3 metric tons. The use of electric propulsion makes possible a reduction in required weight to accomplish the orbit transfer and consequently brings about an increase in net cargo to the lunar surface.

TABLE 3-1. REFERENCE CHEMICAL SYSTEM

Δ Orbit Transfer by Chemical Rocket	
Δ Saturn V Launch Vehicle	
Δ Weights	
Launch Vehicle	2700. Metric Tons
Earth Orbit	109.
Lunar Orbit	31.7
Lunar Surface	12.7
Δ Orbit Transfer Stage is	77.3 Metric Tons

The relationship between mass of orbit transfer stage and lunar cargo is shown in Figure 3-7. Points are spotted to show the characteristics of a nuclear rocket system as well as the all-chemical system, both using a Saturn V earth launch vehicle. As the orbit transfer stage decreases to zero mass, the cargo increases to 43.6 tons. This value is almost attainable by using lunar base propellant manufacture and/or accepting extremely long trip times. Electrical propulsion does have the flexibility to be sized along most of the length of this curve.

The use of the nuclear rocket to replace the S-IV B stage of the Saturn V vehicle has been investigated and performance predicted for two trajectory modes. In the first mode the load mounted above the S-II stage is sufficiently low (approximately 109 tons) that it can be placed in a circular earth orbit by just two stages of the Saturn V. Using this orbital start approach (which is the same as that used for the electrical propulsion system), the net lunar payload is 16.8 tons, a 32 percent increase over the chemical rocket system. The second approach is based on maintaining a heavier load on the S-II stage as in Apollo, whereby the vehicle is in a suborbital trajectory after second stage burnout. The nuclear rocket is then started from the suborbital trajectory, similar to that followed by the S-IV B stage. This approach yields 21.3 tons of net lunar cargo*, a 68 percent increase over the chemical rocket approach.

The suborbital start of the nuclear rocket certainly stands out as the preferred approach from the viewpoint of performance. However, this approach can involve many nuclear

* Johnson, P.G., "A Summary of Nuclear Rocket Applications", AIAA Paper No. 64-388, 1st AIAA Annual Meeting, June 29-July 2, 1964.

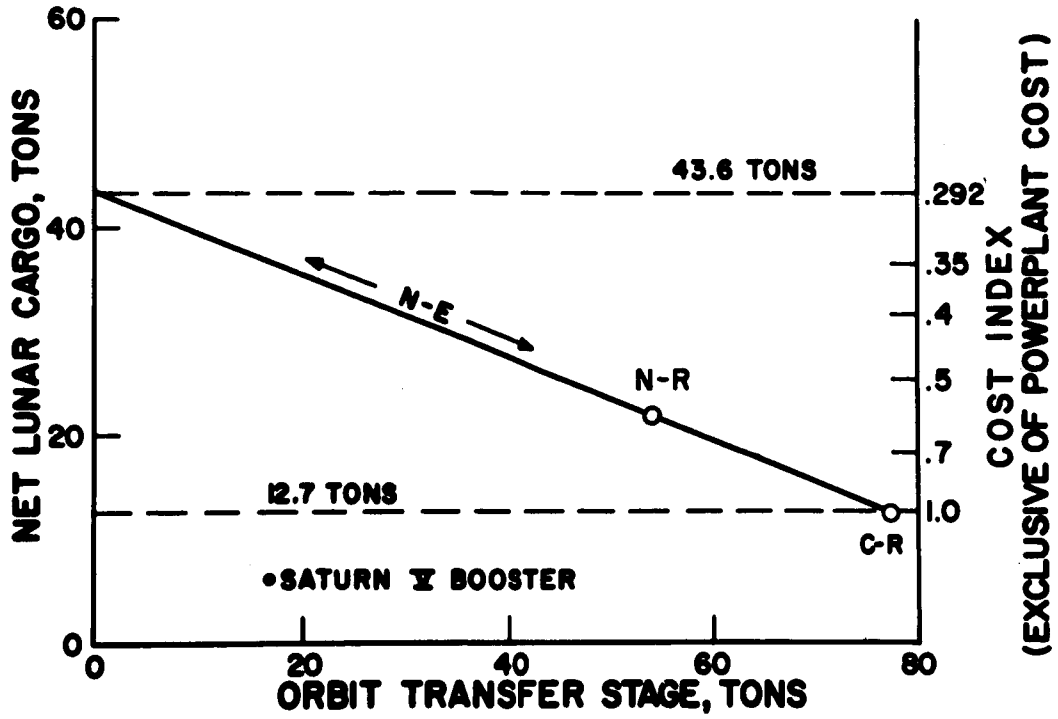

Figure 3-7. Variation of Lunar Cargo and Cost with Size of Orbit Transfer Stage

hazards and much further study is necessary to determine the acceptability of the sub-orbital start.

The cargo increase brought about by use of the nuclear rocket does not represent an equivalent reduction in transportation cost because of the cost to develop and manufacture this stage. The relative cost advantage of the nuclear rocket approach is shown in Figure 3-8 as a function of the net increase of the nuclear rocket stage over the S-IV B stage it replaces. The parameter, cost index, represents the cost per unit mass delivered normalized to that for the chemical rocket. A basic cost per Saturn V is assumed at $100,000,000. The ratio of costs is the important consideration in the economic evaluation. (The cost index for a $10,000,000 nuclear rocket stage associated with a $50,000,000 Saturn V vehicle is the same as a $20,000,000 nuclear rocket stage associated with a $100,000,000 Saturn V.)

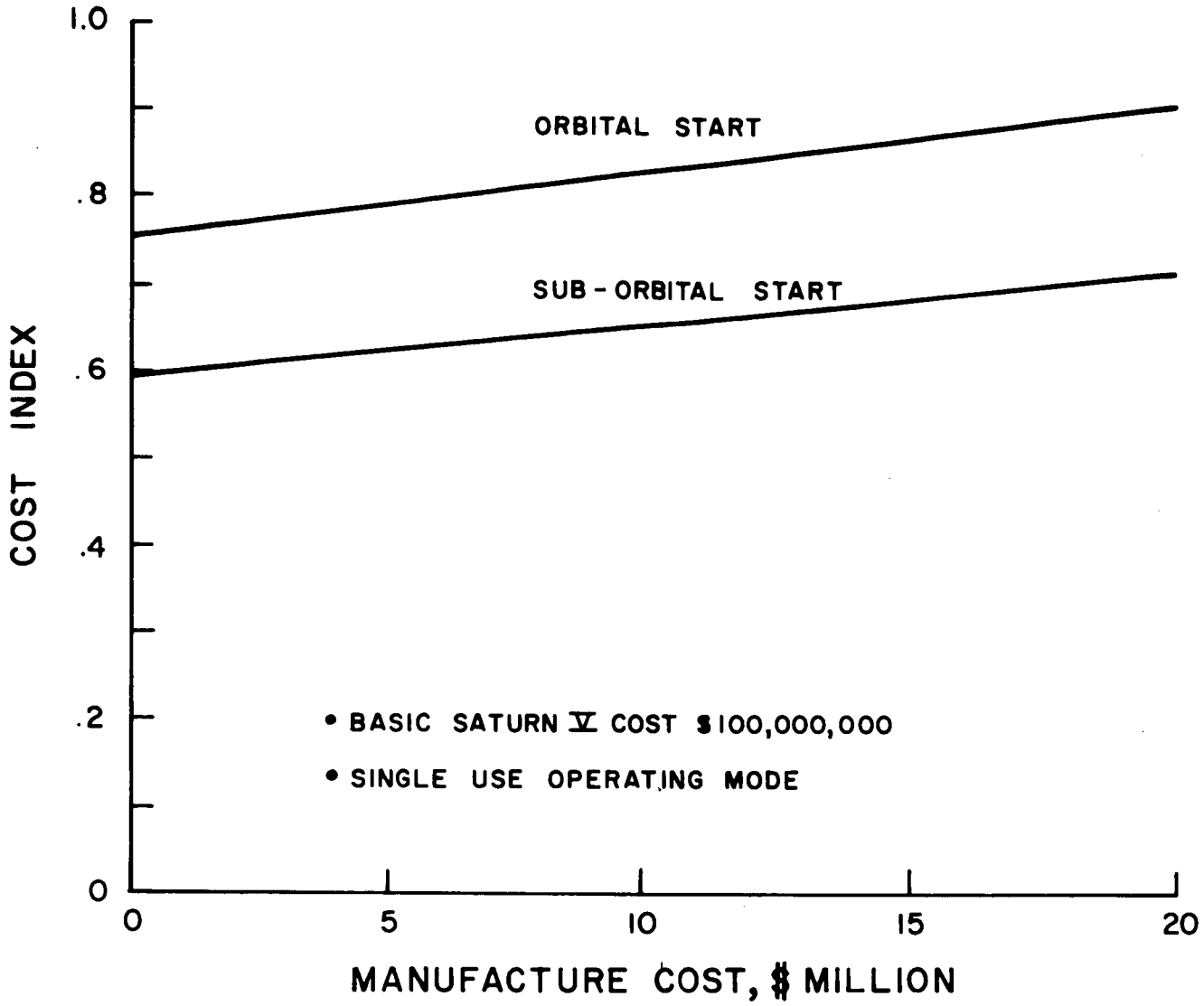

Figure 3-8. Effect of Manufacture Cost on Nuclear Rocket Stage Performance

The cost index shows the savings per launch, and this savings has to be applied against amortization of the development cost. A parametric representation is shown in Figure 3-9 to show the crossover point where the development cost is written off, and true costs savings are realized. For each billion dollars of nuclear rocket development cost, 750 tons and 370 tons are required for the orbital and suborbital start nuclear rocket systems,

respectively, assuming a $10,000,000 nuclear rocket stage and $100,000,000 Saturn V. Thus, it appears that the nuclear rocket approach offers substantial cost improvement over the chemical rocket. In the 15 years of lunar operation previously discussed, the cumulative cargo requirement was 2000 tons. Referring to Figure 3-9, the suborbital nuclear rocket brings about a $4,300,000,000 cost savings.

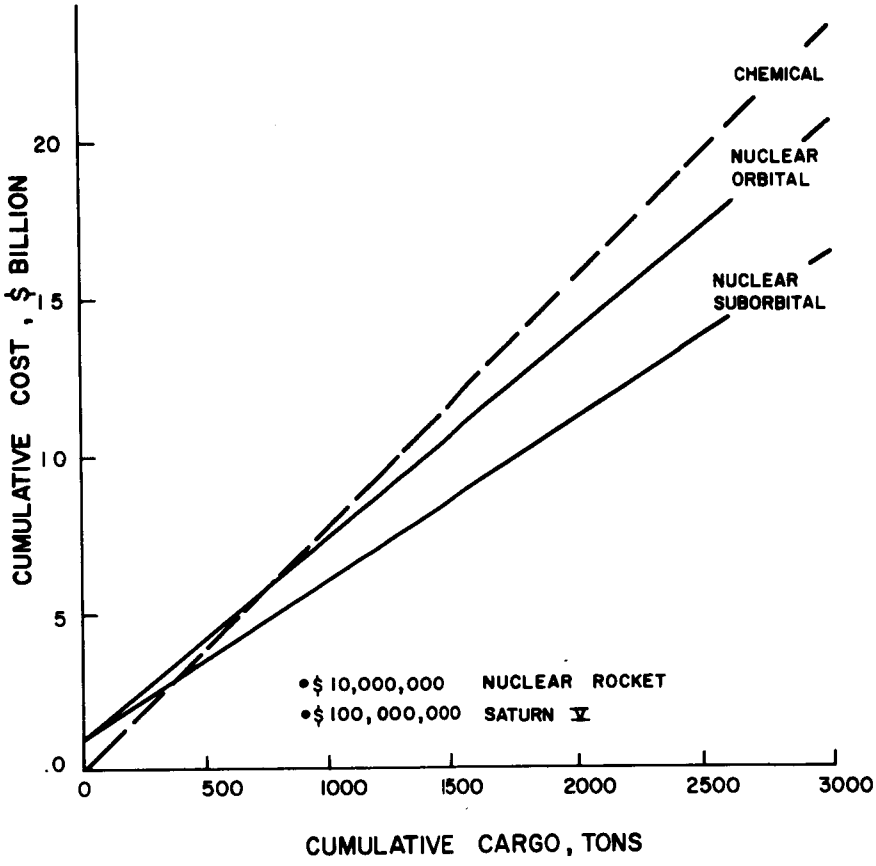

Figure 3-9. Cost Advantage of Nuclear Rocket

As shown previously in Figure 3-7 the nuclear electric system can be sized over a wide range of lunar payloads. The tradeoff needs to be made between acceptable trip time and competitive cost index with both the chemical rocket and the nuclear rocket which was shown to range between 0.6 and 0.9 in Figure 3-8. A comparable parametric graph is shown in Figure 3-10, where the cost index is described for a range of nuclear powerplant manufacture costs and lunar cargos.

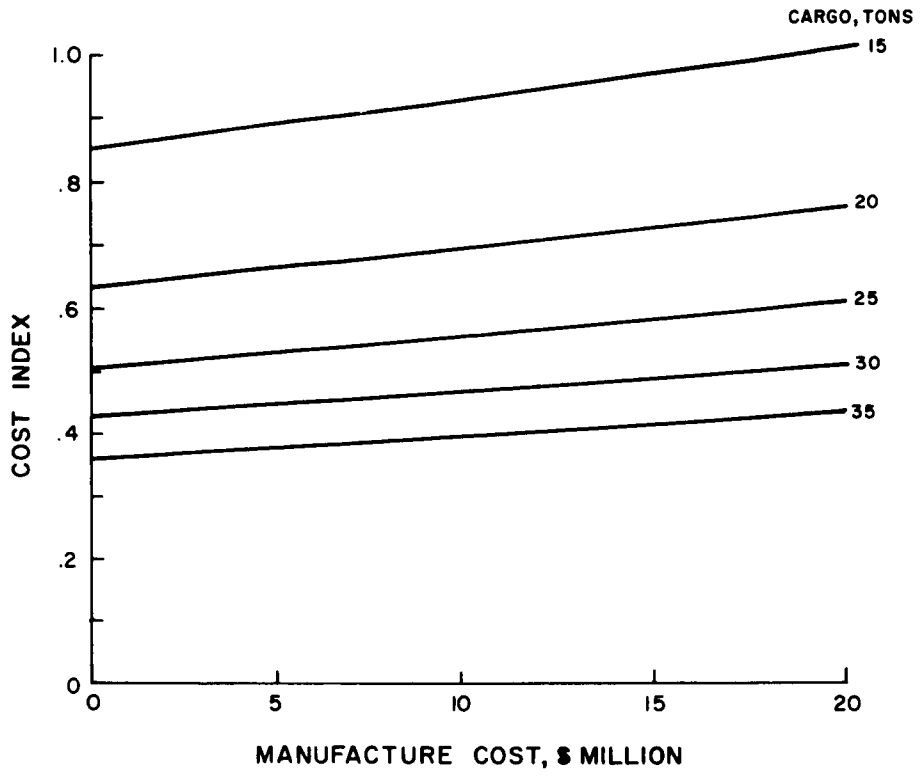

Figure 3-10. Effect of Manufacture Cost on Electrical Propulsion Stage Performance

The large cargo sizes shown are within the range attainable with electrical propulsion as shown by the sample case in Table 3-2. The net lunar cargo is 30.8 tons, delivered in 3280 hours by a nuclear electric system based on the SNAP-50 type powerplant and electron bombardment thrustors.

The cumulative cost savings to be realized after the development cost investment is presented in Figure 3-11. The crossover point for the 30-ton cargo size system is about 250 tons to amortize $1,000,000,000 of electric propulsion system development. The cost savings after 2000 tons of cargo are delivered is $6,600,000,000. The electrical propulsion system at 30-ton cargo size is shown to be quite advantageous. The 250-ton crossover point corresponds to the requirement for the lunar exploration phase of lunar activity. Thus, the electrical propulsion system development cost is covered even if lunar operations cease after the exploratory period. This is not quite the case for the nuclear rocket.

TABLE 3-2. TYPICAL NUCLEAR-ELECTRIC VEHICLE CHARACTERISTICS

Δ Operating Mode

One-Way Trip

Δ Technology

SNAP-50 Powerplant

Beryllium Radiator

Electron-Bombardment Thrustor

Saturn V Launcher

Δ Performance

Outbound Propulsion Time = 3280 Hr

Thrustor Exhaust Velocity = 43 km/sec

Net Electrical Power = 1.9 mwe

New Lunar Cargo = 30.8 tons

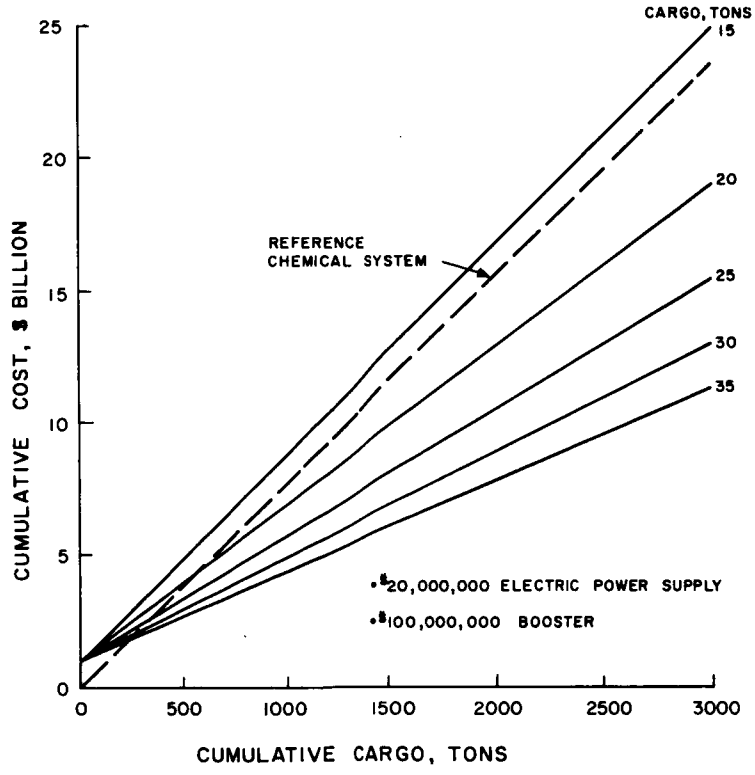

Figure 3-11. Cost Advantage of Electrical Propulsion

The lunar exploration activity is shown to be an important consideration in the advancement of electrical propulsion. The conduction of this activity is more probable because it follows on the heels of Apollo and completes that mission by providing the answers to justify the lunar conquest. The lunar base scientific activities cannot proceed unless sufficient justification is advanced during the exploration. Thus, the scientific period of lunar operation provides a poor reference for design and analysis of the space transport system because of the lesser certainty on its need, timing and requirements. It is better if the electrical propulsion system is justified as sound on the basis of the lunar exploration activity, and it is then available for growth into more advanced lunar operations.

The performance data in Figure 3-2, Figure 3-4, and Table 3-2 can be utilized to determine the range of lunar expeditions possible using the operational approach shown in Figure 3-6. As presented above the use of two Saturn V's can provide ten men plus 15 tons of supplies to the lunar surface, wherein one Saturn V transports the lunar landing stage to lunar orbit by means of electrical propulsion, and the second Saturn V provides the crew in a fast trip using chemical rocket propulsion. For ten men, the 15 tons of supplies is sufficient for a five week expedition, according to Figure 3-2. By decreasing the number of men, more supplies can be carried and the lunar staytime can rapidly be increased. This tradeoff is shown in Figure 3-12. A datum point of interest is the six-man, six-month expedition, which can be accomplished by two Saturn V's. The provision of a second Saturn V with electrical propulsion increases the staytime of the ten-men expedition to one-year as shown on a second curve in Figure 3-12, which is another datum point of interest. Performance for other combinations of electrical propulsion and chemical propulsion transports are shown. A third expedition of interest is the 18-man, 18-month expedition requiring a total of five Saturn V's. This represents a very ambitious expedition and should be capable of enormous scientific achievement.

The comparison of the mixed electrical and chemical propulsion approach with the all-chemical propulsion approach is shown in Figure 3-13. The all-chemical propulsion approach is shown to require approximately double the number of Saturn V boosters. This difference in boosters should represent a 50 percent cost reduction per expedition using the

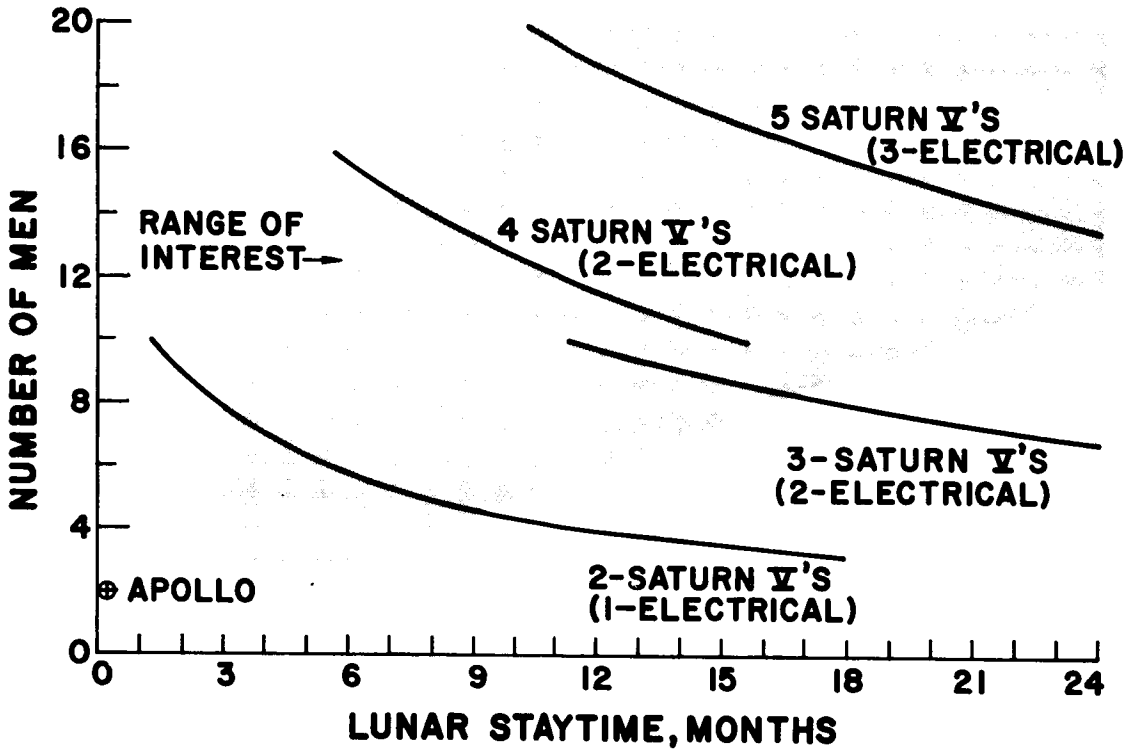

Figure 3-12. Requirements for Lunar Expedition with Electrical Propulsion

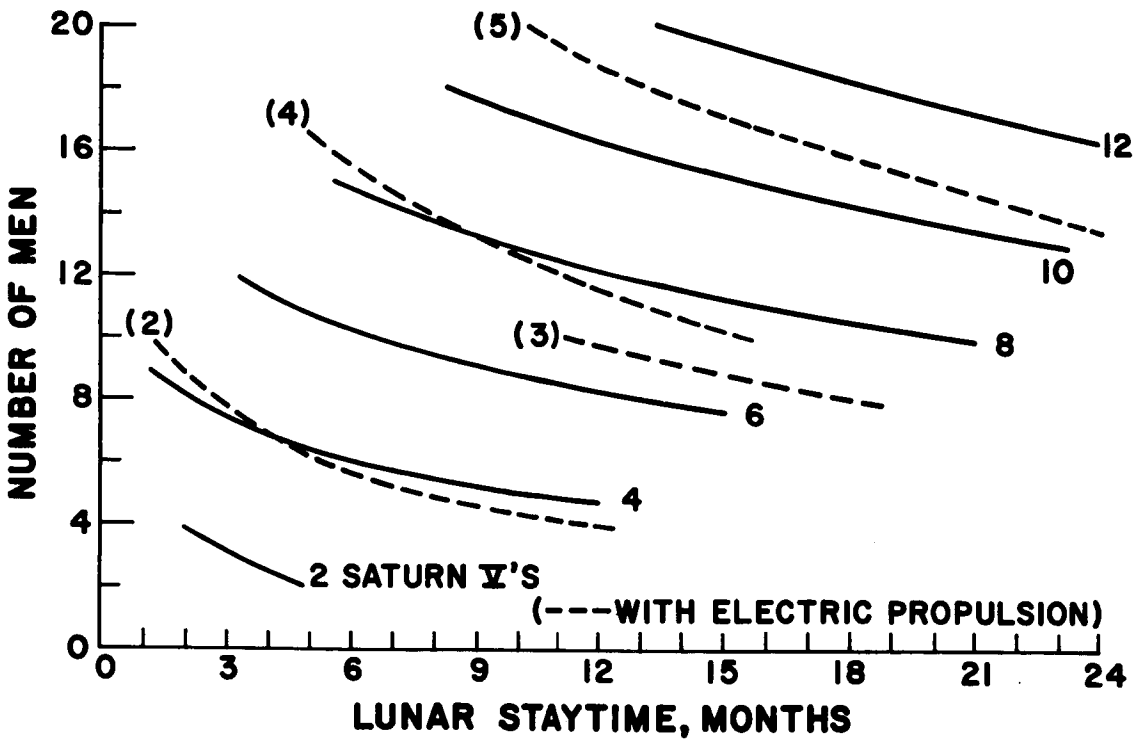

Figure 3-13. Requirements for Lunar Expedition Using Three-Man Apollo Type System

electrical propulsion system. An additional advantage is the simplification of the launching operation wherein the launching of the unmanned electrical propulsion space vehicles precedes the manned chemical rocket space vehicle by four to six months.

In the case of the ten-man semi-permanent scientific base, the cumulative number of Saturn V boosters required to transport both equipment and personnel is shown in Figure 3-14 as a function of the base life. Results are presented for both chemical rocket and electrical propulsion systems and for six-month and twelve-month crew rotation periods using the range of equipment requirements described in Figure 3-3. Again, a substantial advantage is shown for electrical propulsion. Also, the crew duty period is shown to have almost as much influence as the spread in equipment mass estimates to construct and support the base.

The inverse relationship of the data in Figure 3-14 is the level of lunar activity that can be supported by a designated Saturn V launch rate. These results are presented in Figure 3-15. The base size ranges between six and twenty men for a six-Saturn V-per-year launch rate. A launch rate of ten Saturn V vehicles per year could support thirty men on the lunar surface at a transportation cost of one billion dollars per year, assuming the Saturn V vehicle cost is under $100,000,000. The total cargo for thirty men over a decade is between 1500 and 2700 tons.

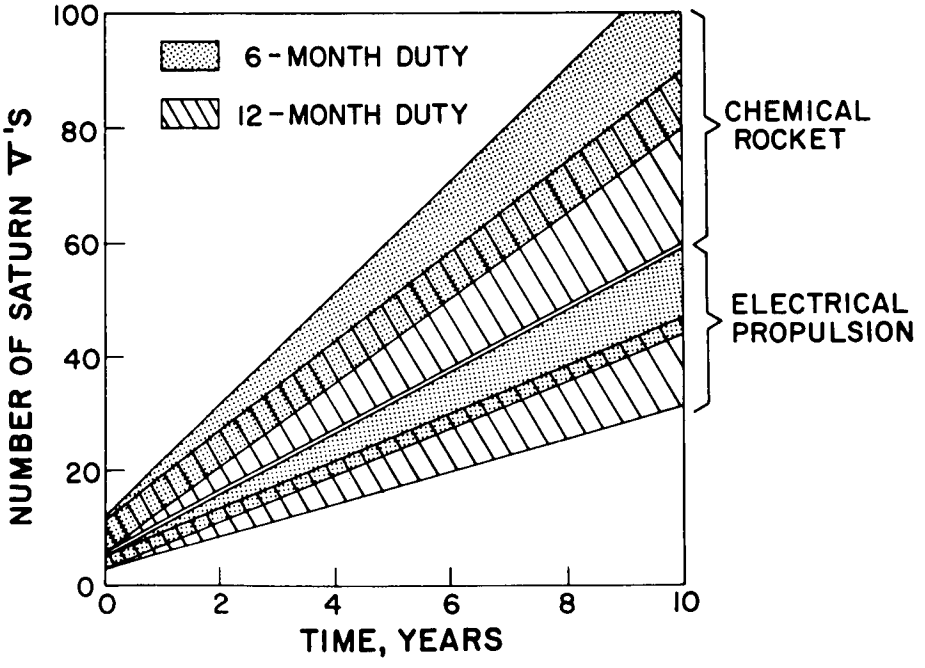

Figure 3-14. Booster Requirements for Ten-Man Lunar Base

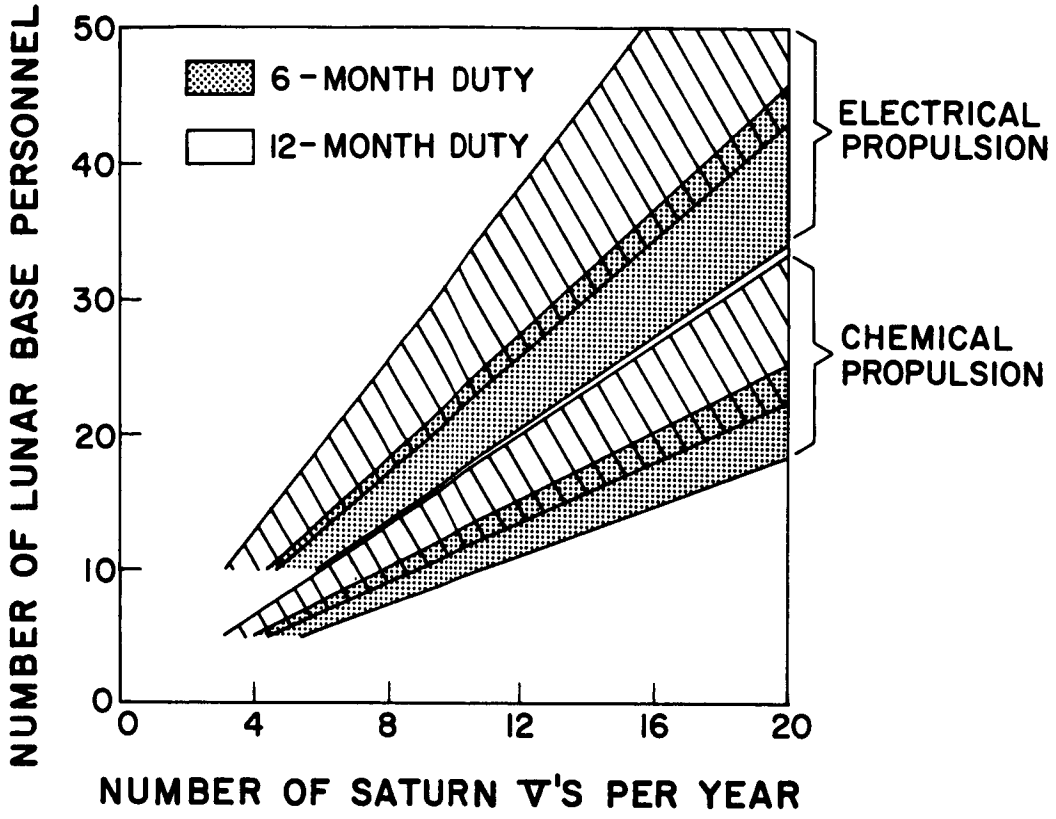

Figure 3-15. Lunar Base Size vs. Booster Launch Rate

The size of lunar landing craft transported from earth orbit to lunar orbit is limited on the small side by economic considerations as shown previously, and on the large side by acceptable trip time and power supply life rating. An optimization study conducted for the electrical propulsion system using ion jet thrustors yielded the performance curves in Figure 3-16, which shows the cost index as a function of trip time for various cumulative cargo requirements. In this graph the development cost and mission failures are included in the cost index calculation. The details used in this study are presented in Appendix B. The powerplant is assumed at 10 kg/KWe, which corresponds closely to the potential of the SNAP-50 type system.

Similar performance is shown in Figure 3-17 for the hybrid arc jet. Little difference is noticed between Figures 3-16 and 3-17 at the long trip times, where the cost index is economically attractive. Increasing cargo requirement improves the advantage of electrical propulsion. However, most of the advantage has been realized by 2000 tons.

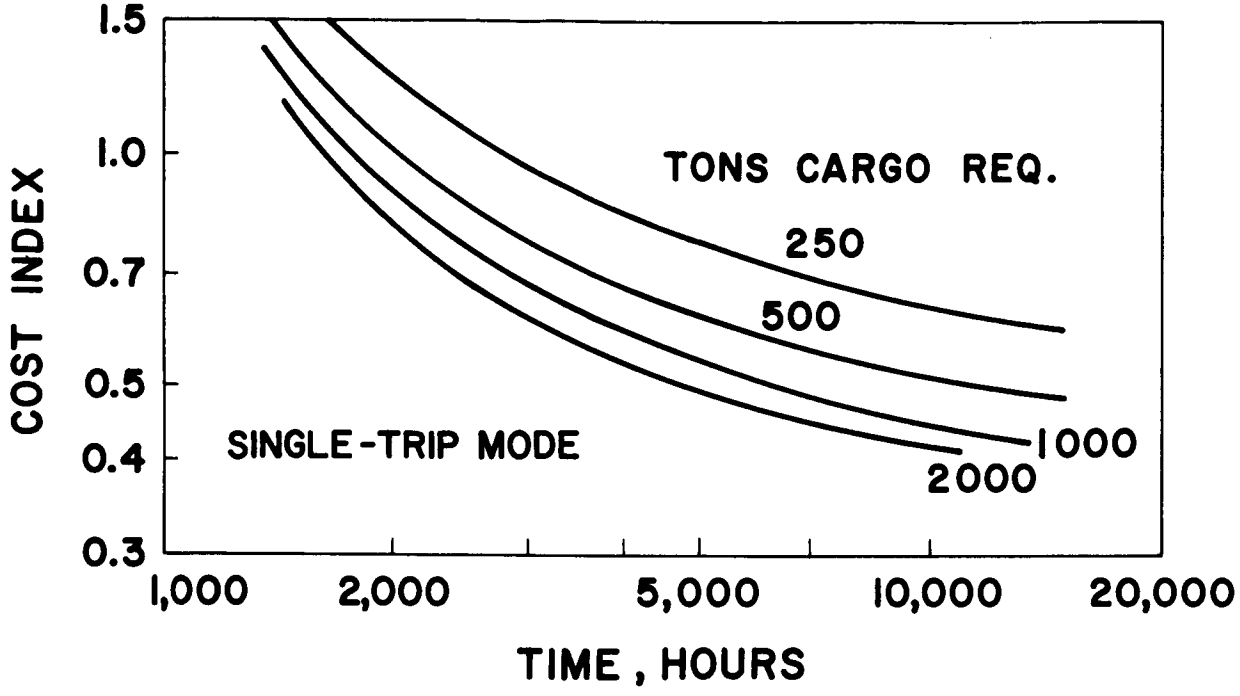

Figure 3-16. Trip Time Variation with Cumulative Lunar Cargo Requirement with Ion-Jet Lunar Cargo Thrustor

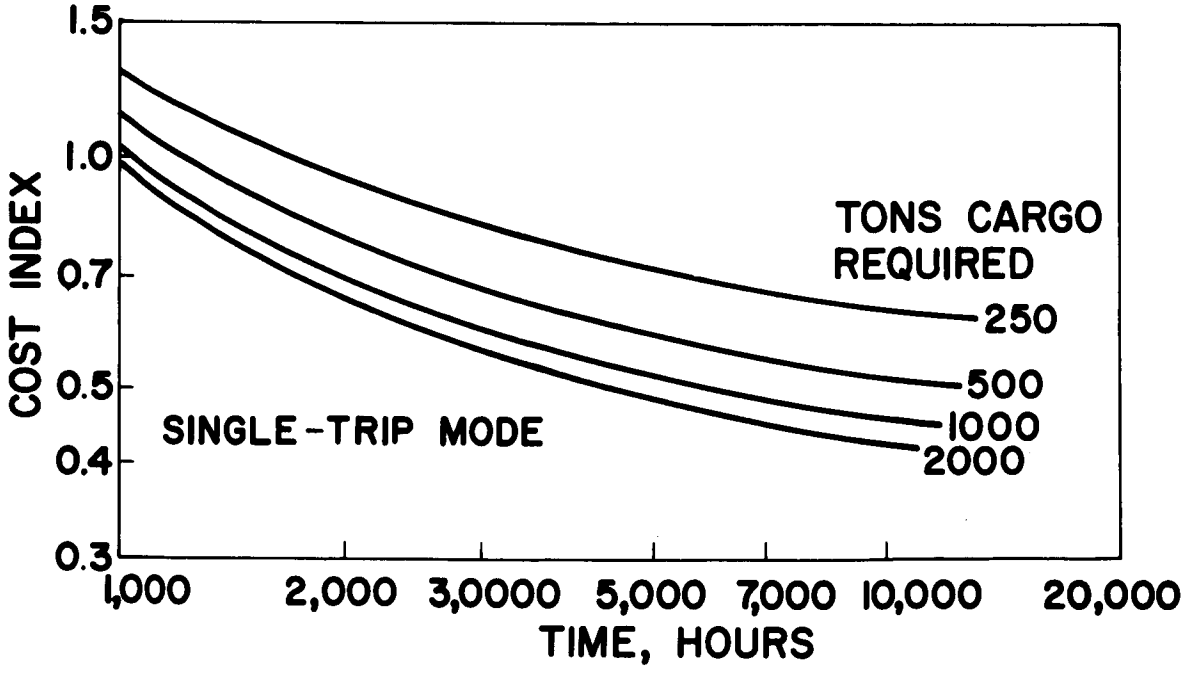

Figure 3-17. Trip Time Variation with Cumulative Lunar Cargo Requirement with Hybrid Arc Jet

Cross plots of Figures 3-16 and 3-17 are presented in Figures 3-18 and 3-19. From these curves the advantage of long trip times is quite apparent. A goal of a four-to six-month trip time system is desirable to obtain a good economic advantage. Trip times greater than six months may be undesirable from the viewpoint of mission operations. The four to six month trip is also advantageous from the power supply development.

The influence of booster cost on economics of electrical propulsion is shown in Figure 3-20. A Saturn V booster cost in excess of $100,000,000 provides a clear advantage to electrical propulsion. A booster cost below $50,000,000 tends to make electrical propulsion system rather sensitive to booster cost, within the assumptions used for generation of these curves.

The variation of cost index with development cost of the nuclear power supply and electrical propulsion systems is presented in Figure 3-21. This item, development cost, has the effect of increasing proportionally the crossover point of cumulative lunar cargo necessary to amortize the development.

The potential of reducing logistic costs for support of lunar operations using electrical propulsion appears very promising. The boundary values for use in a detailed optimization study need more intensive study. Once these bounds are defined the electrical propulsion system optimization can proceed in a methodical manner. Principal considerations are tonnage to be delivered and indirect participation in personnel transportation. The personnel represent a transport task of equal magnitude to the cargo. From this very preliminary study a lunar equivalent (including men plus supplies) cargo requirement of 2000 metric tons appear to be a reasonable goal of the logistics requirement.

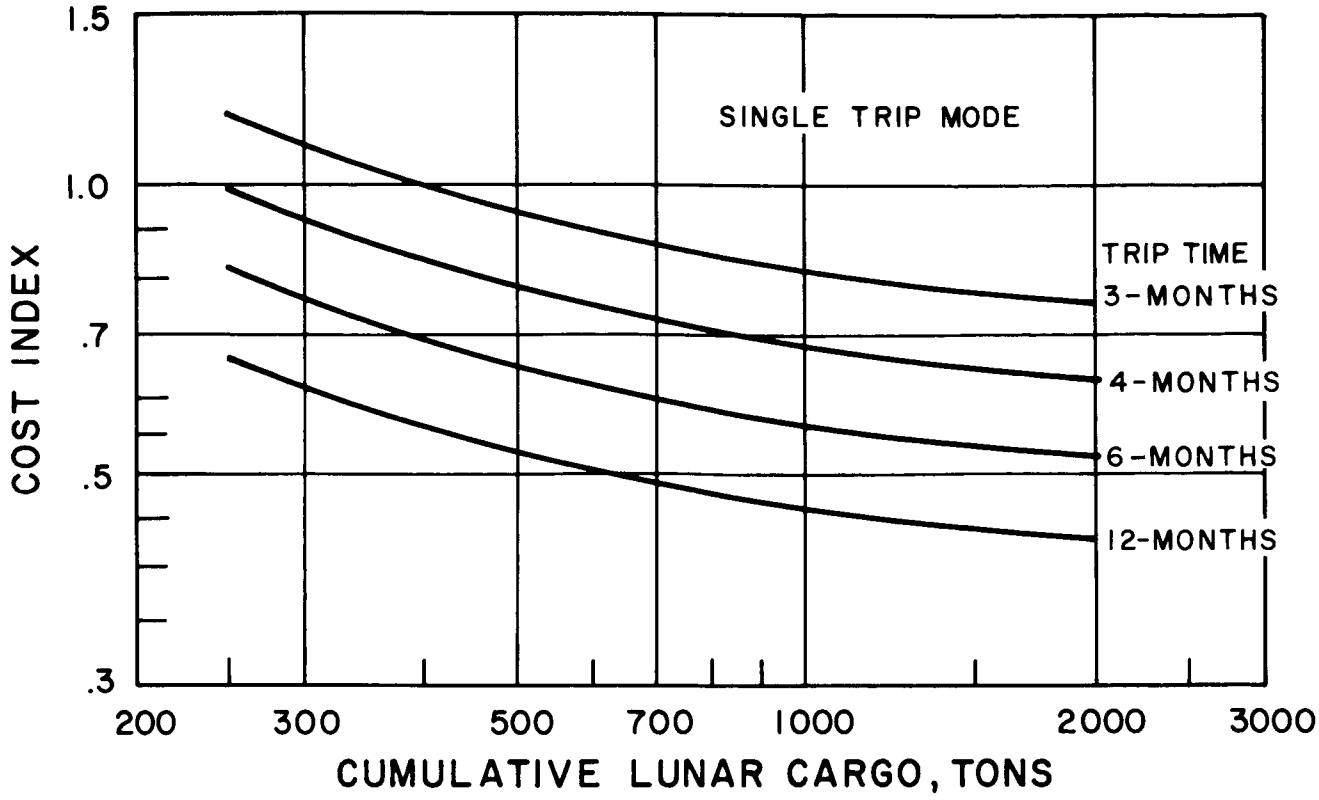

Figure 3-18. Cumulative Lunar Cargo Variation with Trip-Time Requirement with Ion-Jet Thrustor

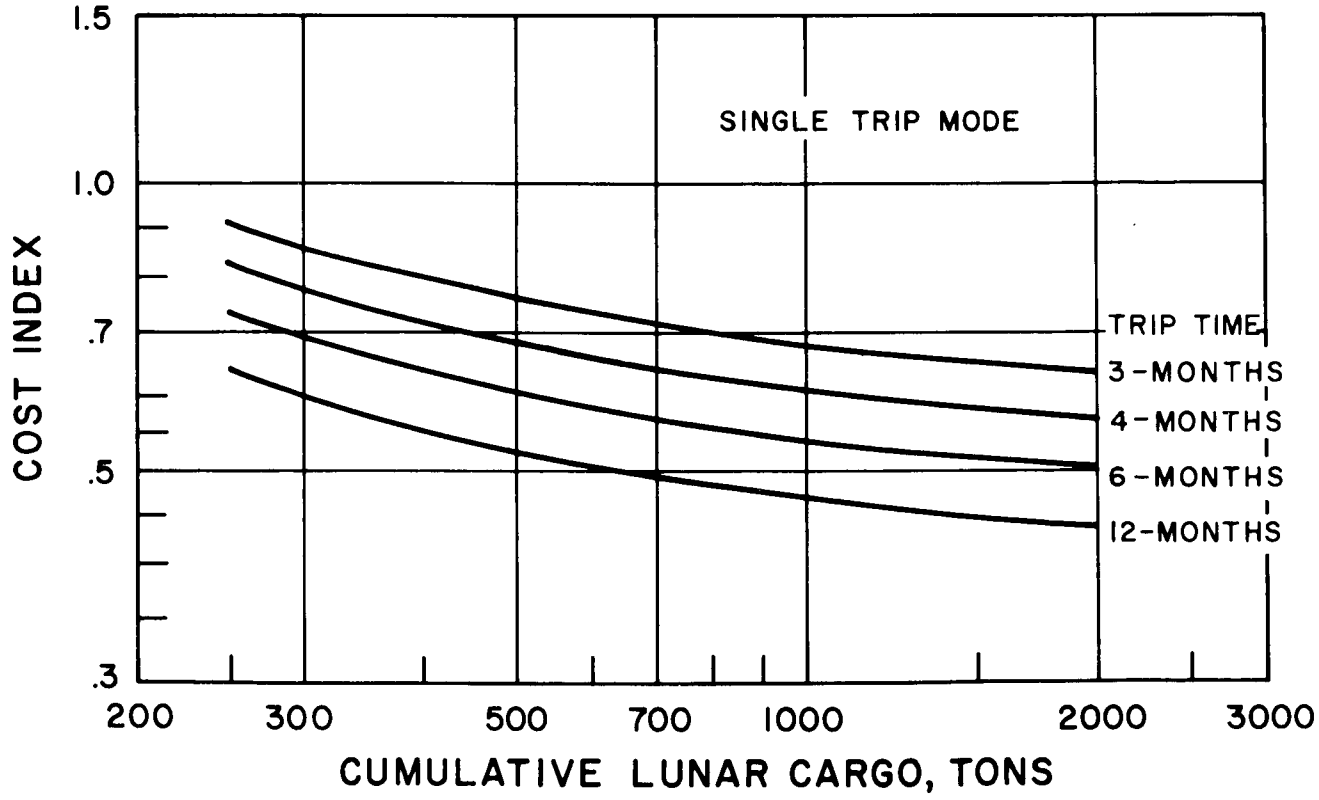

Figure 3-19. Cumulative Lunar Cargo Variation with Trip- Time Requirement with Hybrid Arc-Jet

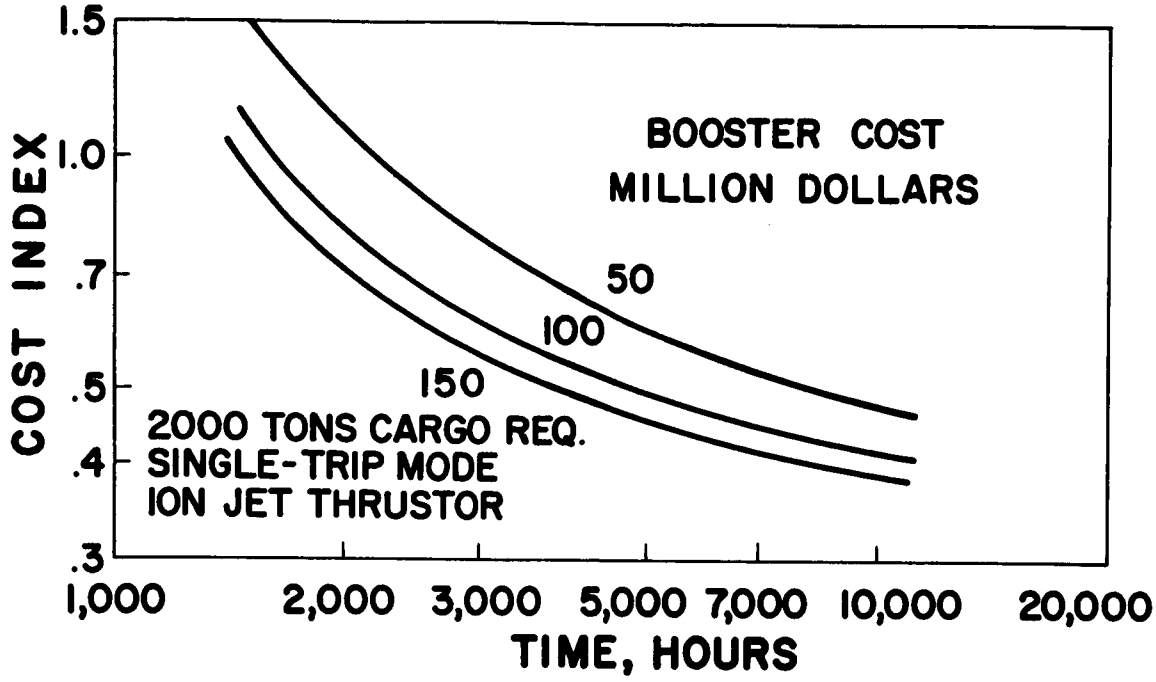

Figure 3-20. Trip Time Variation with Booster Cost

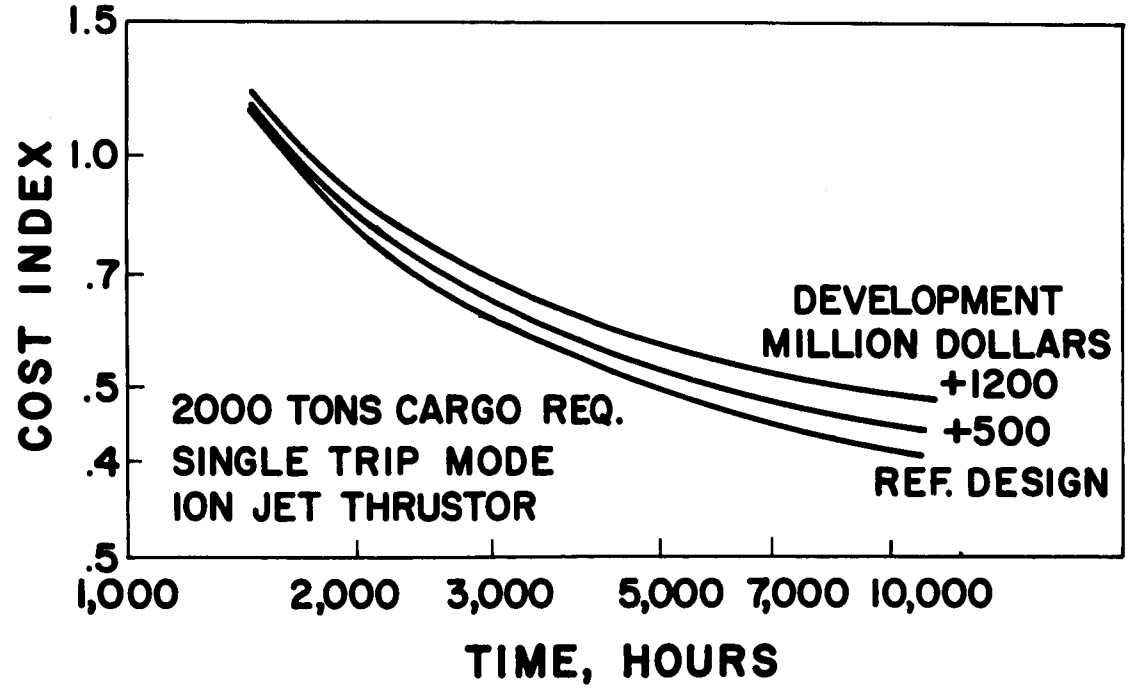

Figure 3-21. Trip Time Variation with Development Cost

SECTION 4
TRAJECTORY ANALYSIS

The earth-moon orbit-to-orbit transfer problem has been analyzed by considering the individual two-body problems of earth-vehicle and moon-vehicle trajectory characteristics and by patching the two together at an earth-moon transition point. The results of these individual studies were used to develop an empirical model of the overall earth-moon transfer problem as a function of pertinent propulsion system and geometric parameters. The multi-variable LEADER optimization process was then used to identify the functional variation of the optimum transfer propulsion requirements.

A. EARTH DEPARTURE TRAJECTORY

The two-body two-dimensional equations of motion of the Earth departure trajectory can be written in terms of the instantaneous orbit elements as:

$$\frac{dP}{dt} = \frac{2\,RT}{V_o} \tag{1}$$

$$\frac{de}{dt} = \frac{S \sin v + T\,(\cos E + \cos v)}{V_o} \tag{2}$$

$$\frac{dv}{dt} = \frac{PVo}{R^2} + \left[\frac{S \cos v - T \sin v\,(1 + \frac{R}{P})}{e\,V_o}\right] \tag{3}$$

The notation is illustrated in Figure 4-1. The results of trajectory calculations derived from numerical integration of equations (1) through (3) indicate that a transverse thrust orientation (S=O) results in Earth departure propulsion requirements which are within a few percent of the optimum. The trajectory results also indicate that the true anomaly (v) is an extremely slowly varying parameter. The preceding equations can, therefore, be simplified by the following assumptions:

$$\frac{dv}{dt} = 0 \tag{4}$$

$$S = 0 \tag{5}$$

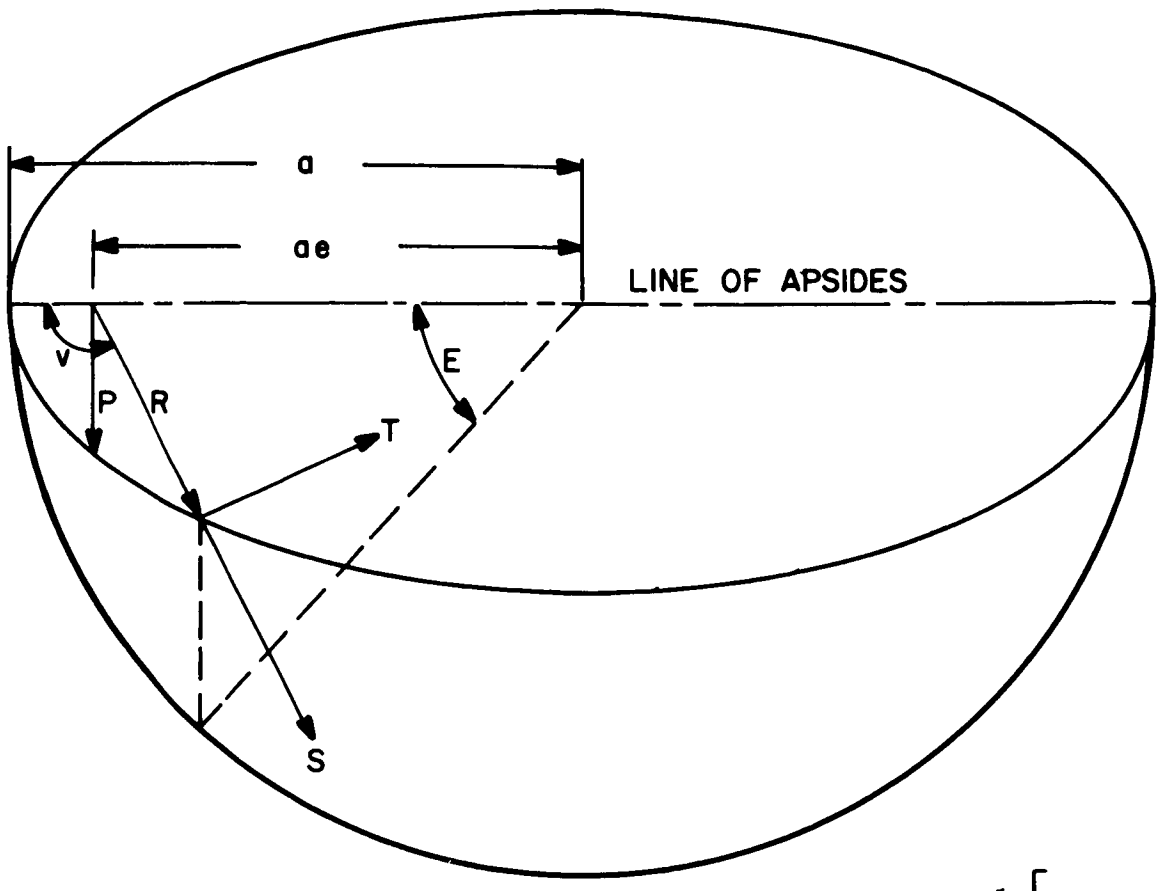

Orbit Radius, R

Semi-Major Axis, a

Orbit Eccentricity, e

True Anomaly, v

Orbit Parameter, $P = R(1+e \cos v)$

Eccentric Anomaly, $E = \cos^{-1}\left[R(e+\cos v)/P\right]$

Gravitational Constant, GM

Circular Velocity, $V_o = \sqrt{GM/P}$

Radial component of Acceleration, S

Transverse Component of Acceleration, T

Figure 4-1. Orbit Geometry and Nomenclature

Equations (3), (4), and (5) can then be combined and rearranged to produce:

$$Z = \frac{P^2 T}{GM} = \frac{e\,(1 + e \cos v)^3}{\sin v\,(2 + e \cos v)} \tag{6}$$

Equation (6) can then be differentiated with respect to time to obtain:

$$\frac{dP}{de} = \frac{(2 + 8\ e \cos v + 3e^2 \cos^2 v)(P)}{(1+e \cos v)\ (2 + e \cos v)\ 2e} \tag{7}$$

A second equation for $\frac{dP}{de}$ can be obtained by combining equations (1), (2), (4), and (5):

$$\frac{dP}{de} = \frac{2R}{\cos E + \cos v} = \frac{2P}{e + 2\cos v + e\cos^2 v} \tag{8}$$

Equations (7) and (8) can then be combined to obtain:

$$\cos^2 v\,(3\cos^2 v - 1)\,e^3 + 2\cos v\,(7\cos^2 v - 2)\,e^2 + 6\,(3\cos^2 v - 1)\,e + 4\cos v = 0 \tag{9}$$

The results of a numerical evaluation of equations (6) and (9) are illustrated in Figure 4-2. These data can be represented empirically by the following equations:

$$\begin{aligned} e &= 1.5\,\mathbb{Z} \text{ for } \mathbb{Z} < .3 \\ &= \sqrt{.7\mathbb{Z} - .05} \text{ for } \mathbb{Z} > .3 \end{aligned} \tag{10}$$

$$e\cos v = .51533\,\mathbb{Z} - .14133\,\mathbb{Z}^2 \tag{11}$$

Equation (1) can now be rewritten as:

$$\int \frac{(1 + e\cos v)\,dP}{2\,P^{1.5}} = \frac{T\,dt}{\sqrt{GM}} \tag{12}$$

Equations (6) and (11) can then be combined to give:

$$e\cos v = 0.51533\,\frac{P^2 T}{GM} - 0.14133\,\frac{P^4 T^2}{(GM)^2} \tag{13}$$

The instantaneous acceleration can then be written in terms of the initial acceleration and the thruster jet velocity:

$$T = \frac{T_o}{1 - T_o(t/V_j)} \tag{14}$$

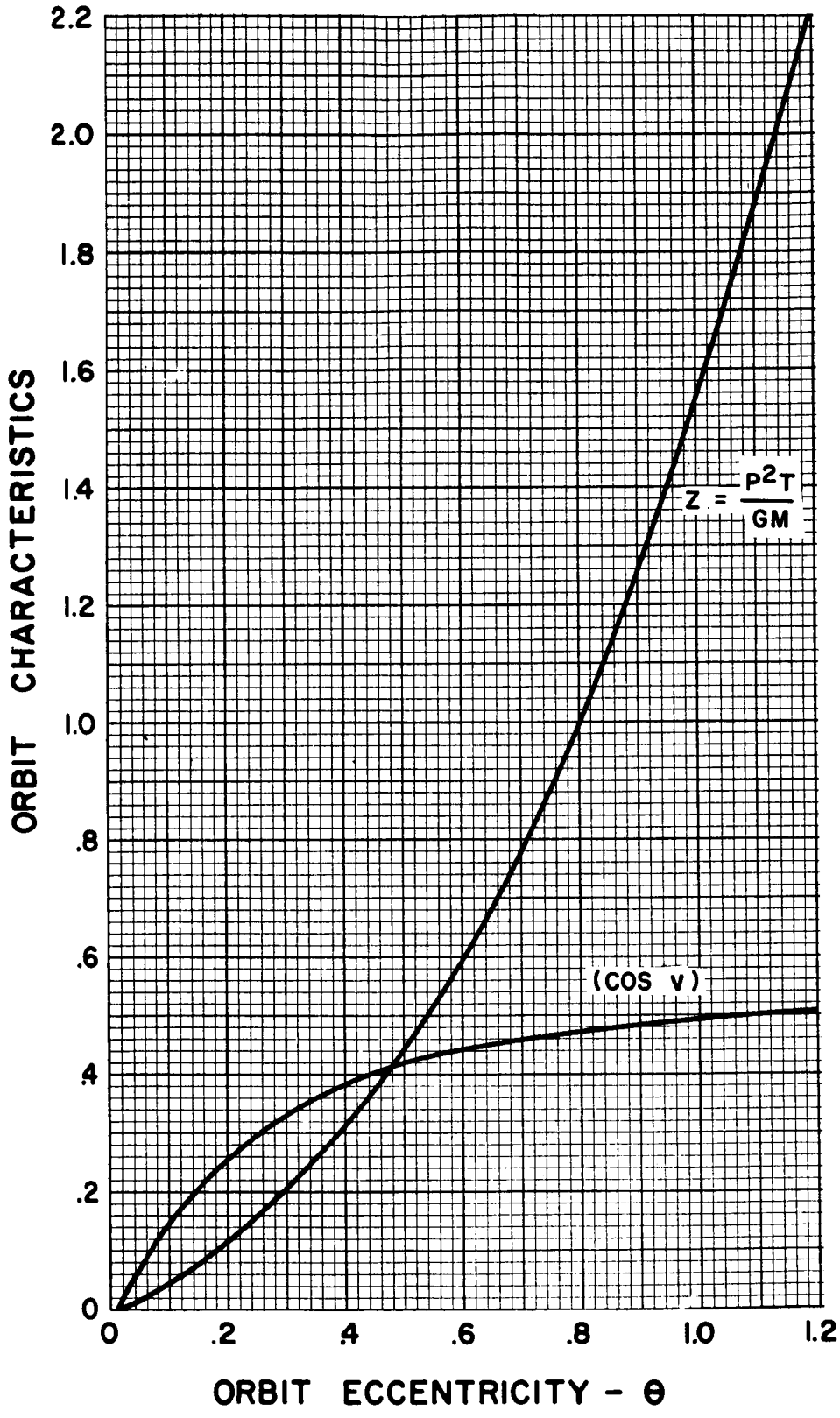

Figure 4-2. Low Acceleration Orbit Characteristics with Transverse Thrust

Equations (12), (13), and (14) can then be combined to give:

$$\int \frac{T_o \, dt}{\sqrt{GM\,(1 - T_o\, t/V_j)}} = \int \frac{\left[1 + .51533 \frac{P^2 T}{GM} - .14133 \frac{P^4 T^2}{(GM)^2}\right] dP}{2\, P^{1.5}} \qquad (15)$$

Equation (15) can then be integrated if the accelerations on the right hand side of the equation are assumed to be constant at the initial value. The result is:

$$\Delta V = -V_j \ell_n \left[1 - \frac{T_o\, t}{V_j}\right] = V_o \left[1 - \frac{P_o}{P_f} (1 - .17178\, Z_f + .02019\, Z_f^2)\right] \qquad (16)$$

Equations (6), (10), and (16) can then be used to determine the characteristics of an Earth departure orbit as a function of the initial propulsion parameters and the magnitude of the propulsion effort measured in terms of characteristic velocity.

Figures 4-3 and 4-4 illustrate the differences between the actual Earth departure orbital characteristics obtained from a numerical integration of the equations of motion and the comparable data determined from the preceding empirical procedure. Figure 4-3 presents the variations in orbital eccentricity and characteristic velocity as a function of the orbit parameter - P. These data have been calculated for an initial 480 Km circular orbit, an initial $(10)^{-4}$ thrust-weight ratio, and a specific impulse of 5000 seconds and have been used to calculate orbital velocity characteristics at an assumed Earth-Moon transition point 340,000 Km from the Earth. Figure 4-4 contains the resulting variation in orbital velocity obtained from the equation:

$$V = \sqrt{GM \left[\frac{2}{R} - \frac{1 - e^2}{P}\right]} \qquad (17)$$

The Lunar orbit velocity is plotted as the vertical line at 1.24 Km/sec. The terminal electric propulsion requirements for converting the Lunar approach orbit to a low altitude circular orbit about the moon will be dependent upon the vector difference between the Earth departure and Lunar orbit velocities. The differences between the actual and empirical

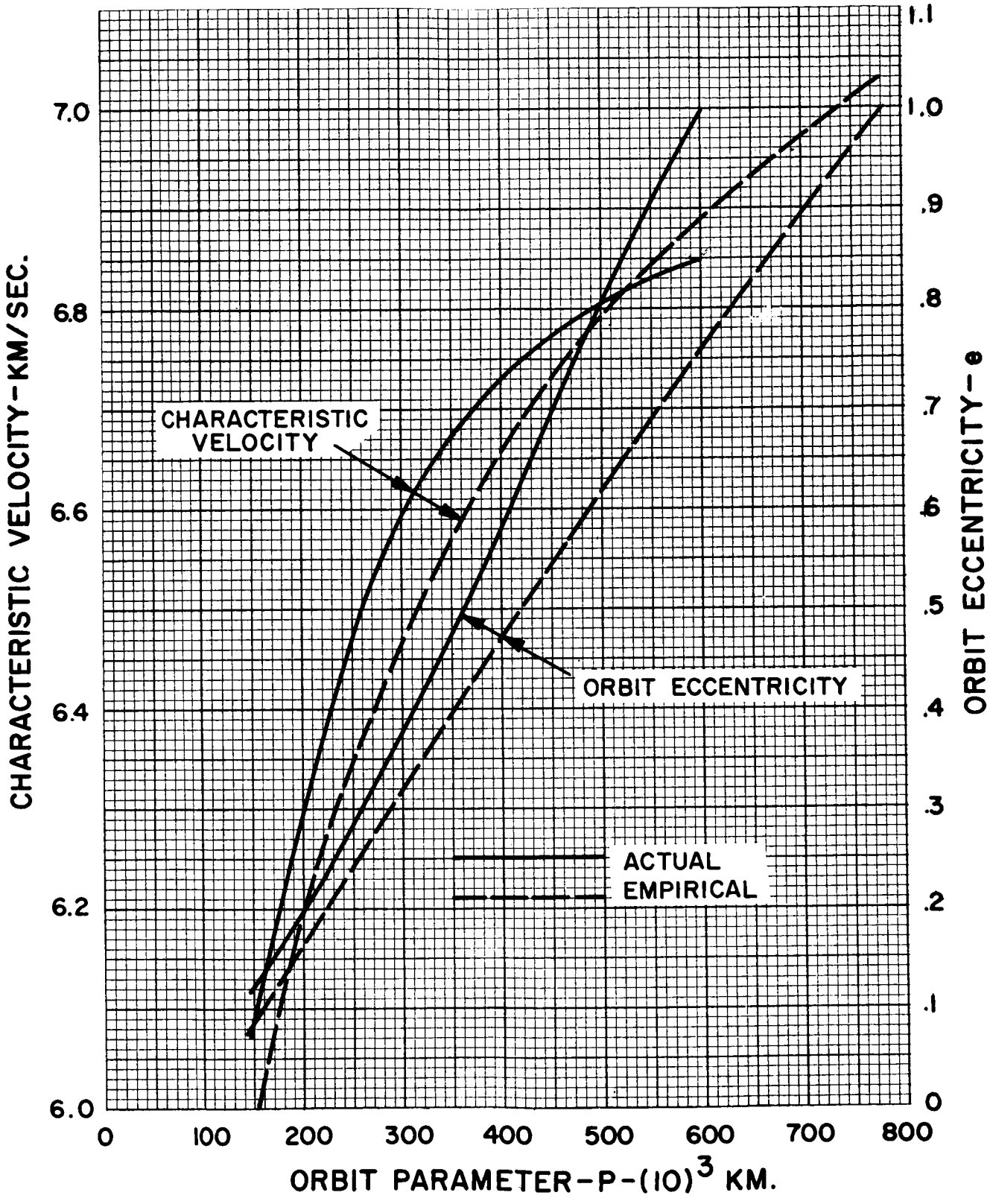

Figure 4-3. Earth Departure Trajectory Characteristics at 10^{-4} Thrust-Weight Ratio and 5000 Sec. Specific Impulse

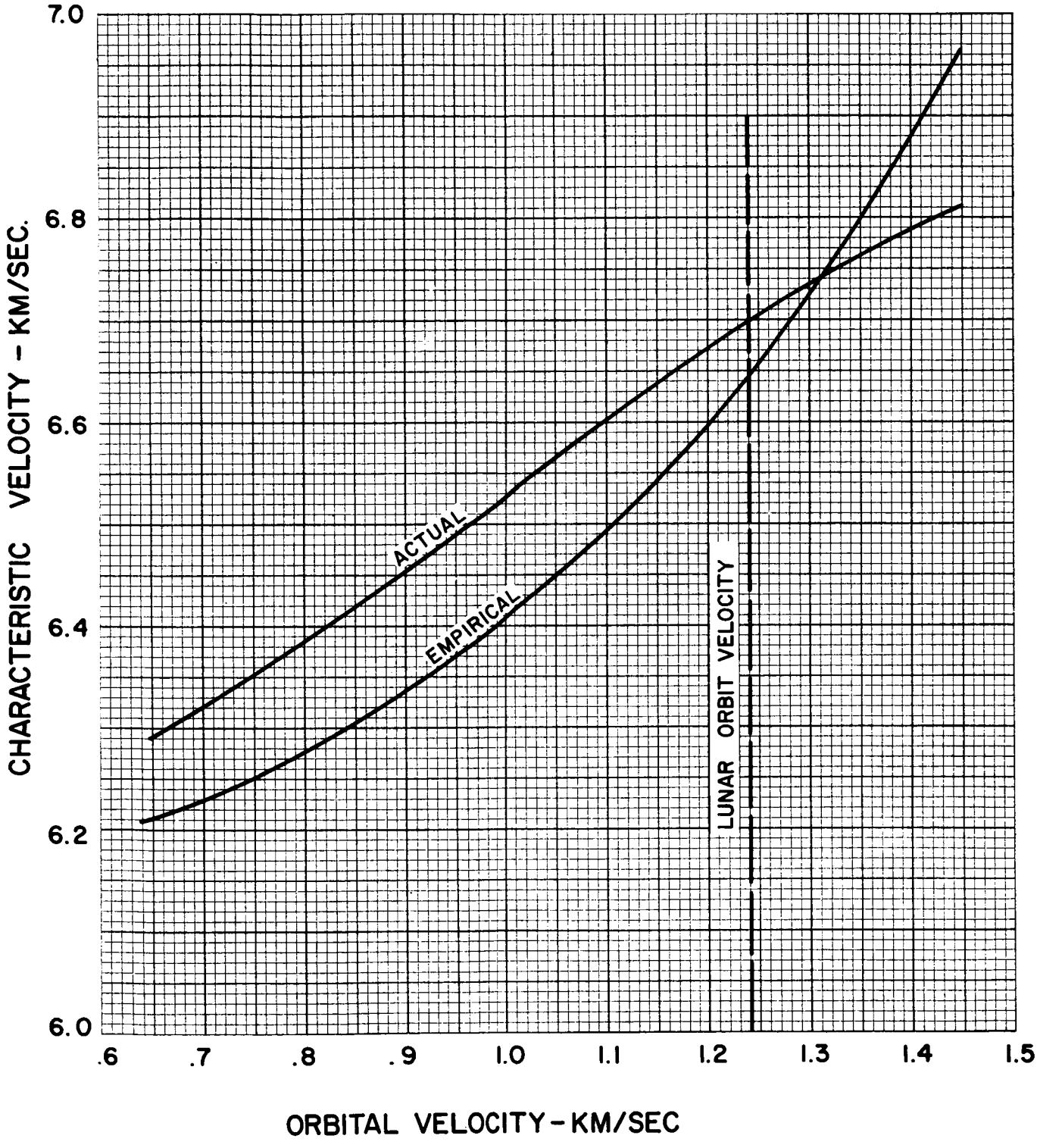

Figure 4-4. Orbital Velocity Characteristics at 340,000 Km, 10^{-4} Thrust-Weight Ratio and 5000 Sec. Specific Impulse

characteristics can be evaluated for a constant terminal propulsion requirement by entering Figure 4-4 at constant orbital velocity. The resulting difference in Earth departure characteristic velocity requirements are determined to be of the order of 1.5 percent. The preceding empirical analysis can, therefore, be concluded to introduce an error of 1.5 percent in the departure propulsion requirements.

B. EARTH-MOON TRANSITION

The third-body perturbation due to the action of the Moon on the Earth departure orbit will be the vector difference of the Lunar acceleration of the vehicle and the Lunar acceleration of the Earth:

$$a_{mp} = \frac{GM_m}{r^2} \rightarrow \frac{GM_m}{R_m^2} \tag{18}$$

Figure 4-5 defines the nomenclature used in this section. A three-body trajectory analysis could be conducted by performing a numerical integration of equations (1), (2), and (3) with the radial and transverse components of the above Lunar perturbation added to the thrust acceleration. Conversely, the error incurred by ignoring the Lunar perturbation can be minimized by terminating the Earth departure analysis at a point where the Lunar perturbation is less than the acceleration due to the Earth's central force:

$$a_{mp} < \frac{GM_e}{R^2} = a_e \tag{19}$$

Similarly, the third-body perturbation due to the action of the Earth on the subsequent Lunar approach trajectory will be the vector difference of the Earth's acceleration of the vehicle and the Earth's acceleration of the Moon:

$$a_{ep} = \frac{GM_e}{R^2} \rightarrow \frac{GM_e}{R_m^2} \tag{20}$$

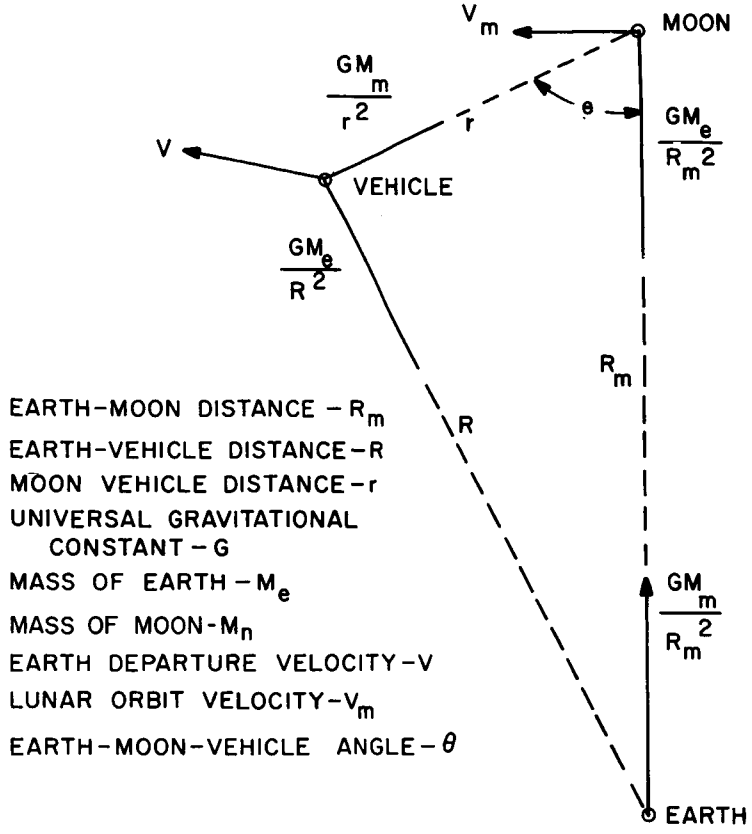

Figure 4-5. Earth-Moon Transition Geometry

The comparable third-body error is again minimized by initiating the Lunar approach analysis at a point where the Earth perturbation is less than the acceleration due to the Lunar central force:

$$a_{ep} < \frac{GM_m}{r^2} = a_m \tag{21}$$

The conditions prescribed by equations (19) and (21) can be imposed simultaneously by the use of an Earth-Moon transition point defined by the equation:

$$\frac{a_{mp}}{a_e} = \frac{a_{ep}}{a_m} \tag{22}$$

The Earth departure trajectory can be transformed into an equivalent Lunar approach trajectory at this transition point.

Equation (22) defines the radius of the Lunar sphere of influence. This equation has been analyzed by H.S. London* and shown to lead to the following relationship:

$$\left[\frac{M_m}{M_e}\right]^2 \sqrt{1 + \left(\frac{r}{R_m}\right)^4 - \frac{2Xr}{R_m^2}} = \left[\frac{r}{R}\right]^{-4} \sqrt{1 + \left(\frac{R}{R_m}\right)^4 - 2\left(1 - \frac{X}{R_m}\right)\left(\frac{R}{R_m}\right)} \tag{23}$$

where $X = r \cos \theta$. The law of cosines can be applied to the diagram of Figure 4-5 to obtain:

$$\left(\frac{R}{R_m}\right) = \sqrt{1 - \frac{2X}{R_m} + \left(\frac{r}{R_m}\right)^2} \tag{24}$$

Equation (24) can then be expanded by binominal series to obtain:

$$\left(\frac{R}{R_m}\right) = 1 - \frac{X}{R_m} + \frac{r^2 - X^2}{2R_m^2} + \frac{X(r^2 + X^2)}{2R_m^3} \tag{25}$$

where terms of the order of $\left[\frac{r}{R_m}\right]^4$ have been ignored. Equations (24) and (25) can then be combined with equation (23) and the fourth and higher order terms ignored as before:

$$\left[\frac{r}{R_m}\right] = \left\{\frac{M_m}{M_e}\left[1 - 2\left(\frac{r}{R_m}\right)\cos\theta + \left(\frac{r}{R_m}\right)^2\right]\right\}^{.4} \left\{\frac{\left[1 - 2\left(\frac{r}{R_m}\right)^2 \cos\theta\right]}{\left[1 + 3\cos^2\theta - 2\left(\frac{r}{R_m}\right)\cos\theta\,(2 + \cos\theta)\right]}\right\}^{.1} \tag{26}$$

Figure 4-6 summarizes the results of a numerical evaluation of equation (26) indicating that the radius of the sphere of influence varies between 13.6 percent and 17.4 percent of the Earth-Moon distance. The data of Figure 4-6 have been represented empirically in order to avoid the need for subsequent iterative solutions of equation (26)

$$\left[\frac{r}{R_m}\right] = 1.358\ (10)^{-1} - 9.7467\ (10)^{-6}\,\theta + 8.1274\ (10)^{-6}\,\theta^2 - 3.6426\ (10)^{-8}\,\theta^3 \tag{27}$$

*London, H.S. "A Study of Earth-Satellite to Moon-Satellite Transfer Using Non-Chemical Propulsion Systems", U.A.C. Report R-1383-1, East Hartford, 1959.

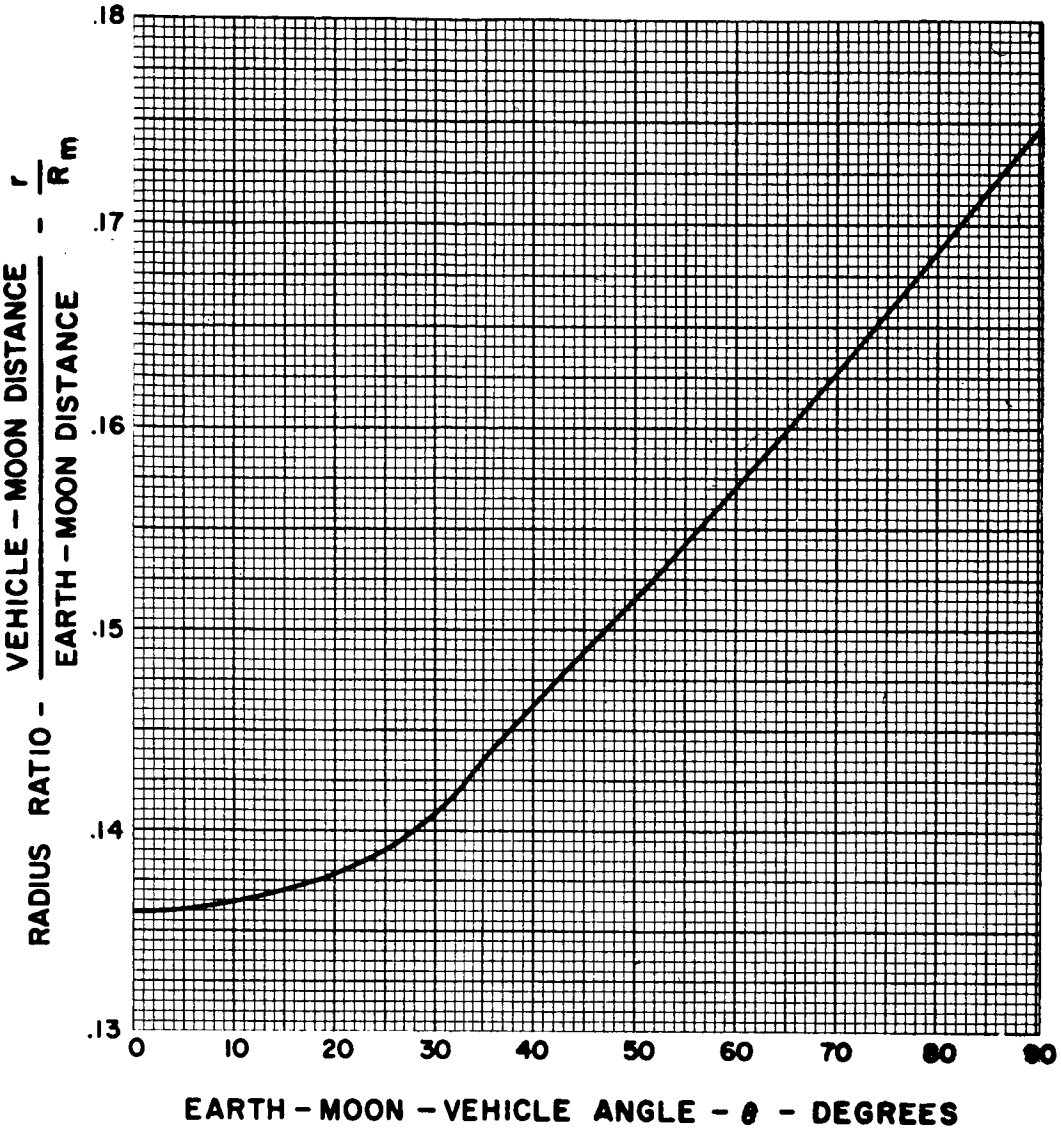

Figure 4-6. Lunar Sphere of Influence

The Earth departure trajectory can be transformed into an equivalent Lunar approach trajectory by the use of the following equations:

$$\bar{V} = V \rightarrow V_m \tag{28}$$

$$P = \frac{(\bar{V} \times r)^2}{GM_m} \tag{29}$$

$$e = 1 - \frac{2P}{r} + \frac{P\bar{V}^2}{GM_m} \tag{30}$$

$$v = \cos^{-1} \frac{1}{e} \left(\frac{P}{r-1} \right) \tag{31}$$

C. LUNAR APPROACH TRAJECTORY

The basic characteristics of the Lunar approach trajectory are similar to the Earth departure trajectory. The principal difference lies in the use of an initial highly elliptical or hyperbolic approach orbit and a terminal low altitude circular orbit instead of the reverse situation. The empirical procedures described in section 4.A can, therefore, be adapted to the Lunar approach case by the following:

$$\mathbb{Z}_o = \frac{e^2 + .05}{.7} \tag{32}$$

$$P_o = \sqrt{\frac{\mathbb{Z}_o \, GM_m}{T_o}} \tag{33}$$

$$V_f = \sqrt{\frac{GM_m}{P_f}} \tag{34}$$

$$\Delta V = V_f \left[1 - \sqrt{\frac{P_f}{P_o}} \quad (1 - .17178 \, \mathbb{Z}_o + .02019 \, \mathbb{Z}_o^2) \right] \tag{35}$$

Note that the subscript -o- refers to the initial state of the Lunar approach trajectory.

The initial Lunar orbit parameter -P_o- obtained from equation (33) represents the value required to achieve an optimum descent spiral to the desired low altitude orbit. It must, therefore, be identical with the corresponding value obtained from equation (29). This requirement imposes a constraint on the relationship between the Earth departure trajectory and the corresponding Earth-Moon-Vehicle angle. An iterative calculation has been avoided by the introduction of the arbitrary penalty function:

$$\Delta V_p = 2\sqrt{GM_m} \left| \sqrt{\frac{1}{P}} - \sqrt{\frac{1}{P_o}} \right| \tag{36}$$

The above penalty function is then added to the characteristic velocity of equation (35) and the total minimized. This serves to drive the penalty function to zero thereby forcing the orbit parameter from equation (29) to be identical with the optimum value obtained from equation (33).

D. TRAJECTORY MODEL

The results of the preceding sections have been combined in order to develop an overall empirical trajectory model that could be used in conjunction with the multi-variable LEADER optimization technique to determine the optimum low-acceleration Earth-Moon orbit-to-orbit propulsion requirements. The resulting trajectory model is summarized in Table 4-1.

The model contains four types of functions: parameters, independent variables, dependent variables, and the objective function. The parameters are maintained constant during each optimization run and, consequently, can be varied in discrete steps to generate a series of parametric studies. The parameter class, therefore, includes the initial thrust-weight ratio, specific impulse, initial Earth orbit altitude, and terminal Lunar orbit altitude. Program constants are also included in this class. The independent variable class includes the Earth departure orbit parameter, the Earth-Moon-Vehicle angle, and the Lunar true anomaly. Although starting values of each of these parameters are required to initialize an optimization calculation, the optimization process will determine the optimum values of these variables. The dependent variable class includes all of the trajectory variables required to define the objective function which is the parameter to be optimized. The trajectory model contains the ability to minimize any one of the following functions through the selection of the appropriate value of the switching function - B:

Earth Departure Characteristic Velocity (for Lunar Fly-by Trajectories)
Total Low Thrust Characteristic Velocity (for Lunar Orbiter Trajectories)
High Thrust Lunar Landing Characteristic Velocity

The optimization process is bounded by a series of constraints. The first six constraints are specified by the lower and upper bounds indicated for the three independent variables. Constraints 6 through 11 impose additional constraints upon the various dependent variables.

TABLE 4-1. LUNAR TRANSFER TRAJECTORY MODEL

Parameters

No.	Description	Symbol	Value	Units
P1	Initial Thrust-Weight Ratio	TWR		
P2	Specific Impulse	I_{sp}		seconds
P3	Sea Level Gravitational Constant	g_o	9.81235	m/sec^2
P4	Earth Gravitational Constant	GM_e	$3.98528(10)^{14}$	m^3/sec^2
P5	Lunar Gravitational Constant	GM_m	$4.90076(10)^{12}$	m^3/sec^2
P6	Initial Earth Orbital Radius	R_o	$6.855(10)^6$	meters
P7	Lunar Orbit Parameter	P_m	$3.83245(10)^8$	meters
P8	Lunar Orbit Eccentricity	e_m	.0549	
P9	Lunar Orbit Momentum	H_m	$3.90812(10)^{11}$	m^2/sec
P10	Terminal Orbit Radius	R_5	$1.770(10)^6$	meters
P11	Conversion Factor	A	$1.745329(10)^{-2}$	rad./deg.
P12	Conversion Factor	C	1.0	
P13	Switching Function	B	-1, 0, 1	
P14	Lunar Radius	R_6	$1.738(10)^6$	meters

Independent Variables

No.	Description	Bounds	
X1	Normalized Departure Orbit Parameter	0	1
X2	Normalized Orbit Angle	0	1
X3	Normalized Lunar True Anomaly	0	1

Dependent Variables

No.	Equation	Description	Units
G1	$P = (1 + 2X1)\ 2(10)^8$	Departure Orbit Parameter	meters

TABLE 4-1. LUNAR TRANSFER TRAJECTORY MODEL (Cont'd)

No.	Equation	Description	Units
G2	$\theta = 90\ (2X2-1)$	Orbit Angle	degrees
G3	$\phi_m = 180\ (2X3-1)$	Lunar True Anomaly	degrees
G4	$a_o - (TWR)\ g_o$	Initial Acceleration	m/sec^2
G5	$V_j = g_o\ I_{sp}$	Jet Velocity	m/sec
G6	$Z_1 = a_o\ P_1^2/GM_e$	Escape Parameter	
G7	$V_o = \sqrt{GM_e/R_o}$	Earth Orbital Velocity	m/sec
G8	$\Delta V_e = V_o \left[1 - \sqrt{\frac{R_o}{P_1}}\ (1 - .17178Z_1 + .02019Z^2)\right]$	Departure Char. Vel.	m/sec
G9	$a_4 = a_o \exp^{\Delta V_e/V_j}$	Capture Acceleration	m/sec^2
G10	$R_m = \frac{P_m}{1 + e_m \cos\ (A\ \phi_m)}$	Earth-Moon Distance	meters
G11	$R_3 = R_m \left[.1358 - 9.7467(10)^{-6}\theta + 8.1274(10)^{-6}\ \theta^2 - 3.6426(10)^{-8}\ \theta^3\right]$	Lunar Transition Radius	meters
G12	$R_2 = \left[R_m^2 + R_3^2 - 2\ R_m R_3 \cos\ (A\theta)\right]^{1/2}$	Earth Transition Radius	meters
G13	$e_2 = \sqrt{.7Z_1 - .05}$	Departure Eccentricity	

TABLE 4-1. LUNAR TRANSFER TRAJECTORY MODEL (Cont'd)

No.	Equation	Description	Units
G14	$\cos \phi_2 = \frac{1}{e_2}\left[\frac{P_1}{R_2} - 1\right]$	Departure True Anomaly	
G15	$\sin \phi_2 = \sqrt{1 - \cos^2 \phi_2}$		
G16	$H_2 = \sqrt{P_1 \, GM_e}$	Departure Momentum	
G17	$V_{t2} = \frac{H_2}{R_2}$	Departure Transverse Vel.	m/sec
G18	$V_{r2} = H_2 e_2 \sin \phi_2 / P_1$	Departure Radial Vel.	m/sec
G19	$V_{tm} = H_m / R_m$	Lunar Transverse Vel.	m/sec
G20	$V_{rm} = H_m \, e_m \sin (A \, \phi_m) / P_m$	Lunar Radial Vel.	m/sec
G21	$V_{t3} = V_{r2} \sin \alpha - V_{t2} \cos \alpha + V_{rm} \sin \theta - V_{tm} \cos \theta$	Approach Transverse Vel.	m/sec
G22	$V_{r3} = V_{r2} \cos \alpha + V_{t2} \sin \alpha + V_{rm} \cos \theta - V_{tm} \sin \theta$	Approach Radial Vel.	m/sec
G23	$H_3 = R_3 \, V_{t3}$	Approach Momentum	m/sec
G24	$P_3 = H_3^2 / GM_m$	Approach Orbiter Parameter	meters

TABLE 4-1. LUNAR TRANSFER TRAJECTORY MODEL (Cont'd)

No.	Equation	Description	Units
G25	$e_3 \cos \phi_3 = \frac{P_3}{R_3} - 1$		
G26	$e_3 \sin \phi_3 = P_3 \, V_{r3}/H_3$		
G27	$e_3 = \sqrt{(e_3 \sin \phi_3)^2 + (e_3 \cos \phi_3)^2}$	Approach Eccentricity	
G28	$R_{pl} = P_3/(1+e_3)$	Initial Perilune Radius	meters
G29	$e_t = \frac{R_{pl} - R_6}{R_{pl} + R_6}$	Landing Eccentricity	
G30	$P_t = (1-e_t) R_{pl}$	Landing Parameter	meters
G31	$\Delta V_{11} = \left[(1+e_3)\sqrt{\frac{GM_m}{P_3}} + 2_{et}\sqrt{\frac{GM_m}{P_t}} \right]$	Landing Char. Vel.	m/sec
G32	$Z_4 = \frac{e_3^2 + .05}{.7}$	Capture Parameter	
G33	$e_3 \cos \phi_4 = .51533 \, Z_4 - .14133 \, Z_4^2$		
G34	$R_4 = \frac{P_3}{1 + e_3 \cos \phi_4}$	Initial Capture Radius	meters
G35	$P_{30} = \frac{Z_4 \, GM_m}{a_4}$	Optimum Approach Par.	meters
G36	$V_5 = \sqrt{GM_m/R_5}$	Terminal Orbit Vel.	m/sec

TABLE 4-1. LUNAR TRANSFER TRAJECTORY MODEL (Cont'd)

No.	Equation	Description	Units
G37	$\Delta V_c = V_5 \left[1 - \sqrt{\frac{R_5}{P_{30}}} \left(1 - .17178 Z_4 + .02019 Z_4^2\right) \right]$	Capture Char. Vel.	m/sec
G38	$\Delta V_p = 2\sqrt{GM_m} \left[\sqrt{\frac{1}{P_3}} - \sqrt{\frac{1}{P_{30}}} \right]$	Penalty Function	m/sec
G39	$\Delta V_1 = \Delta V_c + \Delta V_p$	Corr. Capture Char. Vel.	m/sec
G40	$\sin \theta = \sin (A\theta)$		
G41	$\cos \theta = \cos (A\theta)$		
G42	$\sin \alpha = \frac{R_m \sin \theta}{R_2}$		
G43	$\cos \alpha = \frac{R_2^2 + R_3^2 - R_m^2}{2 R_2 R_3}$		

Objective Function

$$Y = -C \left[B^2 \Delta V_e + .5B (B+1) \Delta V_1 + (1-B^2) \Delta V_{11} \right]$$

Constraints

No.	Equation
7	$\left[\cos^2 \phi_2 - 1 \right] < 0$
8	$V_{r3} < 0$
9	$\left[R_6 - R_{p1} \right] < 0$
10	$\left[R_4 - R_3 \right] < 0$
11	$\left[P_3 - P_{30} \right] < 0$

Note that constraint 11 forces the penalty function (G38) to be positive and the optimization process drives it to zero. This approach eliminates the need to use the absolute magnitude of the penalty function as indicated in the previous section.

E. TRAJECTORY OPTIMIZATION RESULTS

The lunar trajectory model of Table 4-1 has been combined with the multiple-variable LEADER optimization technique* in order to investigate the characteristics and the requirements of optimum lunar transfer trajectories. These studies have considered the requirements for both lunar fly-by and lunar capture into a low altitude circular orbit. The effects of variations in initial thrust-weight ratio, specific impulse, and Earth-Moon distance have been examined.

Figure 4-7 illustrates the effects of Earth-Moon distance. The top curve contains the variation in Earth-Moon distance as a function of the Lunar orbit true anomaly. Note that the distance varies from 362,000 Km to 405,000 Km during the Moon's synodic period. The middle curve illustrates the variation in total low thrust characteristic velocity for establishing a terminal circular orbit about the moon at an altitude of 32 Km (20 miles). It includes both the Earth departure propulsion requirements and the terminal Lunar capture and descent propulsion requirements. The propulsion requirements are seen to minimize at a true anomaly of 50 degrees corresponding to an Earth-Moon distance of 370,000 Km and at a characteristic velocity of 7.86 Km/sec. The total variation is extremely small, however, and of the order of one percent. The bottom curve contains the comparable data for an optimum fly-by past the moon in which low thrust propulsion is used only for Earth departure. These data are quite similar to the orbiter requirements in that they minimize at a true anomaly of 50 degrees and indicate a total variation of one percent over the complete range of Earth-Moon distances.

Figure 4-8 illustrates the results of a comparable study of the effects of variations in initial thrust-weight ratio. These data have been based on the optimum true anomaly of 50 degrees. The top two curves contain the variation in low thrust characteristic velocity requirements for both the orbiter and fly-by modes of operation. These data have been investigated over a thrust-weight ratio range from $2.5(10)^{-5}$ to $4(10)^{-4}$ and illustrate a variation

* Brown, H., "Spacecraft Electric Generating and Propulsion System Integration Study," ASD-TDR-63-428, Cincinnati, 1963.

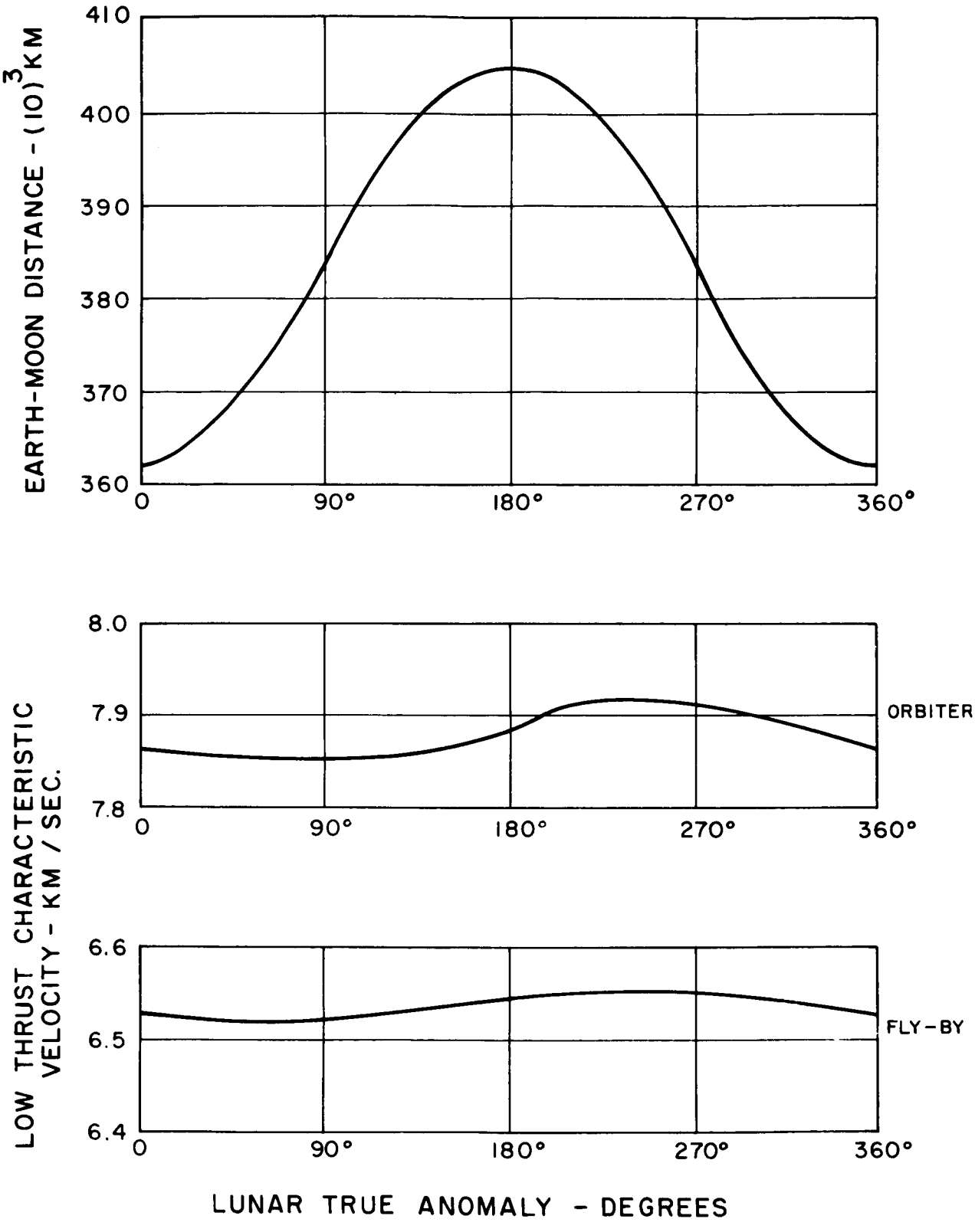

Figure 4-7. Effect of Earth-Moon Distance on Optimum Propulsion Requirements

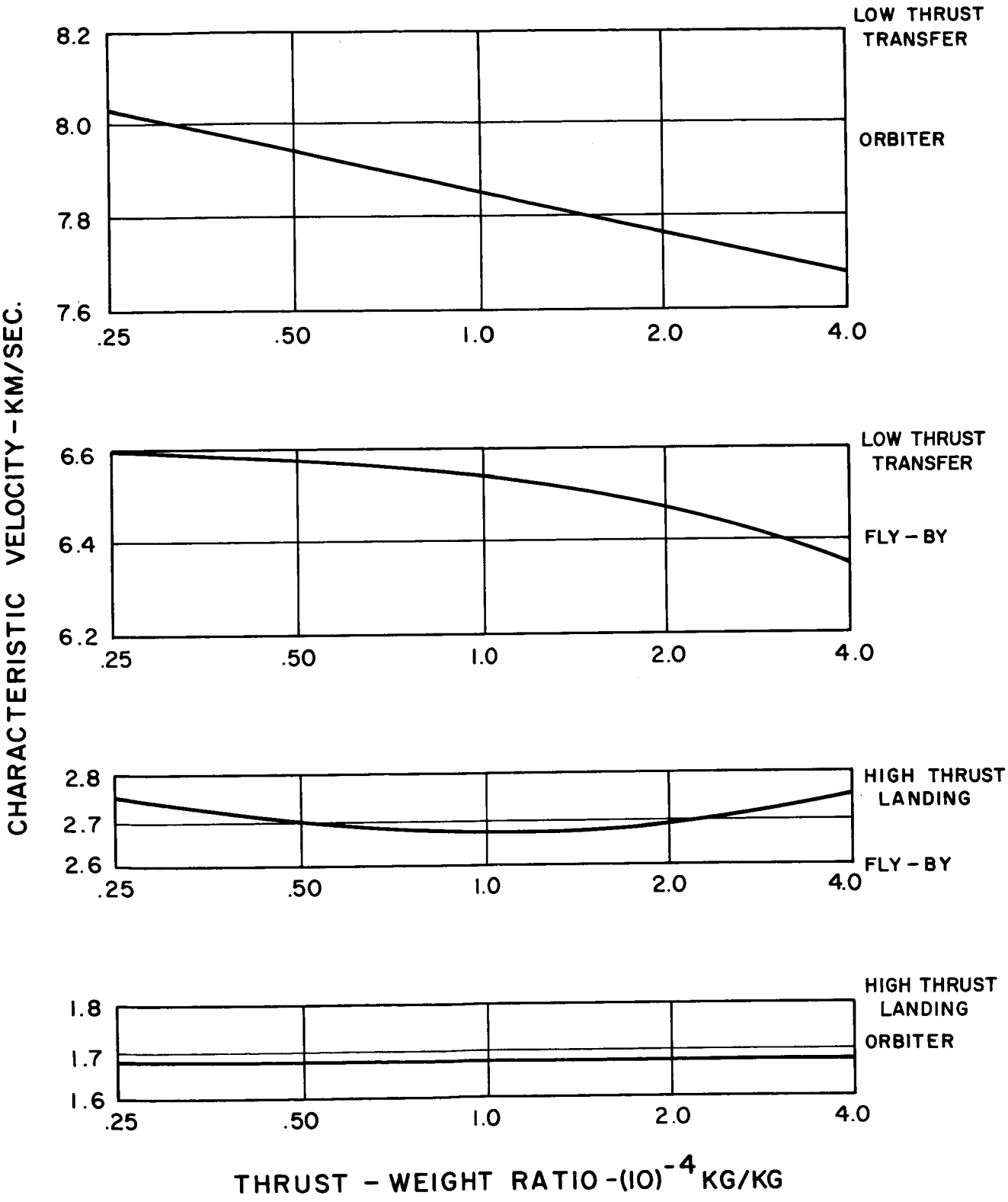

Figure 4-8. Effect of Thrust-Weight Ratio on Optimum Propulsion Requirements

of the order of 5 percent. The bottom two curves contain the corresponding variation in ideal high thrust characteristic velocity requirements for a terminal soft landing on the surface of the moon. These variations are seen to be of the order of 0 to 3 percent. Similar studies were conducted to determine the effects of variations in specific impulse over the range of 3000 seconds to 10,000 seconds. These variations were found to be an order of magnitude smaller than the above variations due to initial thrust-weight ratio.

As a result of the above investigations, it has been concluded that a constant characteristic velocity - independent of Earth-Moon distance, initial thrust-weight ratio, and specific impulse - is a reasonable assumption for this first round study of lunar ferry missions. Subsequent studies should, however, include the variations shown in Figures 4-7 and 4-8. These studies have, therefore, been based on an orbiter characteristic velocity of 7.85 Km/sec and a fly-by velocity of 6.54 Km/sec corresponding to a thrust-weight ratio of $(10)^{-4}$ and the optimum lunar true anomaly of 50^{o}.

Table 4-2 summarizes the basic characteristics of the nominal transfer trajectory obtained from the above optimization studies. The most significant features are the low orbit eccentricities associated with both the Earth departure and the lunar approach trajectories. These data were obtained for the orbiter mode of operation. The comparable optimum fly-by mission utilizes the identical Earth departure trajectory and characteristic velocity but does not use any low thrust lunar approach propulsion. This would, therefore, result in an elliptical fly-by past the moon at a closest approach altitude of 23,670 Km.

TABLE 4-2. NOMINAL TRANSFER TRAJECTORY CHARACTERISTICS

Earth Departure	Initial Circular Orbit Altitude	R_o	480	Km.
	Transfer Orbit Parameter	P_1	304,000	Km.
	Eccentricity	e_1	.342	
	Characteristic Velocity	ΔV_e	6.50	Km/sec.
Earth-Moon Transition	Lunar True Anomaly	v	50.8	degrees
	Earth-Moon Vehicle Angle	θ	52.8^o	degrees
	Earth-Moon Distance	R_m	370,000	Km.
	Earth-Vehicle Distance	R_2	336,000	Km.
	Moon-Vehicle Distance	R_3	61,600	Km.
	Geocentric Velocity-Vehicle	V_2	1.36	Km/sec.
	-Moon	V_m	1.38	Km/sec.
	Selenocentric Velocity-Vehicle	V_3	.24	Km/sec.
Lunar Approach	Approach Orbit Parameter	P_3	39,200	Km.
	Eccentricity	e_3	.443	
	Terminal Circular Orbit Altitude	R_5	32	Km.
	Characteristic Velocity	ΔV_c	1.35	Km/sec.
Total	Characteristic Velocity	ΔV	7.85	Km/sec.

SECTION 5
ELECTRICAL PROPULSION SYSTEM ANALYSIS

This section discusses the factors which provide bounds and establish a baseline for the parametric analysis of the electrically propelled lunar cargo vehicle. These considerations involve the spacecraft elements, such as nuclear-electric power supply, electrical propulsion system and lunar landing craft, and the operational modes, such as single-trip, multiple-trip ferry, and multiple-engine ferry. The constraints imposed by these items are state-of-the-art dependent. The starting point for 1975 operational status and the directions for growth in improved performance and capability are indicated.

A. SPACE VEHICLE CHARACTERISTICS

A preliminary analysis and design of the lunar cargo transport vehicle and its component elements has been made to provide a baseline for the performance estimates and to bound the range of variables. Such parameters as powerplant specific weight, thrustor performance, and cargo fraction of the landing vehicle can be determined to a sufficient accuracy for evaluation of the potential of the mission and to provide direction for future effort.

A typical lunar cargo space transport is illustrated in Figure 5-1. The nuclear power supply is contained within a conical shaped shell forming one end of the spacecraft. The reactor and shield assembly is located near the apex of the cone and the conical surface itself is formed by a fixed configuration space radiator used for heat rejection from the electrical generation system. The electrical generation system is contained within a cylindrical can mounted inside the conical radiator. The cylindrical end of the spacecraft contains the chemical rocket powered landing craft for soft landing the lunar cargo from orbit to the lunar surface. The thrustors and propellant tanks for the electric propulsion system are also mounted in this section.

An alternate configuration for the lunar cargo transport vehicle is shown in Figure 5-2. Two particular features have been changed from the design shown in Figure 5-1. The containment vessel for the electrical generation system has been modified to consist of the upper section of radiator near the reactor-shield assembly, rather than a separate container

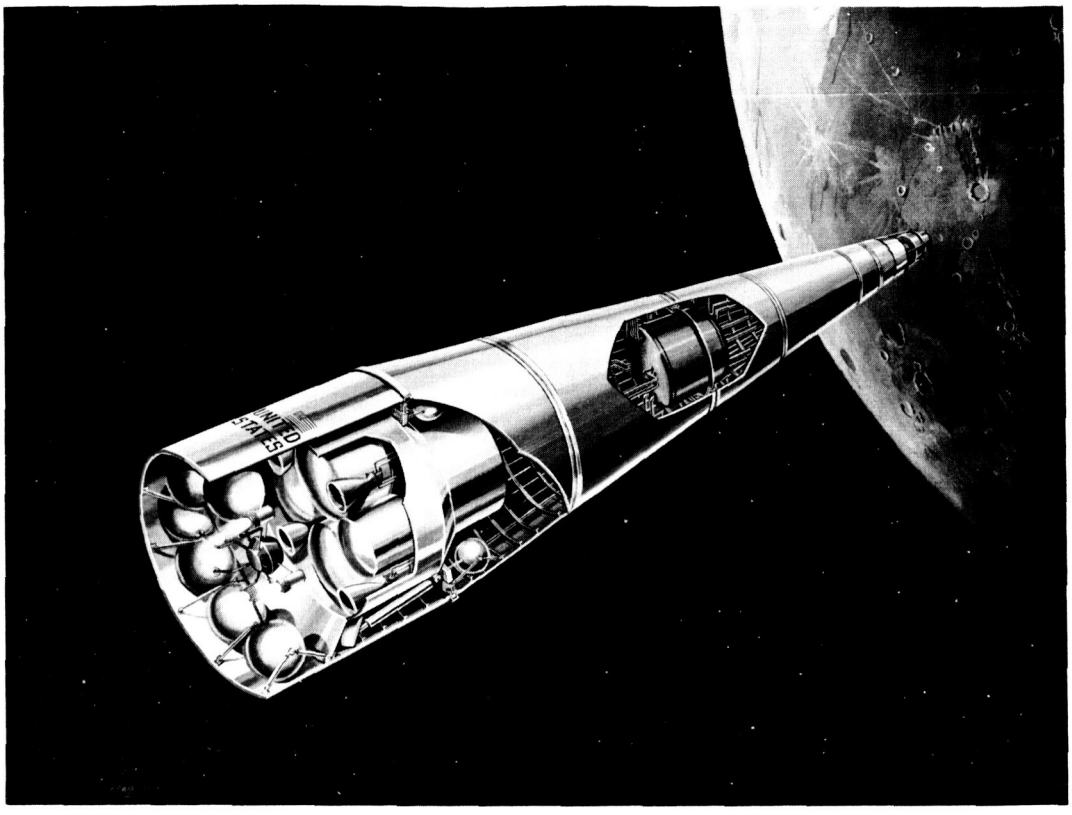

Figure 5-1. Typical Lunar Cargo Vehicle Design

within the radiator being used. Also, the base diameter of the landing vehicle has been increased to the full 10 meter diameter of the Saturn V, which lowers its center of gravity and eliminates an extra containment shell. This step requires the landing legs to be mounted externally. This vehicle is shown in its launch configuration in Figure 5-2(a), and in the outbound flight configuration in Figure 5-2(b). The landing pads are folded upward during launch to avoid interference with the booster, and downward during flight to avoid interference with thermal heat rejection and scattering of nuclear radiation. During launch an aerodynamic shroud could be applied locally over them.

The nuclear power supply, which is shown by itself in Figure 5-2(c), can be propelled back to earth orbit for reuse for (1) transporting another lunar lander, (2) mating to another space vehicle for interplanetary voyages initiating from either lunar or earth orbits, (3) mating to a space station to provide auxiliary power, or (4) landing with the lunar landing craft to serve as a lunar surface power supply. In case the nuclear power supply is landed, additional shielding is required around the reactor. This shield is carried in the base of the

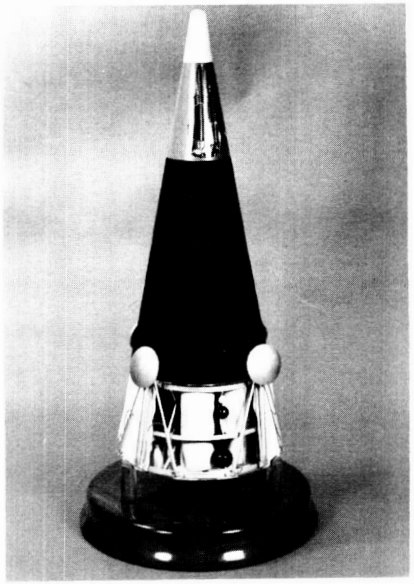

(a) Launch Configuration

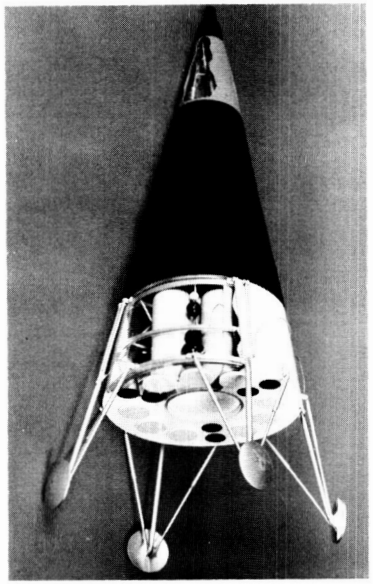

(b) Outbound Flight Configuration

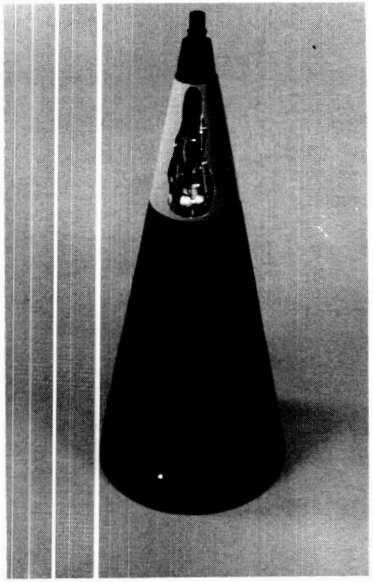

(c) Nuclear Power Supply

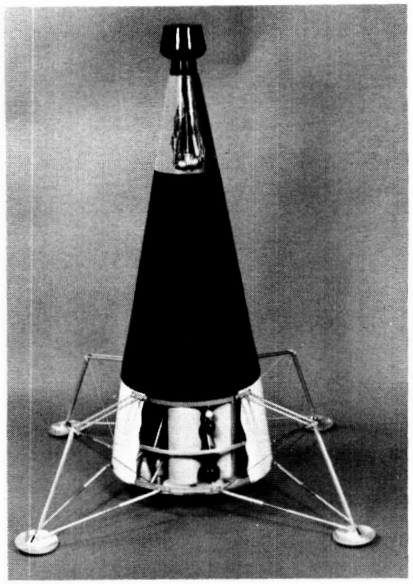

(d) Lunar Surface Power Supply

Figure 5-2. Single Powerplant Lunar Cargo Vehicle (Sheet 1 of 2)

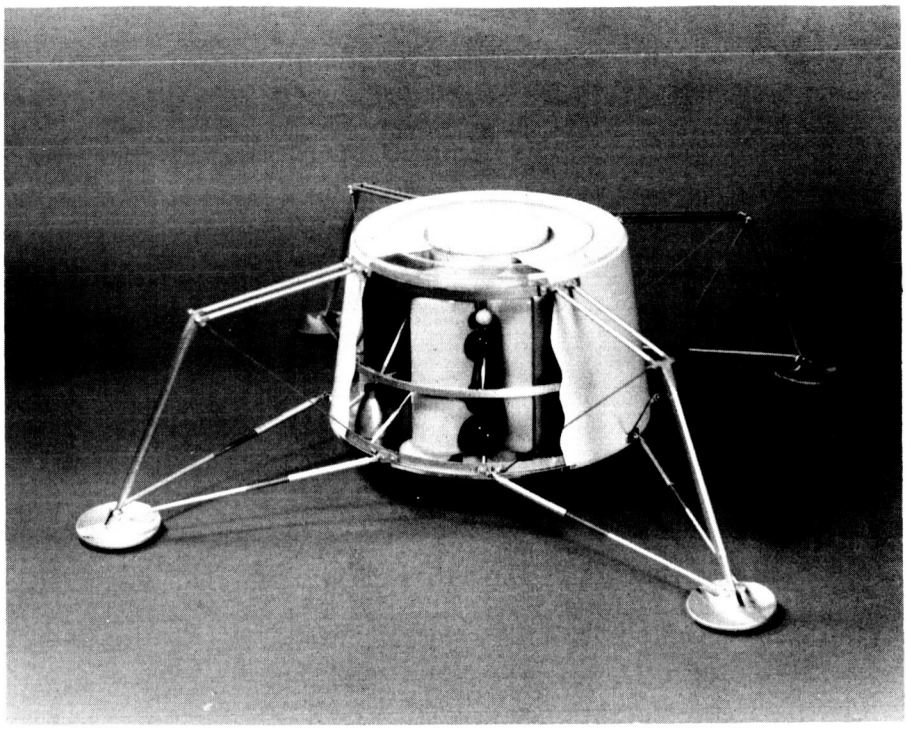

(e) Cargo Lander Version

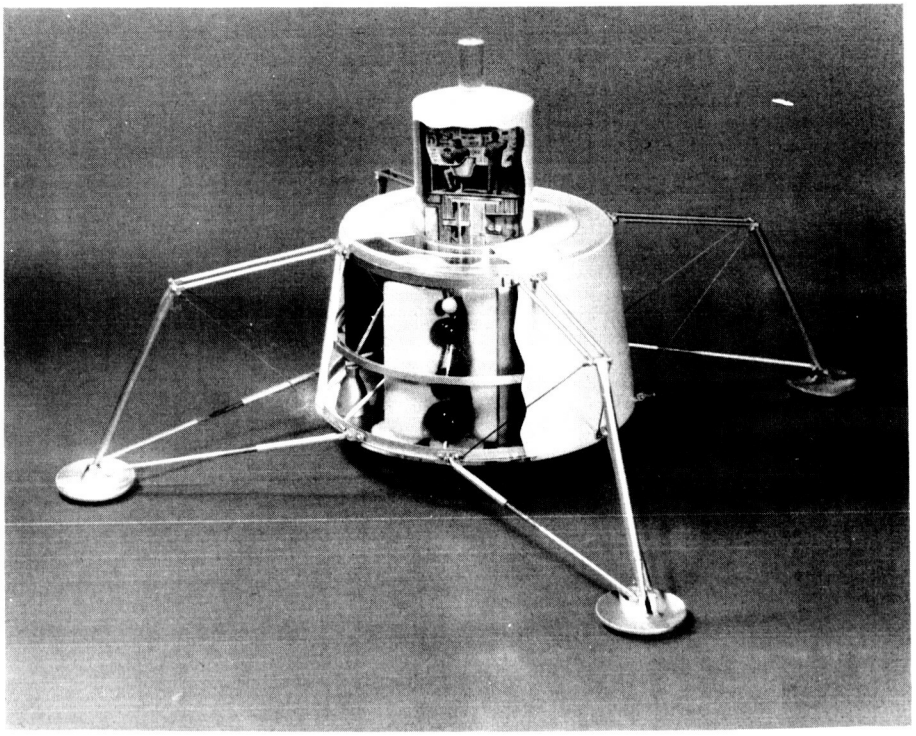

(f) Lunar Shelter Lander Version

Figure 5-2. Single Powerplant Lunar Cargo Vehicle (Sheet 2 of 2)

landing craft until after touchdown on the lunar surface. Then the shield, which is split into two parts by a plane passing through the axis of symmetry, is lowered from a storage location at the center of the lander, translated horizontally to opposite sides of the vehicle, and lifted to position about the reactor by movement on two sets of rails. After the shield is in place, personnel can approach the nuclear power supply and perform assignments in a base facility packaged in the base of this same vehicle. The lunar base facility in this case could be an energy depot, repair shop, or manufacturing plant to exploit lunar resources. A comparison of typical performance characteristics of this lunar cargo system, with and without landing the nuclear power supply, are listed in Table 5-1.

TABLE 5-1. NET LUNAR CARGO CHANGE FOR LANDING OF NUCLEAR POWER SUPPLY

SPACE PROPULSION	CHEMICAL	ELECTRIC	ELECTRIC
Landing Mode	Without Power Supply	Without Power Supply	With Power Supply
Weights, tons			
Electric Power Supply	0	7.4	7.4
Reactor Shield	0	1.2	10.3
Electric Engine Propellant	-	25.0	25.0
Electric Propulsion System (Dry)	-	2.9	2.9
Chemical Landing Craft (No Cargo)	19.0	41.7	46.5
Cargo	12.7	30.8	16.9
TOTAL	--	109.0	109.0

As shown above, considerable advantage is shown for electrical propulsion, and the landing of the nuclear power supply still leaves a respectable mass allowance for a lunar surface facility, which would be manned only after landing.

The nuclear power supply can also be separated from the landing craft in lunar orbit and either a cargo module or a shelter landed as shown in Figures 5-2(e) and 5-2(f). The cargo version would be approached after landing and the supplies unpacked. The lunar shelter version could be manned in lunar orbit and contain provisions for seating the men during descent.

1. Nuclear Electric Power Supply

The nuclear electric power supply has three principal component parts: (1) nuclear heat source, (2) heat engine power generator, and (3) rejection system for waste heat. The nuclear heat source considered for this mission is the nuclear reactor wherein heat is generated by nuclear fission. The heat is used in a thermodynamic energy converter dissipating waste heat via the space radiator to generate electricity. This heat engine can take the form of any of the following energy conversion systems:

1. Rankine
2. Brayton
3. Thermionic
4. Thermoelectric
5. MHD

The powerplant presently of interest for use in electrical propulsion is the SNAP-50/SPUR, which operates on the Rankine cycle and is being funded on a technology development basis. The contemplated power size of this powerplant is 300 KWe, but the technology is reasonably applicable to multi-megawatt power levels. The powerplant schematic is illustrated in Figure 5-3, and typical power loads of the various components are presented. Lithium is used as a heat transport medium to generate potassium vapor in a boiler separate from the reactor. The potassium traverses a simple Rankine cycle with the following processes:

1. Heat addition (liquid to vapor phase change in a boiler)
2. Expansion (generation of shaft power in a turbine)
3. Heat rejection (vapor to liquid phase change in a condenser)
4. Pressurization (liquid pumping in a dynamic pump)

The heat rejection is also indirect. Liquid metal circulates between the compact condenser and the space radiator to dissipate the waste heat from the power conversion system. This approach allows the radiator, which is rather large, to be more easily integrated with the space vehicle and launch booster.

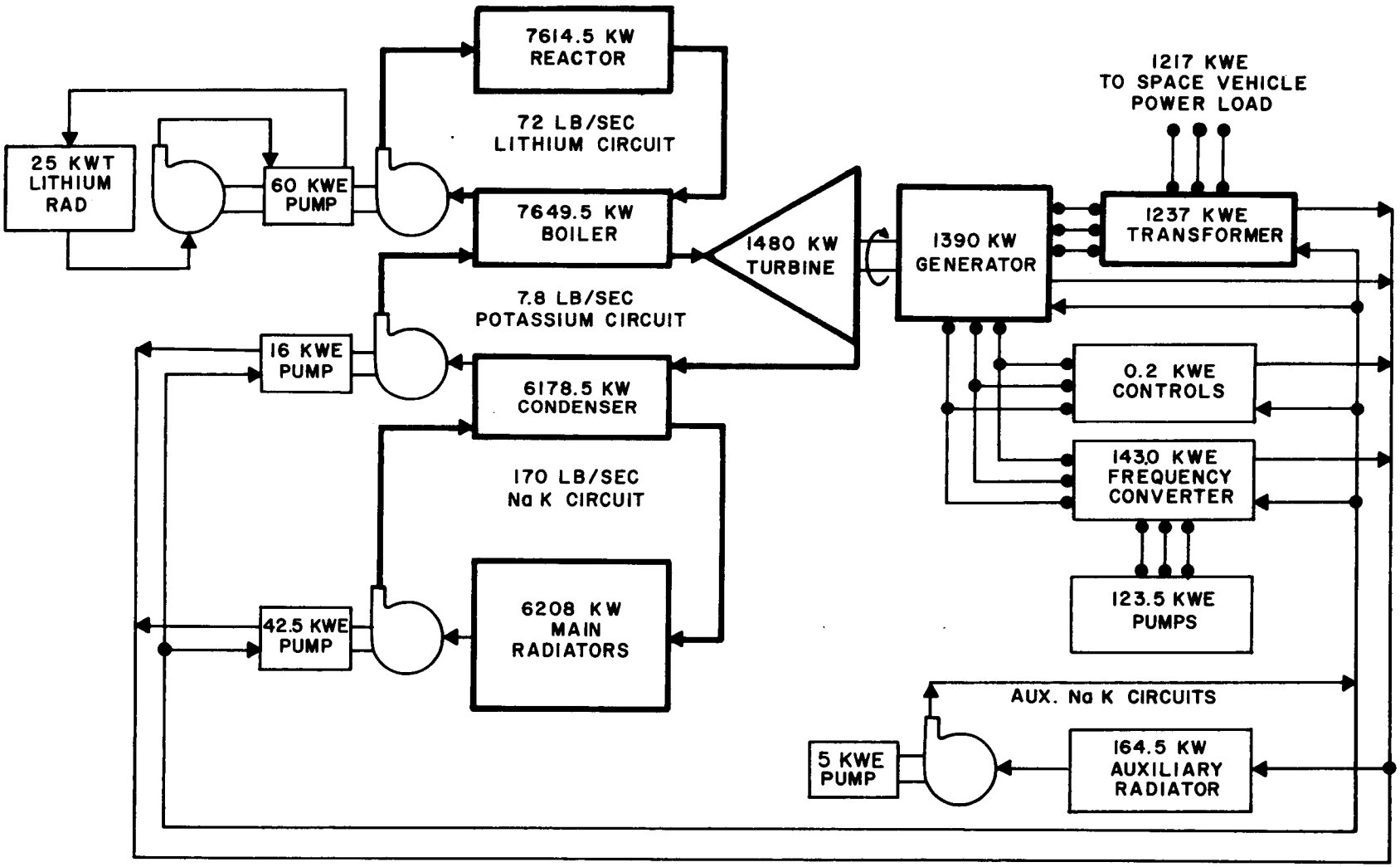

Figure 5-3. Rankine Cycle Powerplant Schematic and Energy Balance

The main power conversion components, i.e., reactor, boiler, turbo-generator, condenser and pumps, can be packaged compactly for ease of manufacture, testing, and transportation of this portion of the system. A typical arrangement is presented in Figure 5-4, which shows four separate Rankine cycle systems coupled to a single reactor. The containment vessel for the power generator system is designed to provide environmental control of the equipment inside. The vessel can be evacuated to permit backfilling with inert gas to protect refractory metal components. Liquid metal coolant tubes are mounted to the containment vessel wall using it as an auxiliary radiator for thermal control of temperature limiting components such as generator, transformers, motor pumps and controls. A convenient cooling arrangement is as follows:

1. Each primary circuit lithium pump contains a secondary flow impeller, which provides bearing lubricant and motor cooling. The effluent from these elements circulate through tubes mounted to the inside of the containment vessel, thereby using it as a fin for radiation of the waste heat to space.

2. Each secondary and tertiary pump also contains a secondary flow impeller for circulating bearing lubricant and motor coolant. However, in this case the effluent circulates through a compact heat exchanger to dissipate the waste heat to an auxiliary coolant.

3. The turbogenerator assembly also contains a pump impeller for bearing lubricant and generator coolant, which circulates low temperature liquid potassium via a compact heat exchanger to an auxiliary coolant.

4. An auxiliary cooling system is provided for each generation system. The auxiliary coolant removes heat from the auxiliary heat exchanger of the motor pump and turbogenerator assemblies, transformers and control systems and circulates through the auxiliary radiator, which is a portion of the conical shell of the containment vessel.

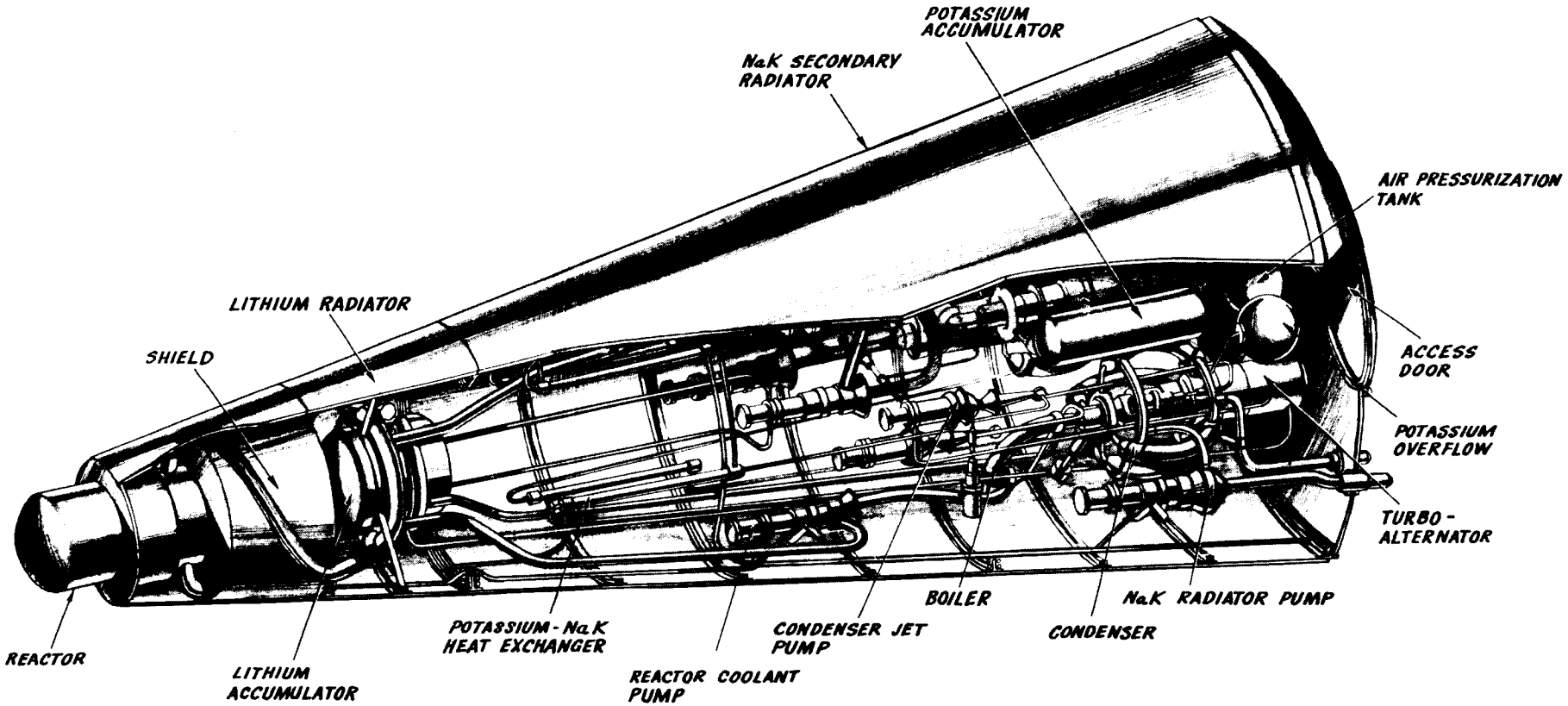

Figure 5-4. 1200 KW_e Power Conversion System Packaging

The purpose of separating the auxiliary cooling of the primary lithium pumps from the remainder of the system is related to the starting conditions and liquid metal freezing temperatures. Lithium freezes at 186°C (367°F) whereas potassium freezes at 63.7°C (147°F). The protection against freezing during the time prior to powerplant startup is provided by an auxiliary heat source and, thus, the portion of power system to be maintained above 186°C (367°F) is narrowed to the primary liquid metal system, which is thermally isolated from the remainder of the power system except in the boiler. Prior to startup the boiler would be empty of potassium. Thus, the heat losses from the primary system are limited to the dry piping from the boiler to the other potassium components, and to the small portion of radiator for primary pump cooling. The rest of the primary system can be blanketed with insulation.

The containment vessel, in addition to providing "atmosphere" and thermal control to the power generation system, also provides meteoroid protection and mounting structure for the components. The entire assembly then mounts on top of a main radiator assembly, which is also shaped as a frustum of a cone.

In small size powerplants (under one megawatt electric), the powerplant weight tends to be dominated by the reactor and nuclear radiation shield. The reactor is sized on the basis of requirements for criticality, heat transfer, and fission gas release. Many design assumptions and materials selections are involved in the weight determination and this material has been presented in various publications.

For use in this study, a reactor reflector outside diameter of approximately 50 centimeters has been assumed for the 1200-kilowatt (electric) size powerplant. The reactor is assumed to be shaped as a right circular cylinder with a 60 centimeter separation distance between the front plane of the active core and the front plane of the nuclear radiation shield. The sizing of the reactor for large powers can be accomplished by assuming constant power density and length to diameter ratio. The weight of the reactor is assumed at 1000 kg; and the life, at 12 months. The variation of reactor diameter and weight is shown in Figure 5-5 for variations in power and operating life.

A shield is required to protect the power generation system and lunar cargo from the nuclear radiation generated by the reactor. The elements most sensitive to radiation are the payload electronics and the integrated dose that is tolerable is quite difficult to estimate at the present time. Allowable doses are assumed to be 10^6 rads of gammas and 10^{11} nvt of fast neutrons. The shield is generally shaped in the form of the frustum of a cone with the axis along the centerline of the spacecraft. The diameter of the shield section closest to the reactor and the shield cone angle are selected so that the payload is completely shielded from a direct view of the reactor. The shield is composed of tungsten and lithium hydride, or other equivalent materials, for gamma absorption and neutron absorption, respectively. The lithium hydride is encased in stainless steel. The weight of the shield required for a 50 centimeter diameter reactor to shadow a 10-degree (half-angle) conical volume containing radiator, power generation system and lunar landing craft is 1500 kilograms. The variation of shield weight with reactor diameter and cone angle is presented in Figure 5-6.

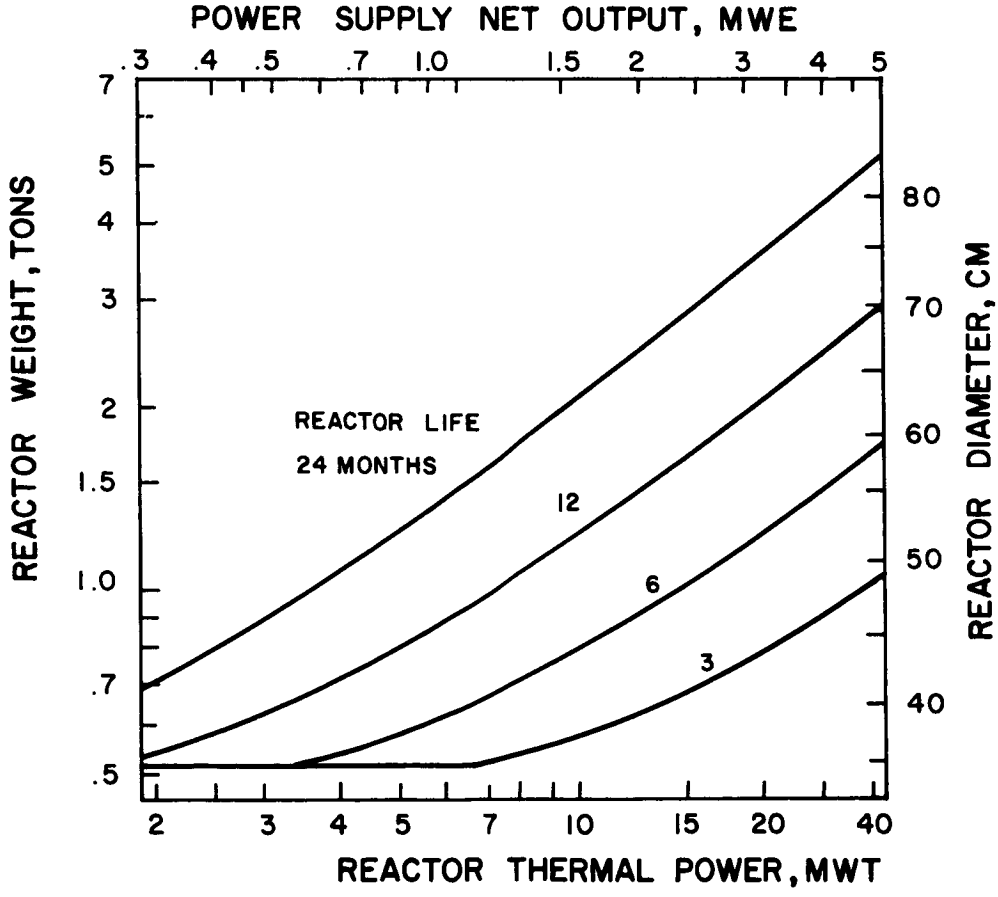

Figure 5-5. Reactor Weight and Diameter Characteristics

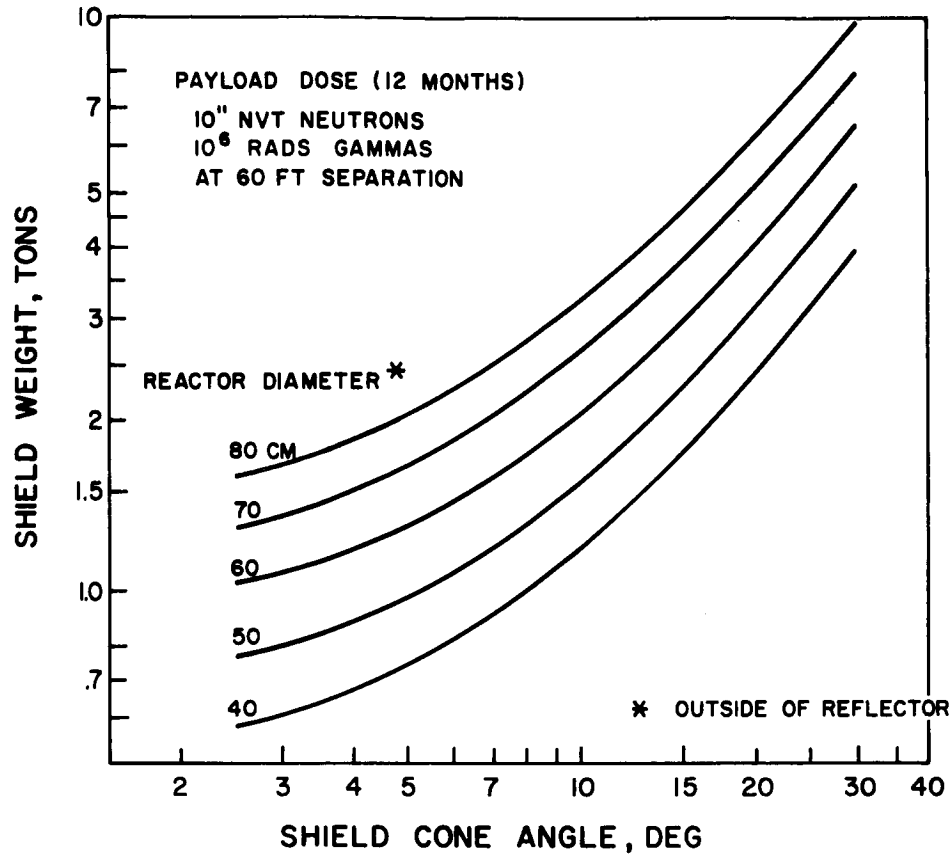

Figure 5-6. Shield Weight Characteristics

The major component of the power generation system is the turbogenerator, which is illustrated in Figure 5-7. The estimated weight of this unit is 470 kg for 467 kva gross output, yielding 300 KWe net power to the electrical propulsion system. The turbine is a conventional axial flow type with four to six stages. The generator can be either an axial-gap design as shown in Figure 5-7, or a radial-gap design of approximately equal mass.

The boiler, condenser and motor pumps can take any of several forms. In the mission study only their approximate mass is significant. A weight tabulation of the power generation system plus reactor and shield is presented in Table 5-2. This weight summary includes all of the elements illustrated previously in Figure 5-4.

The complete powerplant arrangement is shown in Figure 5-8. This design locates the reactor and shield near the apex of a 10^{o} cone with the auxiliary radiators occupying that surface area nearest the shield. The remainder of the conical surface is assigned to the primary radiators. Figure 5-9 schematically depicts the allotment of areas and the thermal loads associated with the various cooling functions.

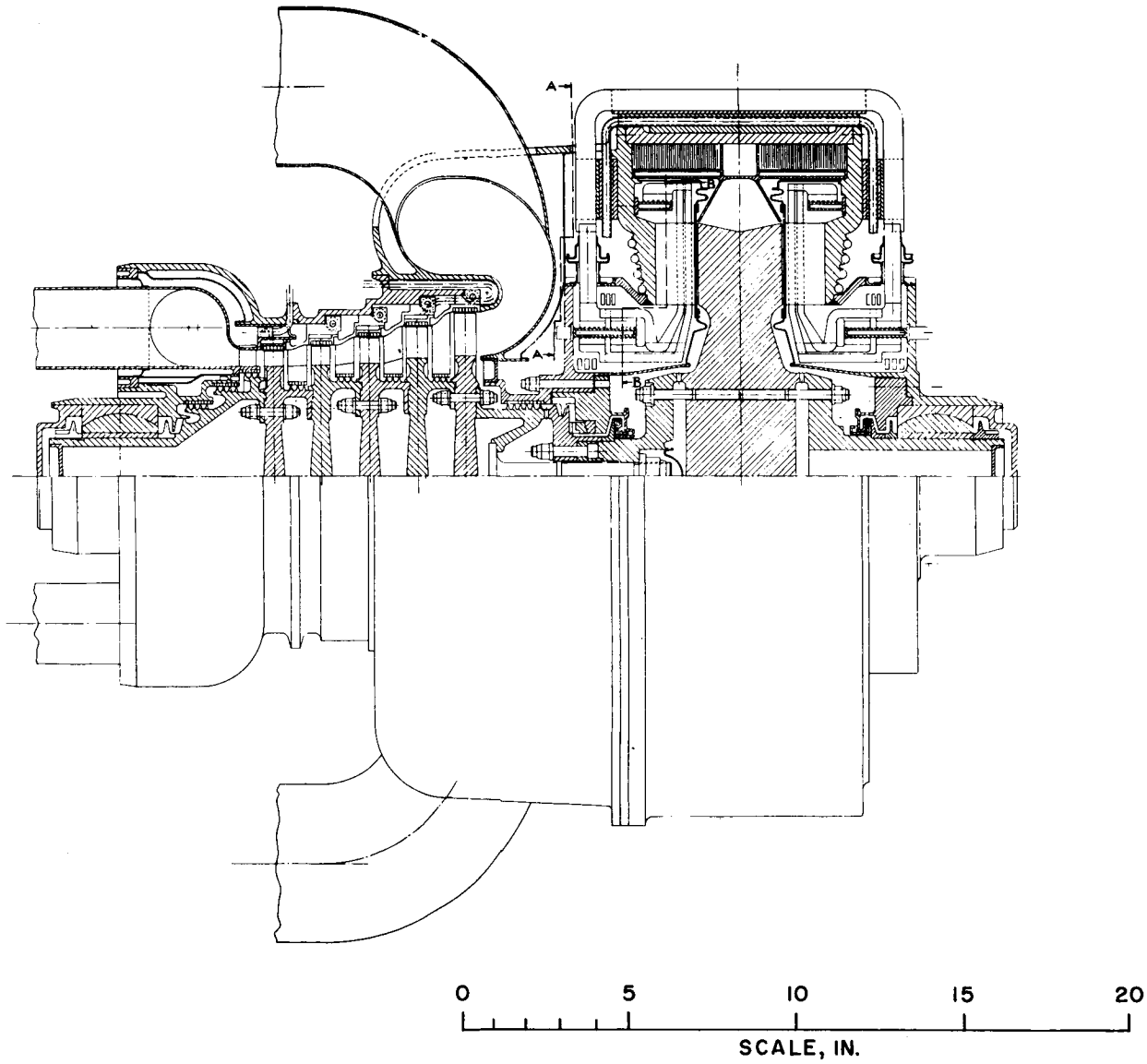

Figure 5-7. 300 KVA Turbogenerator with 14.5 Inch Diameter Generator Rotor

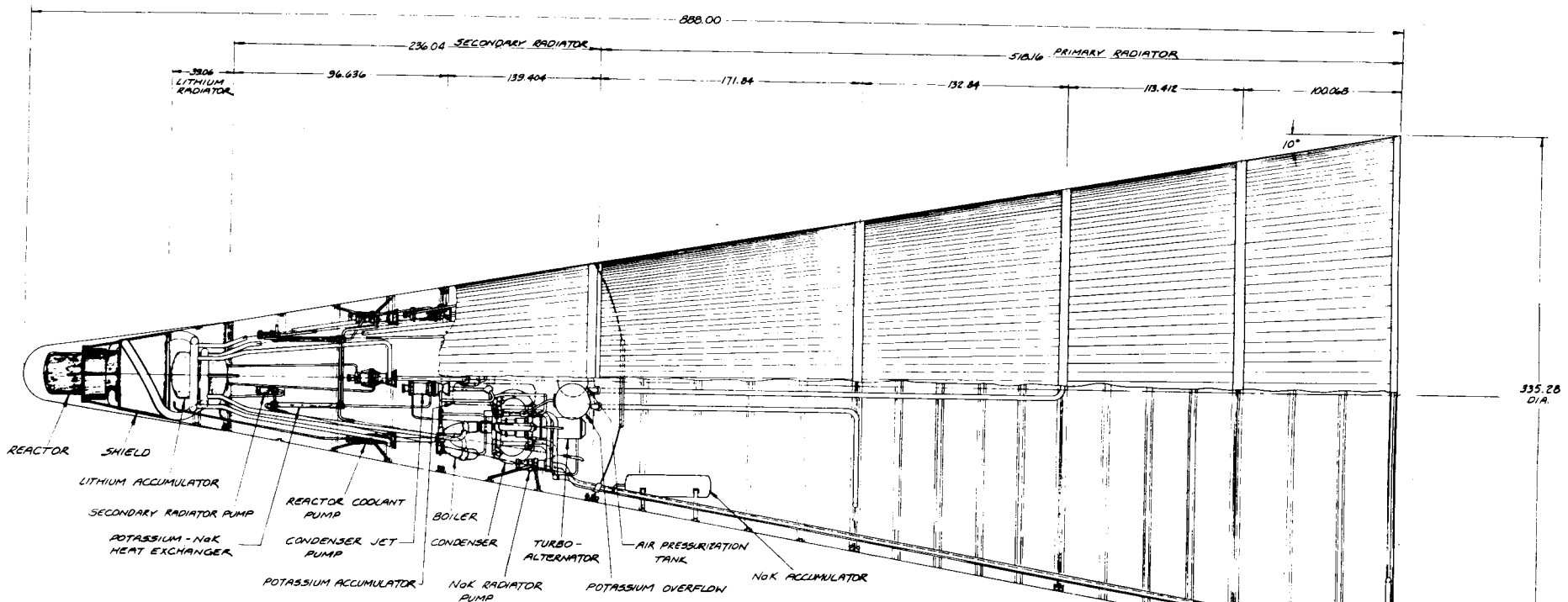

Figure 5-8. Typical Rankine Cycle Powerplant for Lunar Cargo Operation

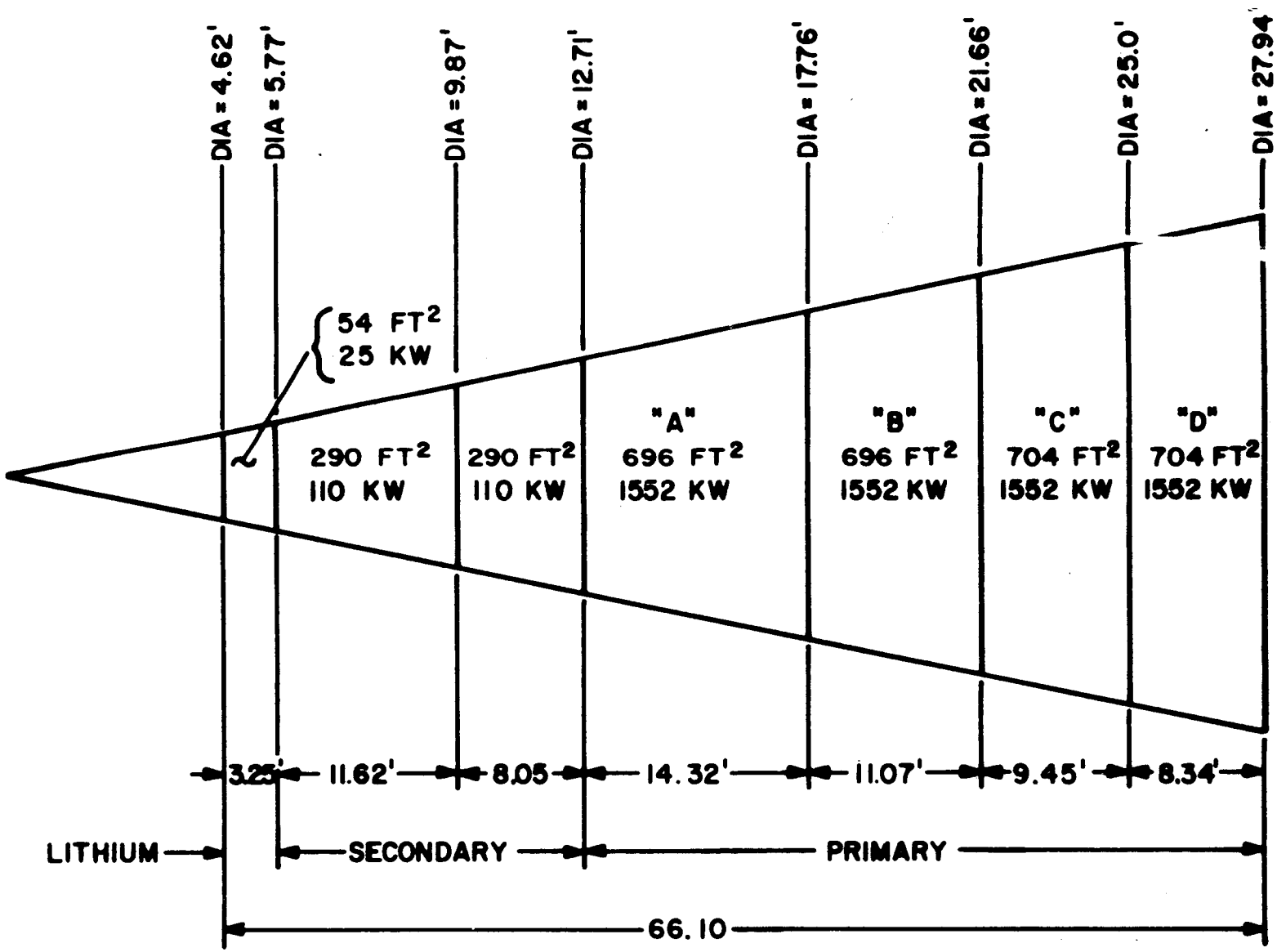

Figure 5-9. Radiator Areas and Thermal Loads

TABLE 5-2. WEIGHT SUMMARY
OF 1200 KW_e ELECTRICAL GENERATION SYSTEM ASSEMBLY
(as per Figure 5-4)

			kg (lbs)
Reactor			1000 (2200)
Shield			1500 (3300)
Reactor Support Structure			50 (100)
Power Conversion Equipment			3650 (8040)
Turbogenerators (4)	1880	(4140)	
Boilers (4)	360	(800)	
Condensers (4)	290	(640)	
Primary Loop Pumps	160	(360)	
Condensate Pumps	70	(160)	
Primary Radiator Pumps	230	(500)	
Controls	70	(150)	
Piping	140	(300)	
Accumulators	180	(400)	
Brackets, Fasteners, etc.	270	(590)	
Auxiliary Radiators			360 (800)
Basic Radiator	260	(570)	
Structural Frames	10	(30)	
Attachment Rings	50	(110)	
Meteoroid Bumpers	10	(20)	
Brackets, Fasteners, etc.	30	(70)	
Pressure Bulkhead			50 (110)
Insulation			230 (500)
Aerodynamic Nose Fairing			140 (300)
TOTAL*			6980 (15360)

* Nuclear Power Supply Exclusive of Main Radiator.

The upper portion of the powerplant comprises the EGS (electrical generation system) module. This group of components, intended to be developed as a unit, includes the reactor, shield, auxiliary radiators, turbo-machinery and associated equipment. The auxiliary radiators, which provide cooling for the primary loop pumps, condensate pumps and generators, form the lateral walls of a pressure tight vessel; the remaining boundaries are provided by the reactor shield assembly and the convex pressure bulkhead. Inside the EGS module, four SNAP-50 type turbogenerator units are arranged symmetrically about the vehicle center line. Fluid networks for these units are configured in a manner such that only the primary loop is common to all units; the secondary and tertiary loops are completely independent so that a failure or malfunction in one of these loops will not affect the operation of the remaining units. The piping network is illustrated schematically in Figure 5-3. The arrangement shown uses four primary radiator pumps; however, the number may vary depending upon the degree of segmentation desired in the primary radiator system.

The reactor is supported by a conical shell which extends the length of the shield and transmits the structural loads into the radiator matrix. By arranging the primary loop piping in a spiraling manner about the shield (see Figure 5-4), it is possible to imbed the lines in the shield without providing a direct radiation path. This arrangement has the further advantage in that the reactor support cone can now be used to provide a hermetic seal for the primary loop piping which would otherwise require individual jacketing in the exposed areas. Prior to launch, during the preheat phase, the entire EGS module can be pressurized with an inert gas. After the launch has been completed, the gas is bled off so as not to induce undue stress in the pressure hull when system start-up is effected. Since it is speculated that in-flight repairs will be feasible at this time, access is provided to the turbo-machinery by means of a port in the pressure bulkhead. Components in the EGS module are positioned to provide a four-foot diameter passage way along the center line. In the event that difficulties are encountered prior to start-up, it may be desirable to repressurize the compartment to facilitate repairs; for this purpose, inert gas tanks are included. Thermal control within the compartment is provided by means of multi-layer foil insulation on the high temperature components. The ambient temperature in the compartment during operation is expected to be near that of the auxiliary radiators. On the large diameter end of the auxiliary radiators,

providing the interface for the primary radiator, is a thermal joint which accommodates the differential expansion of the two radiator systems and provides a high resistance thermal path between them.

The primary radiator illustrated is sized to provide the required heat rejection capacity on four equal area bays, each of which is composed of two 180^{o} panels. The 10^{o} cone angle was selected so that approximately 50 percent of the primary radiator area is located on the cone at a diameter less than 260 inches. Separation at this diameter privides a convenient interface with the Saturn I booster and affords sufficient primary radiator area to allow full power testing of two of the turbogenerator units or a partial power test of the entire system. For test flights then, the upper two primary radiator bays and the EGS module form the payload for a Saturn I launch. Although the overall length of this package exceeds the current Saturn I envelope limitations, the shallow cone angle and relatively low payload weight may combine to provide an acceptable combination for test flights.

Located immediately aft of the primary radiator and serving as an adapter section between the 28 foot diameter radiator base and the 33 foot diameter boost vehicle, is the lunar cargo landing vehicle. Details of the lander design are deliniated in Section 5.A.3 and it is sufficient to point out here only those aspects of the design which influence the powerplant.

The most significant factor requiring consideration is the problem of thermal control between the lander and the primary radiator. Since the chemical propellants stored in the lander are likely to be of the cryogenic variety, it is necessary to provide an extremely high resistance thermal path between these components. The interchange of radiant energy can be minimized by the use of low emissivity coating on the inner surface of the radiator and multi-layer foil insulation on the upper surface of the lander. Conduction heat transfer can be controlled by the use of a high thermal resistance joint; this type of interface will also be required to allow unrestricted thermal expansion of the radiator.

Power conversion equipment for the electric thrustors, propellant, and the electric thrustors themselves, are incorporated into the lander design.

Radiators were designed using the SPARTAN III and the CRASS computer codes*. The procedure employed was to use the Spartan program to determine an optimum design with respect to thermal and meteoroid protection requirements with the resulting configuration then being analyzed for structural integrity using the CRASS program. In some instances, several iterations through this loop are required before a satisfactory design is evolved.

Since the radiators are intended to serve as the primary structure and withstand the launch loads, they are analyzed for general instability, local instability and panel instability under an equivalent axial load. The equivalent axial load was assumed to increase linearly along the vehicle length at a rate of 16,200 pounds per foot, as illustrated by Figure 5-10. This equivalent load is scaled from the loads predicted at the Saturn V booster interface, during "max q α" conditions, with Apollo spacecraft payload.

The 54 square meter lithium pump cooling radiator uses the shared fin design to provide four distinct fluid loops. The coolant circulated in this radiator is lithium hence requires a refractory metal tube liner within the beryllium armor. The secondary radiator occupies two bays and is composed of four separate fluid circuits; each bay accommodating two shared-fin loops. Thermal load for these radiators originates at the alternators and condensate pumps and is transferred to the radiators via potassium to NaK heat exchangers. Although the original requirements for the secondary radiators specified a heat rejection capacity of 165 kilowatts, the design presented has a capability of rejecting over 200 kilowatts. This apparent overdesign results from consideration of the structural requirements of the vehicle at this point and the volume required for packaging the turbo-machinery.

Analysis of the primary radiator bays indicates only minor additions are necessary to provide structural adequacy. The configuration selected for this concept does not provide sufficient primary radiator area to allow the use of unlimited area designs; the weights presented are therefore slightly greater than the absolute minimum weight attainable for this type of radiator. Details of the radiator designs are presented in Table 5-4 and a weight summary for the launch configuration is given by Table 5-5.

---

* Code names for internally generated computer programs.

Thermal and reliability requirements assumed for this study are listed in Table 5-3 below.

TABLE 5-3. RADIATOR REQUIREMENTS

PRIMARY RADIATOR

Thermal Load - 6208 KW
Inlet Temperature - 675°C (1246°F)
Coolant - NaK
Armor and Fin Material - Beryllium
Liner Material - Stainless Steel
Segmentation - 4 loops
Mean Time to Failure - 50,000 hrs
Area Limit - 260m^2 (2800 ft^2)

SECONDARY RADIATOR

Thermal Load - 165 KW
Inlet Temperature - 308°C (586°F)
Coolant - NaK
Armor and Fin Material - Beryllium
Liner Material - Stainless Steel
Segmentation - 4 loops
* Mean Time to Failure - 1.1×10^5 hrs.
Area Limit - 54 m^2 (580 ft^2)

LITHIUM PUMP COOLING RADIATOR

Thermal Load - 25 KW
Inlet Temperature - 315°C (600°F)
Coolant - Lithium
Armor and Fin Material - Beryllium
Liner Material - Columbium
Segmentation - 4 loops
* Mean Time to Failure - 1.17×10^6 hrs
Area Limit - 5 m^2 (54 ft^2)

* Combined mean time to failure for the auxiliary radiators is 100,000 hours. Distribution is based on radiator area.

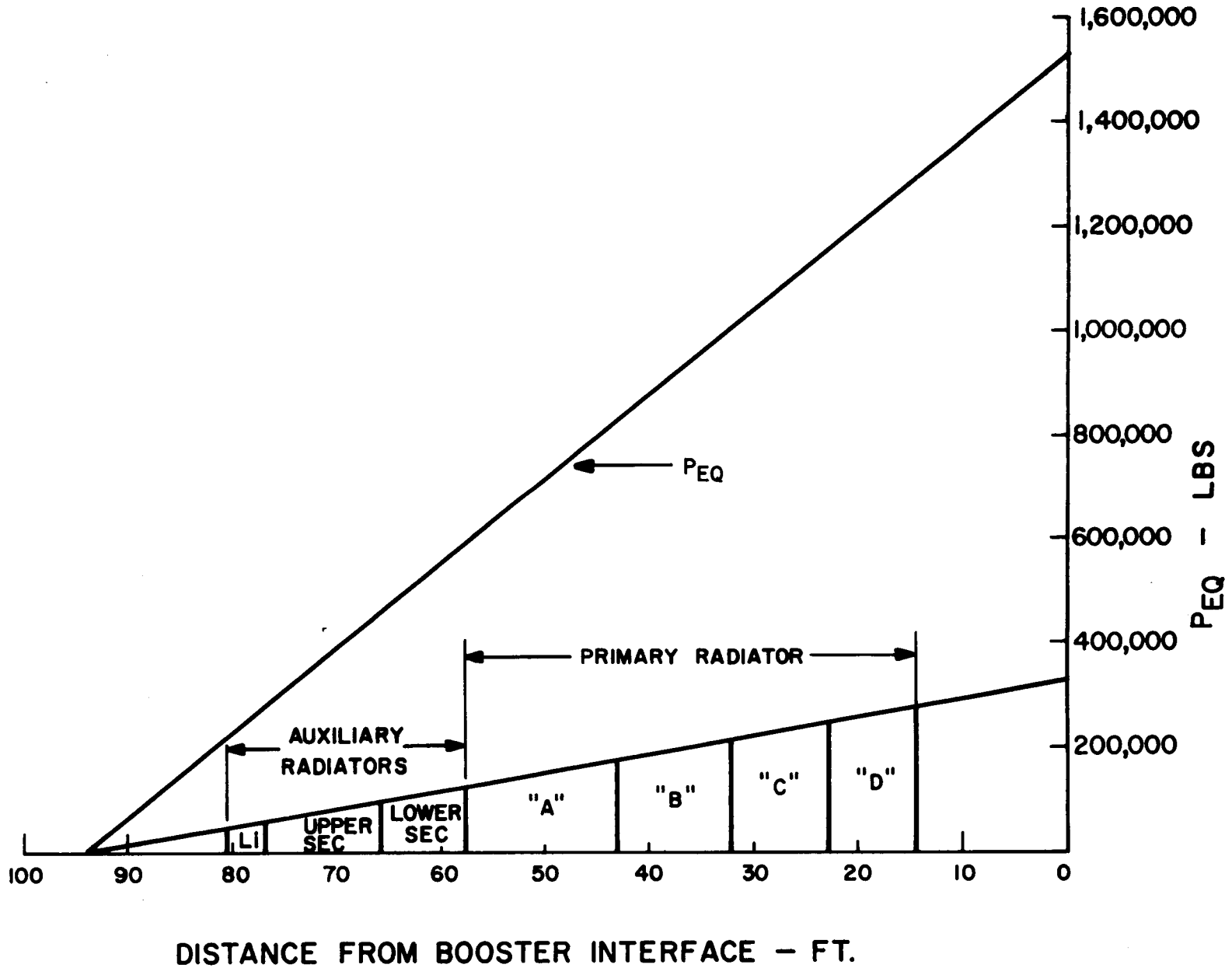

Figure 5-10. Lunar Cargo Vehicle Equivalent Axial Load

TABLE 5-4. RADIATOR DETAILS

	UNITS	PRIMARY A	PRIMARY B	PRIMARY C	PRIMARY D	SECONDARY UPPER	SECONDARY LOWER	LITHIUM PUMP RAD.
Heat Rejected	KW	1552	1552	1552	1552	110	110	25
No. of Panels	---	2	2	2	2	2	2	2
Header Length	Ft.	23.9	31.0	36.6	41.5	12.3	17.7	8.2
No. of Tubes per Panel	---	103	135	173	191	50	70	36
Liner Inside Diameter	In.	.28	.24	.21	.21	.18	.18	.18
Fluid Inlet Temperature	^{o}F	1246	1246	1246	1246	586	586	600
Fluid Δ T in Radiator	^{o}F	205	205	205	205	86	86	15
Fin Thickness	In.	.060	.060	.060	.060	.045	.045	.040
Tube Length	Ft.	14.4	11.0	9.2	8.1	11.6	7.8	3.2
Feed Line Diameter	In.					1.0	1.0	.50
Radiating Efficiency	%	81	80	81	80	86	85	85
Radiating Area	Ft^2	704	702	700	701	288	283	54
Basic Radiator Weight	Lbs.	1063	1136	1197	1332	242	258	64
No. of Structural Frames	---	4	4	3	3	3	4	1
Weight of Structural Frames	Lbs.	23	44	50	68	7	11	1
Weight of Longitudinal Stiffeners	Lbs.	--	--	--	--	--	7	--
Structural Margin of Safety	---	.11	.51	.25	.17	.17	.46	.50
Total Radiator Weight	Lbs.	1086	1180	1247	1400	250	276	65

A preliminary design of a 1200 KWe nuclear power supply prepared at the beginning of the study is presented in Figure 5-11. This design preceded that shown in Figures 5-2 and 5-8, and is the layout for the illustration in Figure 5-1. The details shown for header to tube connections in Figure 5-11 would be used for either arrangement of power supply. The more recent layout in Figure 5-8 is more advantageous for packaging and support of the electrical generation system components. Weights for both layouts are approximately the same.

TABLE 5-5. WEIGHT SUMMARY
OF 1200 KW_e NUCLEAR POWER SUPPLY
(as per Figure 5-8)

		kg	(lbs)
Reactor		1000	(2200)
Shield		1500	(3300)
Reactor Support Structure		50	(100)
Power Conversion Equipment		3650	(8040)
Auxiliary Radiators		360	(800)
Pressure Bulkhead		50	(110)
Insulation		230	(500)
Aerodynamic Nose Fairing		140	(300)
Subtotal (EGS Assembly)		6980	(15360)
Primary Radiator		2760	(6090)
Basic Radiator	2150 (4730)		
Structural Frames	80 (180)		
Attachment Rings	210 (470)		
Meteoroid Bumpers	70 (160)		
Brackets, Fasteners, etc.	250 (550)		
TOTAL		9740	(21450)
Weight per Kilowatt		8.1	(17.9)

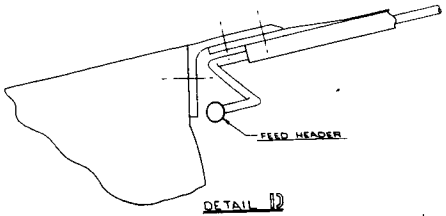

DETAIL 12
SCALE 1/1

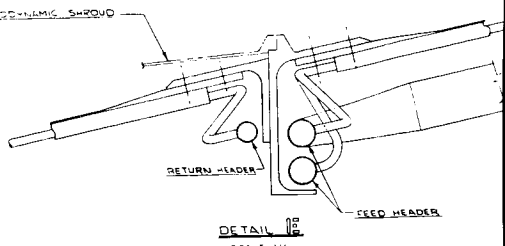

DETAIL 11
SCALE 1/1

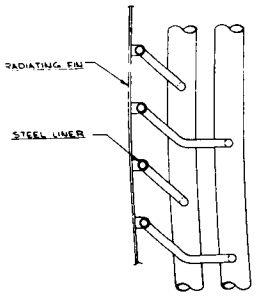

SECTION H-H
SCALE 1/1

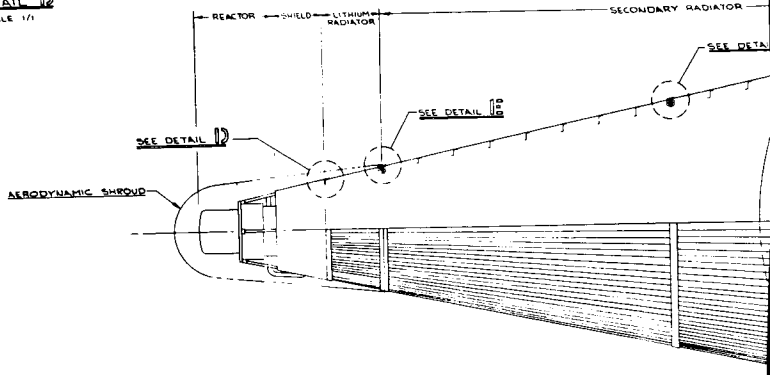

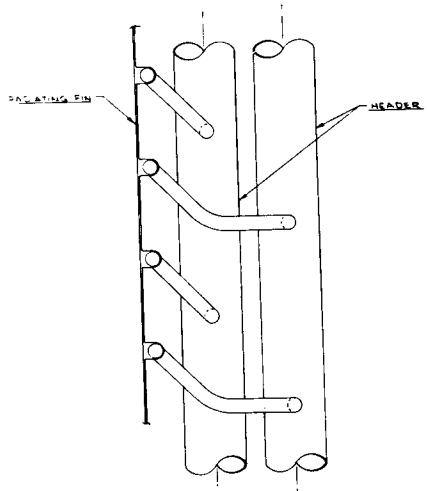

SECTION G-G
SCALE 1/1

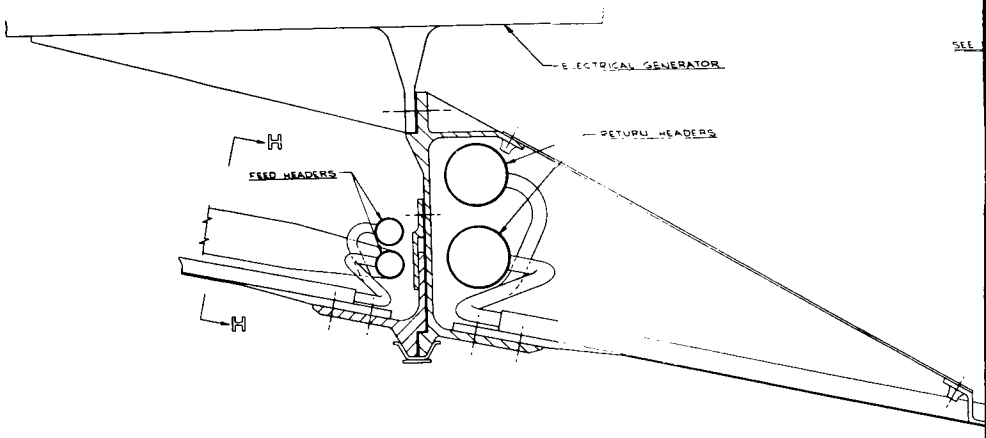

DETAIL 13
SCALE 1/1

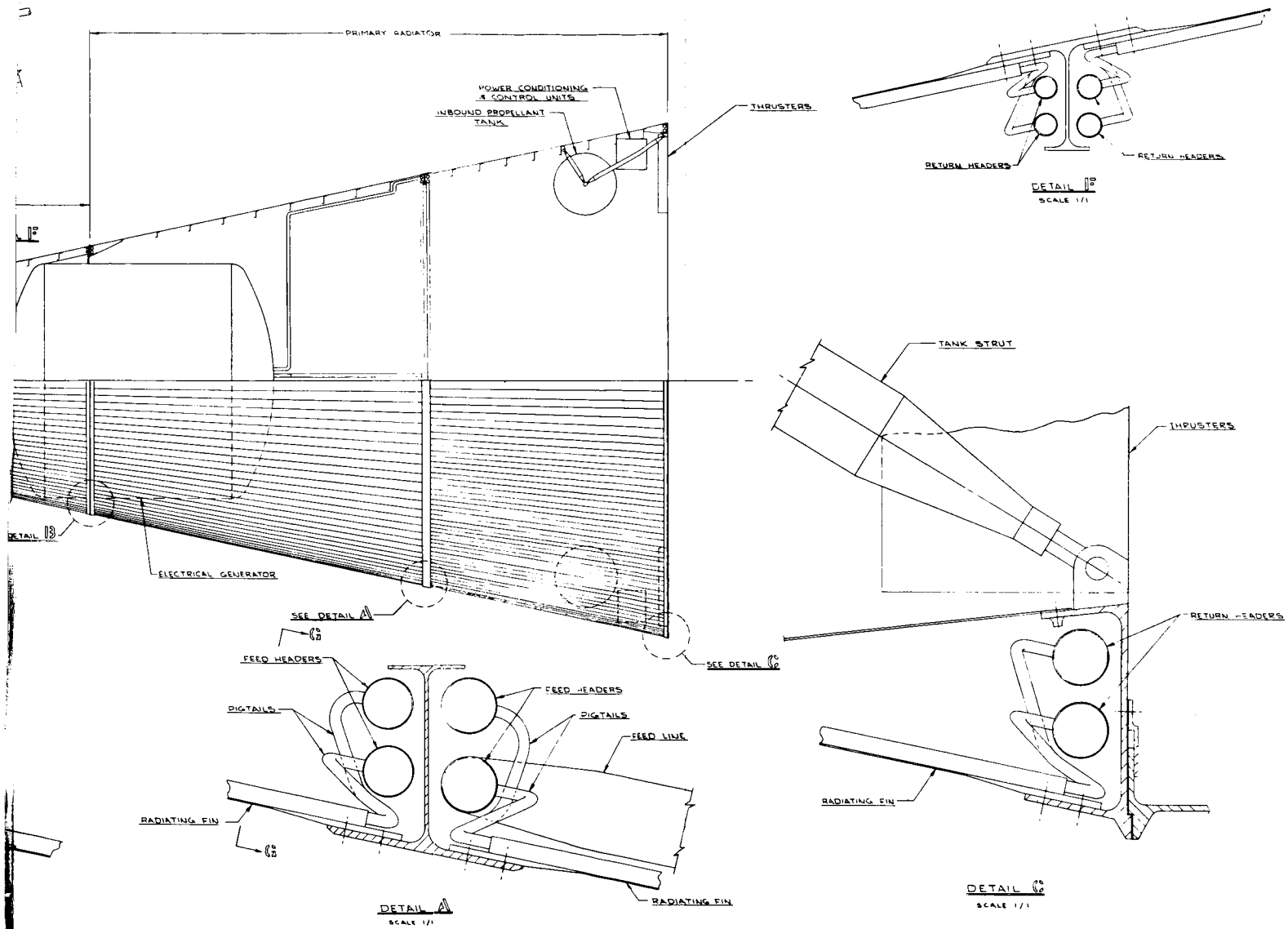

Figure 5-11. Alternate Rankine Cycle Power-plant for Lunar Cargo Operation

The radiator weight varies significantly with requirements for meteoroid protection. An approximate functional relationship for the radiator weight is:

$$W \sim A^{(1+\alpha)} \quad T^{\alpha}$$

where

W = radiator weight

A = radiator area

T = mean time to radiator puncture

The exponent α varies with selection of materials and configuration. An evaluation of this component about the radiator design shown in Figure 5-8, which used beryllium armor and fins, yields the value 0.17. The radiator area varies directly with power, assuming constant fin efficiency, and is designed for 1.2 megawatt (electric) size power supply and 50,000 hours mean time to radiator puncture. This results in a specific weight of 2.61 kg/ KW_e. Thus, the general radiator weight equation is:

$$W = 2.61 \left(\frac{T \quad P}{(50,000) \quad (1.2)} \right)^{.17} \text{kg/KW}_e$$

The mean time to radiator puncture relates to the survivability of the radiator as a function of time. This functional relationship is:

$$R = \exp(t/T)$$

where

R = Probability of no punctures

t = Time of exposure to meteoroids

T = Mean time to puncture

The weight variation with power rating of the turbomachinery, heat exchangers and supporting equipment in the electrical generation system is rather difficult to determine. An acceptable assumption for this equipment is that weight varies directly with power rating, and no adjustment is provided for variation of design life, since life is related more closely to development cost investment.

The information presented above on weight variation of reactor, shield, radiator and electrical generation system components can be combined to show the variation of power supply specific weight with power rating and the influence of other factors such as reactor diameter and radiator mean time to puncture. As previously shown the reactor diameter is a function of power size and lifetime, as well as detail design parameters such as burnup, configuration and materials selection. The variation of power supply specific weight with reactor diameter (outside of reflector) is presented in Figure 5-12, and lines of constant power supply life are shown. The power supply rating appears to influence specific weight only in the range below one megawatt. The power supply life selection between 6 and 24 months can increase specific weight by 16 percent, which is a relatively small amount. The effect of mean time to radiator puncture is shown in Figure 5-13. Again, the variation of power supply specific weight with the design parameters is rather small.

The conclusion is that the power supply weight tends to be directly proportional to power over a wide range of power size and is not significantly affected by any of the design parameters as shown here. The weight is affected by state-of-art considerations which can shift the power supply specific weight upward or downward by a sizable factor. For purpose of mission analysis variations of power supply specific weight can be ignored during the period of conceptual and feasibility studies. A power supply specific weight of 10 kg/KWe appears to be a proper estimate for a SNAP-50/SPUR derived power supply. A range of specific weights of interest for the mission studies is from 5 to 20 kg/KWe.

The power supply specific weight has an almost proportional effect on travel times for the electrically propelled space vehicle. Trip times will vary directly as the sum of power supply plus thrustor weight. The thrustor specific weights tend to range between 1 and 4 kg/KW_e. Thus, a 50 percent decrease in power supply specific weight from 10 kg/KW_e to 5 kg/KW_e, in the case where the thrustor specific weight is 4 kg/KW_e, yields a 36 percent reduction in trip time. The typical effect of power supply specific weight on trip time is shown in Figure 5-14.

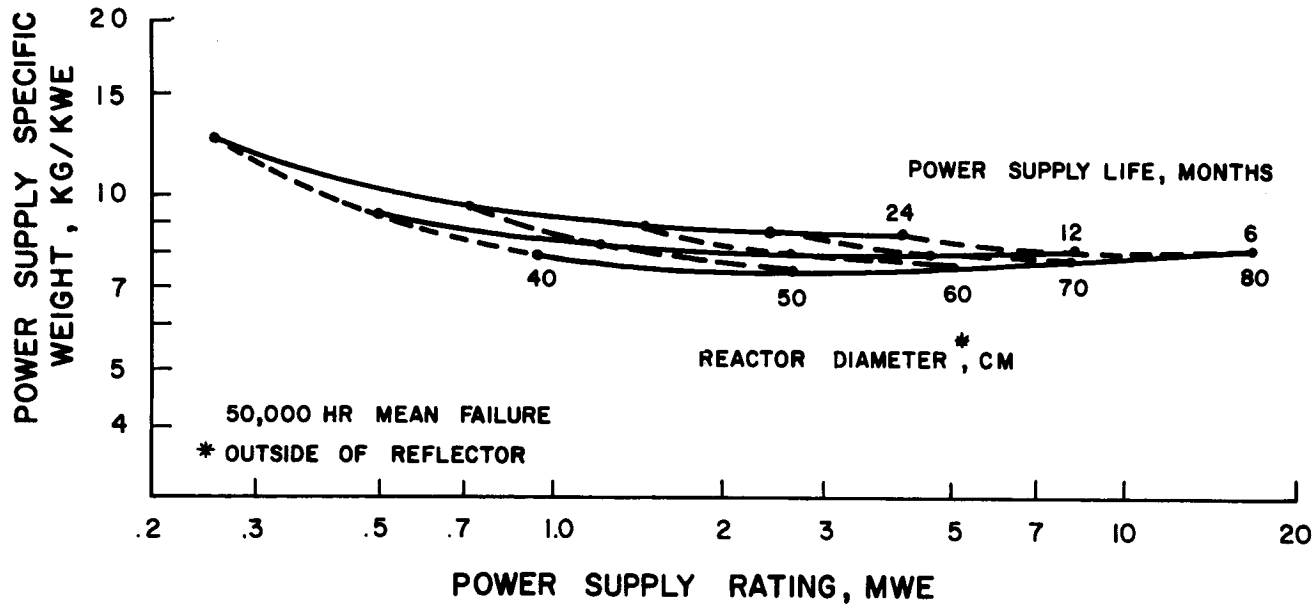

Figure 5-12. Power Supply Specific Weight Variation with Reactor Diameter

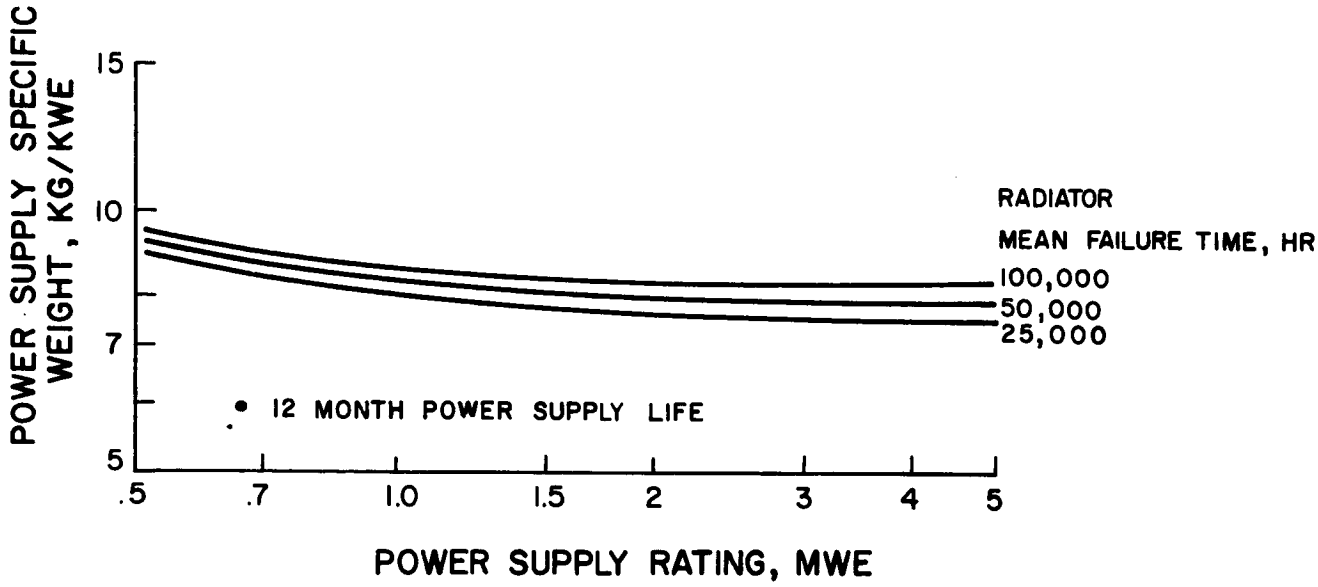

Figure 5-13. Power Supply Specific Weight Variation with Radiator Mean Failure Time

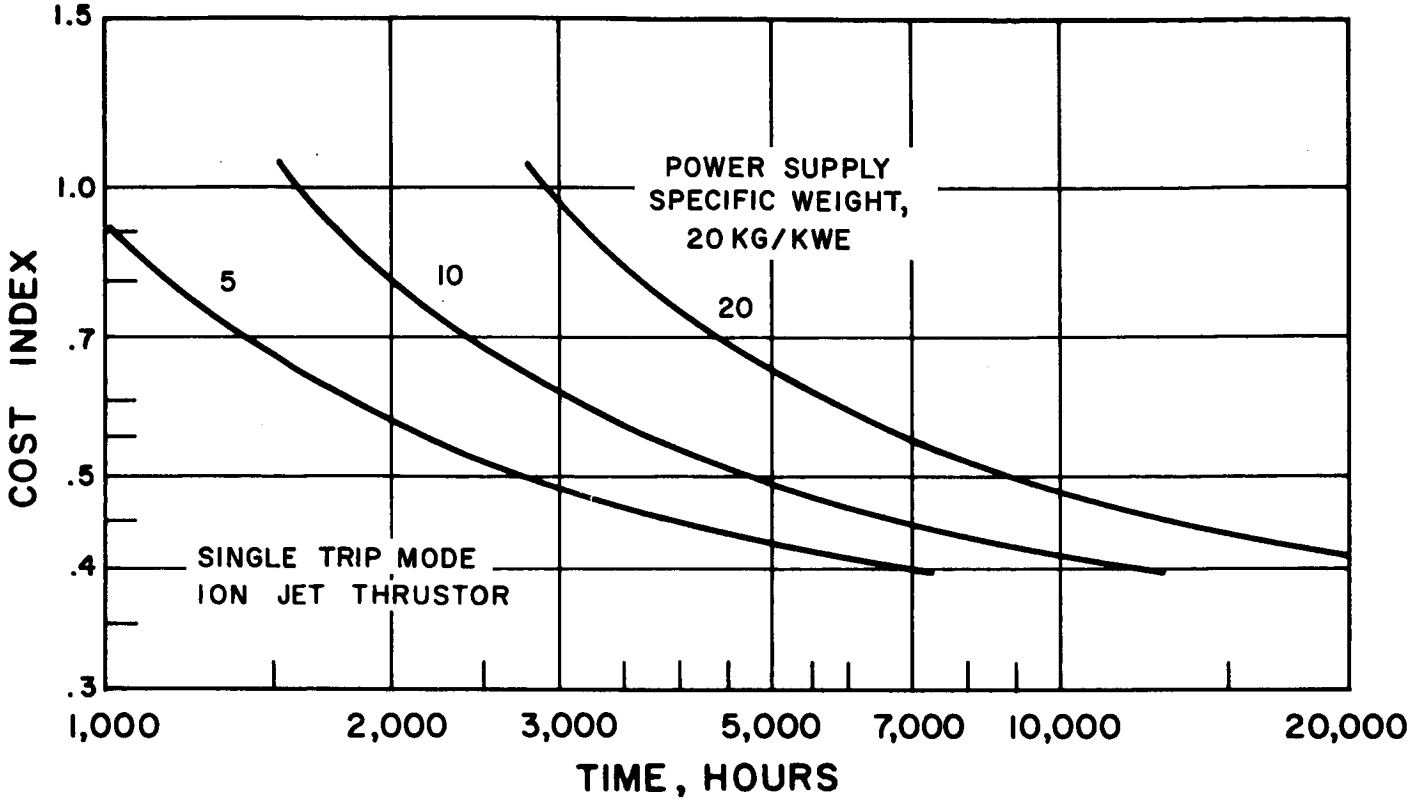

Figure 5-14. Effect of Power Supply Specific Weight on Trip Time

The data in Figure 5-14 shows that cost index is a function of both power supply specific weight and trip time. The trip time corresponds to the life qualification rating of the power supply for the case of the single-trip operating mode. If a requirement is not set for the trip time, then the power supply specific weight can be traded-off against its life rating and costs associated with development and manufacture. A comprehensive study covering these items would reduce the data in Figure 5-14 to a single recommended design point, for each set of assumed boundary conditions, state-of-the-art, etc.

2. Electrical Propulsion System

The electrical propulsion system includes the electric thrustors, propellant tank and feed system, and the power conditioning system. Performance characteristics such as efficiency and specific weight can be predicted over a wide range, depending on the selected concept and state-of-art assumption, and these variations are presented below.

The two basic types of thrustors considered are the ion jet and the hybrid arc jet. The ion jet, or electrostatic ion thrustor, is better understood than the other and, for that reason, has been selected for more general use in this study. Electron bombardment and contact ionization thrustors are both forms of the ion jet, and characteristics of these are presented in some detail below. The hybrid arc jet is defined as an arc jet thrustor with a MHD boost, and many variations of this are discussed in the literature using hydrogen propellant. The most advanced hybrid arc jet, examined only superficially to date, uses lithium propellant and has the potential of 70 percent efficiency over a wide range of specific impulses. A comparison between the various electric thrustors was made during the early phase of this study on the basis of mission performance and the results are presented in Figure 5-15. The hybrid arc jet with hydrogen propellant was considered to be of little interest and was not included in further study. The performance of the electron bombardment and contact ionization thrustor was reasonably close, and the electron bombardment was selected as sufficiently representative of the ion jet class of thrustors.

There are substantial differences of opinion as to the present performance capacities of ion thrustors, and, of course, even greater variations are found in predicting future capabilities. A report, currently being prepared on the use of electric thrustors for manned interplanetary voyages*, contains a treatise on ion thrustors and attempts to steer a middle ground through the controversy. Rather than repeat the entire analysis here, only the results are presented.

*Coates, G. "Study of Low Acceleration Space Transportation Systems Interim Report," GE Document No. 65SD4315.

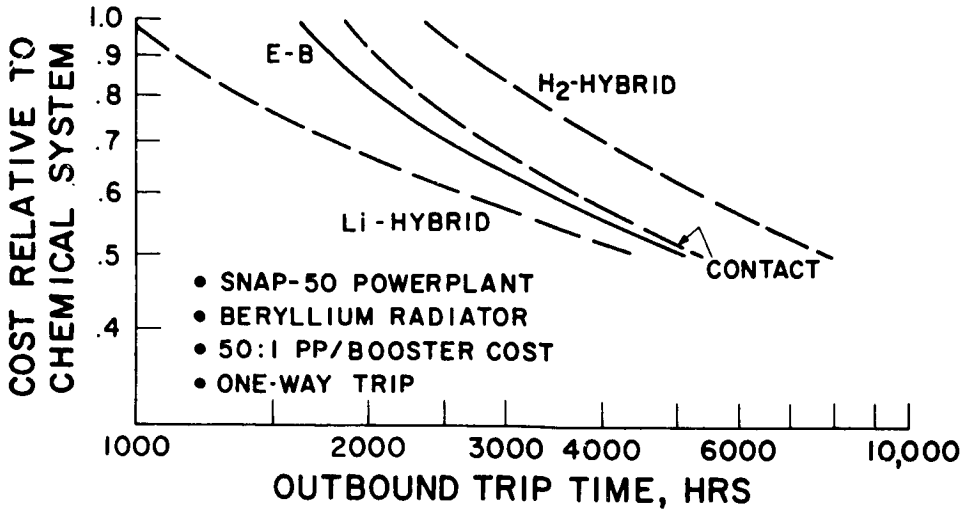

Figure 5-15. Performance Comparison

Three state-of-the-art levels in ion jet thrustor performance, size and weight are postulated for both the electron bombardment and contact ionization thrustor:

a. Electron Bombardment Thrustor

1. The first state-of-the-art level assumes very conservative design from the electrode erosion viewpoint. An average current density (beam current divided by thrustor frontal area) of 12.5 amps/meter^2 is assumed; this is further assumed to correspond to a screen current density of 23 A/m^2. The reduced ion generation losses reported by P. D. Reader* of NASA-Lewis, imply that maximum thrustor efficiency will be obtained at propellant utilizations which are higher than previous practice; the propellant utilizations assumed on this basis are plotted in Figure 5-16. Entering this data into Figure 5-17(a) reveals that the electrode life under these conditions should exceed 20,000 hours at all specific impulse levels. Thus a margin is available if needed for downward revision of the propellant utilization and/or the electrode durability. This would be a realistic design condition for 1970-1975, if the development effort between now and then were concentrated on the cathode lifetime and overall thrustor reliability problems rather than on thrustor efficiency improvements.

* Reader, P.D., "Experimental Performance of a 50-Centimeter Diameter Electron Bombardment Ion Rocket," September 1964, AIAA Paper No. 64-689.

Next, an ion generation loss of 600 ev/ion was assumed at a propellant utilization of 96 percent. This is slightly less than the 650 ev/ion indicated at this utilization in the experimental data of P. D. Reader. A crude estimate of the variation of this loss with propellant utilization was made. The resultant ion generation losses were added to the estimated accel drain current losses and feed, cathode and neutralizer will be negligibly small from the viewpoint of this study. Applying the 50 kg/m^2 figure to the thrustor area data yields a curve of thrustor specific weight versus specific impulse which is also shown in Figure 5-18.

2. The second state-of-the-art level assumes firm confidence in the data of Figure 5-17(a) and improved ion chamber performance. Specifically, an average current density of 25 amps/$meter^2$ (corresponding to a screen current density of 45 A/m^2) was assumed along with an ion generation loss of 500 ev/ion at 95 percent propellant utilization. The propellant utilization was fixed at the minimum value consistent with 10,000 hours life as obtained from Figure 5-17(a). The resultant efficiencies, sizes and weights are shown in Figures 5-16, 5-18 and 5-19. The break in these curves is due to the space-charge limited flow boundary which is encountered at a specific impulse of 4,000 seconds. The discontinuity in weight is due to the addition of a decel electrode.

3. The third state-of-the-art level assumes an average current density of 35 amps/$meter^2$ (screen current density = 64 A/m^2). This assumes that the durability of the accel electrode has been doubled without a weight increase, either through improved design, through the use of beryllium electrodes, or through coating the critical areas of the electrodes. The ion generation losses were again assumed to be reduced, this time to a value of 400 ev/ion at 96 percent propellant utilization. The propellant utilization was assumed to be the same as for the second state-of-the-art level.

b. Contact Ionization Thrustor

1. Copper electrodes and an ionizer current density of 60 amps/$meter^2$ are assumed. The Hughes ionizer performance is assumed to apply, hence a neutral fraction of

1.4 percent is assumed. Figure 5-17(b) indicates a lifetime of more than 20,000 hours for these conditions, along with an electrode spacing of 6 to 8 millimeters. The power required to maintain the proper ionizer temperature (1310^{o}K) was calculated by assuming that the entire ionizer radiates to space with an emissivity of 0.5. This emissivity is somewhat high to account for the miscellaneous small thermal losses due to conduction, radiation from other parts of the thrustor, etc. The power required to heat the propellant and the neutralizer was estimated and added to the estimated accel drain current losses and ionizer heater power to obtain the total losses as a function of specific impulse. The resultant efficiency curve is presented in Figure 5-19.

The frontal area of the thrustor is assumed to be 1-1/2 times the total ionizer area and the mass is assumed to be 80 kg per square meter of frontal area (1-1/3 times the value assumed for the electron bombardment thrustor with a decel electrode). The resultant thrustor frontal area and mass data are presented in Figure 5-18.

2. The second state-of-the-art level retains the copper electrodes and assumes an ionizer current density of 120 amps/meter^{2}. A 10,000 hour life at this current density requires ionizer performance midway between the Hughes and EOS data; i.e., a neutral flux on the order of 1 percent. An electrode spacing of 2.5 mm is assumed; this implies space charge limited flow for specific impulses less than 8,000 seconds.

3. The third state-of-the-art level assumes an ionizer current density of 194 amps/meter^{2}. A lifetime of 10,000 hours can be obtained at this current density with copper electrodes by achieving both the 0.65 percent neutral fraction indicated by EOS and a 60 percent improvement in copper electrode durability (see Figure 5-17(b). This might be done through the use of non-conducting coatings on critical areas. Greater improvement in electrode durability of course permits higher neutral fractions; for instance, doubling the durability (as assumed for the

electron bombardment engine at level 3) permits a neutral fraction of 0.9 percent, while tripling the durability permits a neutral fraction of 1.4 percent.

The desired lifetime can also be obtained easily with the use of beryllium electrodes as shown in Figure 5-17(c). The contact thrustor efficiency at this current density is plotted in Figure 5-19 and the associated weights and areas are plotted in Figure 5-18.

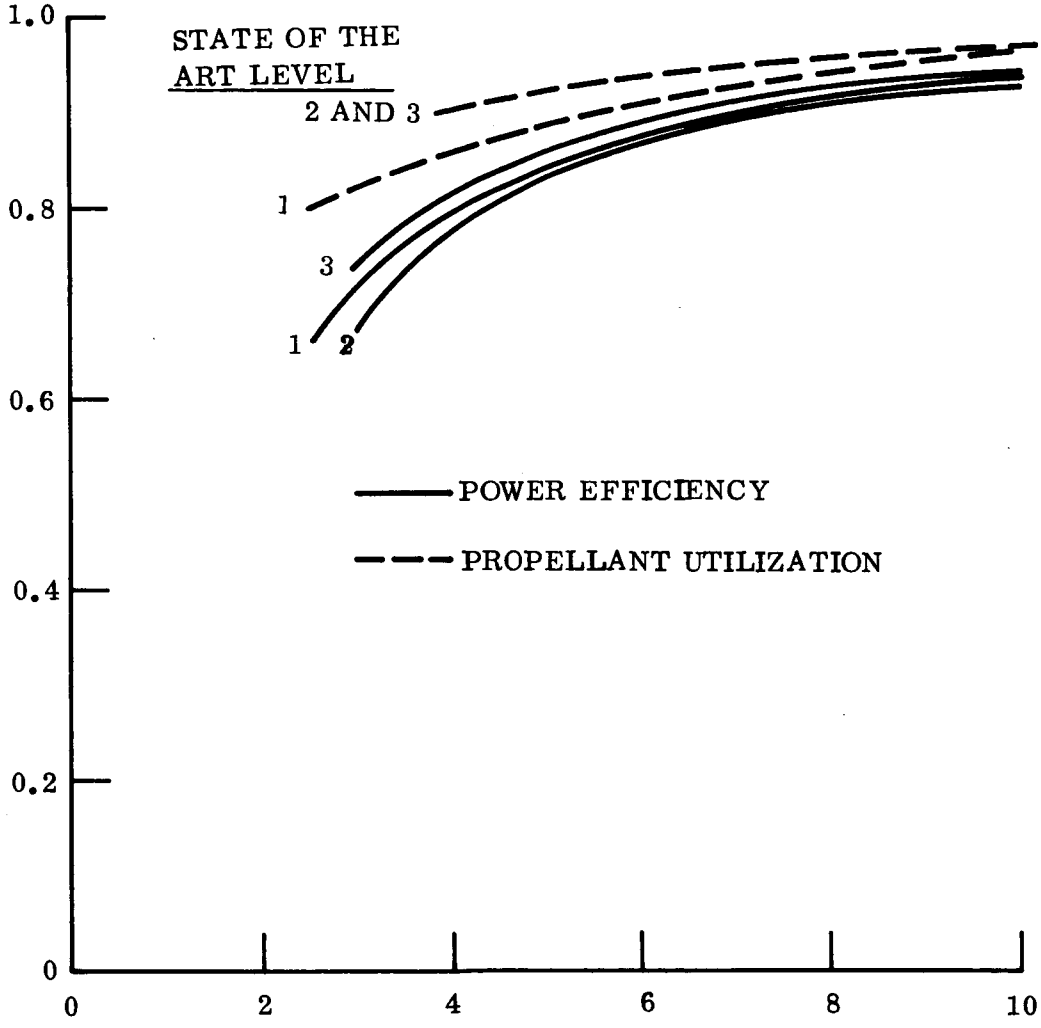

Figure 5-16. Electron Bombardment Thrustor Performance Characteristics

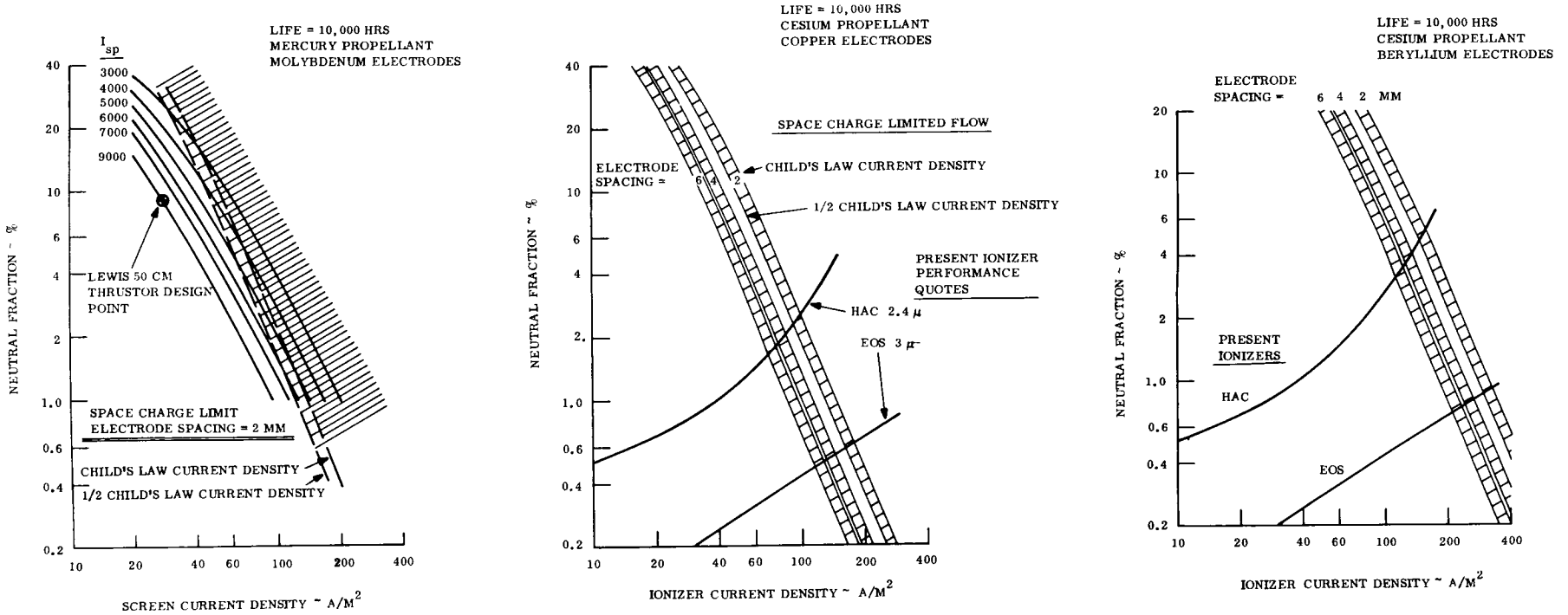

Figure 5-17. Limits Set by Electrode Erosion

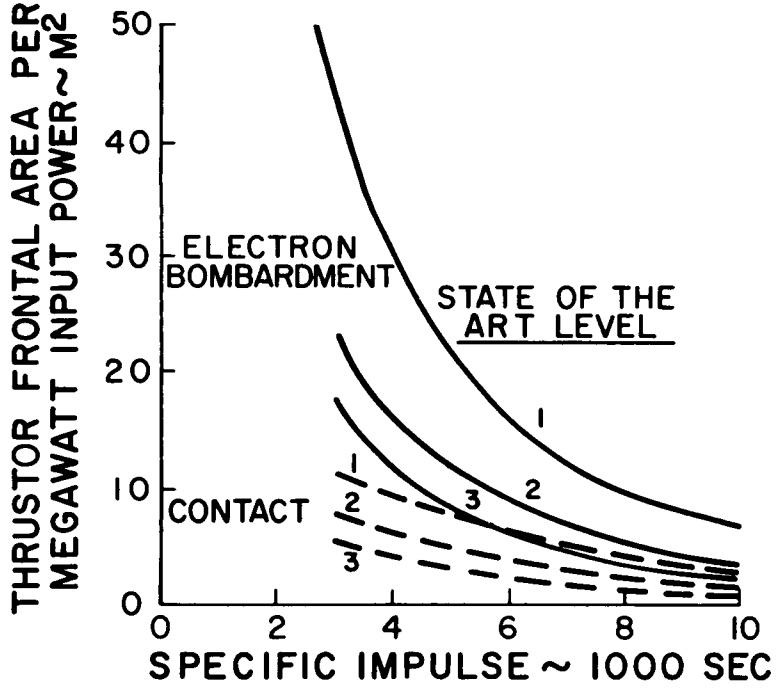

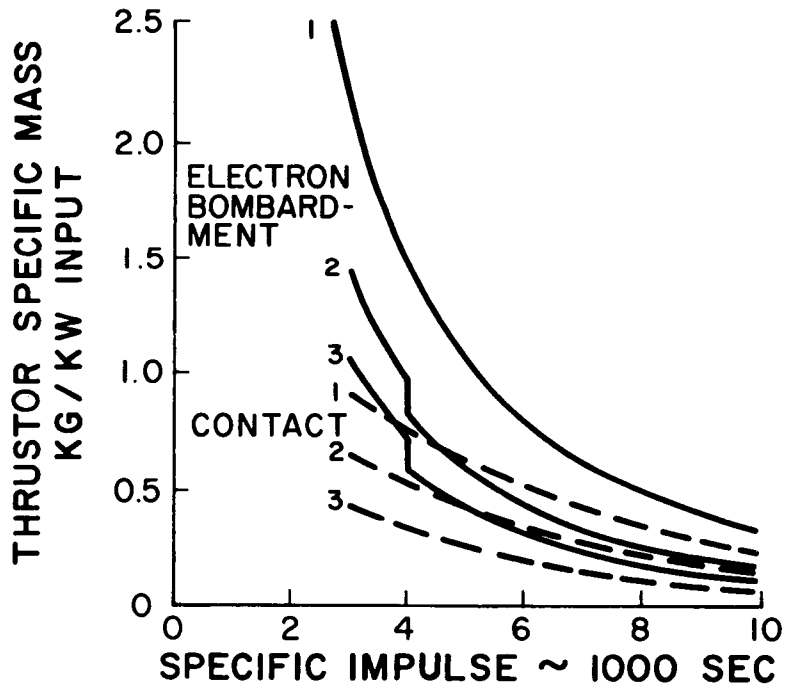

Figure 5-18. Thrustor Size and Weight

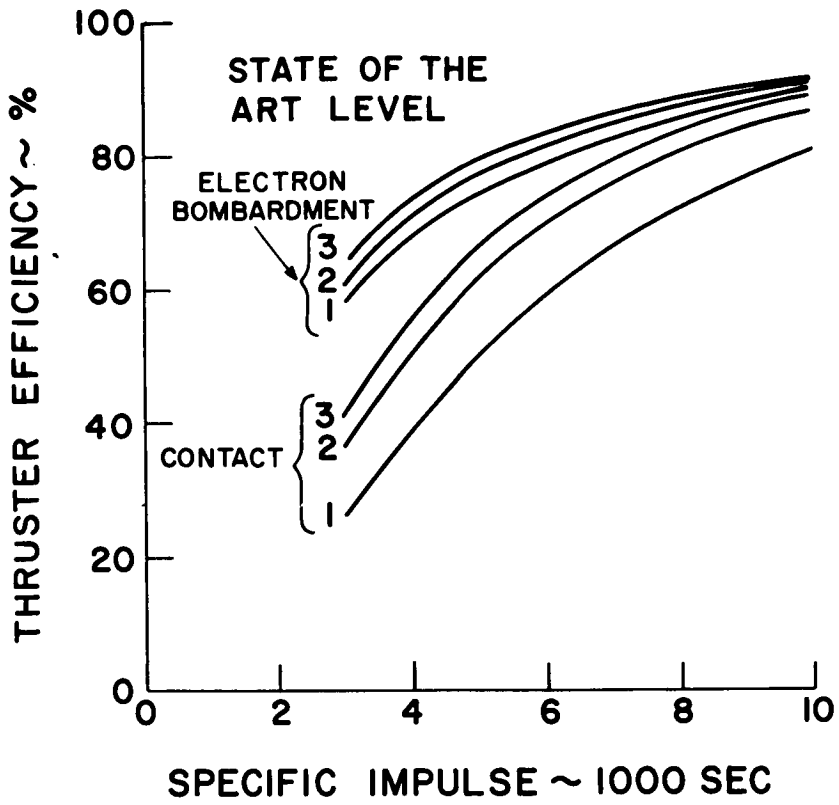

Figure 5-19. Thrustor Efficiencies

The other parts of the electrical propulsion system are the power conditioning and distribution system, and the propellant storage and distribution system. The power conditioning and distribution system is dependant on the selections of thrustor and assumed state-of-art for rectifiers, transformers and other parts. The range of specific weight is between 1 and 3 kg/ KW_e. Since the power supply specific weight (assuming a SNAP-50/ SPUR type system) is in the 10 kg/ KW_e range, the power conditioning and distribution system weight increases the overall power subsystem specific weight by 10 to 30 percent, and this in turn will increase mission trip time and required power supply life rating by an equivalent amount.

The propellants used in all of the electric thrustors considered for the lunar cargo transport system are liquid metals, which are reasonably dense. Estimates of tankage mass are in the range of 5 percent of the propellant mass. Other items such as propellant margin and propellant feed system are apt to account for another 5 percent of propellant mass. Thus, the propellant utilization is assumed at 90 percent of the gross weight of propellant + tank +

structure + feed system. In the case of hydrogen propellant, the propellant utilization is estimated at 80 percent because of the large volume required.

3. Lunar Landing Craft

The Lunar Lander in the launch configuration shown in Figures 5-20 and 5-21, is a conical frustum 5.79 m (228 in.) high, tapering with an 8^{o} half-cone angle to remain within the 10^{o} half-cone angle of the nuclear reactor scatter shield. The base is 10.06 m (396 in.) in diameter to mate with the S-II stage of the Saturn V booster, and the top is 8.25 m (335 in.) in diameter to mate with the powerplant primary radiator.

An adapter section 30.5 m (12 in.) high joins the lander shell to the booster. This section provides access to the bolt circle at the booster interface, contains the booster stage separation system, and accommodates the electrical propulsion thrustors. After launch, a shaped charge separates the lander from the adapter so that the adapter remains with the S-II stage.

The electron bombardment thrustors, each 1.5 m in diameter, are arranged in three groups of three. Each group is fed by a single mercury propellant tank. The spherical propellant tank is mounted above the thrustors, along with associated power conditioning and controls equipment. The thrustors are jettisoned after use in lunar orbit to minimize the lander mass.

The cargo compartment, located on the lander axis, is 3.66 m (12 ft.) in diameter and 5.49 m (18 ft.) high for a volume of 57.6 m^3 (2036 ft^3). However, the cargo compartment may be extended inside the primary radiator to an overall length of 18 m (59 ft.) to accommodate low density cargoes or oversize items of equipment.

Separation of the lander from the powerplant is accomplished by a shaped charge at the ring joining the lander to the primary radiator. Braking from lunar orbit is provided by six RL-10 engines. Propellant for these engines is stored in cylindrical tanks; six with liquid hydrogen and three with liquid oxygen. Throttle control is used to adjust descent speed. A secondary propulsion system using N_2O_4 and UDMH-N_2H_4 is used to provide attitude control torques.

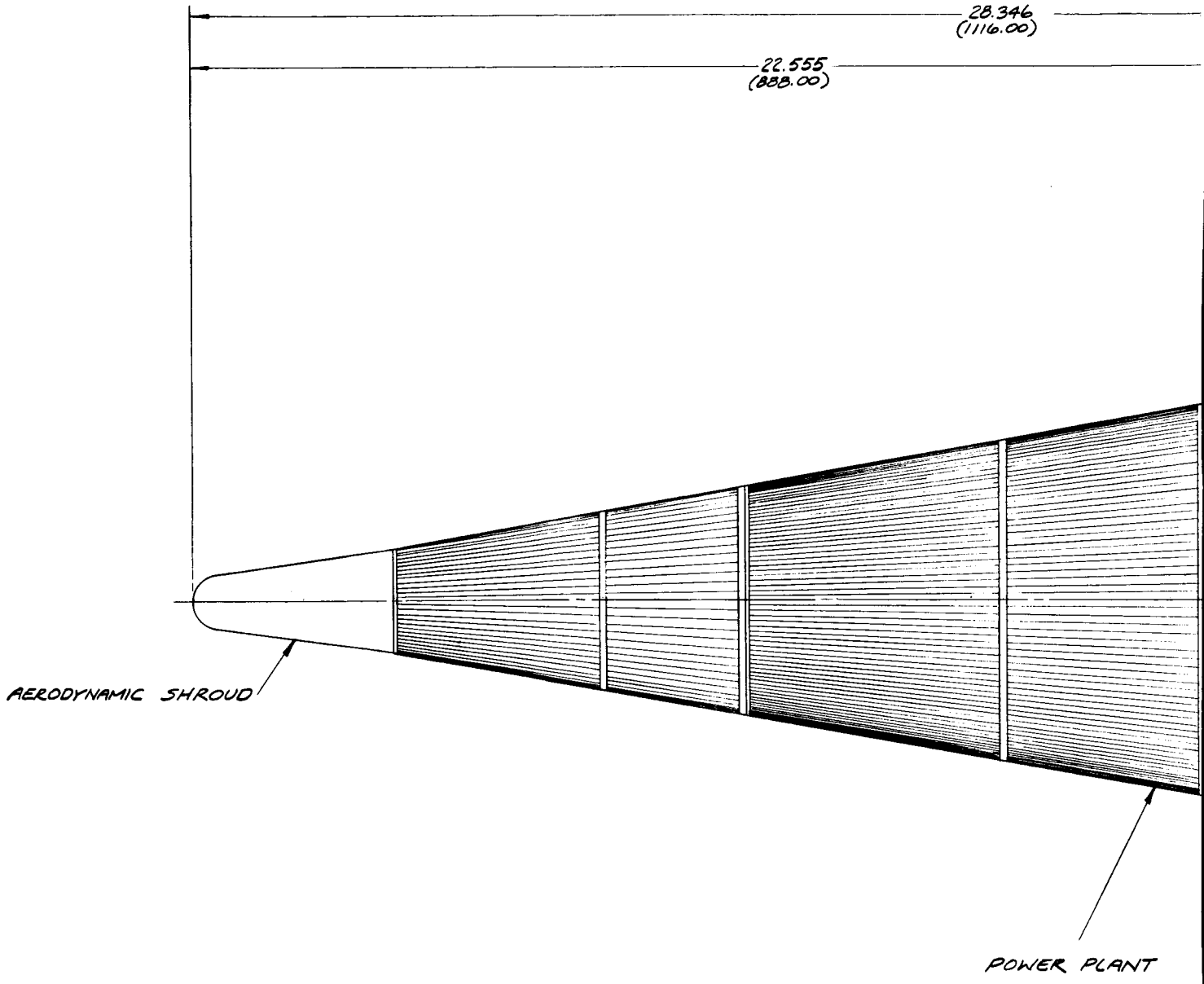

SCALE:- METERS

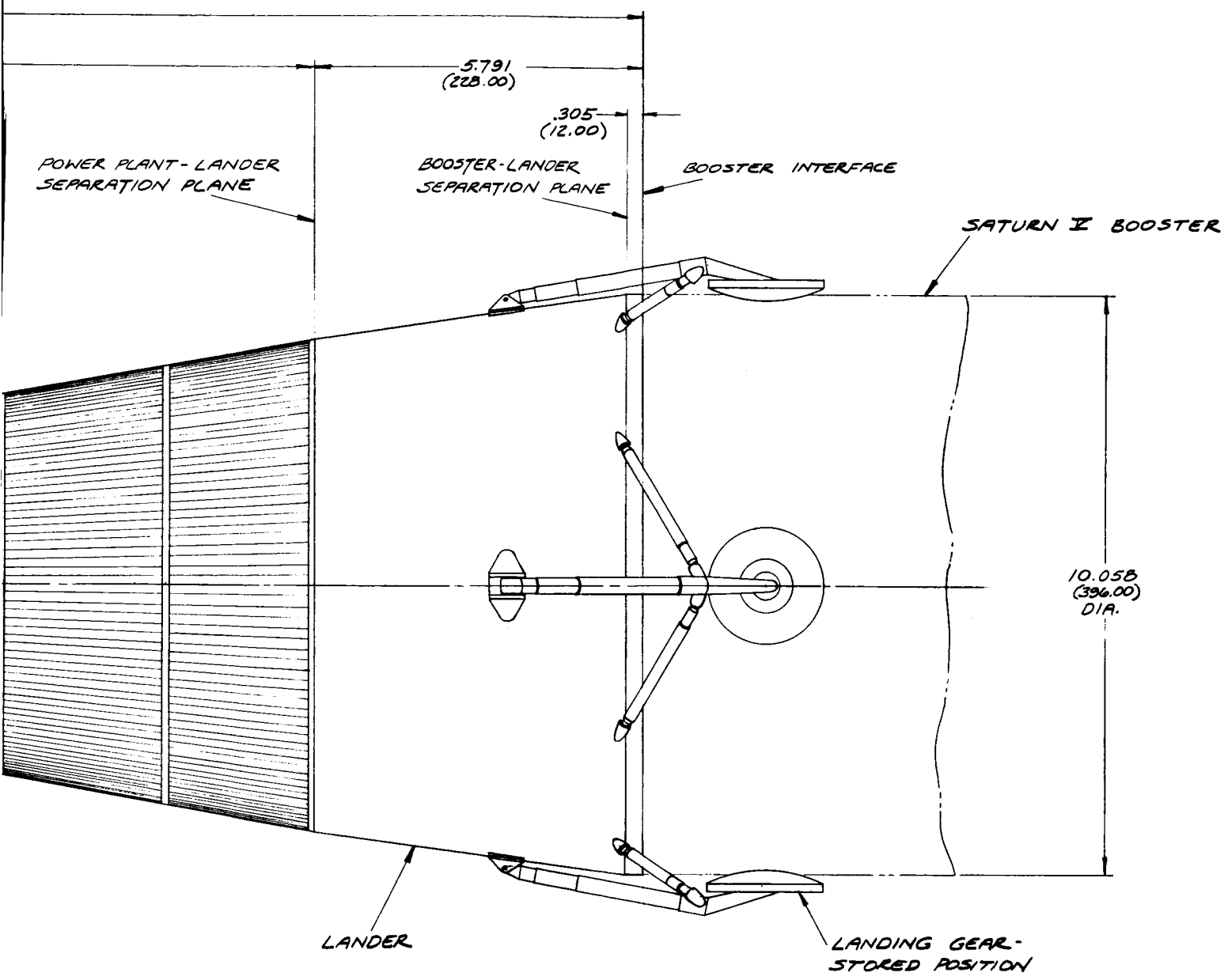

Figure 5-20. General Arrangement of Electrically Propelled Lunar Cargo Vehicle

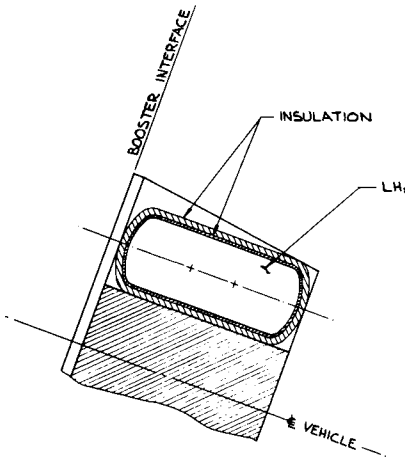
BOOSTER INTERFACE
INSULATION
LH_2 TANK
℄ VEHICLE

SECTION **B - B**

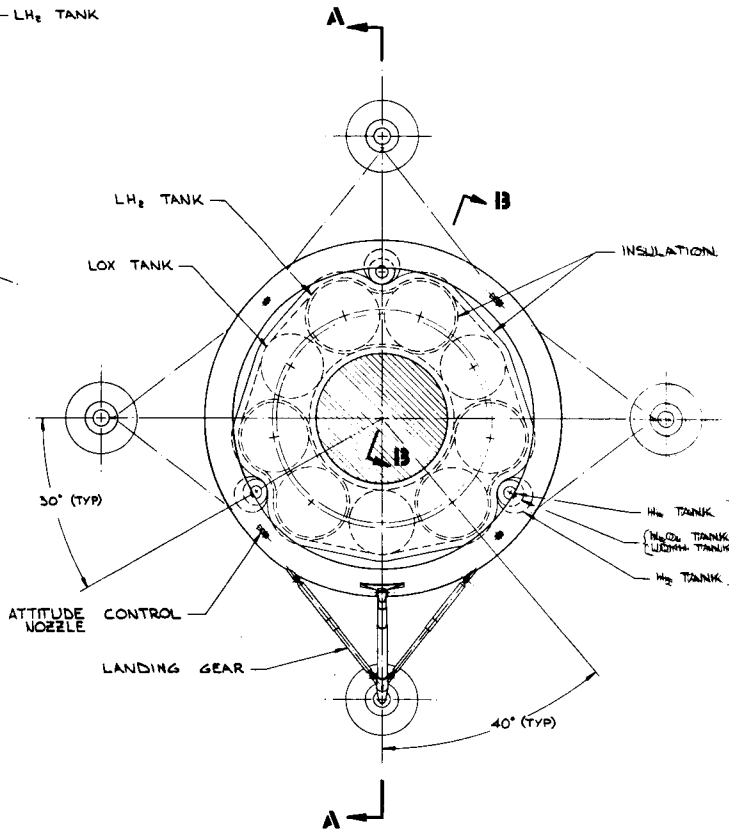
A
B
LH_2 TANK
LOX TANK
INSULATION
30° (TYP)
He TANK
N_2O_4 TANK
UDMH TANK
H_2 TANK
TYP 3 PLACES
ATTITUDE CONTROL NOZZLE
LANDING GEAR
40° (TYP)
A
B

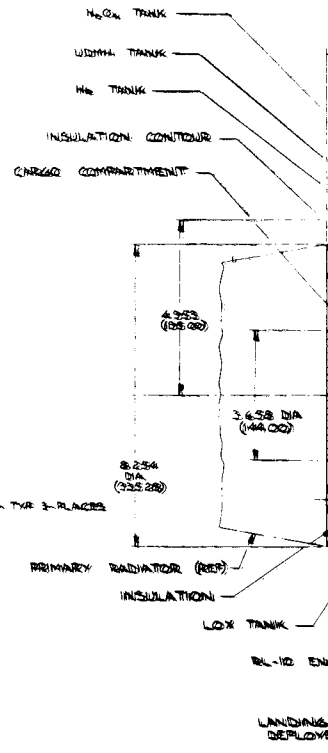
N_2O_4 TANK
UDMH TANK
He TANK
INSULATION CONTOUR
CARGO COMPARTMENT
4.953 (195.00)
3.658 DIA (144.00)
8.254 DIA (325.28)
PRIMARY RADIATOR (REF)
INSULATION
LOX TANK
RL-10 EN
LANDING
DEPLOY

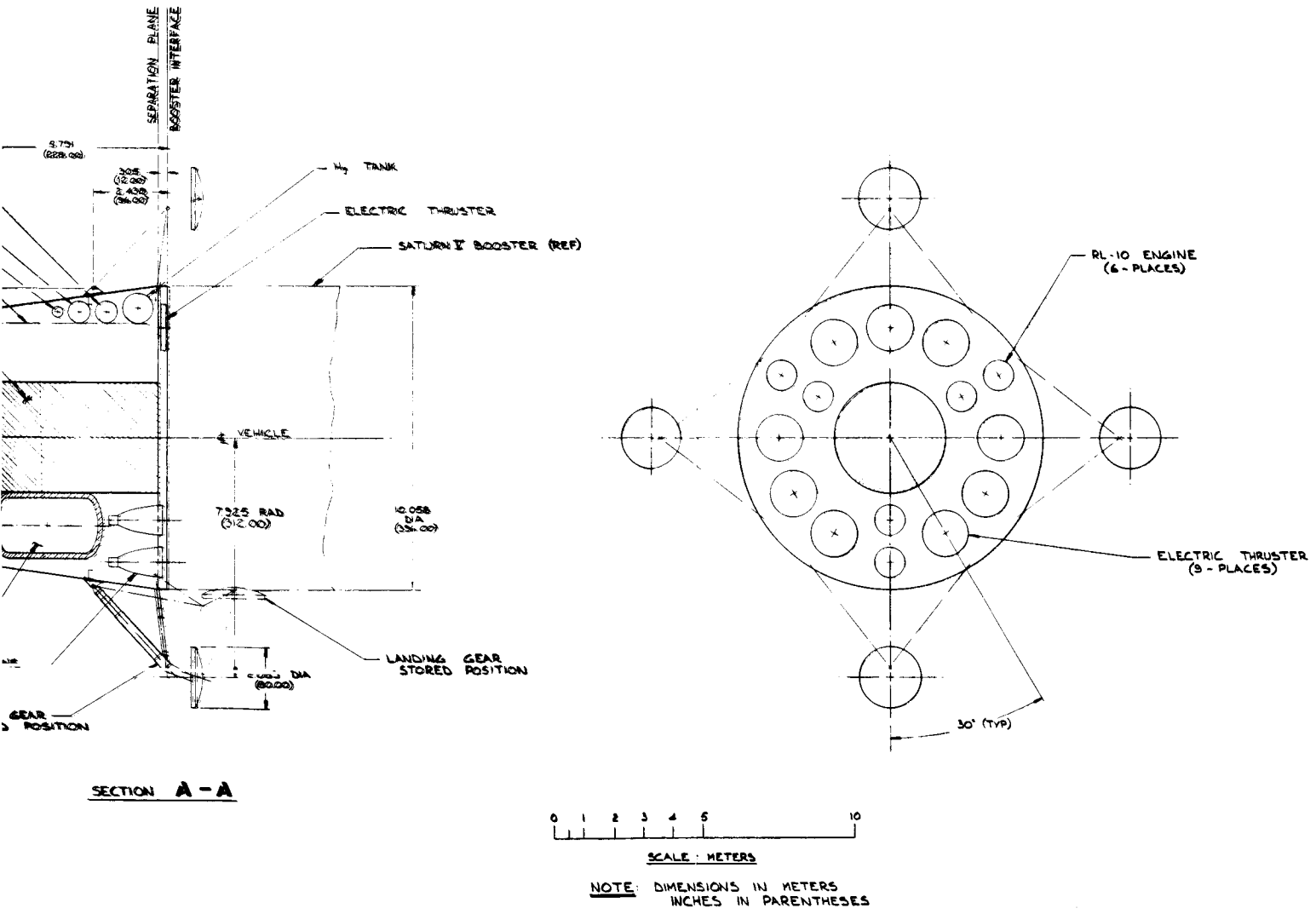

Figure 5-21. General Arrangement of Lunar Landing Craft

Four landing legs are mounted externally on the lander. During launch, the legs are folded against the side of the vehicle with the feet in contact with the unpressurized upper skirt on the S-II stage. After launch and prior to booster separation the legs are extended into landing position. In this position, the landing feet lie on a circle 15.8 m (52 ft.) in diameter.

The six RL-10 engines provide a total braking thrust of .4 MN (90,000 lbf). Propellant is liquid oxygen/ liquid hydrogen stored in cylindrical aluminum tanks surrounding the cargo compartment; six with liquid hydrogen and three with liquid oxygen. The tanks are covered with a multiple layer radiation barrier insulation (e.g., aluminized mylar) to reduce propellant boil off. Mission analysis indicates that the optimum ratio of propellant boil off mass to insulation mass is approximately 2. The following assumptions were used in determing the insulation requirements:

LH_2 Storage Temperature:	$38.3^{o}K$ ($-423^{o}F$)
LOX Storage Temperature:	$108^{o}K$ ($-297^{o}F$)
Lander Ambient Temperature:	$288^{o}K$ ($26^{o}F$)
LH_2 Heat of Vaporization:	442kJ/ kg (190 BTU/ lbm)
LOX Heat of Vaporization:	213 kJ/ kg (92 BTU/ lbm)
Storage Time:	5000 hr.
Insulation Conductivity:	$.173\ mW/m^{o}K\ \left(10^{-4}\left(\frac{BTU\text{-}ft}{ft^2\ hr\ ^{o}F}\right)\right.$
Insulation Density:	$35\ kg/m^2$ ($2.2\ lbm/ft^3$)

The insulation is wrapped around all tanks collectively rather than individually in order to minimize the boundary surface area. To eliminate heat transfer from the LOX tank to the LH_2 tank, additional layers of insulation are wrapped around the LH_2 tank, in accordance with the difference in storage temperatures. Since insulations of this type exhibit considerable anistropy in conductivity, each layer will be essentially isothermal. To minimize heat leaks through the insulation, the tanks are supported by tubular struts of glass fabric laminate.

The lander ambient temperature can be maintained close to sink temperature if heat transfer from the primary radiator is minimized. Conduction from the primary radiator is greatly reduced by partial separation of the joint between the radiator and the lander. After launch

and prior to start up of the nuclear powerplant, the structural attachment can be severed, retaining only a pinned connection of sufficient size to carry the loads due to electrical propulsion thrusting and attitude control torques. The pinned connections would permit radial expansion of the higher temperature primary radiator. Radiation from the primary radiator is reduced by using a low emissivity surface treatment on the inside surface of the radiator and by insulation acrosss the top of the lander.

The secondary propulsion system, used to provide attitude control torques, is assumed to have the following characteristics:

Total Impulse:	3.12 MN-sec. (700,000 lbf-sec)
Fuel:	UDMH-N_2H_4
Oxidizer:	N_2O_4
Oxidizer/ Fuel Ratio:	1.64
Operating Pressure:	1.72 MN/ m^2 (250 psi)
Pressurizing Gas:	He
Helium Storage Pressure:	34.5 MN/ m^2 (5000 psi)

The lander primary structure consists of an outer shell and three ring frames. The shell resists axial compression and bending loads while the ring frames distribute the concentrated loads of the cargo and tank supports, and the landing legs. The outer shell is beryllium with longitudinal stiffeners, sized by comparison with the bending test data of M. F. Card*. The equivalent axial load on the outer shell obtained by combining axial and bending loads at the maximum " $q\alpha$ " launch condition, is estimated to be 7.12 MN (1.6×10^6 lbf) for a .90 launch probability.

Propellant tanks for the primary, secondary, and electrical propulsion systems are supported by pin-ended struts attached to the three ring frames. Design loads are assumed to result from dynamic response to booster vibration during launch, assuming a 1 g longitudinal input at the booster interface and a transmissibility of 10. The cargo compartment

* Card, M. F., "Bending Tests of Large-Diameter Stiffened Cylinders Susceptible to General Instability", NASA TN D-2200, April 1964.

is supported primarily by the center ring so that the inertia loads of the cargo on lunar landing will relieve the vertical reactions on the ring from the landing legs.

The landing legs are pin-ended tubular steel struts with aluminum honeycomb for energy absorption in each main strut. The energy absorption capability is based on a free fall from 3 m above the lunar surface and landing on two of the four legs. The feet are sized to limit the soil bearing pressure to 41.2 KN/m^2 (6 psi). The landing legs are designed to withstand the loads resulting from 6 g axial and 1 g lateral deceleration (earth g's reference) on two of the four legs. The landing loads cause critical bending in the central ring to which the main strut pivot fittings are attached. This ring is assumed to be titanium with an ultimate tensile strength of 1.24 GN/m^2 (180,000 psi).

Table 5-6 shows the mass breakdown for the lunar lander for a range of lander sizes.

TABLE 5-6. MASS BREAKDOWN FOR VARIOUS LUNAR LANDER SIZES

	A	B	C
Primary Structure, lb	5740	4710	4180
Outer Shell	2430*	1840*	1840**
Ring Frames	1500	1310	1110
Landing Gear	1900	1560	1230
Primary Propulsion, lb	83625	69280	54670
Propellant (useable)	64500	53100	41700
Propellant Boil off	7360	6250	5020
Insulation	3205	2730	2190
Tankage	3490	2970	2380
Engines & Accessories	4470	3730	2980
Support Structure	600	500	400
Secondary Propulsion, lb	2635	2635	2635
Propellant	2285	2285	2285
Tankage	180	180	180
Engines & Accessories	25	25	25
Support Structure	145	145	145
Cargo (including structure)	78000	63375	48515
TOTAL, lb	170,000	140,000	110,000
Cargo Fraction	.46	.45	.44

* 130 lbs remains with booster

** 520 lbs remains with booster

A lunar cargo lander configuration has been considered in which the nuclear powerplant is landed with the cargo section. The changes in the lander from the all-cargo configuration include redesign of the landing legs and associated portions of the primary structure. To enable use of the nuclear powerplant for a lunar base, an auxiliary shield and means for assembling it must be provided.

The landing weight of this configuration remains the same as the all-cargo configuration described previously; therefore, much of the lander remains unchanged, including the primary and secondary propulsion systems. However, the addition of the nuclear powerplant results in a significant change in the center of gravity. In order to provide the same margin of stability on touchdown, it is necessary to increase the landing leg span to approximately 24 m (79 ft). The weight of a simple, pivotted main strut to reach this span would be prohibitive. In addition, a leg folded for launch in the same manner as that used on the all-cargo configuration would have its foot in contact with the pressurized tank wall of the S-II booster stage. Therefore, a folding leg, shown in Figure 5-22, was chosen. During launch the legs are folded against the side of the lander shell structure with the feet up so that they do not interfere with booster separation.

The deployment sequence is shown in Figure 5-23. Deployment is initiated by driving leg "A" about hinge "B". During the first 11.5^{o} of rotation, struts "C" increase in length by telescoping, locking in the extended position when strut "D" passes over center. Rotation of strut "A" then continues until the leg is in the landing position. Travel is limited by cables "E" which feed out from reels inside the lander shell.

At touchdown, members "A" and "E" present a rigid truss and energy is absorbed by honeycomb structure in the telescoping sections of struts "C" and "D". Struts "A" and "D" act as pin ended columns in compression, while cables "E" are always in tension. Struts "C" are in tension due to the vertical landing loads, but may be put in compression by lateral landing loads. The legs are designed to withstand the loads resulting from 6 g axial and 1 g lateral deceleration (earth g's reference) on two of the four legs.

For lunar base operation of the nuclear powerplant additional shielding is required beyond the 10^{o} half angle cone provided by the existing shield. Increasing the size of the fixed shield to provide hemispherical coverage would result in a prohibitive center of gravity location, for both the launch and lunar landing conditions, as well as presenting an undesireable aerodynamic shape. An acceptable solution is to provide auxiliary shielding that is used only during lunar base operation, as shown in Figure 5-24.

A fixed, cylindrical tungsten shield around the reactor provides sufficient shielding so that the base of the powerplant can be safely approached by personnel with the reactor shut down. After lunar landing, the two auxiliary shield segments of lithium hydride can then be removed from the cargo compartment and placed in position at the base of the lander. From this position the shield segments can be raised on tracks up the side of the radiator by cables. When pulled into position, the shield segments interlock with each other and the fixed shield.

When the nuclear powerplant is to be replaced, the auxiliary shield segments can be removed and used on the replacement powerplant. The ultimate solution, after lunar soil properties are known, would be to provide only a shell which could be filled with lunar soil to act as an auxiliary shield.

For space operation of the nuclear powerplant, separation joints are provided between primary and secondary radiators and between the powerplant and the lander. These joints are separated after launch to permit thermal expansion and limit thermal conduction. Sufficient tension capability is retained to carry the bending loads due to attitude control torques. When the powerplant is landed on the lunar surface, these joints must be capable of withstanding the landing loads. With an ideal landing, no tension loads occur and the joints have sufficient shear and compression capability. However, to allow for the effects of elastic rebound and unusual dynamic conditions, it would be desireable to increase the tension capability of the joints prior to lunar landing. This could be accomplished by actuators which clamp the two rings of the joint together.

Once the powerplant has landed, the problem of heat conduction across the joints occurs again by the introduction of a compression load due to lunar gravity. The actuators clamping the rings of the joint together should then be released and the joint separated by contacts of high thermal resistance.

A summary of mass values is presented in Table 5-7.

TABLE 5-7. WEIGHT SUMMARY OF LUNAR LANDING CRAFT

Powerplant		18,690 lbs
Auxiliary Shield		20,000
Primary Propulsion		83,625
Secondary Propulsion		2,635
Primary Structure		9,930
Outer Shell*	2,430	
Ring Frames	1,960	
Landing Gear	5,000	
Cargo (Including Structure)		35,660
		170,000 lbs

* 130 lbs remains with S-II stage.

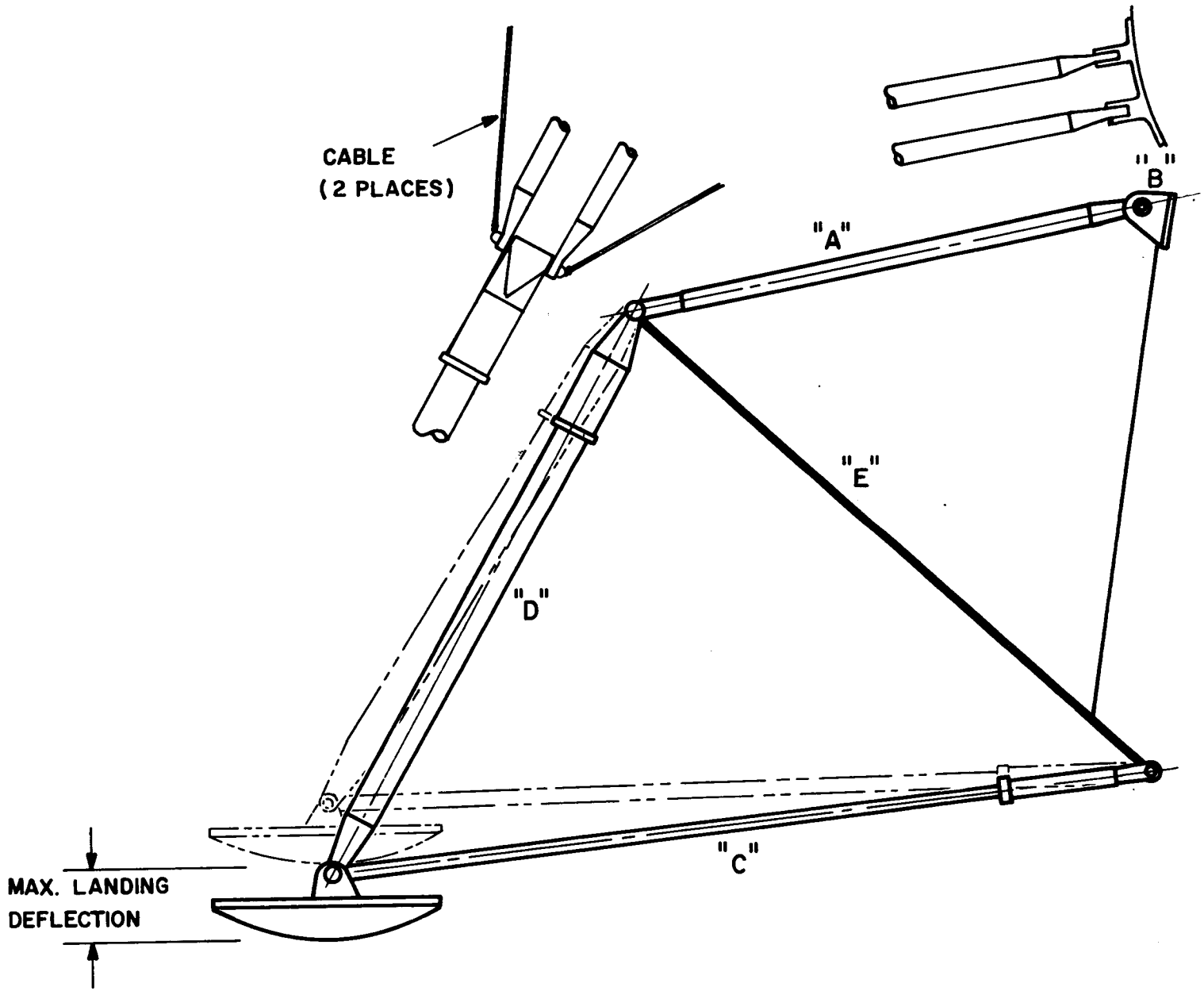

Figure 5-22. Lunar Landing Leg (for Lunar Cargo Vehicle with Powerplant)

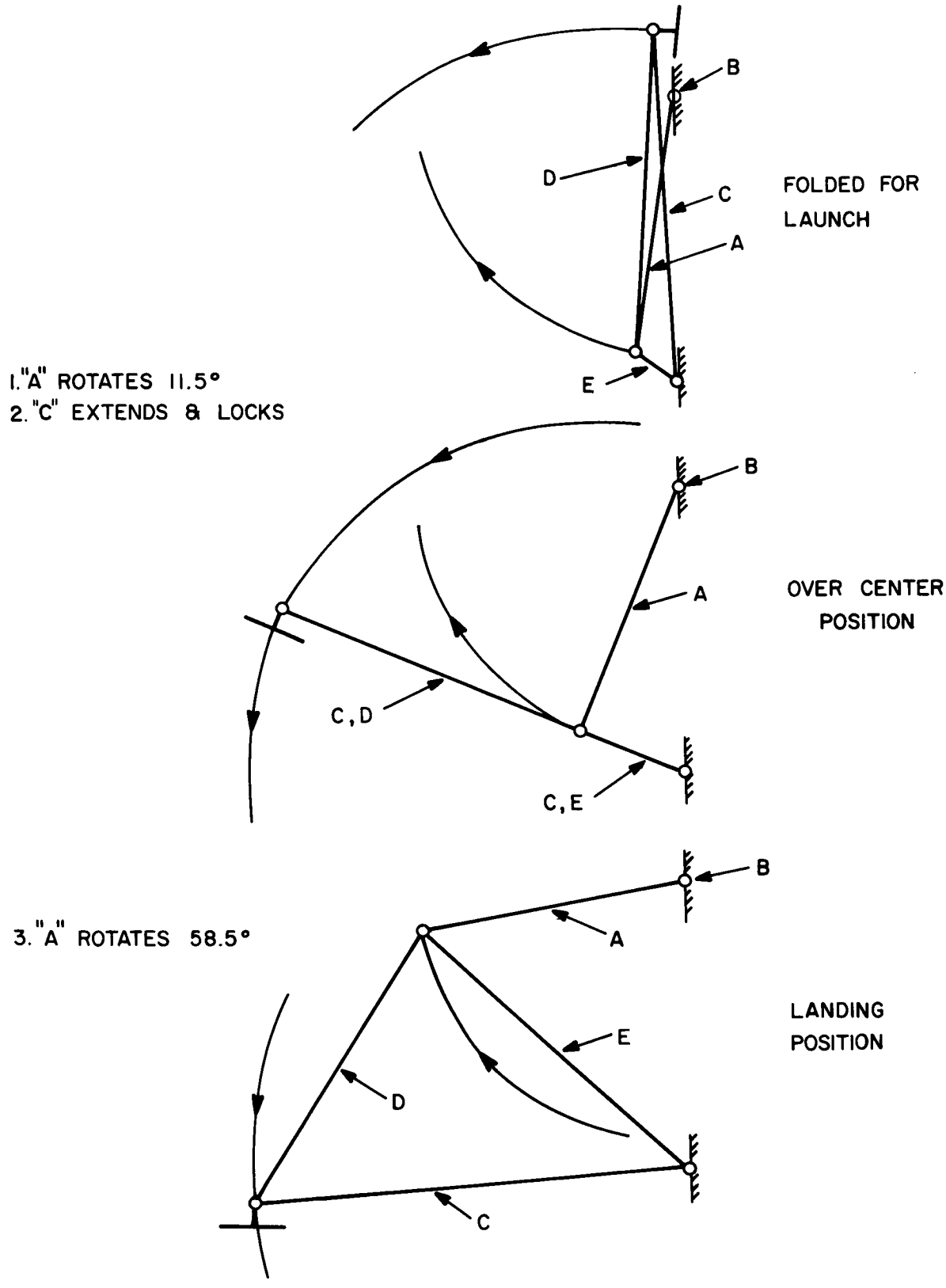

Figure 5-23. Landing Leg Deployment

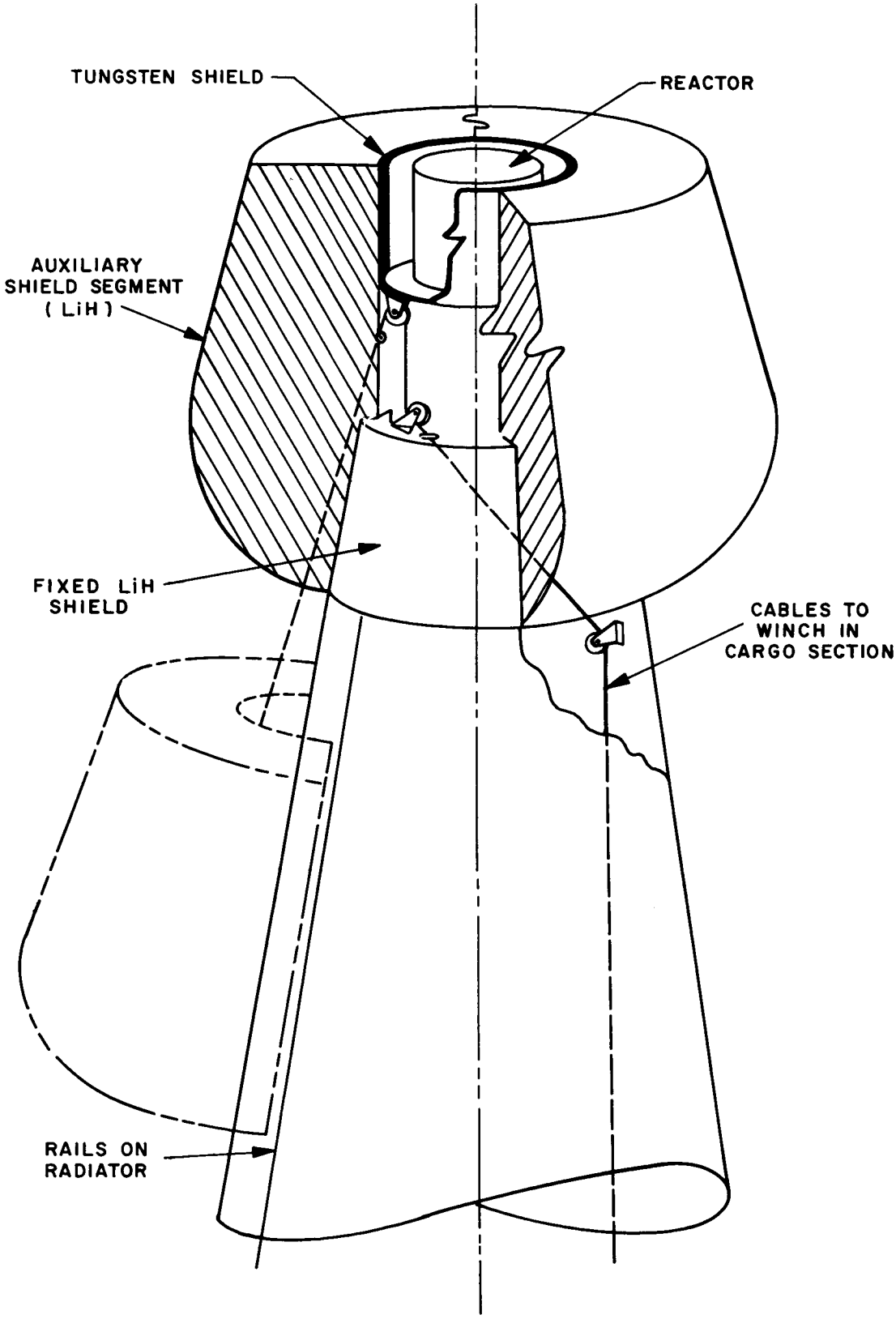

Figure 5-24. Auxiliary Shield

B. MISSION OPERATIONAL MODES

The carrier vehicles for the logistic materials transported from the earth's surface to the lunar surface can be configured for many varying operational modes. Either single-use or re-usable vehicles can be considered for each of the three steps in the transportation pattern, i.e., earth launch, orbit transfer, and lunar landing.

In the present study only the single-use Saturn V class of booster is considered for the first transportation step, i.e., ascent from the earth's surface to circular orbit. The key influence of the earth launch system on lunar logistics is the cost per unit mass to orbit. Additional influences are booster payload mass, geometry, center of gravity, interface acceleration pattern, ground handling procedures and launch procedure. The results achieved, based on the use of the Saturn V, can generally be converted to application to other boosters of interest.

Many operational variations exist for the orbit transfer phase as shown in Table 5-8. The one-way trip mode requires abandonment of a nuclear power supply in lunar orbit after each mission. However, this scheme is mechanically least complicated because space rendezvous and assembly are not required. The single powerplant shuttle not only requires orbital mating but has an inherent matching difficulty between its initial voyage and subsequent voyages because the powerplant in the initial launch displaces either electric system propellant or lunar landing craft. This situation is improved by launching two vehicles to mate in earth orbit for the first outbound voyage. Because the number of powerplant trips is expected to be limited to about four (as a result of the powerplant life limitation), the initial voyage is quite influential in establishing optimum powerplant and landing vehicle size. The use of multiple powerplants is a second approach towards finding a more favorable powerplant and landing vehicle size compromise. More than two powerplants are probably not of interest because of the configuration problems brought about by the need for nuclear radiation shielding.

TABLE 5-8. BASIC OPERATIONAL MODES

- Δ One Way Trips
  - Single-Use Powerplant
- Δ Single Powerplant Shuttle
  - One or Two Initial Launches
  - Two to Four Outbound Trips
- Δ Multiple Powerplant Shuttle
  - Two or Three Powerplants

In both the single and multiple powerplant shuttle operational modes, many options exist for disposition of electrical thrustors and propellant tanks. These options are:

1) Maintaining constant landing vehicle size between successive voyages and allowing thrustor jet velocity to vary

2) Maintaining constant thrustor jet velocity between successive voyages and allowing landing vehicle size to vary

3) Allow both landing vehicle size and thrustor jet velocity to vary between successive voyages to minimize transportation cost at constant powerplant life (or to minimize powerplant life at constant transportation cost)

4) Utilization of either constant, or variable specific impulse thrustors permanently mated to the powerplant (requiring in-space fluid line connections)

5) Utilization of separate electrical thrustors for the outbound orbit transfer permanently mated to the outbound propellant tanks, which are discarded in lunar orbit and replaced in earth orbit

6) Utilization of inbound electrical thrustors permanently mated to the powerplant requiring in-flight fluid line connections for the inbound thrustors only

7) Utilization of inbound electrical thrustors mated to the inbound propellant tanks abandoned in either earth orbit or later abandoned in lunar orbit, in either case thrustor and tank being replaced in earth orbit

8) Utilization of inbound electrical thrustor and propellant tank permanently mated to the powerplant and sized to accomplish all of the inbound voyages eliminating re-supply requirements.

The above options for the lunar logistic operational mode yield a large number of space vehicle configurations, which are classified by Figure 5-25. In the present study, performance estimates have been generated for the best of these many combinations.

The third and last transportation phase to be considered is the descent from lunar orbit to the lunar surface. A high thrust propulsion system such as nuclear or chemical rockets is necessary. Only the chemical rocket has been considered to date. The multiple-use lander appears to be at a disadvantage in terms of cargo delivery efficiency as shown in Figure 5-26 when propellants are supplied from the earth for both descent and ascent phases. The value of a multiple-use lander is the savings in not having to repetitively transport landing equipment and structure from the earth. However, reuse requires the transportation of additional propellant for a portion of the descent phase and for the entire ascent phase. This supplied material will exceed the mass of landing material for all situations. For example, a landing structure mass fraction of 0.15 yields a 0.4 cargo fraction of net material inserted in lunar orbit from earth using a single-use lander; and a 0.34 cargo fraction, using a multiple-use lander. Thus, it appears that only single-use lunar landers are of interest. The exploitation of lunar resources to manufacture chemical propellants will alter this conclusion and make the re-useable lunar lander the better approach.

Electrical propulsion has a unique degree of freedom advantage relative to high thrust rocket propulsion in that the thrustor jet velocity can be conveniently selected to match the available propellant to the characteristic velocity requirement for the voyage. As a result each division of booster payload into positive values for cargo, nuclear powerplant and electric thrustor propellants provides a real solution with a required thrustor jet velocity and resultant trip time. Thus, a parametric representative of trip time can be made as a function of lunar cargo and powerplant size selection. This representation is a function of several design states-of-art such as:

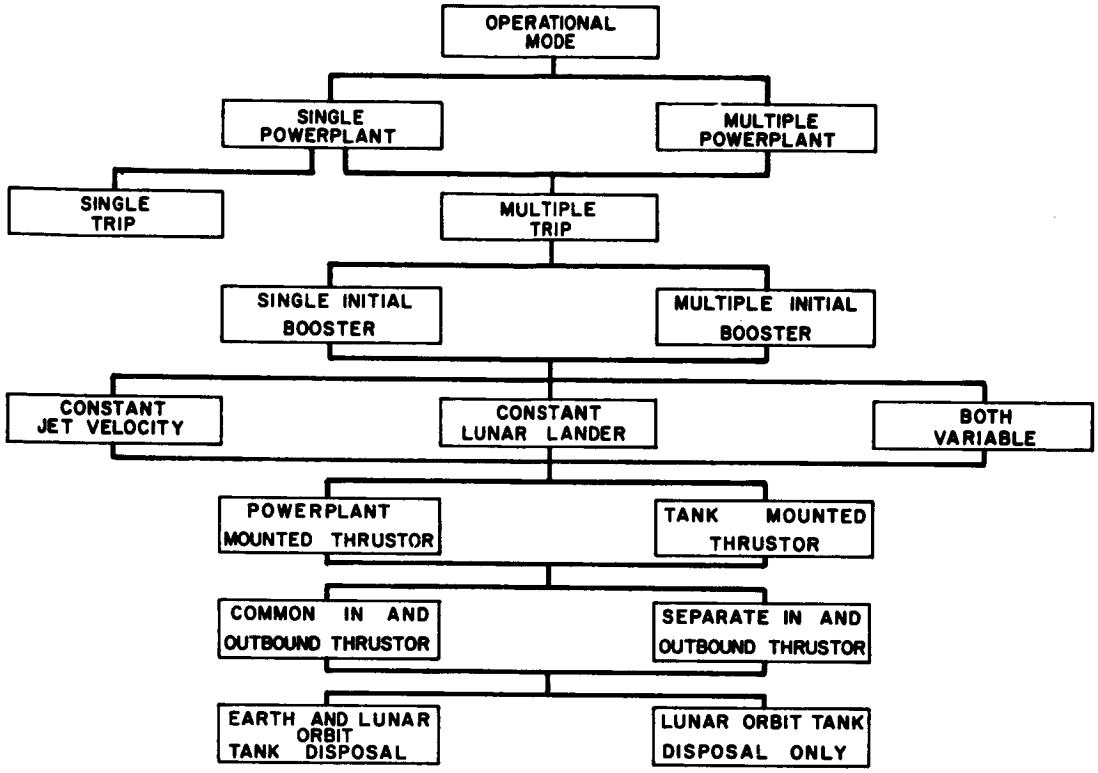

Figure 5-25. Lunar Cargo Vehicle Options

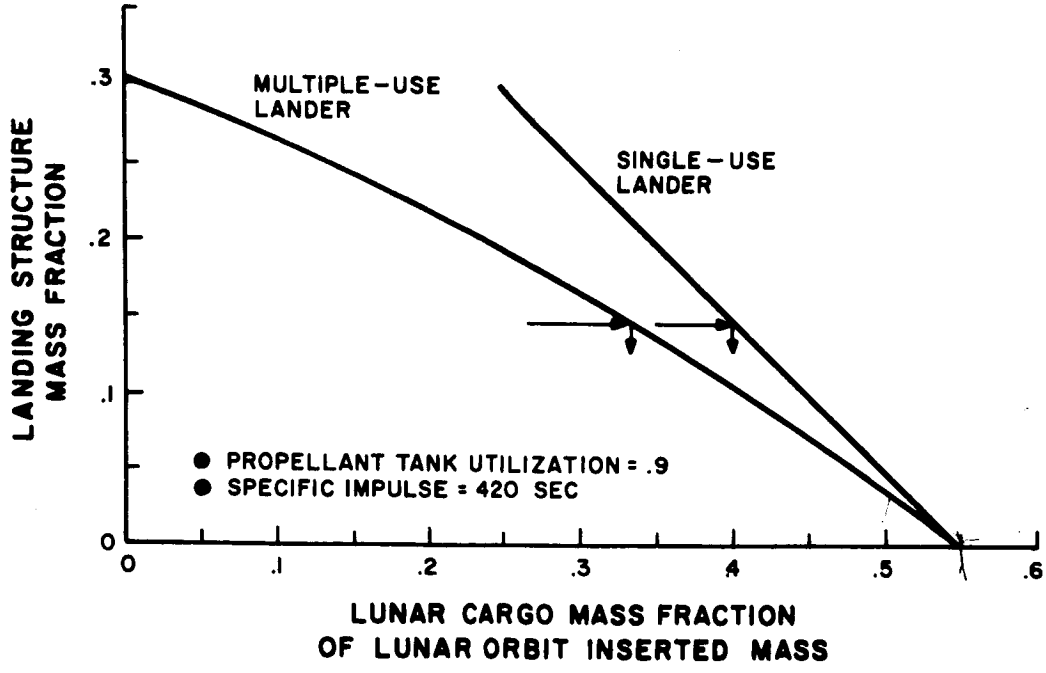

Figure 5-26. Comparison of Single-Use and Multiple-Use Lunar Landing Vehicles

1) Powerplant specific weight
2) Thrustor specific weight
3) Thrustor efficiency
4) Electric propellant tank utilization
5) Lander cargo fraction
6) Booster net orbital payload.

The following sections contain descriptions of the calculation approaches, assumptions and constraints imposed on each of the operational modes in this investigation.

1. Single Trip

The single trip mode performance is relatively simple to calculate and a convenient approach is described in Table 5-9. The characteristic velocity requirement and initial gross weight of the electric-propelled cargo vehicle are functions of the earth launch booster payload and orbit altitude capacity. The powerplant specific weight and a number of empirical parameters for thrustor performance and vehicle structure and tankage are determined by design studies. Other empirical parameters are obtained from cost studies. After all the equations and variables have been defined, two independent variables remain for consideration in an optimization study and these two variables can be selected in a number of ways. In Table 5-9 the design parameters selected are power rating of the nuclear-electric power supply and specific impulse of the electric thrustor. This selection allows direct computation of the performance characteristics.

A different selection of independent variables is desirable for performing an optimization study. This combination is system cost and qualified life, which cannot generally be used to obtain a direct solution. Several optimization approaches can be used. The power rating and specific impulse can be varied to minimize specific payload cost. Also, lines of either constant power rating, specific impulse, lunar cargo mass, or other desired variable can be plotted on a graph of specific payload cost versus power system life rating and the optimum performance curve drawn tangent to the bottom of the constant parameter curves. This latter approach is illustrated in Figure 5-27, where lines of constant lunar cargo mass per vehicle were used to generate the optimum performance curve by graphical means.

TABLE 5-9. SINGLE TRIP FERRY CALCULATION

Constraints		Characteristic Velocity	ΔV
		Initial Gross Weight	W_o
		Powerplant Specific Weight	w
Design Parameters		Power Rating	P
		Specific Impulse	I_{sp}
Equation	1	Final Vehicle Weight	$W_1 = W_o \exp^{-\Delta V/g I_{sp_2}}$
	2	Specific Power	$(P/T) = A_o + A_1 I_{sp} + A_2 I_{sp}$
	3	Thrustor Specific Weight	$w_e = B_1 + B_2 I_{sp}^{B_3}$
	4	Power-Propulsion Weight	$W_p = (w+w_e) P$
	5	Payload	$W_{pl} = W_1 - W_p - (W_o - W_1) w_t$
	6	Cost	$C = C_b + W_p C_p + (W_o - W_1) C_{pp}$
	7	Specific Payload Cost	$C_{pl} = \frac{C}{W_{pl}}$
	8	Trip Time	$t = \frac{(W_o - W_1) I_{sp} (P/T)}{3600P}$

The result of each of these optimization approaches is the elimination of at least one, and possibly two, independent variables to describe performance for each combination of constraints and assumed constants such as booster capability, power supply specific weight and cost. The optimization produces a specific payload cost as a function of power system life rating, which can minimize at either a finite or infinite value of powerplant life rating, depending on the cost relationships used. Thus, the absolute minimum of specific payload cost may be of less interest than the specific payload cost at particular powerplant life ratings.

The performance of the ion jet and arc jet thrustors are compared in Figure 5-28 for the single trip mode. The ion jet has a poor efficiency characteristic at specific impulse levels below 4000 seconds, whereas the hybrid arc jet efficiency is inclined to be fairly constant,

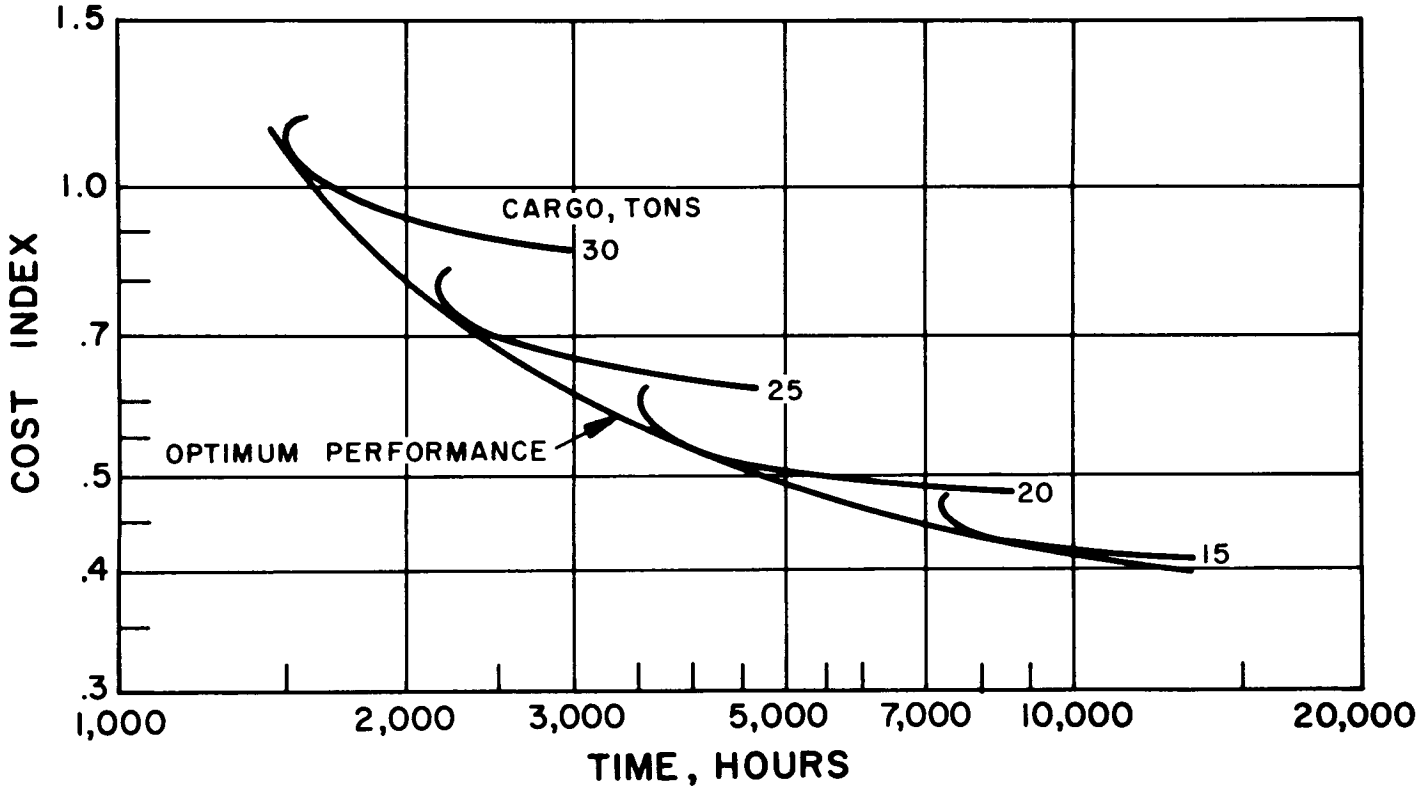

Figure 5-27. Optimization for Single Trip, Ion Jet Lunar Cargo System

if a non-dissociating propellant such as lithium is used. The difference in performance between the ion jet and the 70 percent efficient hybrid arc jet is shown to be small at low cost index values, which is the range of interest.

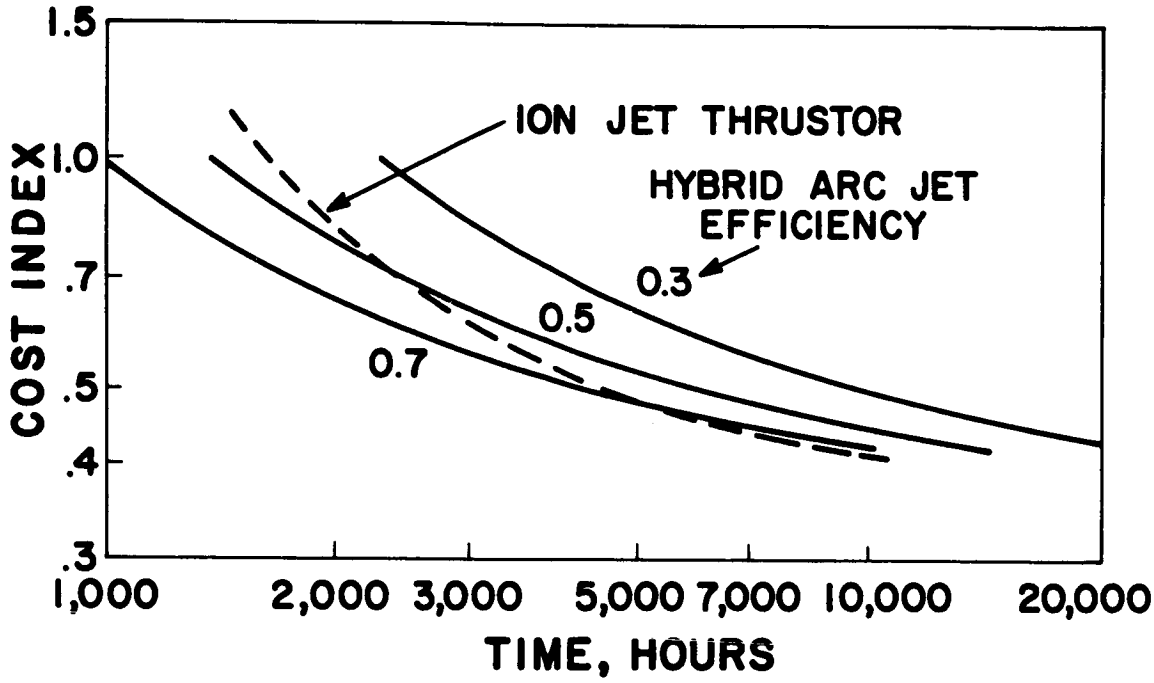

Figure 5-28. Trip Time Comparison Between Ion-Jet and Hybrid Arc-Jet Lunar Cargo System

An analytical technique to minimize specific payload cost at constant trip time with respect to specific impulse is described below. The specific payload cost equation of Table 5-9 was first simplified by eliminating the relatively minor effects of propellant tankage and propellants costs. Then it was differentiated with respect to specific impulse and the results, equated to zero:

$$\left.\frac{\partial C_{pl}}{\partial I_{sp}}\right|_t = 0 = \left[W_1 - W_p\right] C_p \frac{\partial W_p}{\partial I_{sp}} - \left[C_B + W_p C_p\right]\left[\frac{\partial W_1}{\partial I_{sp}} - \frac{\partial W_p}{\partial I_{sp}}\right] \qquad (1)$$

Equation (1) can then be rewritten as:

$$\frac{\partial W_1}{\partial W_p} = \frac{C_B + W_1 C_p}{C_B + W_p C_p} \tag{2}$$

The parameters, X and Y, were then defined by the equations:

$$X = \frac{3500 t W_p}{W_o} = \left[1 - (W_1/W_o)\right] I_{sp} (P/T) (w + w_e) \tag{3}$$

$$Y = \frac{\Delta V}{g I_{sp}} (W_1/W_o) = \frac{I_{sp}}{W_o} \frac{\partial W_1}{\partial I_{sp}} \tag{4}$$

Equation (3) was evaluated numerically from the propulsion system characteristics of Section 5A and represented empirically by the equation:

$$X = 600,000 + 24,200\, w + 17.9\, w\, I_{sp} \tag{5}$$

Similarly, Equation (4) was evaluated and replaced by the empirical relationship:

$$Y = \left[1.26 + 1.22\,(10)^{-3} I_{sp}\right]^{-1} \tag{6}$$

Equations (3) and (5) were then combined to obtain:

$$\frac{\partial W_p}{\partial I_{sp}} = \frac{W_o}{3600 t} \frac{\partial X}{\partial I_{sp}} = 4.97\,(10)^{-3} \frac{w W_o}{t} \tag{7}$$

Equations (4) and (7) were then substituted into Equation (2) to obtain:

$$\frac{Yt}{4.97(10)^{-3} w I_{sp}} = \frac{C_b + W_1 C_p}{C_b - W_p C_p} \tag{8}$$

An approximate relationship for the optimum specific impulse can be obtained from Equation (8) by combining it with Equations (3) through (6):

$$(I_{sp})_{opt} \cong \sqrt{\frac{C_b t + (166.7 + 4.035\ w)\ W_o C_p}{6.06(10)^{-6}\ w\ (C_b + 1.03\ W_o C_p)}} \qquad (9)$$

The resulting Equation (9) can be added to the equations of Table 5-9 in order to eliminate one of the design degrees of freedom. The other degree of freedom has been retained in order to obtain performance capabilities over a range of trip times.

2. Multiple Trip Ferry

The multiple trip ferry mission profile is illustrated in Figure 5-29. It consists of three types of trips - initial, middle, and terminal. These trips differ from each other by the following:

a. Initial Trip - Either one or two boosters can be used to launch the powerplant and the initial trip propellant and payload vehicle into Earth orbit.

b. Middle Trip - One booster is used for each middle trip to launch its propellant and payload module.

c. Terminal Trip - One booster is used but propellant is provided for only a one-way trip.

All multiple trip missions include an initial and terminal trip. Two trip missions have no middle trip, three trip missions have one middle trip, four trip missions have two, etc.

The one-way performance calculation procedure shown in Table 5-9 can be used for analyzing the terminal trip. Table 5-10 illustrates the corresponding calculation procedure that must be used for the initial and middle round trips. It differs from the one way procedure because of the provision for inbound propellant and for an inbound specific impulse that may be different from the outbound value. The missing equations for specific power and thrustor specific weight are identical to those indicated in Table 5-9. These equations

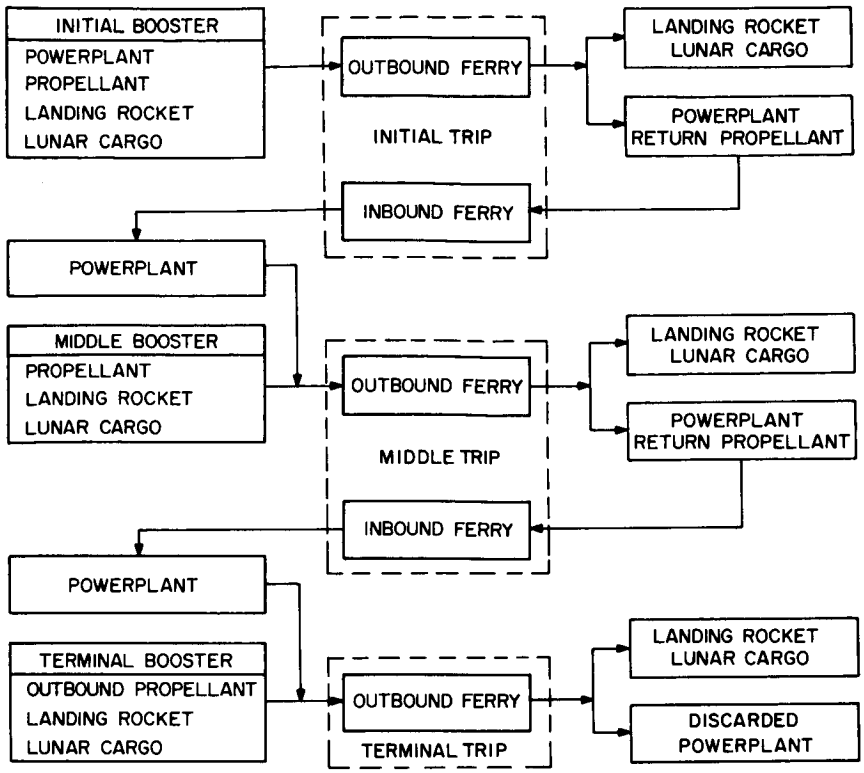

Figure 5-29. Multiple Trip Single Powerplant Model

must, however, be evaluated for both the outbound and inbound engines if separate specific impulse levels are used. Note that the powerplant cost is omitted for the middle and terminal trips. If the middle and terminal trips are assumed to use one booster and the initial trip powerplant, the maximum number of design degrees of freedom will be:

Initial Trip - $(N_b, P, I_{spo}, I_{spi})$	- 4
Middle Trip - (I_{spo}, I_{spi})	- 2
Terminal Trip - (I_{spo})	- 1
Total	- 7

The multiple trip design can be further constrained by the following assumptions:

- The initial trip is restricted to either one or two boosters (1).
- (1) The payload module is identical for all three types of trips (2), or
  (2) A single thrustor and specific impulse is used for all five types of legs (4).

TABLE 5-10. ROUND TRIP FERRY CALCULATIONS

Constraints		Characteristic Velocity	ΔV
		Initial Gross Weight per Booster	W_{oo}
		Powerplant Specific Weight	w
Design Parameters		Number of Boosters	N_b
		Power Rating	P
		Specific Impulse - Outbound	I_{spo}
		- Inbound	I_{spi}
Equations	1	Initial Gross Weight	$W_o = N_b W_{oo}$ (Initial Trip) $= W_{oo} + W_p$ (Remaining Trips)
	2	Power-Propulsion Weight	$W_p = (w + w_{eo} + w_{ei})\, P$
	3	Lunar Arrival Weight	$W_1 = W_o \exp^{-\Delta V/g\, I_{spo}}$
	4	Inbound Mass Ratio	$(W_2/W_3) = \exp^{\Delta V/g\, I_{spi}}$
	5	Earth Arrival Weight	$W_3 = \dfrac{W_p}{1 + (1 - W_2/W_3)\, w_t}$
	6	Lunar Departure Weight	$W_2 = (W_2/W_3)\, W_3$
	7	Payload	$W_{pl} = W_1 - w_t (W_o - W_1) - W_2$
	8	Cost	$C = N_b C_b + W_p C_p + (W_o - W_1 + W_2 - W_3)\, C_{pp}$
	9	Outbound Trip Time	$t_o = \dfrac{(W_o - W_1)\, I_{spo}\, (P/T)_o}{3600P}$
	10	Inbound Trip Time	$t_i = \dfrac{(W_2 - W_3)\, I_{spi}\, (P/T)_i}{3600P}$

The numbers in parentheses above refer to the number of degrees of freedom removed by each constraint. The sections below will describe the results of preliminary studies of the effects of the above constraints.

Performance of the multiple-trip ferry is compared to the single trip mode in Figures 5-30 and 5-31 for ion jet thrustors and hybrid arc jet, respectively. On the basis of power supply life, the single trip mode shows the better performance. However, on the basis of trip time the multiple trip ferry is more advantageous, particularly after the initial outbound trip. The trip time can be reduced 25 percent for the second and subsequent trips relative to the single trip mode at 0.5 cost index using the data in Figure 5-30.

a. Two Boosters for Initial Trip

The reason for considering the use of two boosters to launch the first earth orbit to lunar orbit voyage is to achieve a better match between powerplant size and spacecraft gross mass on both the first and subsequent trips. As mentioned previously, the powerplant mass displaces electric propulsion system propellant and/or lunar landing craft on the first earth launch as compared to launches for subsequent trips. The two booster approach consists of the following steps:

(1) Launch #1: Assembly consisting of nuclear power supply, lunar landing craft, electric thrustors and a part of the electric-thrustor-propellant is mounted on top of a Saturn V booster and launched into a parking orbit.

(2) Launch #2: Assembly consisting of a second lunar landing craft and the remainder of the electric-thrustor-propellant is mounted on a second Saturn V booster and launched into orbit for rendezvous with the first launched spacecraft. Vehicles are coupled, they proceed to lunar orbit for release of the two landers, and the powerplant is propelled back to earth parking orbit.

(3) Launch #3: Assembly consisting of lunar landing craft and replacement electric-thruster-propellant is launched into the parking orbit to rendezvous with the nuclear powerplant. The voyage then proceeds as before.

(4) Subsequent Launches: Process is repeated until power supply either fails or wears out.

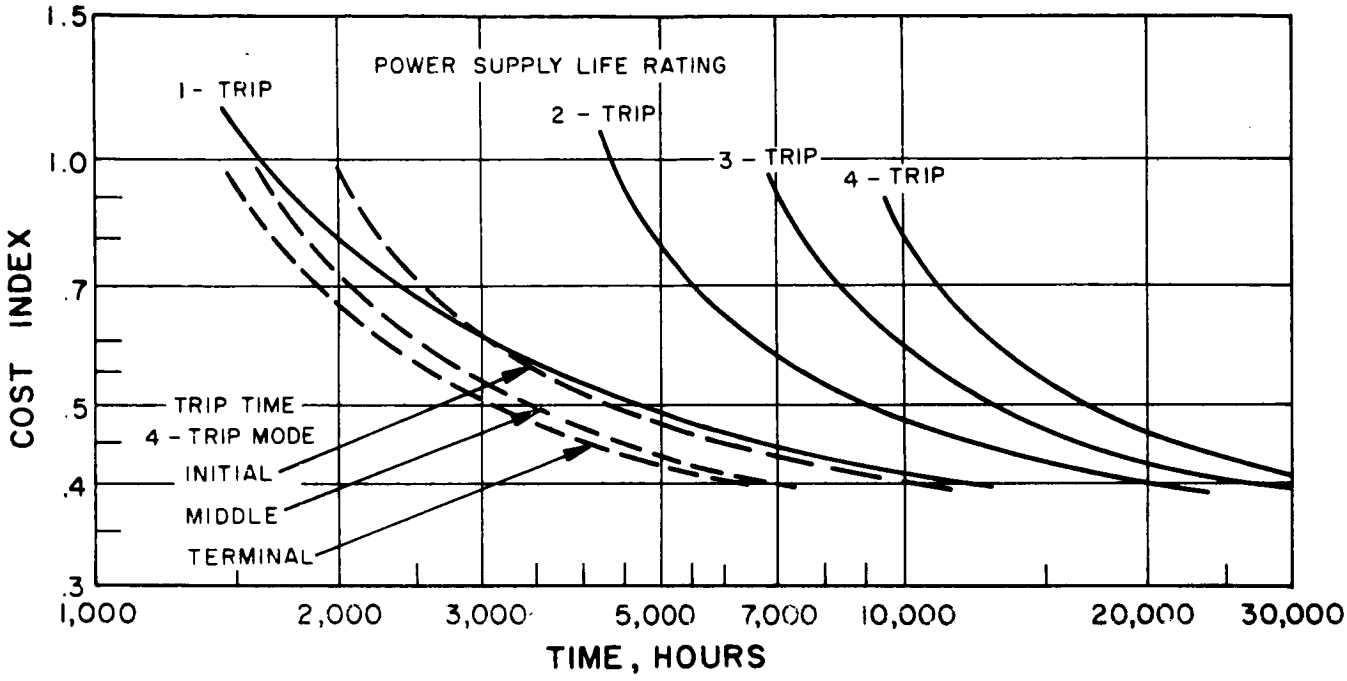

Figure 5-30. Effect of Number of Trips on Power Supply Life and Trip Time with Ion Jet Thrustor

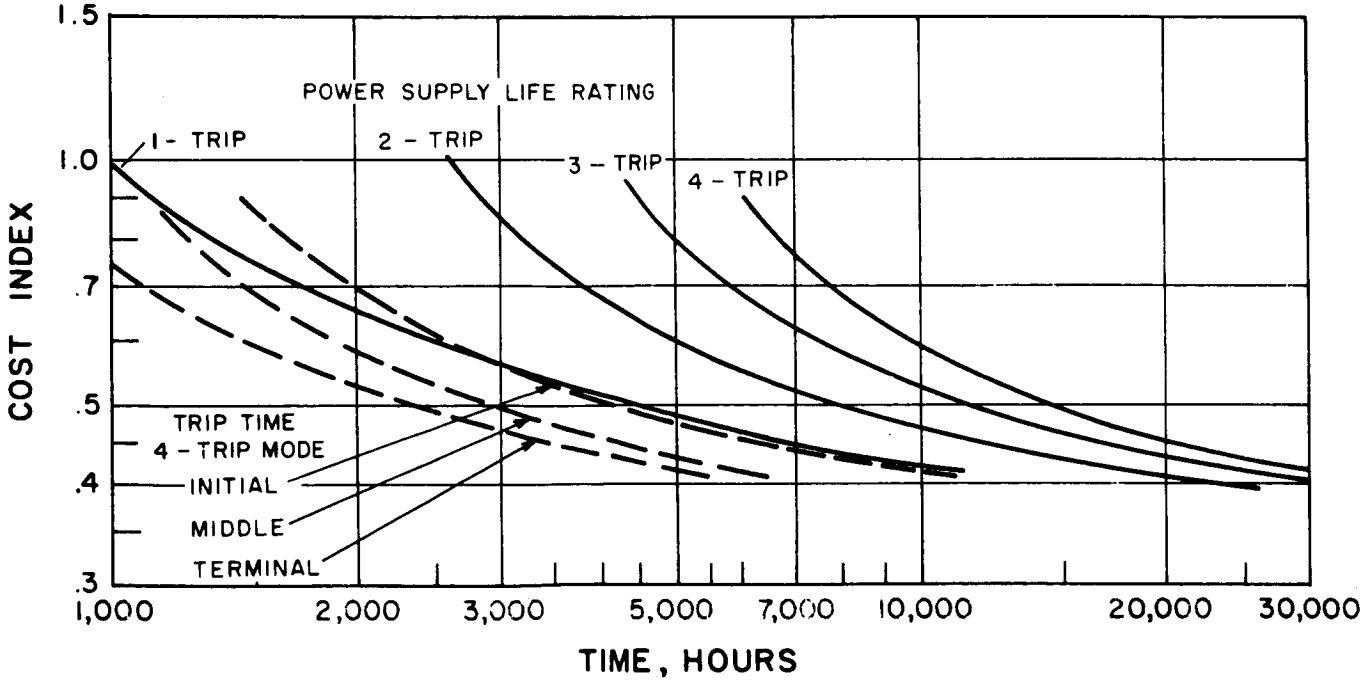

Figure 5-31. Effect of Number of Trips on Power Supply Life and Trip Time with Hybrid Arc Jet Thrustor

A performance comparison between the one and two initial booster approach is presented in Figures 5-32 and 5-33. These data indicate that the use of two boosters for the initial trip yields a negligible change on the basis of power supply life. The two-booster approach does have an advantage in trip time for the middle and terminal trip as shown in Figure 5-32. This would be an important reason for selection of the two-initial booster operating mode.

b. Constant Lunar Lander Size

The assumption that the lunar cargo module be fixed at a constant size between successive voyages will constrain two of the five specific impulse levels and permit an optimization of the remaining three. As a result of fixing the cargo module size, five different specific impulses are still required to provide the proper characteristic velocity for the various outbound and inbound voyages. The specific impulses for each of the three outbound types of trips are closely related to electric power supply and lunar landing craft sizes. The two types of inbound trip specific impulses can be made equal and optimized together, or made equal to one of the outbound specific impulses. Thus, the different values of specific impulses required can number three to five.

The design problem when using a fixed lander size is the method of installation of thrustors. The choices are:

(1) Use of a variable specific impulse thrustor mounted permanently to the powerplant

(2) Use of several non-variable specific impulse thrustors, one size for each specific impulse requirement, and mounted permanently to the powerplant.

(3) Use of a separate fixed specific impulse thrustor for each propulsion stage mounted to the propellant tank and discarded after use

(4) Use of a separate fixed specific impulse, propellant tank mounted thrustors for each of the outbound voyages and a powerplant mounted fixed specific impulse thrustor for the inbound voyages.

A constant size lunar lander mission model has been developed from the equations of Tables 5-9 and 5-10 and used to run a series of parametric optimization studies with the

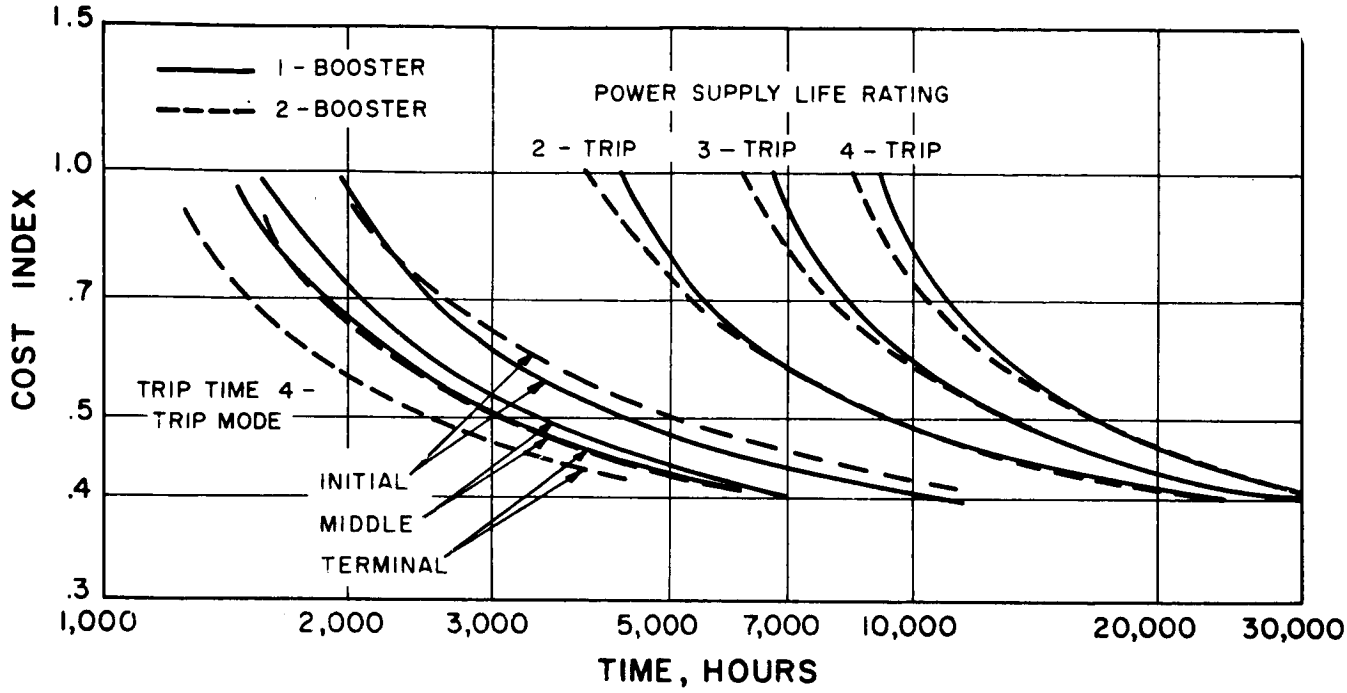

Figure 5-32. Effect of Number of Boosters on Initial Trip with Ion Jet Thrustors

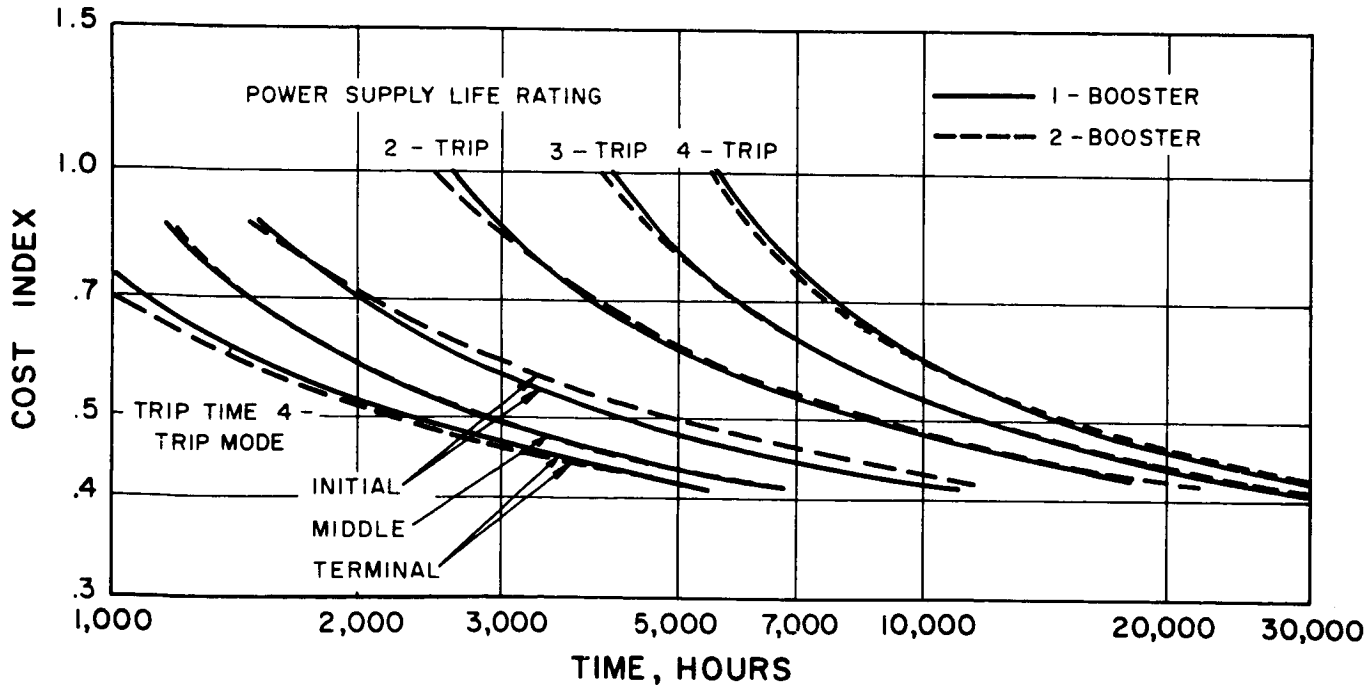

Figure 5-33. Effect of Number of Boosters on Initial Trip with Arc Jet Thrustors

LEADER optimization program of H. Brown*. These preliminary studies were run with the thrustor weights omitted from the model. Table 5-11 summarizes the results of a typical optimization run for a powerplant specific weight of 13.6 kg/kw (30 lbs/kw). The extremely wide variation in specific impulse is clearly beyond the capabilities of projected first or second generation electron-bombardment thrustors. The flexibility of a hybrid arc-jet thrustor to accommodate this range of values is also in doubt.

The alternative of using a separate thrustor for each segment of the mission would, however, result in a thrustor specific weight of (12 to 17 Kg/Kw) 26 to 38 lbs/kw depending upon whether or not a common power conditioning system can be used for two or more engines. The third possibility of selecting off-optimum performance to force two, three, or four of the specific impulse levels together has not been investigated but does not appear to be any more attractive than the preceding approaches.

Performance characteristics have been estimated for the case where the electric thrustors are integrated with the propellant tanks and resupplied for each successive mission. The general performance results are presented in Appendix A, and typical optimized performance characteristic are presented in Figures 5-34 and 5-35. The performance characteristics associated with zero weight thrustors are also plotted to show the net performance penalty due to the thrustor weight.

c. Constant Specific Impulse

The use of a single thrustor assembly operating at a constant specific impulse throughout the power supply life for all five elements of the multiple trip ferry requires the use of a different size lunar landing craft for the initial, middle, and terminal trips. This approach removes four degrees of freedom from the general design problem and reduces it to a two-dimensional situation similar to the single trip ferry. The results of a typical multiple trip mission calculation is presented in Table 5-12 for a powerplant specific weight of 13.6 kg/KW_e (30 lbs./KW_e) and the use of two boosters for the initial voyage. The lunar

*Brown, H., "Spacecraft Electric Generating and Propulsion System Integration Study," ASD-TDR-63-428, Cincinnati, 1963.

TABLE 5-11. MULTIPLE TRIP MISSION REQUIREMENTS WITH CONSTANT PAYLOAD

Power - MW	3.6		
Total Trip Time-hrs.	10,000		
Trip	Initial	Middle	Terminal
Initial Gross Weight - Kg.	220,000	170,000	170,000
Trip Time-hrs.			
Outbound	1712	2592	2140
Inbound	1473	2082	----
Specific Impulse-sec.			
Outbound	2009	4174	3395
Inbound	5875	8858	----
Payload-Kg.			
Lunar Orbit	70,000	70,000	70,000
Lunar Surface	28,000	28,000	28,000

TABLE 5-12. MULTIPLE TRIP MISSION REQUIREMENTS WITH SINGLE THRUSTOR

Power MW		4.0	
Specific Impulse - sec.		3550	
Total Trip Time - hrs.		10,000	
Trip	Initial	Middle	Terminal
Gross Weight-Kg.	220,000	175,000	175,000
Trip Time-Hrs.			
Outbound	2900	2355	2355
Inbound	1170	1170	----
Payload - Kg.			
Lunar Orbit	81,000	49,000	69,000
Lunar Surface	32,000	20,000	28,000

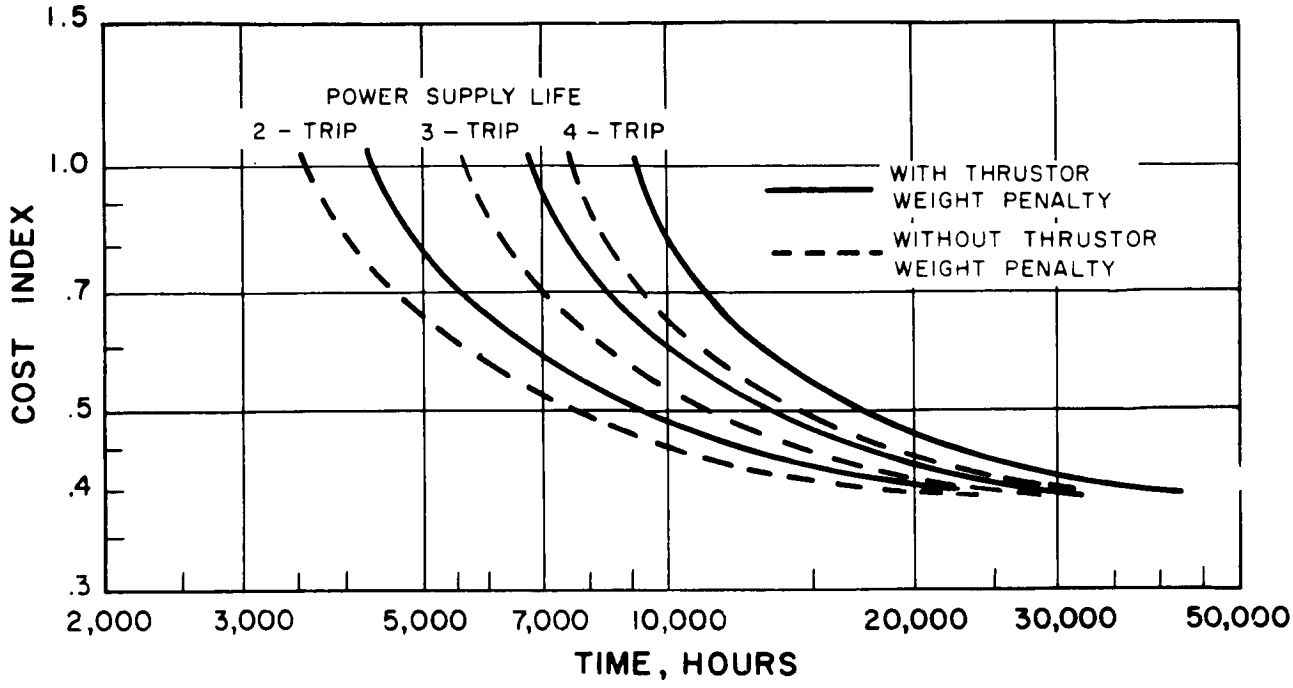

Figure 5-34. Effect of Ion Jet Thrustor Weight Penalty

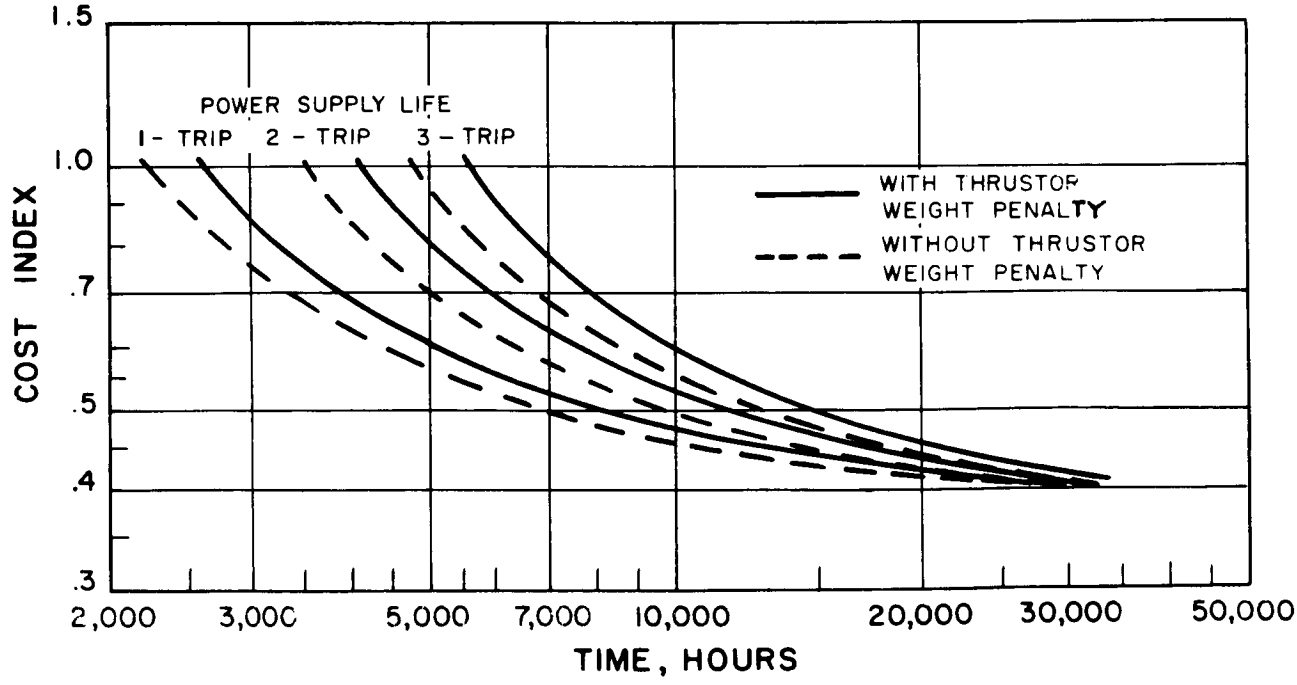

Figure 5-35. Effect of Hybrid Arc Jet Thrustor Weight Penalty

lander gross size varies between 81 tons for the first voyage to 49 tons for the middle voyage (s), with the terminal voyage lander size falling in between at 69 tons. This non-standardization of lander sizes is not desirable for many obvious reasons. However, the performance advantage in terms of trip time and cost may outweigh this disadvantage.

The constant specific impulse approach is compared to the constant lander size approach in Figures 5-36 and 5-37 for both ion jet and hybrid arc jet thrustors, and both one-initial-booster and two-initial-booster operational modes. The performance advantage of the constant specific impulse approach is appreciable, particularly at the short power supply life portion of the curves. These comparisons lead to the conclusion that careful consideration be given to the constant specific impulse approach.

d. Elimination of Tank Dumping in Earth Orbit

In each of the preceding operating modes, the propellant tanks were jettisoned almost immediately after running dry. Separate tanks were provided for the outbound and inbound voyages, and these were discarded after use in lunar orbit and earth orbit, respectively. The disposing of material in low earth orbit may be undesirable for a continuing operation. Thus, an examination was made of operating modes whereby the propellant tanks used for the inbound voyage were retained after running dry and later discarded in lunar orbit.

The obvious scheme to achieve this result is to provide a separate outbound and inbound propellant tank on each launched spacecraft and program the discard of spent propellant tanks so that, at each arrival in lunar orbit, the propellant tanks from the just-completed outbound voyage and the preceding inbound voyage are jettisoned. An alternative approach is to integrate the propellant tank for the inbound voyage with the powerplant and fill it initially with the required propellant for all of the anticipated inbound voyages. The launch vehicles on the second and subsequent trips would provide, therefore, the outbound propellant tank assembly and lunar landing craft. Both of these approaches offer operating advantages at the expense of a small performance and cost penalty, and the range of this penalty is shown in Figure 5-38 and 5-39. The disposal of propellant tanks in high earth orbit, rather than lunar orbit, would yield about 2/3 of that penalty shown in these graphs.

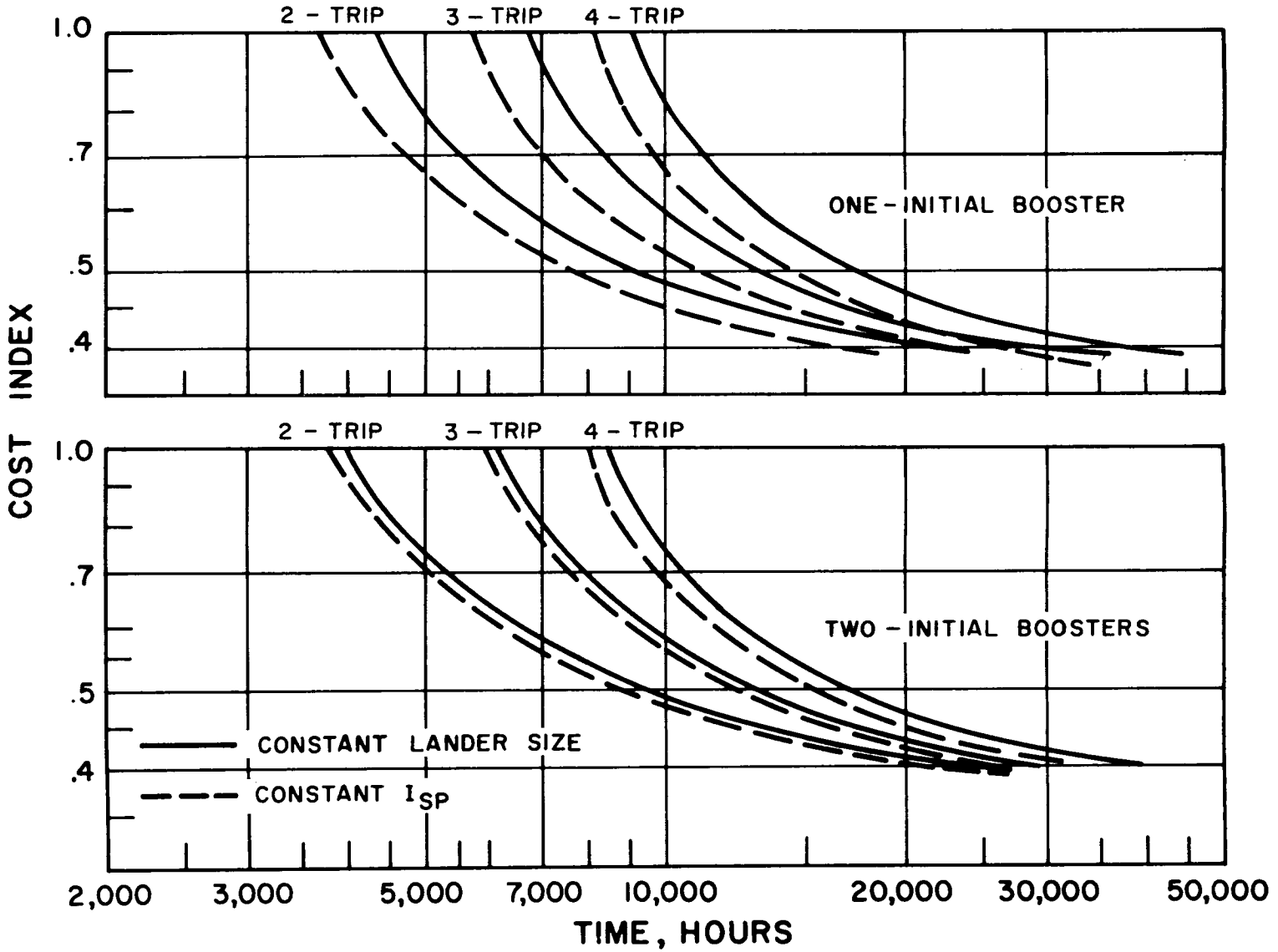

Figure 5-36. Performance of Constant Size Lander Versus Constant Specific Impulse with Ion Jet Thrustor

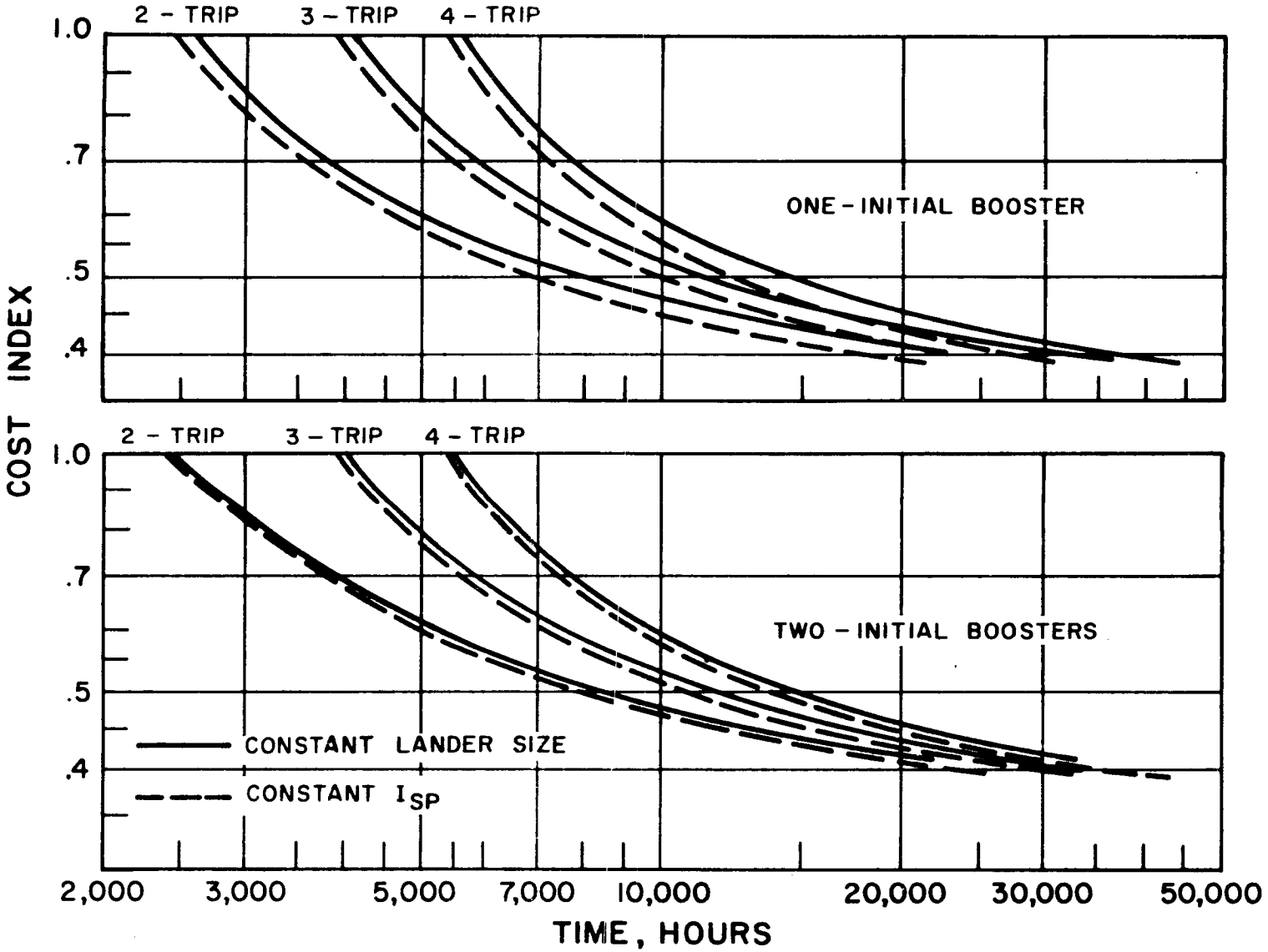

Figure 5-37. Comparison of Constant Size Lander and Constant Specific Impulse Performance with Arc Jet Thrustor

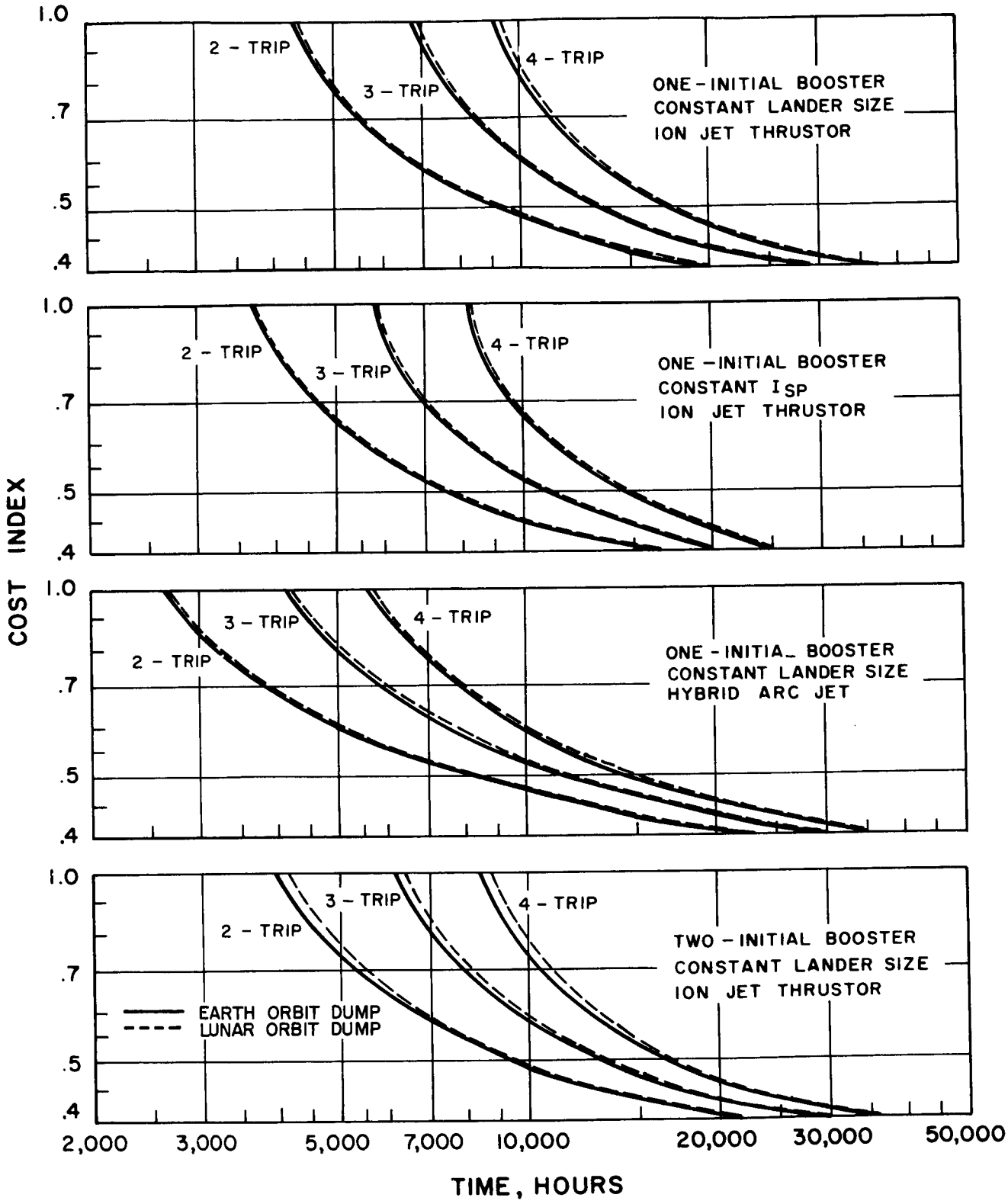

Figure 5-38. Penalty for Retention of Inbound Electric Propulsion System for Dump in Lunar Orbit

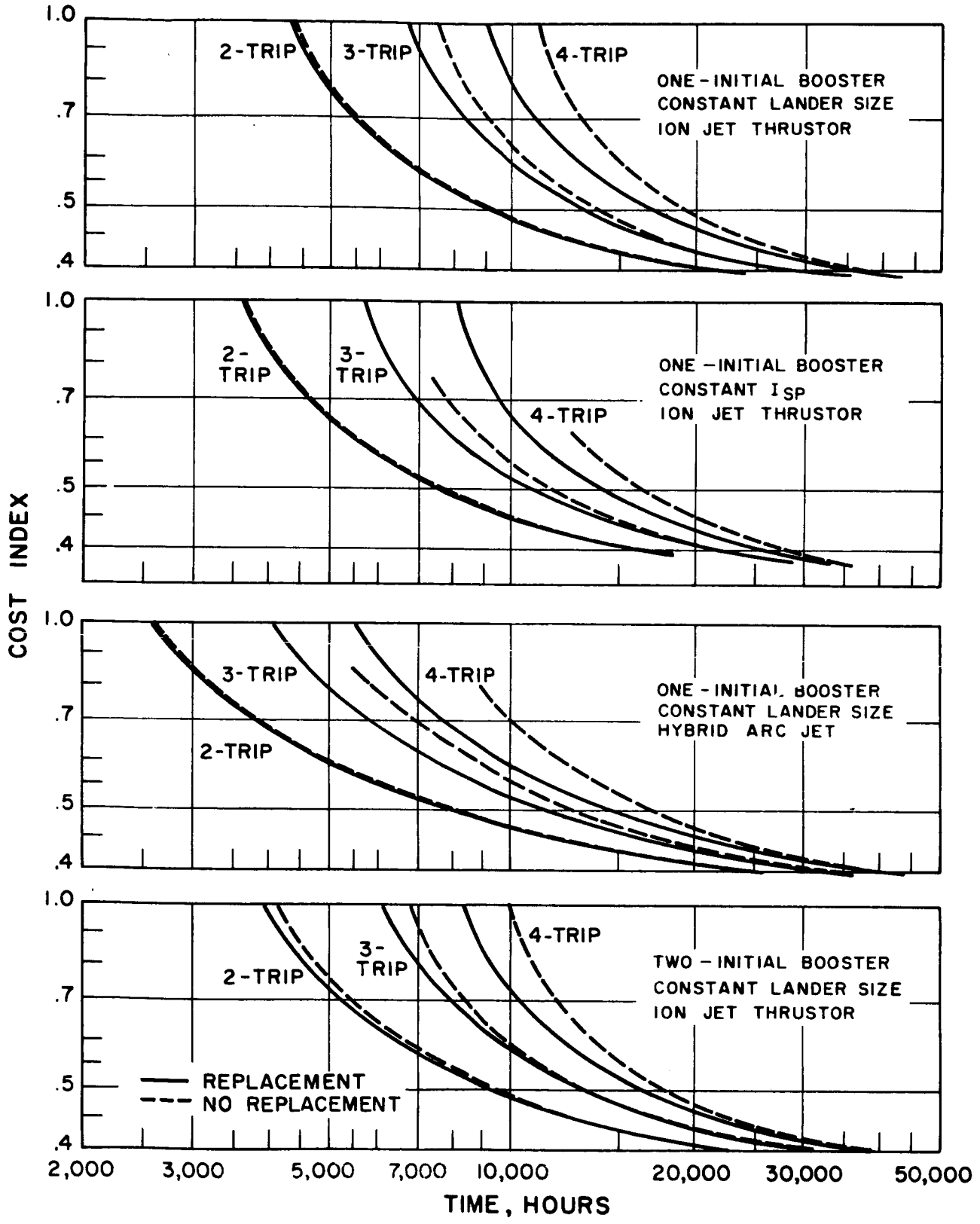

Figure 5-39. Penalty for No Inbound Propulsion System Replacement

In Figure 5-38 the penalty associated with the first scheme is illustrated, i.e., the operational mode where each successive booster provides a new propellant tank for the inbound voyage and the just-emptied inbound propellant tank is retained for disposal in lunar orbit at the next lunar orbit arrival. In Figure 5-39 the penalty associated with the second scheme is indicated, i.e., the operational mode where the entire propellant load for all the inbound voyages is provided on the initial launch vehicle with the powerplant and ultimately discarded with the powerplant in lunar orbit. The penalties are shown for various operating modes involving selections of electric thrustor, number of boosters on initial voyage, constant size lander and constant specific impulse approaches. In general, the penalty becomes negligible at the ends of the curves where cost index is a minimum and power supply life rating is long. At the short life end of the curve the penalty for providing all of the inbound propellant initially is large and increases more so with more numerous trips. However, the low cost end of the curve is the range of real interest and the penalty may be acceptable to avoid littering the space near earth.

Another advantage of the scheme to haul all materials back to lunar orbit for disposal is the reduction of hazards associated with rendezvous of the returning power supply and the next launched spacecraft. The docking procedure and preparation of the coupled spacecraft for the next outbound voyage is simplified, and, therefore, less prone to failures.

3. Multiple Engine Ferry

The multiple engine mission profile is illustrated in Figure 5-40. This mode of operation is visualized as a continuous operation with a new powerplant module added at the beginning of each outbound leg and the oldest powerplant discarded at the beginning of each inbound leg. An alternate approach would involve powerplant replacement on every other round trip. These two modes of operation will be referred to as continuous replacement and alternate replacement modes, respectively, in the following sections.

a. Continuous Replacement

All trips with the continuous replacement mode are identical and, therefore, only a single trip need be considered. The equations of Table 5-10 were used to develop a mission model

of the continuous replacement mode for use in conducting parametric optimization studies with the aid of the LEADER technique. A four degree of freedom model was formulated in terms of the following design variables:

a. Power Rating

b. Outbound Specific Impulse

c. Inbound Specific Impulse

d. Number of Powerplant Modules

This model was used in conjunction with preliminary electric thrustor characteristics obtained from H. Brown* to investigate the relative performance capabilities of orbiter and fly-by delivery modes and to determine the effects of powerplant operating life on mission performance.

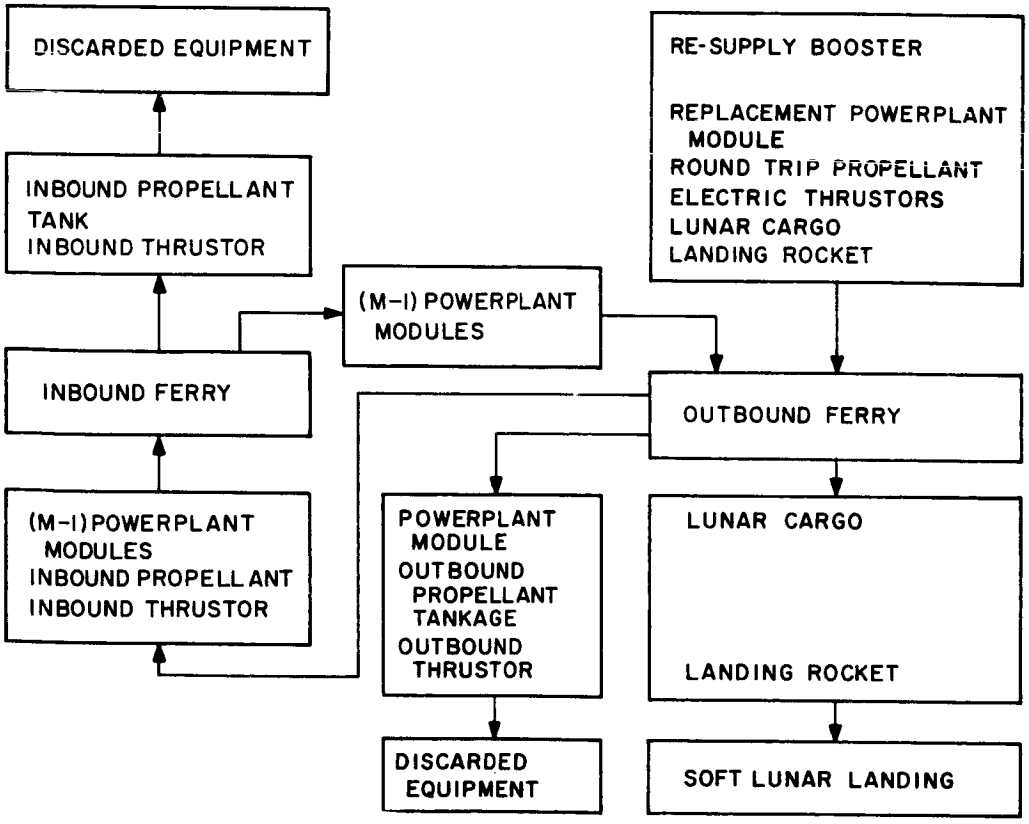

Figure 5-40. Multiple Engine Ferry

*Brown, H., and Widmer, T.F., "Research on Spacecraft and Powerplant Integration Problems - Mission Analysis Topical Report," General Electric TIS No. 64SD505, Philadelphia, 1964.

The results of these studies are summarized in Figure 5-41. The Cost Index, defined in Section 5.B.1, has been plotted against trip time for lines of constant powerplant specific weight. These data have been obtained by minimizing the relative payload cost for maximum powerplant operating times of 10,000 and 15,000 hours. Performance is shown for both the fly-by and the orbiter modes of operation. These results indicate that the payload costs are essentially 20 percent higher for the fly-by mode of operation. It has been concluded, therefore, that the subsequent investigations can be restricted to the orbiter mode of payload delivery. The orbiter performance line with a 15,000 hour powerplant life capability indicates a payload cost reduction of the order of about 5-10 percent. Note that the optimum trip times are essentially the same for 10,000 and 15,000 hour operation. This indicates the use of 50 percent more engine modules with the 15,000 hour operation in order to permit utilization of each engine for a correspondingly greater number of trips before replacement.

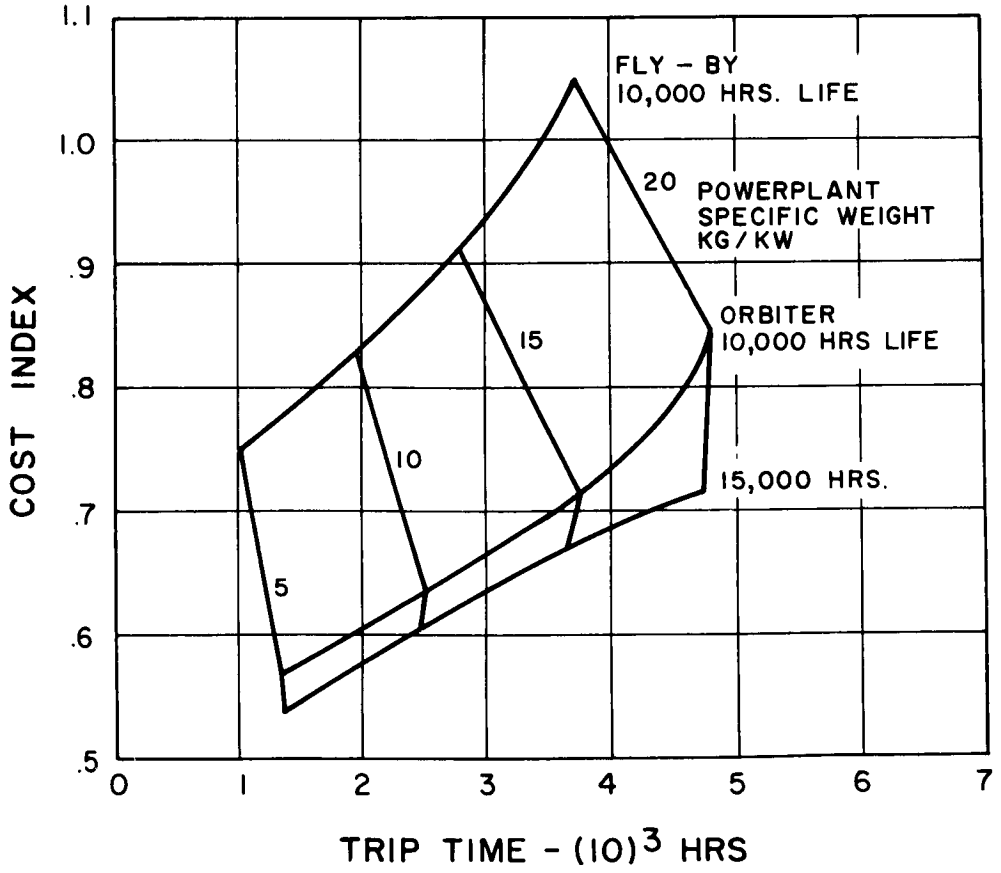

Figure 5-41. Preliminary Multiple Engine Results

The preliminary results assumed separate outbound and inbound thrustors and included extremely modest levels of thrustor specific weight. These results indicated an optimum outbound specific impulse of the order of 3400 seconds and an optimum inbound specific impulse of the order of 4300 seconds. This variation is believed to be beyond the capabilities of a single thrustor with variable specific impulse capabilities. The use of a single thrustor operating at a compromise specific impulse will, however, outperform the dual thrustor approach when the thrustor specific power and specific weight characteristics of Section 5.A are substituted for the data of H. Brown*. The subsequent multiple engine ferry studies have, therefore, been based upon a single thrustor approach.

The performance of the two-powerplant system is compared to the one-powerplant system for the two-trip operating mode in Figures 5-42 and 5-43 using ion jet thrustors and hybrid arc jets, respectively. The two-powerplant system shows a small performance advantage. Other advantages of the multiple powerplant mode are redundancy for the outbound voyage and repetitive use of same size landers and trip times.

b. Alternate Replacement

The alternate replacement mode of operation has been investigated only for a four trip-two engine case in order to permit comparisons with both the two trip-two engine and four trip-four engine cases. A thrustor module has been assumed to be connected to each powerplant and is, therefore, discarded and replaced along with the powerplants. This approach results in the use of a single constant specific impulse level for all outbound and inbound trajectories and in the following repetitive two-trip cycle:

Trip 1 - Launch replacement powerplant, thrustor, propellant, and payload module and mate with old powerplant-thrustor module returned from previous trip. Both powerplants are used for the outbound trajectory to deliver the payload and the subsequent inbound trajectory back to Earth.

Trip 2 - Launch replacement propellant and payload module and mate with the two engine powerplant-thrustor module from previous trip. Both powerplants

*Brown, H., and Widmer, T.F., "Research on Spacecraft and Powerplant Integration Problems - Mission Analysis Topical Report," General Electric TIS No. 64SD505, Philadelphia, 1964.

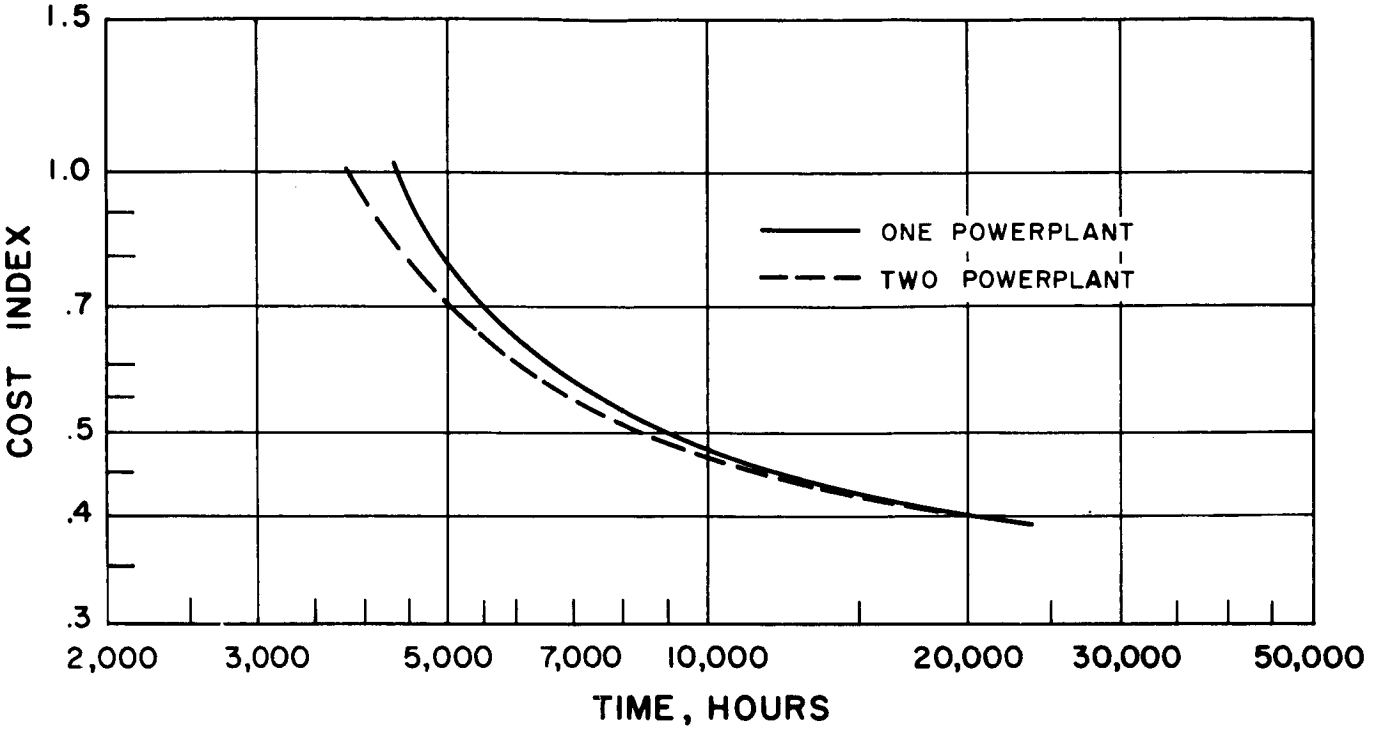

Figure 5-42. Performance of One Vs. Two Powerplant Systems for Two - Trip Mode with Ion Jet Thrustors

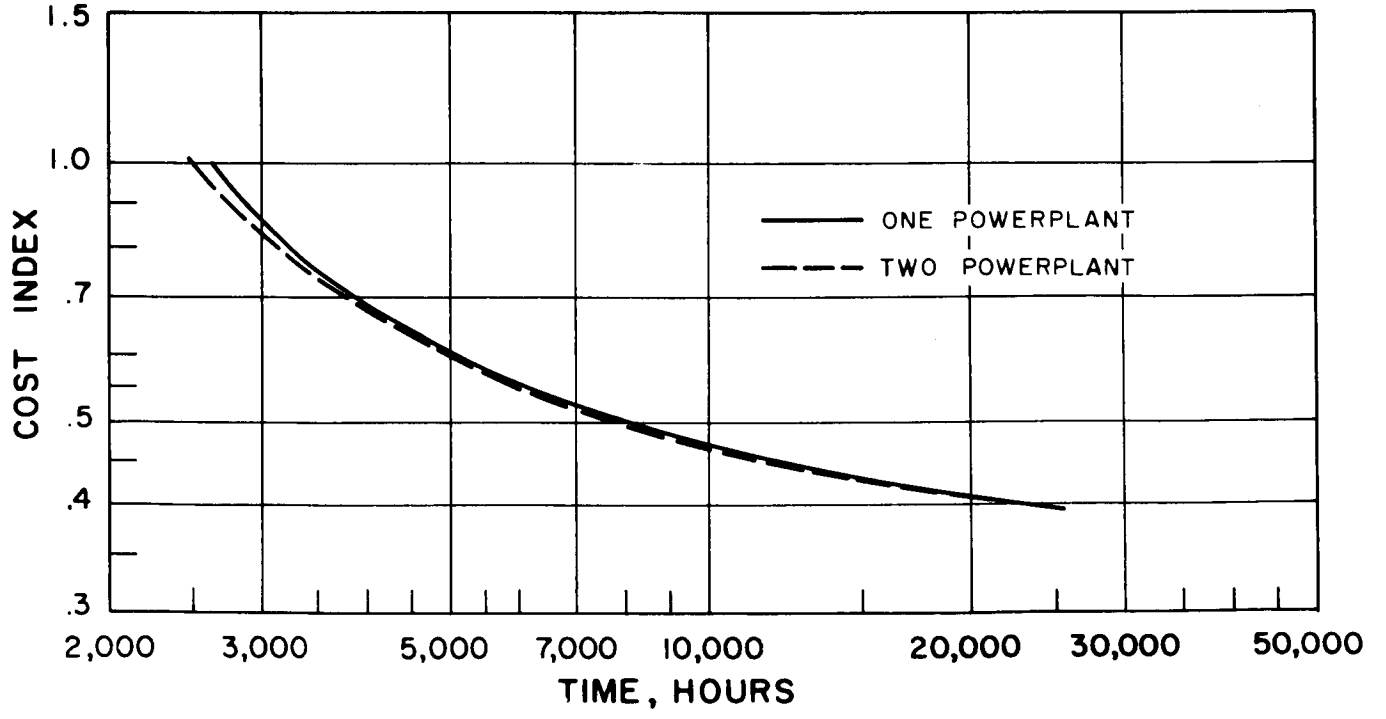

Figure 5-43. Performance of One Vs. Two Powerplant Systems for Two - Trip Mode with Hybrid Arc Jets

are used for the outbound trajectory and the older powerplant-thrustor module discarded at the Moon. The subsequent inbound trajectory is carried out with the remaining powerplant-thrustor module.

This approach requires a different payload module for each trip.

SECTION 6

PERFORMANCE ANALYSIS

One of the major tasks in this study is to develop a generalized analysis of the sustained lunar supply problem based on the use of a reusable, power-limited vehicle or propulsion module. Results of this analysis are to be developed in parametric form, from which the major performance characteristics can be determined for various state-of-the-art assumptions. The results of this effort are presented in this section.

A. TECHNICAL APPROACH

The technical approach and design constraints used in the generation of parametric performance data are presented below. The characteristics of the space vehicle have been simplified to be more generally useful, and the design assumptions are listed. The selection criteria for optimization is minimum cost per unit mass of cargo delivered, and the applicable equation defining the Cost Index is described. A method to properly penalize performance for long trip times has been developed, which is based on probability of vehicle system failure.

1. Spacecraft Characteristics

The analyses of nuclear power supply weight variations presented in Section 5A show that the specific weight changes only slightly with power level and survival probability from meteoroid puncture. The principal influences are the assumptions for the state-of-the-art. As a result, the parametric analysis has been developed to show characteristics at constant values of specific weight ranging from 2.26 kg/KW_e (5 lbs/KW_e) to 18.1 kg/KW_e (40 lb/KW_e). The electric thrustor performance characteristics do vary with the design requirements for any prescribed state-of-the-art, however, and this variation is considered. The electric thrustor type used in the analysis is the electron bombardment ion engine, which was selected because it typifies the ion jet thrustor and has received most widespread attention. The efficiency and weight characteristics assumed are presented in Figures 6-1 to 6-3. The weight includes the portion of the power conditioning equipment located with the thrustor. The weight of power conditioning equipment located near the nuclear power supply is assumed to be included in the nuclear power supply specific weight.

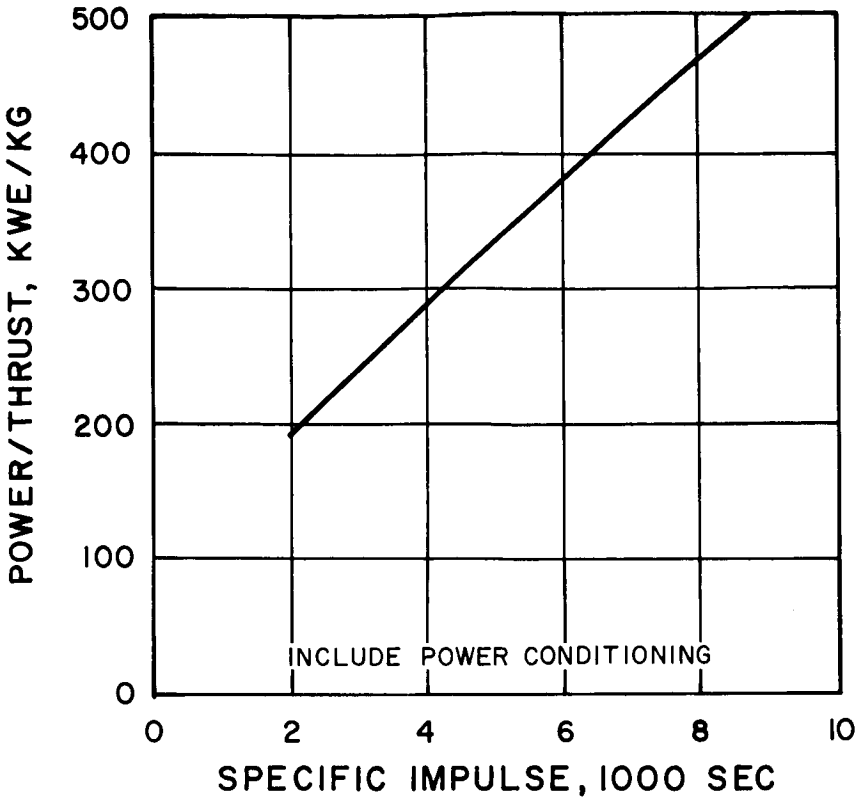

Figure 6-1. Assumed Thrustor Power to Thrust Ratio

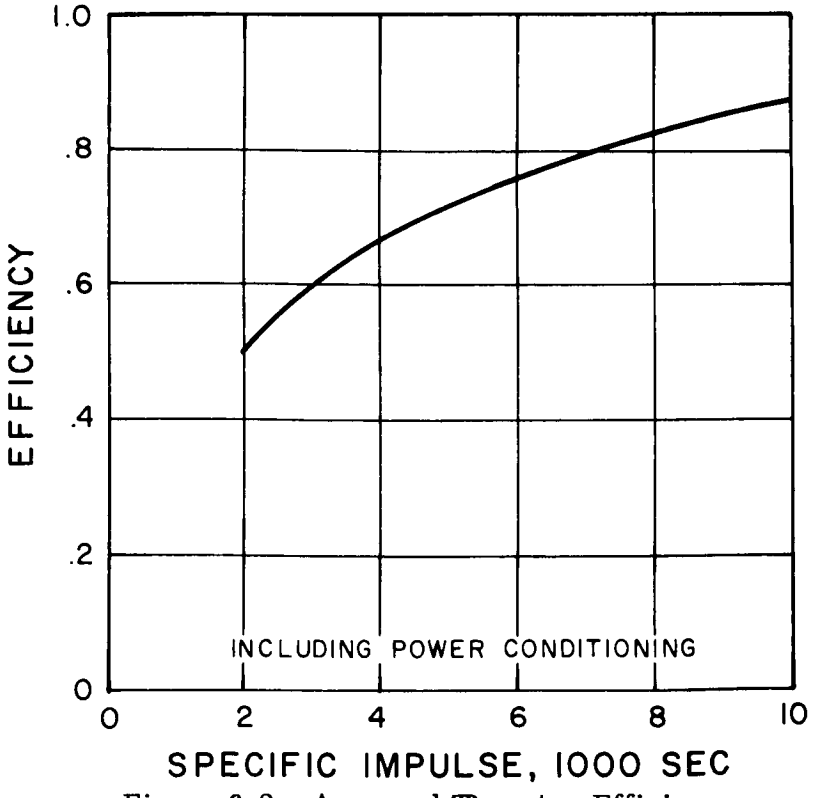

Figure 6-2. Assumed Thrustor Efficiency

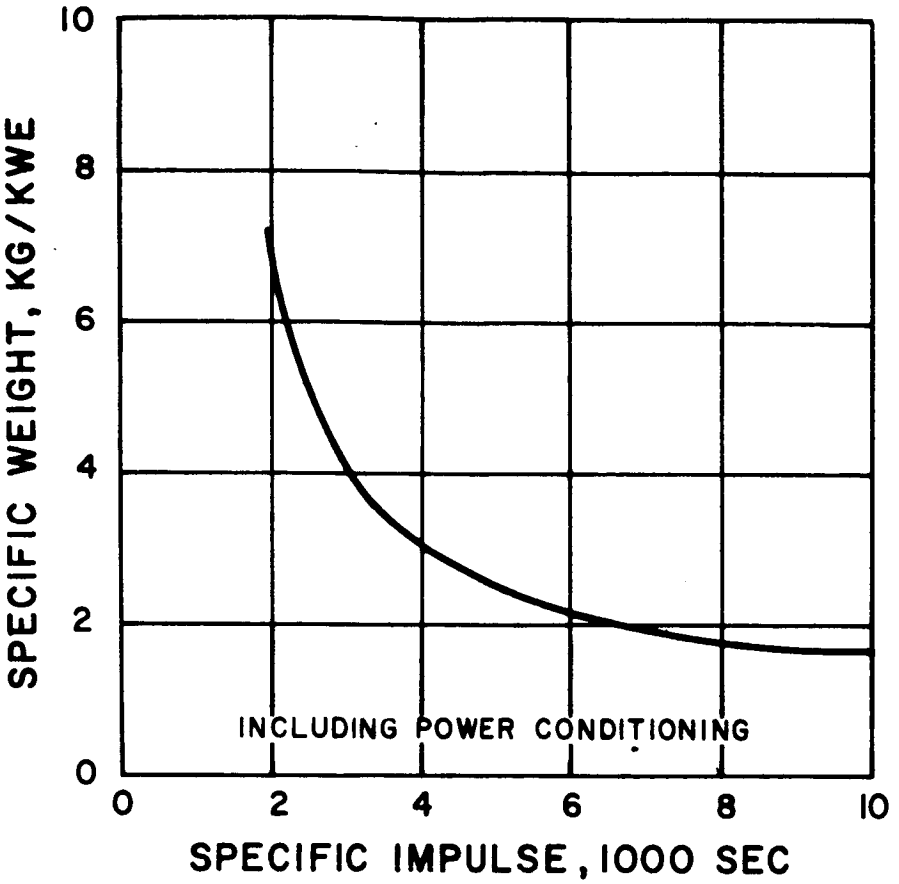

Figure 6-3. Assumed Thrustor Specific Weight

The propellant tank, structure and insulation is assumed constant at ten percent of the gross propellant system weight. Thus, the propellant mass fraction utilization is 0.9 of the total, propellant + tank + structure + insulation.

The lunar landing craft is assumed to have a 0.4 lunar cargo fraction. This completes the accounting of design characteristics of the electrically propelled cargo vehicle. The performance characteristics can readily be corrected to account for change in any of these assumptions.

The operational modes for the multiple-trip case are based on the use of a powerplant mounted thrustor using constant specific impulse between subsequent voyages. Propellant tanks are discarded when dry at the terminal orbits. The single-powerplant, multiple-trip mode uses two booster launches to initiate the first outbound voyage. The objective in this

parametric analysis is to provide comparisons between the single-trip versus multiple-trip selections, and the single-powerplant versus the multiple-powerplant selections.

2. Selection Criteria

The selection criteria for comparison of the electrical propulsion system to the chemical rocket is the cost index, or relative payload cost.

The importance of using minimum costs rather than maximum cargo delivered in the mission optimization is illustrated by the results in Figure 6-4. In this graph the variation of trip time versus optimum powerplant size is plotted as a function of the ratio of powerplant to booster costs and the nuclear/chemical cargo system cost. A powerplant mass fraction of 0.1 can correspond to a 1090 KW_e powerplant assuming a 109,000 kg initial gross weight vehicle and 10 kg/KW_e nuclear power supply. A value of 50:1 for the powerplant/booster cost ratio corresponds to a typical case where the booster specific cost is $40 per kilogram ($120,000,000 Saturn V divided by 3,000,000 kg initial gross weight), and the powerplant specific cost is $2000 per kilogram ($20,000,000 nuclear powerplant of 10,000 kg mass and 100 KW_e capacity). The Nuclear/Chemical Cargo System Cost is synonymous with Cost Index. The performance shown for powerplant/booster cost ratio 1:1 is the case where costs are ignored and the optimization is based on maximizing lunar cargo. The difference between optimum powerplant mass fractions is almost a factor of 2 for powerplant/booster cost equal to 1:1 versus 50:1. Thus, this graph shows the importance of considering costs in the optimization.

A second basis for relating costs is to use the cost to place a unit mass into earth orbit, rather than the booster specific cost based on weight on the launch pad. The Saturn V can place a 109,000 kg mass into earth orbit. Assuming the Saturn cost at $120,000,000, the specific cost to orbit is $1100 per kilogram of payload. In this approach the ratio of nominal

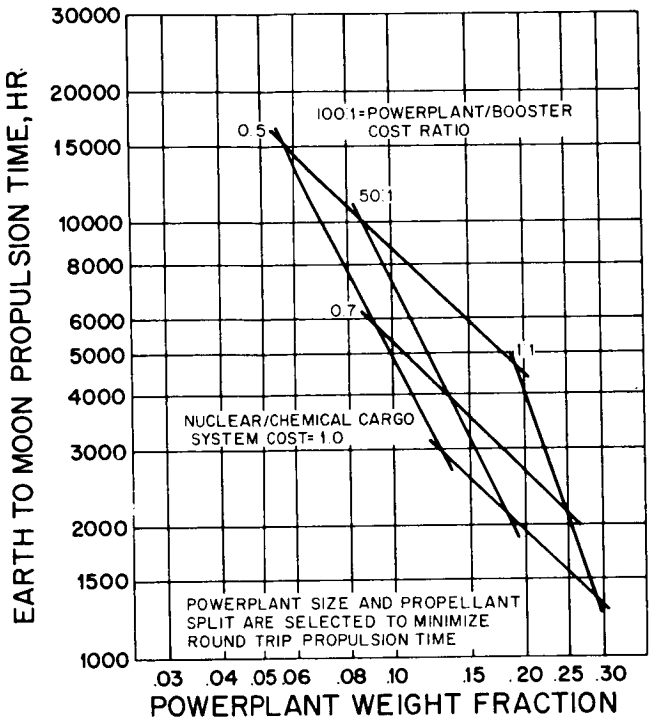

Figure 6-4. Effect of Powerplant/Booster Cost Ratio

powerplant to booster costs is approximately 2:1. The significant features in the optimization study based on costs are their ratios, rather than their magnitudes.

This second approach has been used in the parametric studies presented in Section 6B. The particular assumptions used are presented below, keeping in mind that it is the ratio of costs that is important for purpose of system optimization:

a. Booster Cost (C_b) - \$60,000,000 per Saturn V launch to place a payload of 109,000 kg in a 300 mile circular orbit about the Earth. This results in a booster cost of 550/kg of payload.

b. Powerplant Cost (C_p) - \$1100/kg for the nuclear-electric powerplant, electric thrustors, and associated power conditioning systems. Thus, the ratio of nominal powerplant to booster costs is 2:1.

c. Propellant Costs (C_{pp}) - \$44/kg for the electric thrustor propellant requirements.

The basic Cost Index can, therefore, be obtained from the equation:

$$CI = \frac{(C_b + w\,PC_p + W_{pp}\,C_{pp})/W_{pl}}{C_b/(W_{pl})_c}$$

where $(W_p)_c$ = the lunar payload capability with chemical rocket propulsion

W_{pl} = the lunar payload capability with electrical propulsion

w = specific weight of nuclear power supply

P = power output at nuclear power supply

Parametric studies included in Section 6B indicate the effects of variations in the above powerplant to booster cost ratio from 1 to 4. These variations, therefore, include the range of Saturn V costs from \$30,000,000 to \$120,000,000, the range of powerplant costs from \$500 to \$2000 per kilogram or combinations of the two. The reference Saturn V payload delivery capability is 13,000 kilogram. No additional costs have been included, however, for the upper stage propulsion beyond Earth orbit for the transfer and soft landing operations. Consequently, a cost index of 1.0 implies an actual payload cost of \$4600 per kilogram.

The approach described above only accounts for the manufacturing cost of nuclear power supply, and this is adequate for this first order system optimization. A more refined analysis has been derived, which includes development cost, and this is described in detail in Appendix B. Most of the performance curves showing various effects on Cost Index presented in Section 3 were based on this "refined" procedure. This approach should be expounded in any future effort.

The accuracy of a more refined cost optimization procedure is limited to the accuracy of information utilized. The general parametric results presented in Section 6B have all

of the unknowns grouped into a single parameter, ratio of powerplant to booster costs. As a result the parametric representation can show effects of variation of this parameter. Increasing the complexity of the cost estimation procedure adds many more independent variables to the analysis, and parametric representation of results becomes more difficult. The most logical approach in this situation is to conduct supporting studies on market requirements, development programming and manufacture, so that the range of their variation can be narrowed. Then the performance results can be presented with "influence" factors computed to describe the above mentioned affects.

3. Trip Time Penalty

A method to penalize the performance of the electrically propelled vehicle for long trip times has been devised, which is based on the probability of vehicle losses enroute to the moon. (Total trip time as used herein is synomymous with life rating of electrical power supply and propulsion system.) The vehicle loss penalty is a cost penalty added to the basic cost index to reflect the probability of a powerplant failure and attendant loss of payload during an outbound Earth-Moon transfer or the probability of an inbound powerplant failure which would require replacement before the next outbound leg. The basic assumption used in the development of the survival penalty is the validity of the exponential failure model:

$$R = \exp.^{-t/\theta} \qquad (1)$$

where R is the probability of experiencing a single failure after t hours of operation with a powerplant designed for a mean time to failure of θ hours. The consequences of the failure are dependent upon the degree of redundancy built into the powerplant (number of failures leading to loss of powerplant), the number of engine modules used, and upon whether the failure has occurred during either an outbound or inbound trajectory. A distinction is, therefore, made by this approach between redundancy in which a powerplant is designed to sustain operation until a prescribed number of failures have occurred and modularization in which a number of powerplants are used simultaneously with each individual powerplant lost after a single failure. The survival model has been based upon the assumption that payload delivery can be completed as long as a single operating powerplant module remains. Similarly, it has been assumed that the powerplant can be returned to the earth for re-use if

one operating powerplant module remains. The returned powerplants are re-used for subsequent trips, however, only if they have experienced no previous failures, regardless of the number of failures permitted before the loss of powerplant. This approach results in a survival penalty which is a combination of an outbound penalty and a corresponding inbound penalty. The implementation of these basic ground rules to each of the various modes of lunar ferry operation are discussed in the following sections.

a. Single Trip Mode

The single trip survival penalty is obtained from equation (1) and the following:

$$R_m = 1 - (1-R)^n \tag{2}$$

where R_m is the survival probability and n the number of failures that result in loss of powerplant. The parameter n can also be interpreted as the number of non-redundant powerplant modules used. The survival penalty is then obtained from:

$$C_s = \frac{1}{R_m} \tag{3}$$

The corrected cost index is obtained from the product of the basic cost index and the survival penalty:

$$CI = C_s \times (CI)_b \tag{4}$$

b. Multiple Trip

The multiple trip mode consists of three types of trips:

1. Initial Trip which uses two boosters to launch the powerplant, round-trip propellant, and payload.

2. Middle trip which differs from the initial trip in that a single booster is used to launch the round-trip propellant and the payload; the powerplant being available from the preceding trip. The inbound trip time of the middle trip is identical to that of the initial trip. The outbound trip time and the payload, however, are different.

3. Terminal trip differs from the middle trip in that no return payload is provided and, consequently, the payload can be increased. The terminal outbound trip time is identical to that of the middle trip.

The multiple trip mode, therefore, involves three different trip times and three different payloads for missions of three or more trips. The following nomenclature will be used to differentiate between the different parameters:

Initial outbound trip time	-	t_o
Inbound trip time	-	t_i
Terminal outbound trip time	-	t_t
Initial trip payload	-	$(W_{pl})_1$
Middle trip payload	-	$(W_{pl})_2$
Terminal trip payload	-	$(W_{pl})_n$

Note that a two trip mission will involve only the initial and terminal trips.

The probability of payload delivery on the initial trip can be expressed as:

$$R_o = \exp^{-t_o/\theta} \tag{5}$$

$$R_{m1} = 1 - (1-R_o)^n \tag{6}$$

The second trip will be initiated only if no powerplant failures have occurred during the initial round trip. The probability of payload delivery on the second trip will, therefore, be the product of the probability of no previous failures and the probability of a failure during the second trip.

$$R_i = \exp^{-t_i/\theta} \tag{7}$$

$$R_t = \exp^{-t_t/\theta} \tag{8}$$

$$R_{m2} = R_o R_1 \left[1 - (1-R_t)^n\right] \tag{9}$$

Similarly, the probability of payload delivery for the third trip is:

$$R_{m3} = (R_o R_i)\ (R_t R_i)\left[1 - (1-R_t)^n\right] \tag{10}$$

and for the j th trip is:

$$R_{mj} = (R_o R_i)\ (R_t R_i)^{(j-2)}\ \left[1 - (1-R_t)^n\right] \tag{11}$$

The total probable payload delivered can be obtained by combining the individual probabilities from equations (6), (9), (10), and (11) with the corresponding payload capabilities:

$$(W_{pl})\ (R_m) = \left[1 - (1-R_o)^n\right]\ (W_{pl\ 1}) + R_o R_i \left[1 - (1-R_t)^n\right]\ (W_{pl})_2$$

$$\left[1 + (R_t R_i) + \ldots (R_t R_i)^{(Q-3)}\right] + R_o R_i\ (R_t R_i)^{(Q-2)} \left[1 - (1-R_t)^n\right] (W_{pl})_n \tag{12}$$

where Q is the total number of trips. The result of equation (12) can be used to determine the total delivery probability by dividing by the total nominal payload:

$$W_{pl} = (W_{pl})_1 + (Q-2)\ (W_{pl})_2 + (W_{pl})_n \tag{13}$$

The probable number of boosters required for the mission can be obtained by summing the probable number required for each trip:

$$R_b = N_b + (R_o R_i) + (R_o R_i)\ (R_t R_i) + \ldots\ (R_o R_i\ (R_t R_i)^{(Q-2)}$$

$$= N_b + (R_o R_i) \left[\frac{1 - (R_t R_i)^{(Q-1)}}{1 - (R_t R_i)}\right] \tag{14}$$

The nominal mission cost can then be corrected for the difference between the nominal number of boosters required and the probable requirements:

$$C_c = C - \left[N_b + (Q-1) - R_b\right] C_b \tag{15}$$

The corrected cost from equation (15) can then be combined with the delivery probability from equation (12) to obtain the resulting survival penalty and the corrected cost index:

$$C_s = \frac{C_c}{C\,R_m} \tag{16}$$

$$CI = C_s\,(CI)_b \tag{17}$$

c. Multiple Engine Mode

Two types of multiple engine operations have been considered - one in which an engine replacement is made on every trip and the alternate approach in which the engine replacement is made on every other trip. The mode of operation involving powerplant replacement every trip has been analyzed as a continuous operation in which the first engine is used for its first trip, the second engine for its second trip, the third engine for its third trip, etc. The probability of payload delivery can, therefore, be obtained from the following equations:

$$R_o = \exp^{-t_o/\theta} \tag{18}$$

$$R_i = \exp^{-t_i/\theta} \tag{19}$$

$$R_1 = R_o \tag{20}$$

$$R_2 = R_o\,(R_o R_i) \tag{21}$$

$$R_3 = R_o\,(R_o R_i)^2 \tag{22}$$

etc.

$$R_m = 1 - (1 - R_1)\,(1 - R_2)\,(1 - R_3)\,\ldots \tag{23}$$

where t_o is the outbound trip time and t_i is the inbound trip time. Equation (23) corresponds to the assumption that the payload delivery can be completed as long as one or more operating powerplants are available. The probable number of engines available at earth departure with no previous failures can be obtained from:

$$M_e = 1 + (R_o R_i) + (R_o R_i)^2 + (R_o R_i)^3 + \ldots = \frac{1 - (R_o R_i)^m}{1 - (R_o R_i)} \tag{24}$$

where m is the nominal number of engines. It has been assumed that additional engine replacements will be made prior to earth departure to bring the number of available engines up to the nominal amount. The mission cost must, therefore, be penalized for the additional booster and powerplant costs associated with the unscheduled engine replacement. This cost penalty has been based on the assumption that an extra Saturn V launch will be used periodically in order to maintain a supply of replacement engines at an orbital supply depot and, therefore, the booster cost will be proportional to the ratio of powerplant weight to booster payload capability. The resulting cost penalty can be obtained from the equation:

$$C_p = (M-M_e)\ (C_p + \frac{C_b}{W_{bpl}})\ wP \tag{25}$$

where W_{bpl} is the orbital payload capability of the booster. The resulting survival penalty can then be defined as:

$$C_s = \frac{1 + (C_p/C)}{R_m} \tag{26}$$

The alternate mode involving engine replacement every other trip introduces a variation in the trip times and payload capabilities between two successive trips depending upon whether or not an engine replacement is scheduled. This mode has been analyzed only for a two engine - four trip case. The payload delivery probability must, therefore, be obtained from the relationships:

$$R_1 = \exp^{-t_{1o}/\theta} \tag{27}$$

$$R_2 = \exp^{-t_{1r}/\theta} \tag{28}$$

$$R_3 = \exp^{-t_{2o}/\theta} \tag{29}$$

$$R_4 = \exp^{-t_{2r}/\theta} \tag{30}$$

$$R_{m1} = 1 - (1-R_1)\ (1-R_1R_4) \tag{31}$$

$$R_{m2} = 1 - (1 - R_2R_3)\ (1 - R_2R_3R_4) \tag{32}$$

$$R_m = \frac{R_{m1}(W_{pl})_1 + R_{m2}(W_{pl})_2}{(W_{pl})_1 + (W_{pl})_2} \tag{33}$$

where the subscripts 1 and 2 refer to the first and second trips of the two trip cycle which is carried out twice in the four trip mission. The subscripts o and r refer to the outbound and round-trip times. Equation (33) can then be used in conjunction with equations (25) and (26) to obtain the resulting survival penalty.

B. MISSION PERFORMANCE

The data of the previous sections have been used to generate a series of mission performance maps for the single trip, multiple trip, and multiple engine modes of lunar ferry operation. These data illustrate the effects of powerplant specific weight, trip time, powerplant and booster costs, mean time to failure, number of failures, number of trips, and number of engines on the cost index capabilities of nuclear-electric propulsion.

1. Single Trip Ferry

a. Performance

The nominal single trip performance data are illustrated in Figures 6-5 and 6-6. The data of Figure 6-5 show the variation in cost index as a function of power rating, powerplant specific weight, and trip time for a nominal powerplant to booster cost ratio of 2.0. The survival penalty analysis of Section 5.A.3 has been omitted from these results in order to illustrate ultimate performance capabilities. The cost index improves at constant powerplant specific weight as the power rating is reduced. This trend continues until each line reaches 29 percent payload cost at zero power and infinite trip time. It is obvious, therefore, that some type of trip time penalty must be imposed on the data in order to identify optimum performance capabilities in a meaningful trip time regime.

Figure 6-6 has been derived from the data of Figure 6-5 and from the survival penalty analysis of Section 5.A.3. These data have been based upon a nominal mean time to failure of 10,000 hours and upon a nominal two failures leading to mission abort. The survival penalty increases with increased trip time due to the greater probability of failure and causes the constant powerplant specific weight lines to minimize in the 4500 to 8000 hour trip time

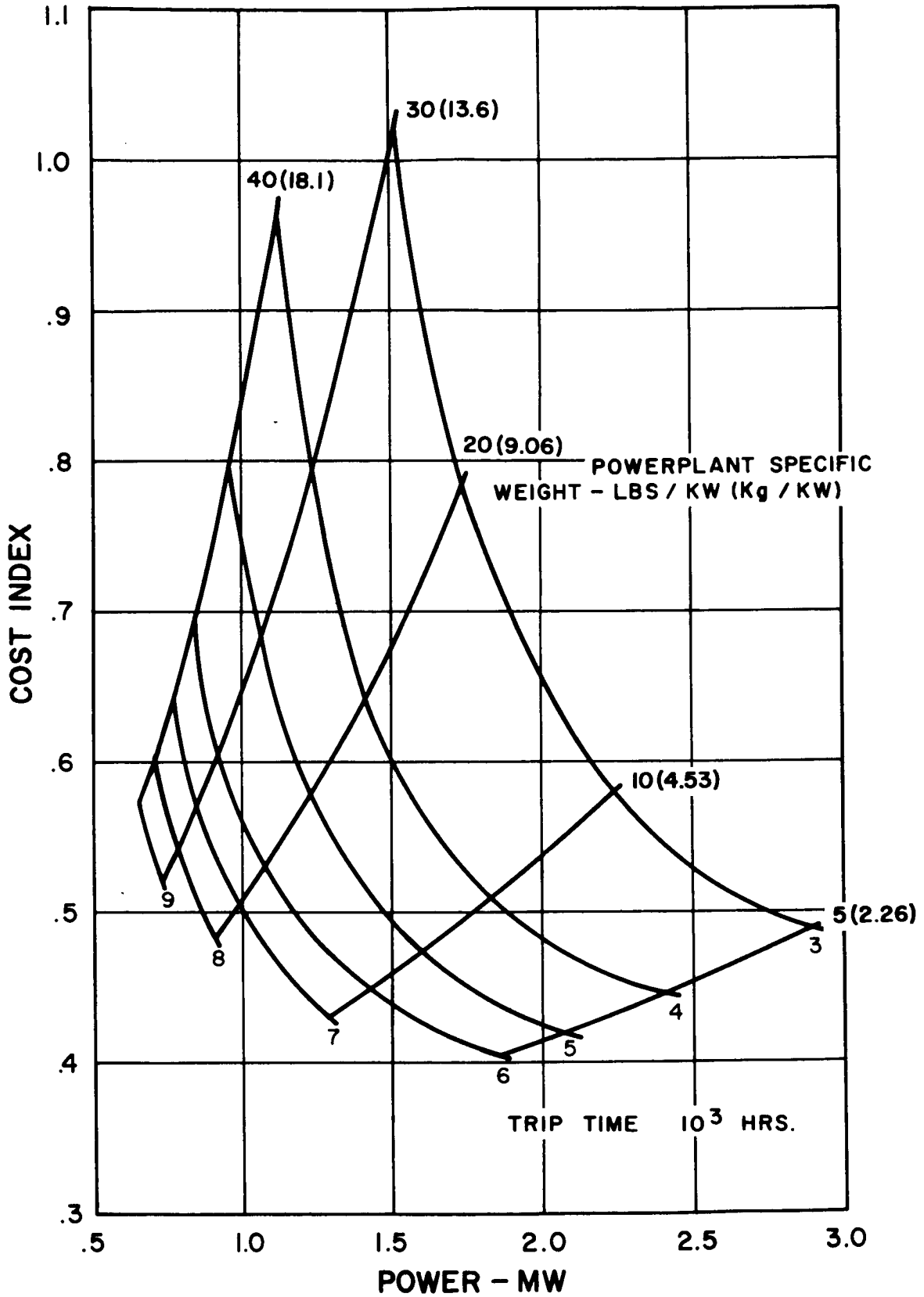

Figure 6-5. Single Trip Ferry Performance with No Survival Penalty

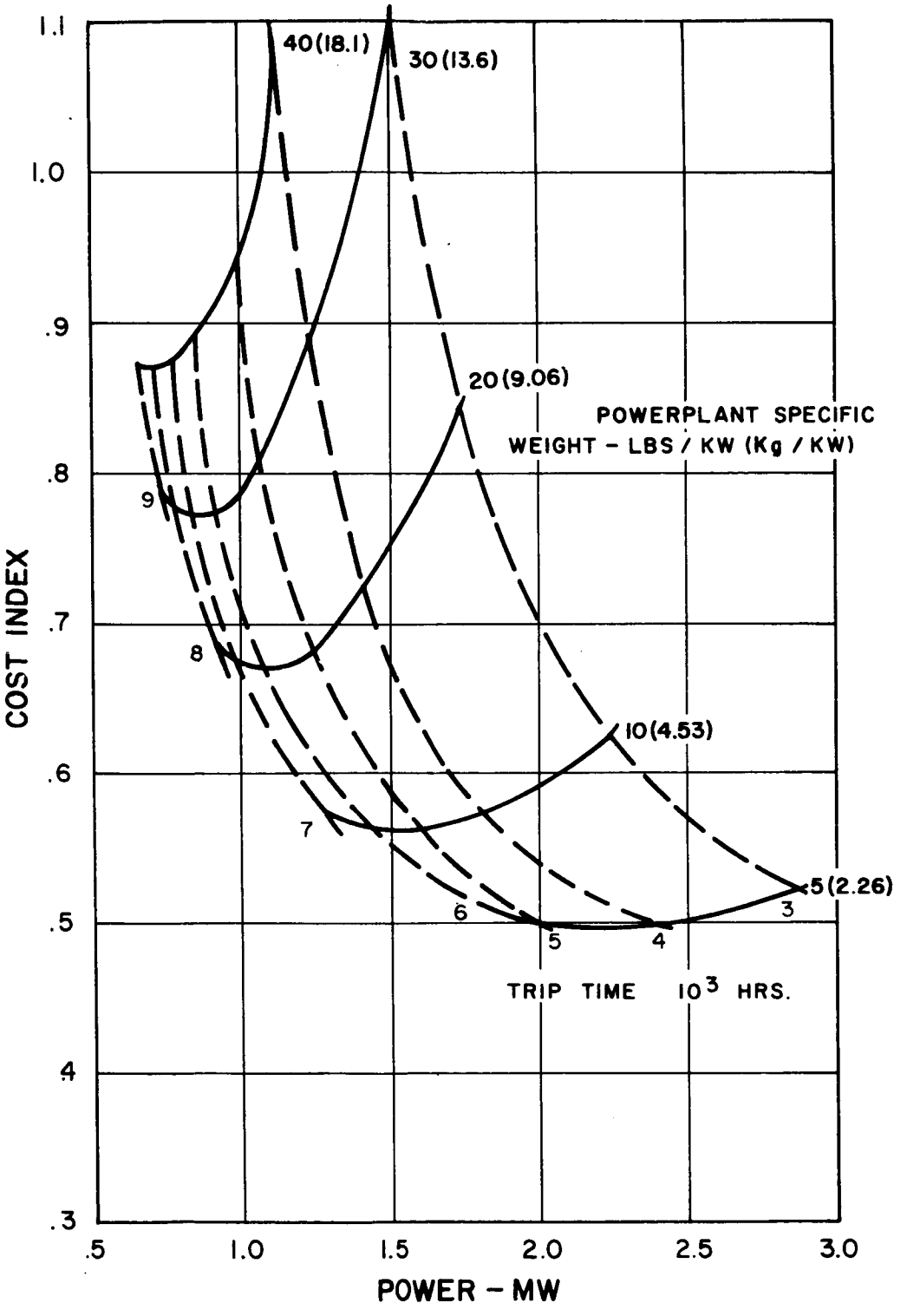

Figure 6-6. Single Trip Ferry Performance with Nominal Powerplant Design.
10,000 Hr. MTTF, 2 Failures to Abort Mission.
Powerplant to Earth Orbital Payload Cost Ratio of 2.

regime. The survival penalties in this region are of the order of 20 to 40 percent.

The indicated points of minimum cost index represent the optimum single-trip ferry performance for the above nominal powerplant specifications. These data have been used as a base point in exploring the effects of variations in powerplant to booster cost ratio, mean time to failure, and number of failures. Parametric data has been generated by varying one parameter at a time while maintaining the others at their nominal values. Figure 6-7 illustrates the performance variation with powerplant to booster cost ratio for the nominal mean time to failure and the nominal number of failures. Performance capabilities are shown for cost ratios of 1, 2, and 4 corresponding to the minimum relative payload cost for each combination of powerplant specific weight and cost ratio. The data for a cost ratio of 2, therefore, is identical to the optimum nominal data from Figure 6-6. These data indicate substantial variations in cost index over the range of powerplant to booster costs shown.

Figure 6-8 contains corresponding data to illustrate the effects of variations in mean time to failure for the nominal powerplant cost ratio and the nominal number of failures. The mean time to failure range of 10,000 to 40,000 hours has been investigated. As in the previous curves, the performance shown represents the minimum cost index obtainable. The shaded region represents operation at a trip time of 10,000 hours which has been imposed as an arbitrary upper limit on trip time. Although a substantial improvement is indicated for increased mean time to failure from 10,000 to 20,000 hours, relatively little gain appears possible beyond 40,000 hours.

Similar data is shown in Figure 6-9 for the effect of the number of failure leading to mission abort. These data are quite comparable to those of the preceding curve and indicate that a single curve might be sufficient to show both effects.

b. Mission Requirements

The cost index data of the preceding section have been obtained with the optimum specific impulse relationship of equation (9) of Section 5. Figure 6-10 contains the resulting variation in optimum specific impulse corresponding to the nominal performance data contained in Figure 6-5 and 6-6. The corresponding lunar surface payload is also shown. Note that the

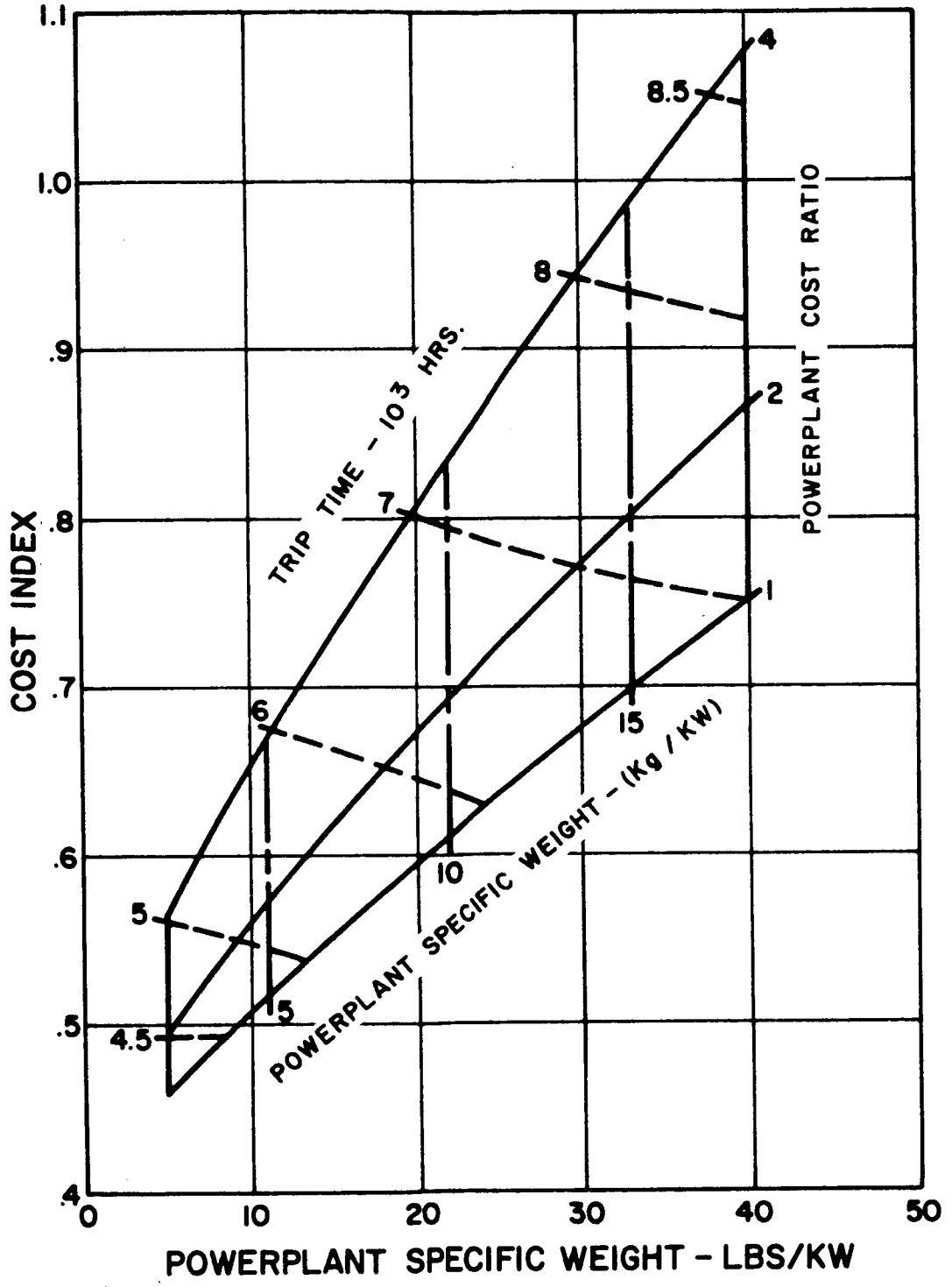

Figure 6-7. Effect of Powerplant and Boost Costs on Single Trip Ferry Performance

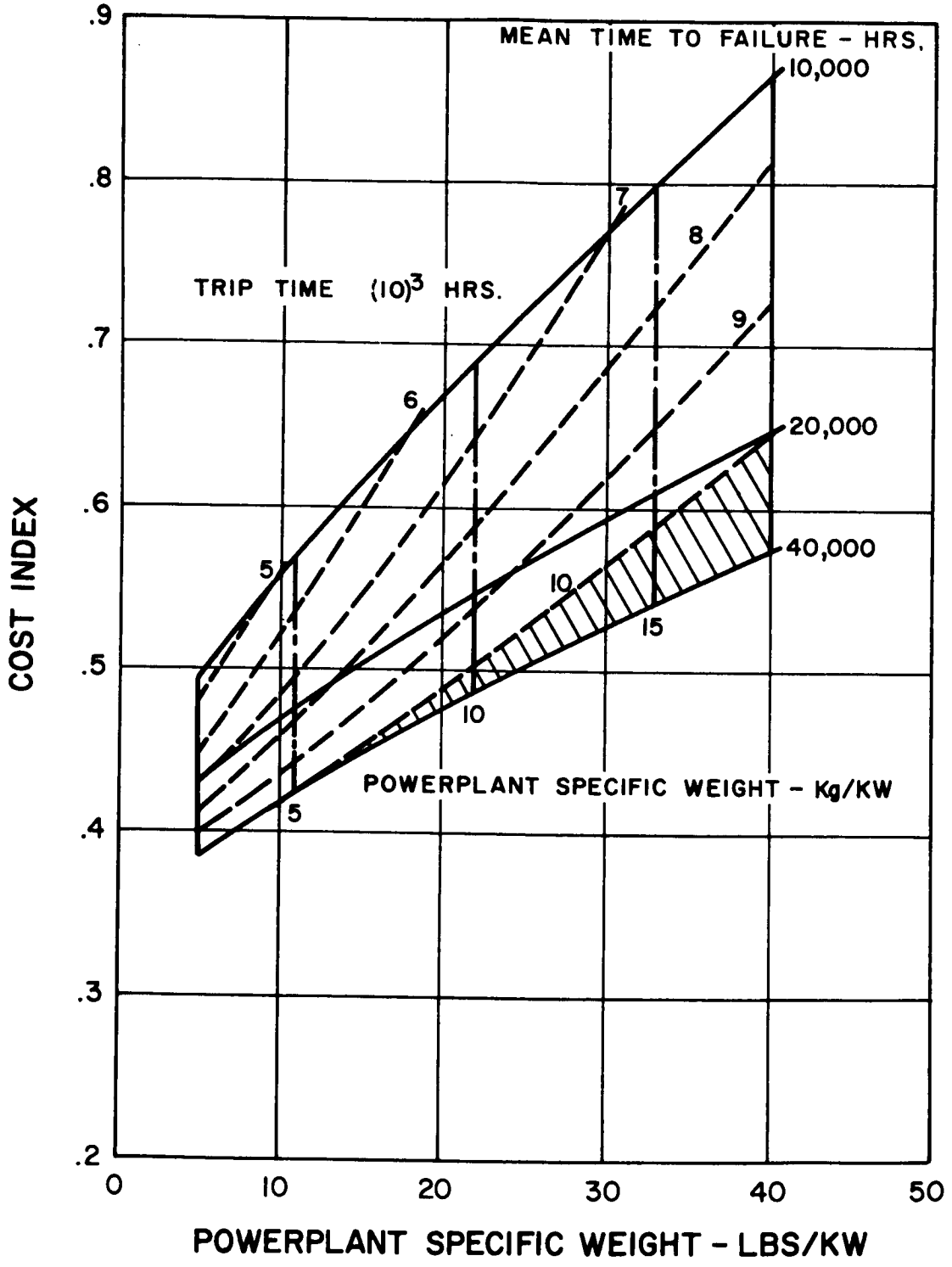

Figure 6-8. Effect of Mean Time to Failure on Single Trip Ferry Performance

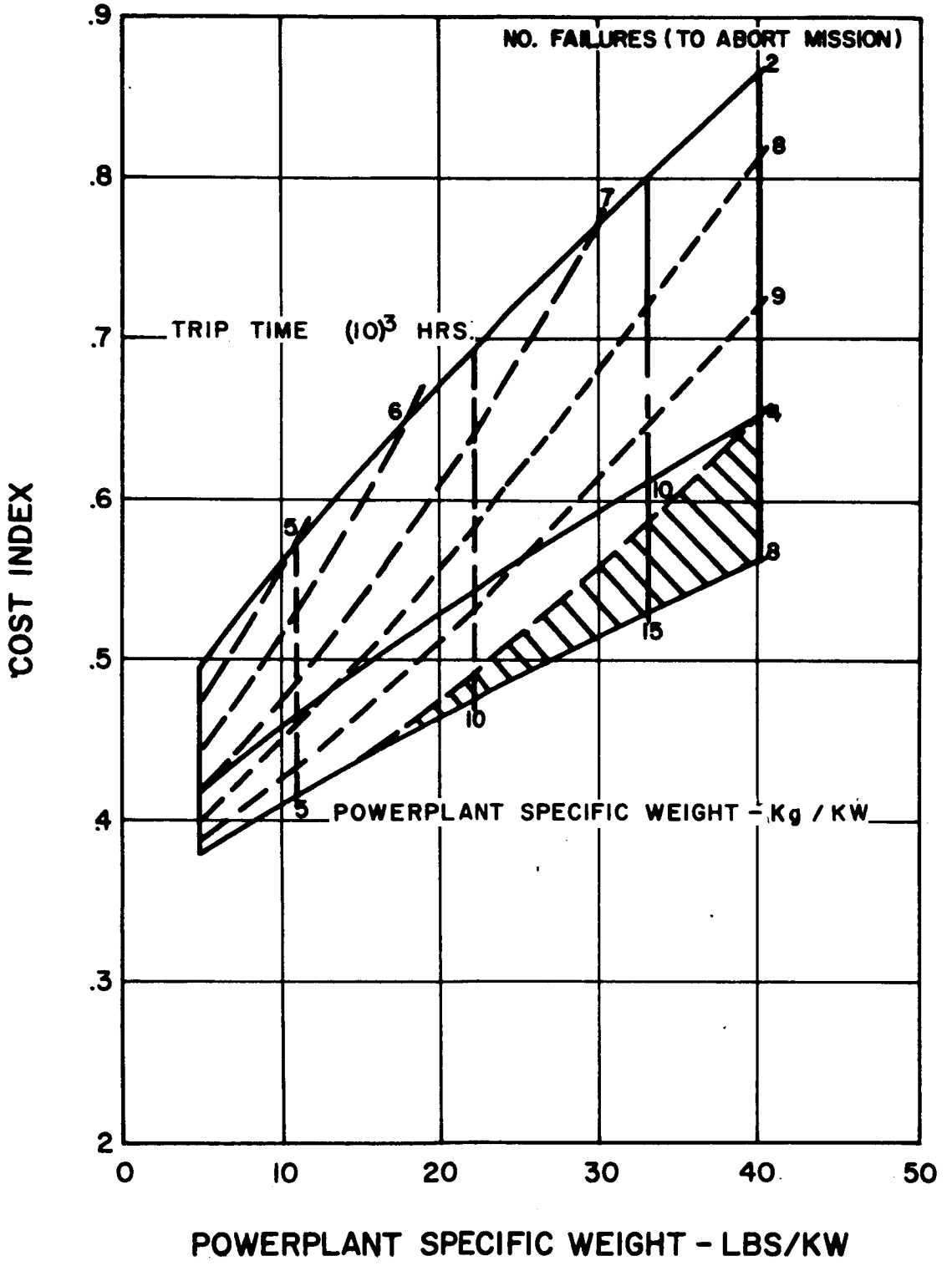

Figure 6-9. Effect of No. of Failures on Single Trip Ferry Performance

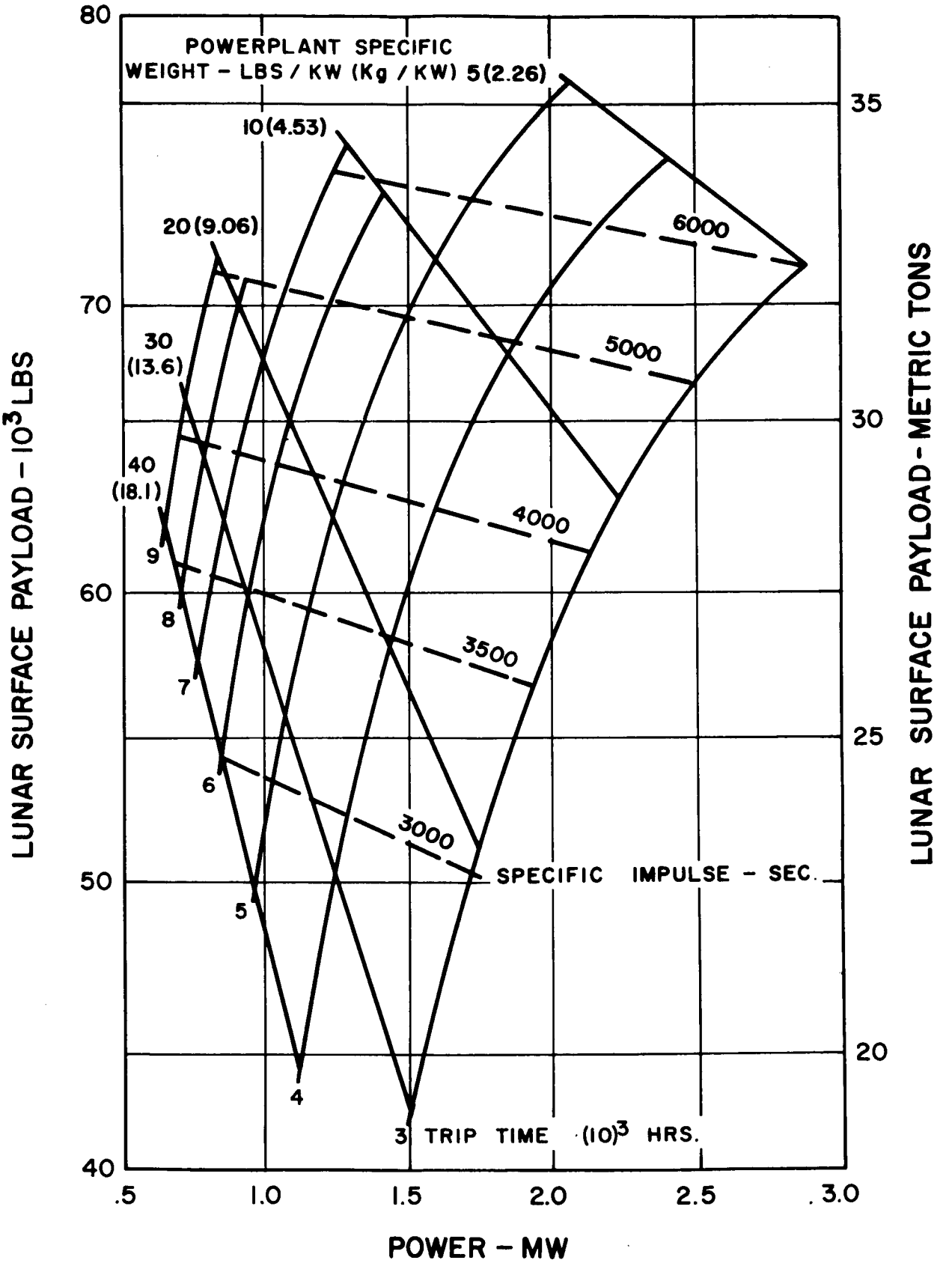

Figure 6-10. Single Trip Ferry Requirements with Nominal Powerplant

nuclear-electric payload capabilities per trip are of the order of 4 to 6 times the corresponding payload capabilities of upper stage chemical propulsion (13,000 kg for trip). Other power-payload mixes are feasible by permitting off-optimum specific impulse operation. This will, however, result in increased cost indexes at constant trip time and powerplant specific weight.

Figure 6-11 contains similar data corresponding to the performance data of Figure 6-7. The data indicates relatively little variation in optimum specific impulse with power rating and, similarly, very little variation in optimum lunar payload per trip with powerplant specific weight. Note that these data have been derived from both the analytical optimization process of equation (9) of Section 5 and the graphical optimization process of Figure 6-6. Figure 6-12 contains the comparable variation in optimum specific impulse and optimum lunar surface payload for both the mean time to failure variation of Figure 6-8 and the number of failures variation of Figure 6-9. These data indicate that the mission performance is dependent upon the ratio of the mean time to failure and the number of failures.

2. Multiple Trip Ferry

a. Optimization Process

Figure 6-13 illustrates the optimization process used in identifying the optimum specific impulse and power requirements for the multiple trip ferry. These data were generated by calculating multiple trip ferry performance over a range of specific impulses and power levels. The data of Figure 6-13 illustrates a set of typical results as obtained for a powerplant specific weight of 20 lbs/KW and for the nominal powerplant characteristics (10,000 hours Mean Time to Failure, payload cost ratio of 2, 2 failures to abort mission, and three trip mission). The envelope around these data, indicated by the dotted line, represent the optimum cost index variation with trip time.

The specific impulse variation with power along this envelope was used to generate the effects of variations in trip time as illustrated in Figures 6-14 and 6-15. The minimum point on the envelope at 15,700 hours trip time and 0.651 relative payload cost has been used as the base point for the parametric studies described in the following section.

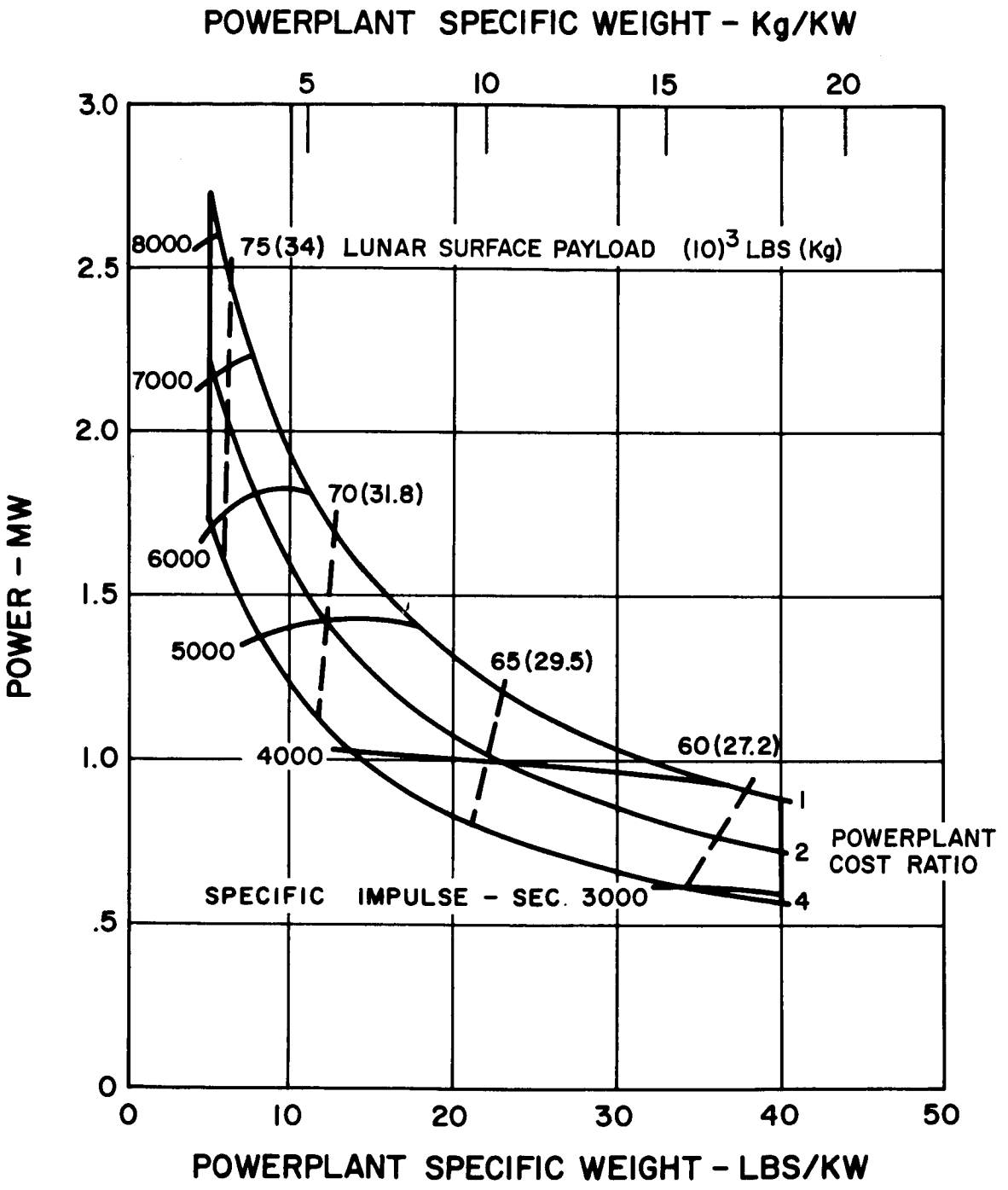

Figure 6-11. Effect of Powerplant and Boost Costs on Single Trip Ferry Requirements

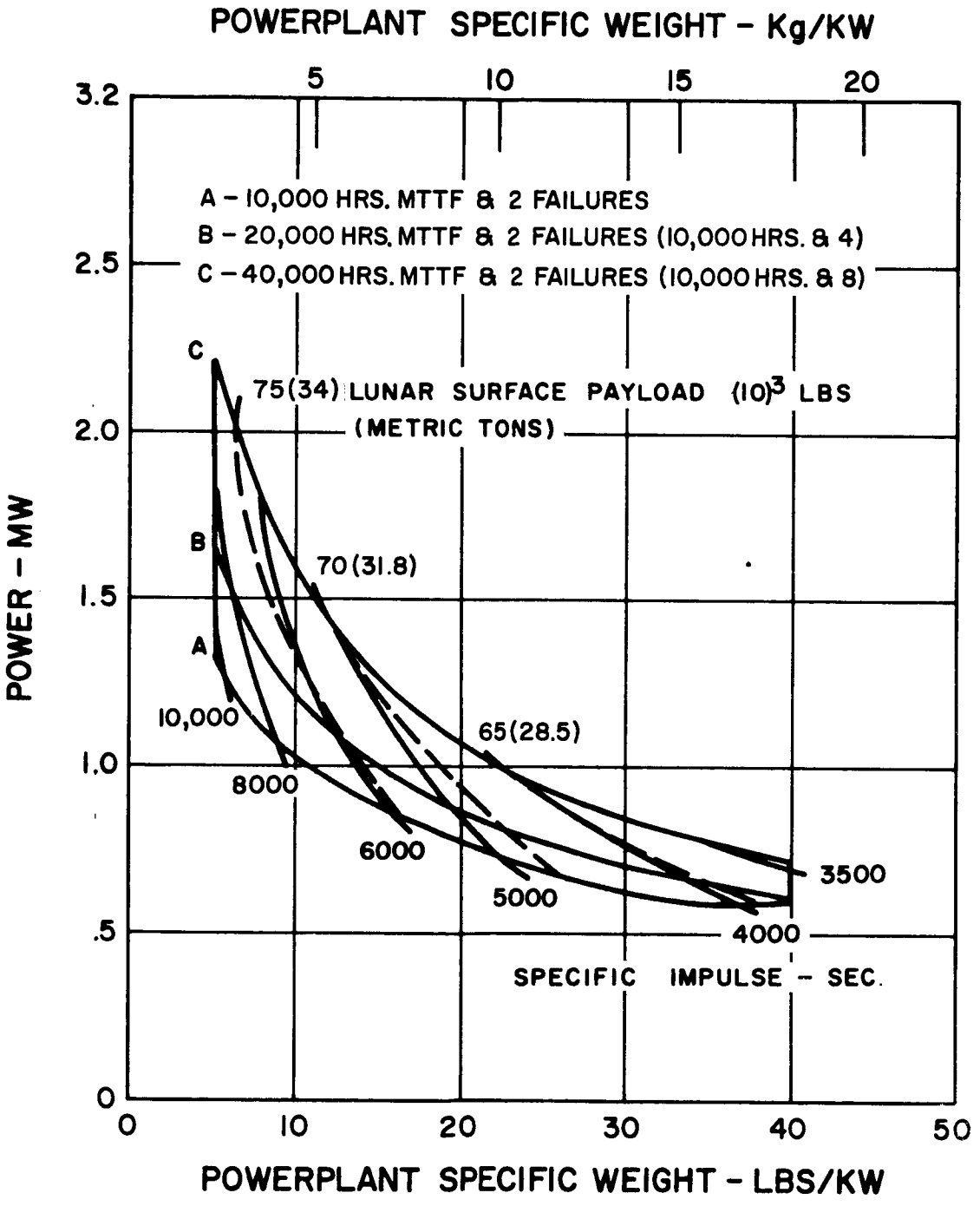

Figure 6-12. Effect of Mean Time to Failure and Number of Failures on Single Trip Ferry Requirements

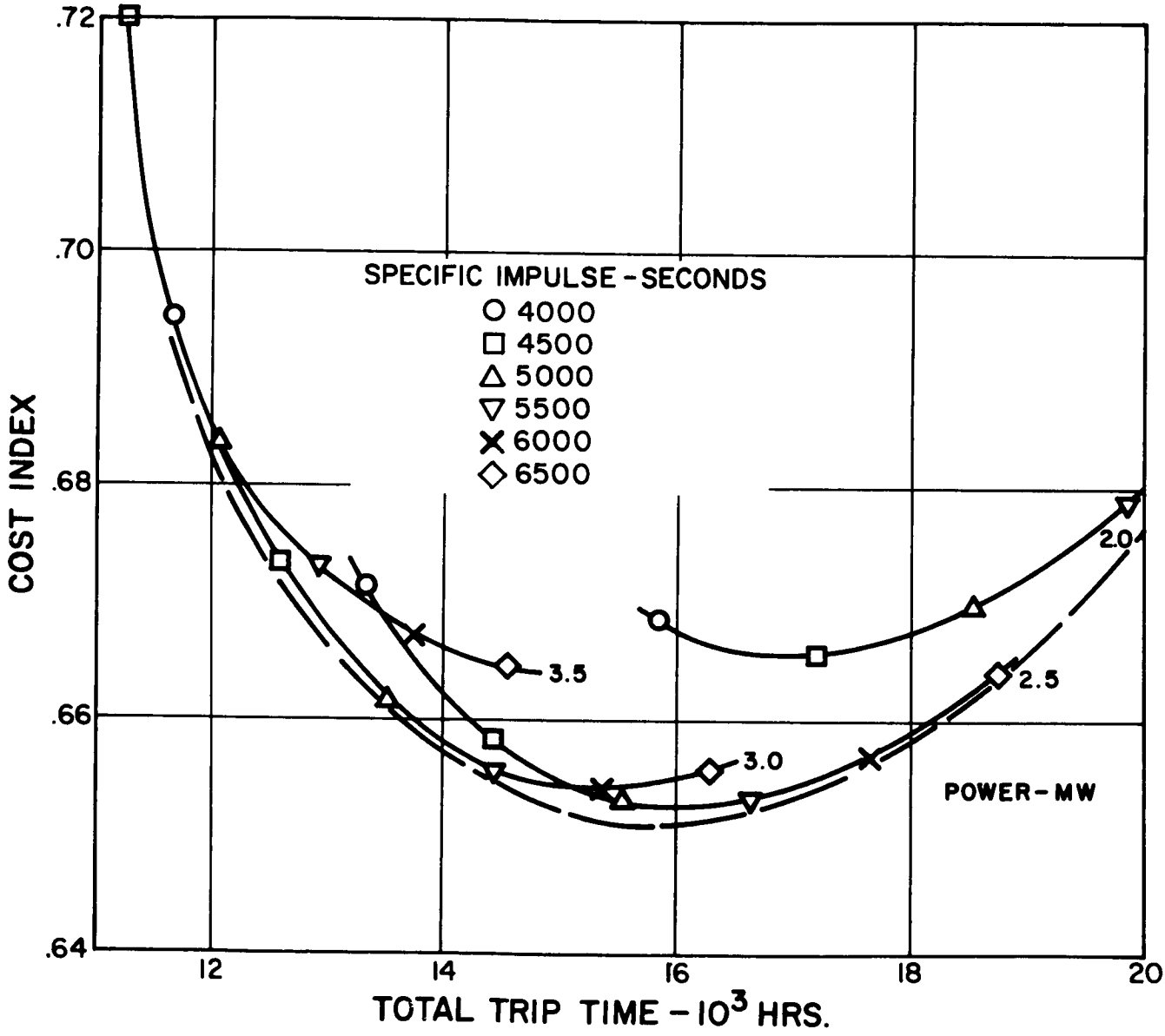

Figure 6-13. Multiple-Trip Working Curve for Nominal Powerplant at 20 lbs/KW Specific Weight

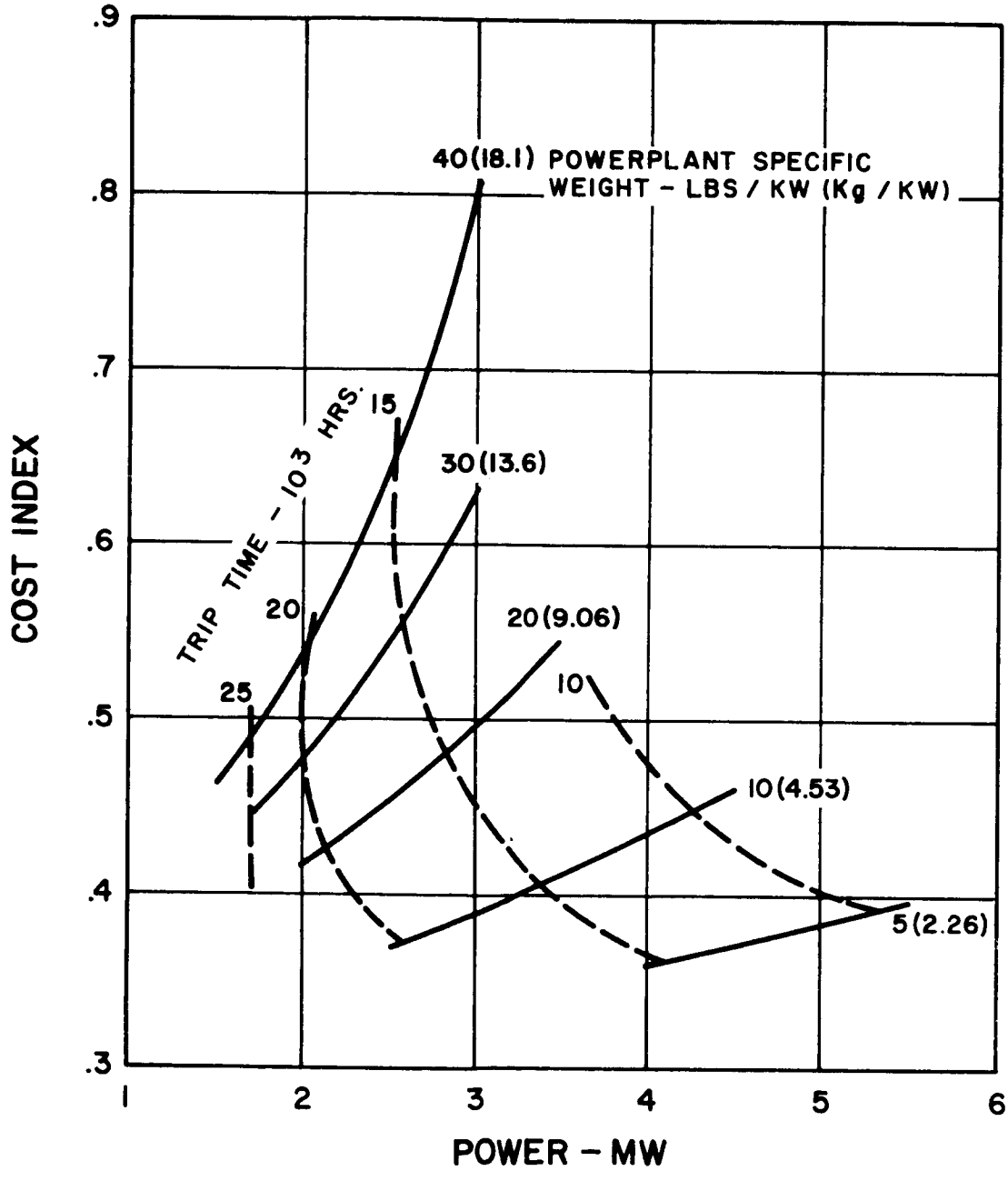

Figure 6-14. Multiple-Trip Ferry Performance with Nominal Powerplant Design - No Survival Penalty

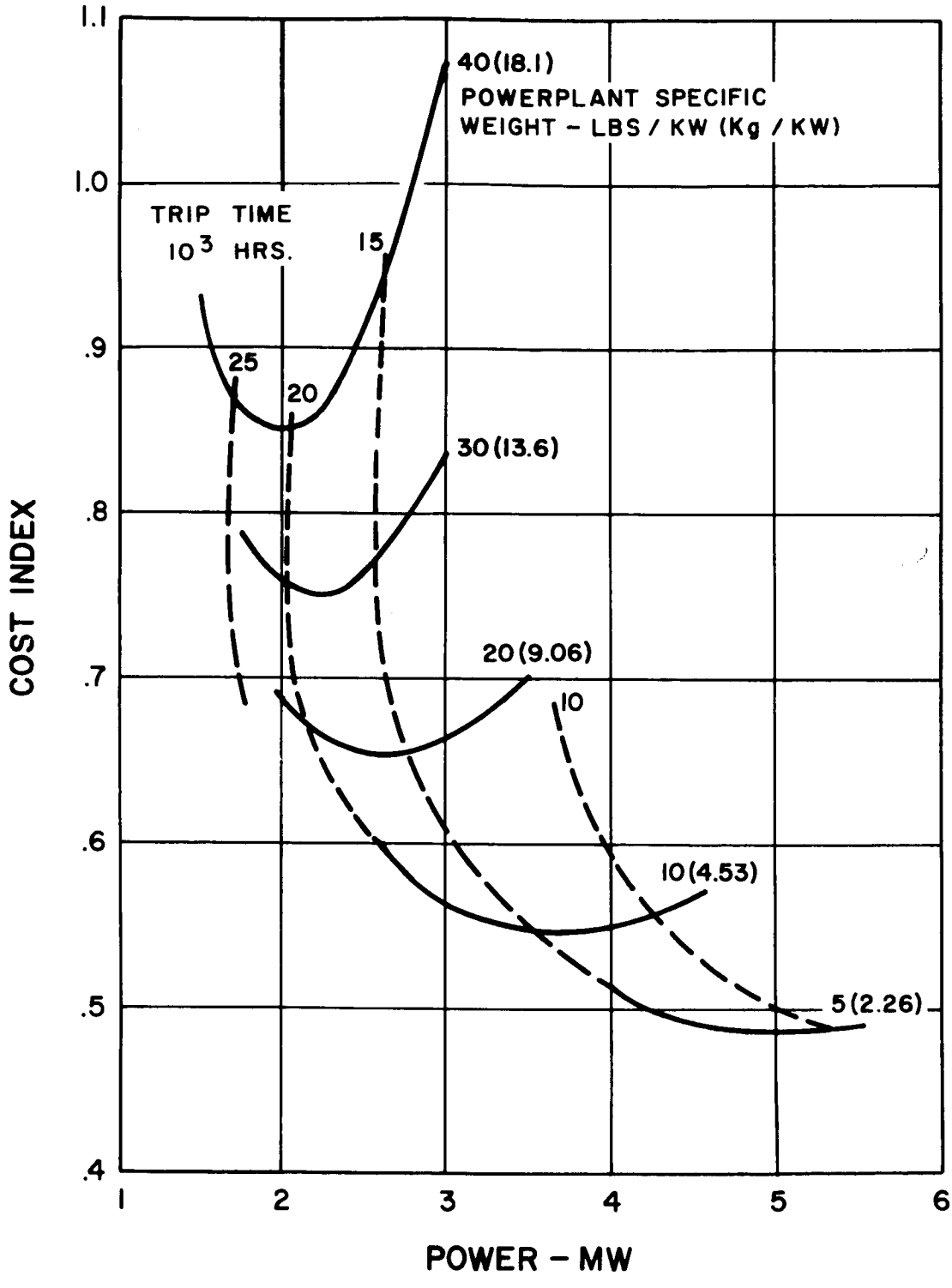

Figure 6-15. Multiple-Trip Ferry Performance with Nominal Powerplant Design - 10,000 Hrs. MTTF, 2 Failures to Abort Mission, Powerplant to Earth Orbit Payload Cost Ratio of 2, Three Trip Mission

The above two-step optimization process has been used to determine corresponding optimum specific impulse and power requirements for each of the remaining powerplant specific weights for the nominal powerplant characteristics and for the various parametric variations investigated. The results of this optimization process are described in the following sections.

b. Performance

The nominal multiple trip performance data are summarized in Figures 6-14 and 6-15. Figure 6-14 illustrates the variation in cost index with powerplant specific weight and trip time with the survival penalty omitted. These data cover the same general range of relative payload costs as the comparable single trip performance of Figure 6-5 but with approximately three times the power and twice the total trip time(for the three trips). Figure 6-15 contains the same nominal performance data but with the survival penalty included in the calculation for cost index. The multiple trip performance appears to be 1 to 2 percent better than that obtained for the single trip mode.

The points of minimum cost index for each powerplant specific weight have been used as base points, as before, in exploring the effects of variations in powerplant to booster cost ratio, mean time to failure, number of failures, and number of trips. The parametric data has been generated by varying one parameter at a time while maintaining the others at their nominal values. Figure 6-16 illustrates the performance variation with powerplant to booster cost ratio for the nominal mean time to failure, the nominal number of failures, and the nominal three trip mission. Data are shown for the nominal cost ratio of 2 and for values of 1 and 4 as well.

Figure 6-17 contains the performance variation for mean time to failure of 10,000, 20,000, and 40,000 hours. Note that the data for 40,000 hours involves total trip times up to 40,000 hours for the nominal three trip mission which would involve single trip times in excess of 10,000 hours. Similar data is illustrated in Figure 6-18 for the effect of 2, 4 and 8 failures. Figure 6-19 illustrates the performance variation for the nominal powerplant for 2,3 and 4 trip missions. These data have been plotted against total trip time with lines of constant cost index in order to obtain a clearer picture of the performance variation with the number of trips. Note that both the cost index and the average trip time is reduced as the number of trips is increased from 2 to 4.

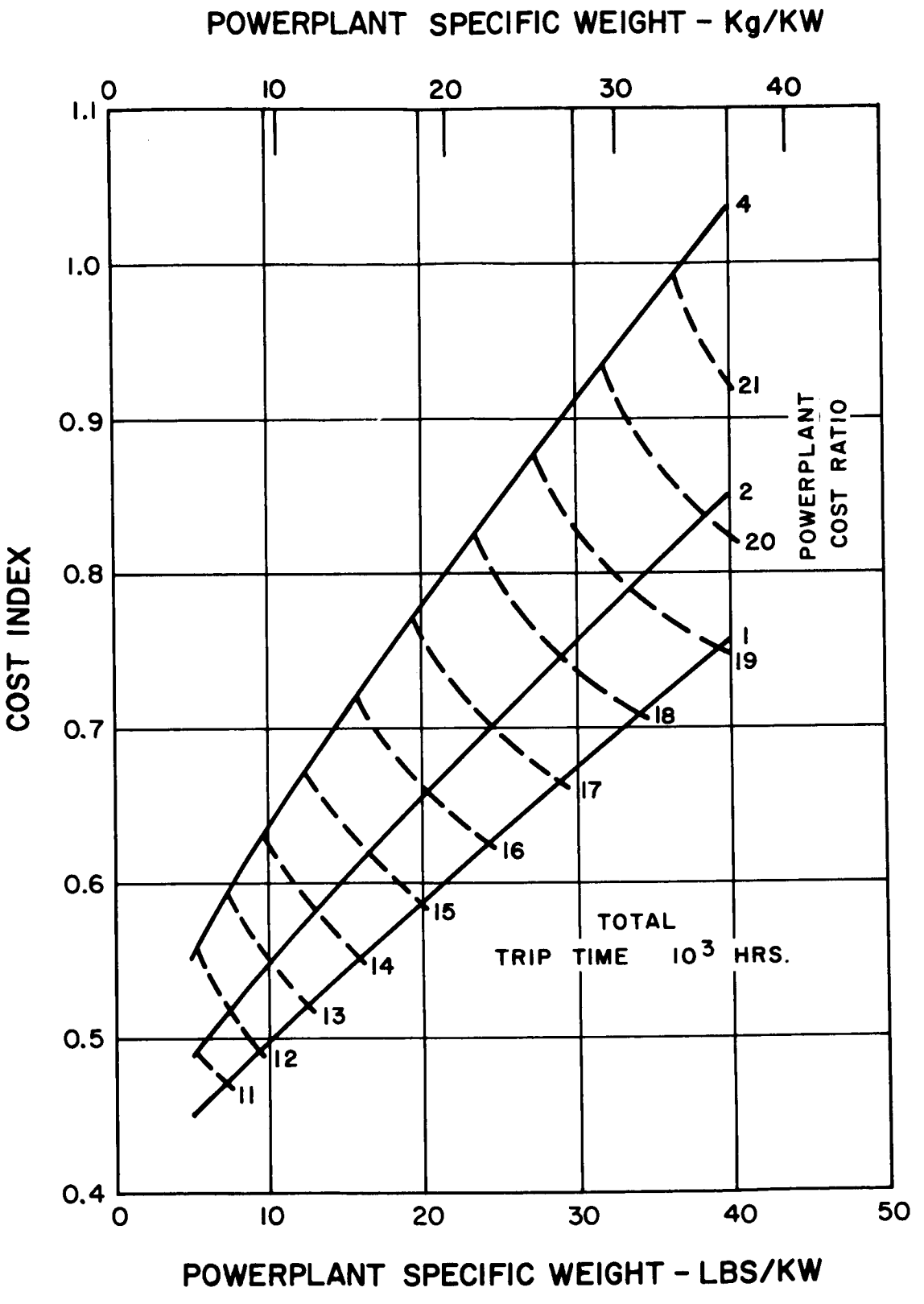

Figure 6-16. Effect of Powerplant Cost Ratio on Multiple-Trip Ferry Performance

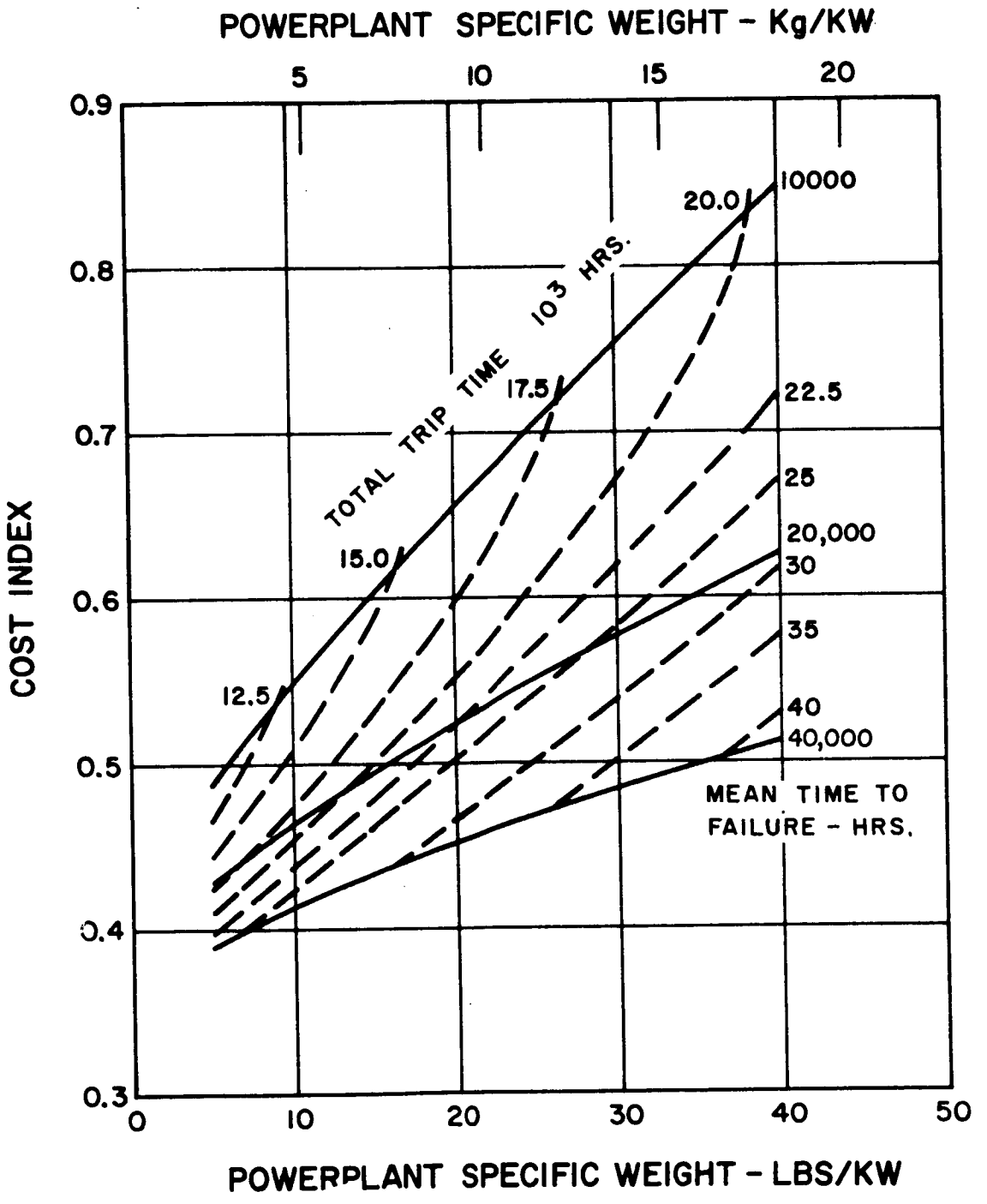

Figure 6-17. Effect of Mean Time to Failure on Multiple-Trip Ferry Performance

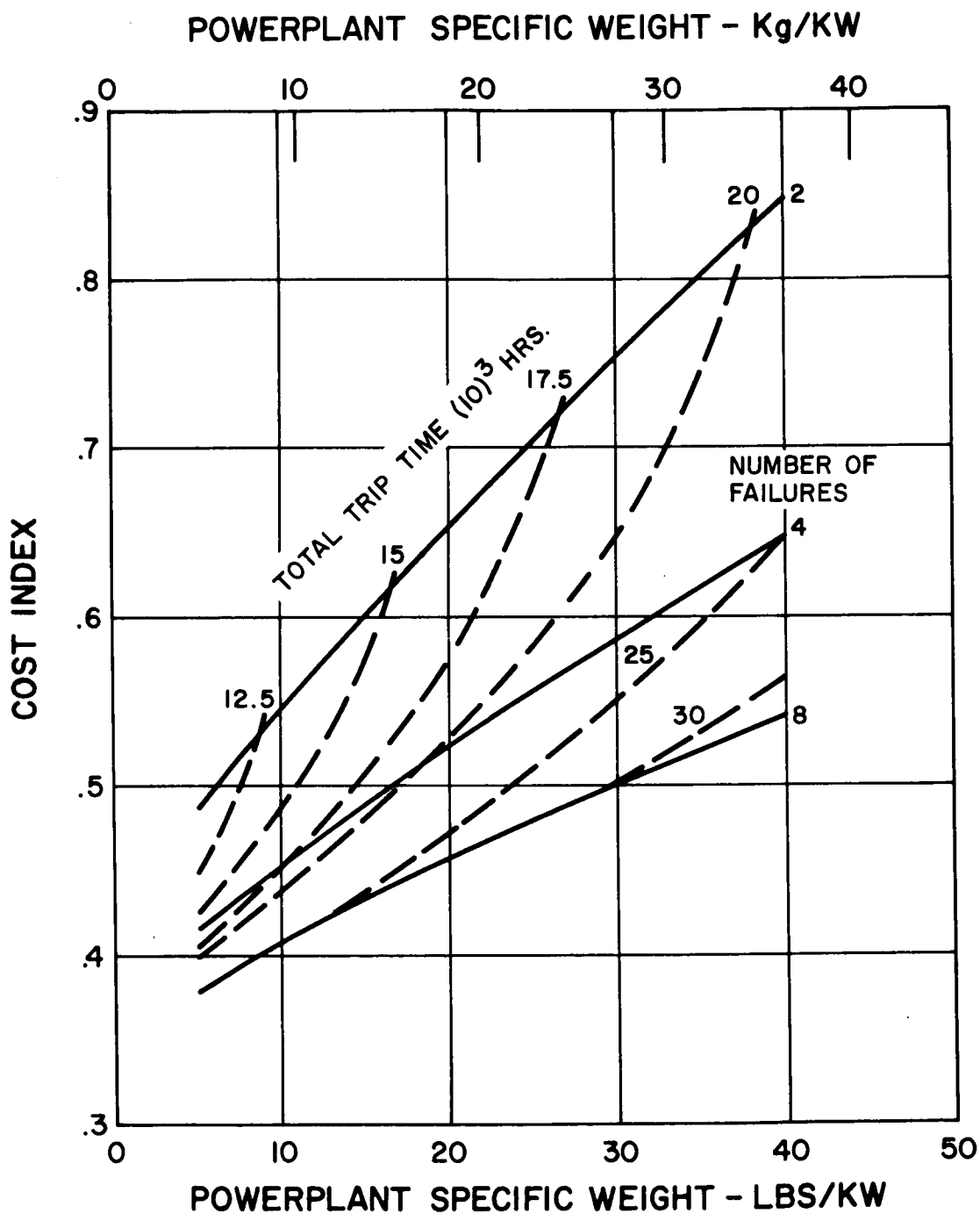

Figure 6-18. Effect of Number of Failures on Multiple-Trip Ferry Performance

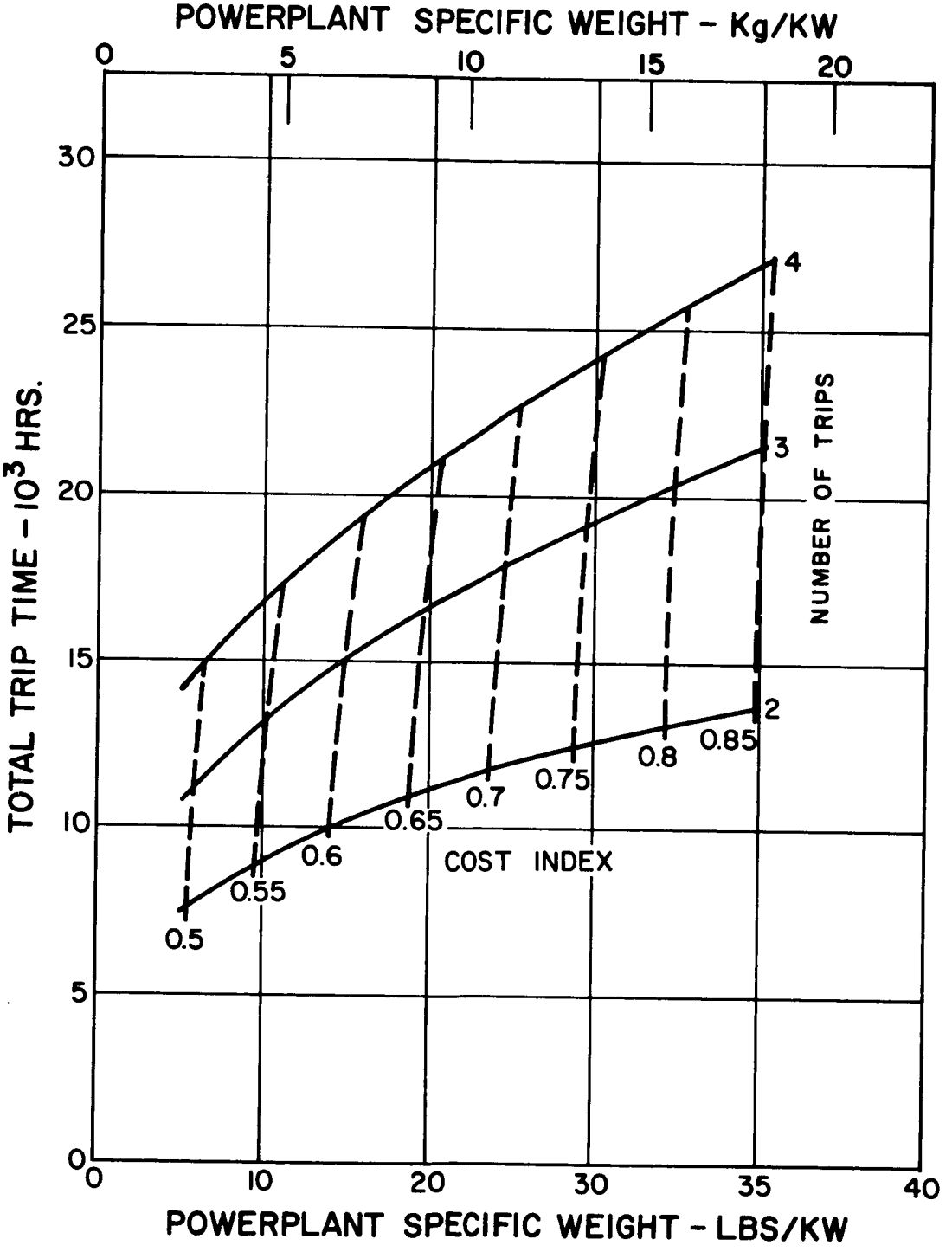

Figure 6-19. Effect of Number of Trips on Multiple-Trip Ferry Performance

c. Mission Requirements

Figures 6-20 through 6-24 contain the mission requirements associated with the performance data of Figures 6-14 through 6-19. These data illustrate the optimum specific impulse and power rating as a function of powerplant specific weight. Total lunar surface payload capabilities are also indicated. Figure 6-20 contains the data for the nominal powerplant corresponding to the performance data of Figures 6-14 and 6-15. These data indicate that the multiple trip ferry can deliver average payloads per trip of the order of 50 percent greater than the single trip for the same relative payload cost.

Figure 6-21 contains similar data for the variation in cost ratio corresponding to the performance data contained in Figure 6-16. Similarly, Figure 6-22 contains the mission requirements for the mean time to failure variation corresponding to the performance data of Figure 6-17, and Figure 6-23 contains the data for the number of failure variation corresponding to the performance data of Figure 6-18. Figure 6-24 illustrates the variation in total lunar surface payload with powerplant specific weight for 2, 3, and 4 trip missions corresponding to the performance data of Figure 6-18. Note that the optimum power and the optimum specific impulse are both independent of the number of trips.

Table 6-1 summarizes the individual outbound and inbound trip times for each of the trips of the multiple trip ferry and also the individual payloads for each trip. These data have been obtained directly from computer results. These results indicate the possibility of utilizing a common lunar landing stage for the middle and terminal trips for most powerplant configurations. The initial trip payload, however, appears to be generally 80 percent higher than the other two and would, consequently, require an additional lunar landing vehicle.

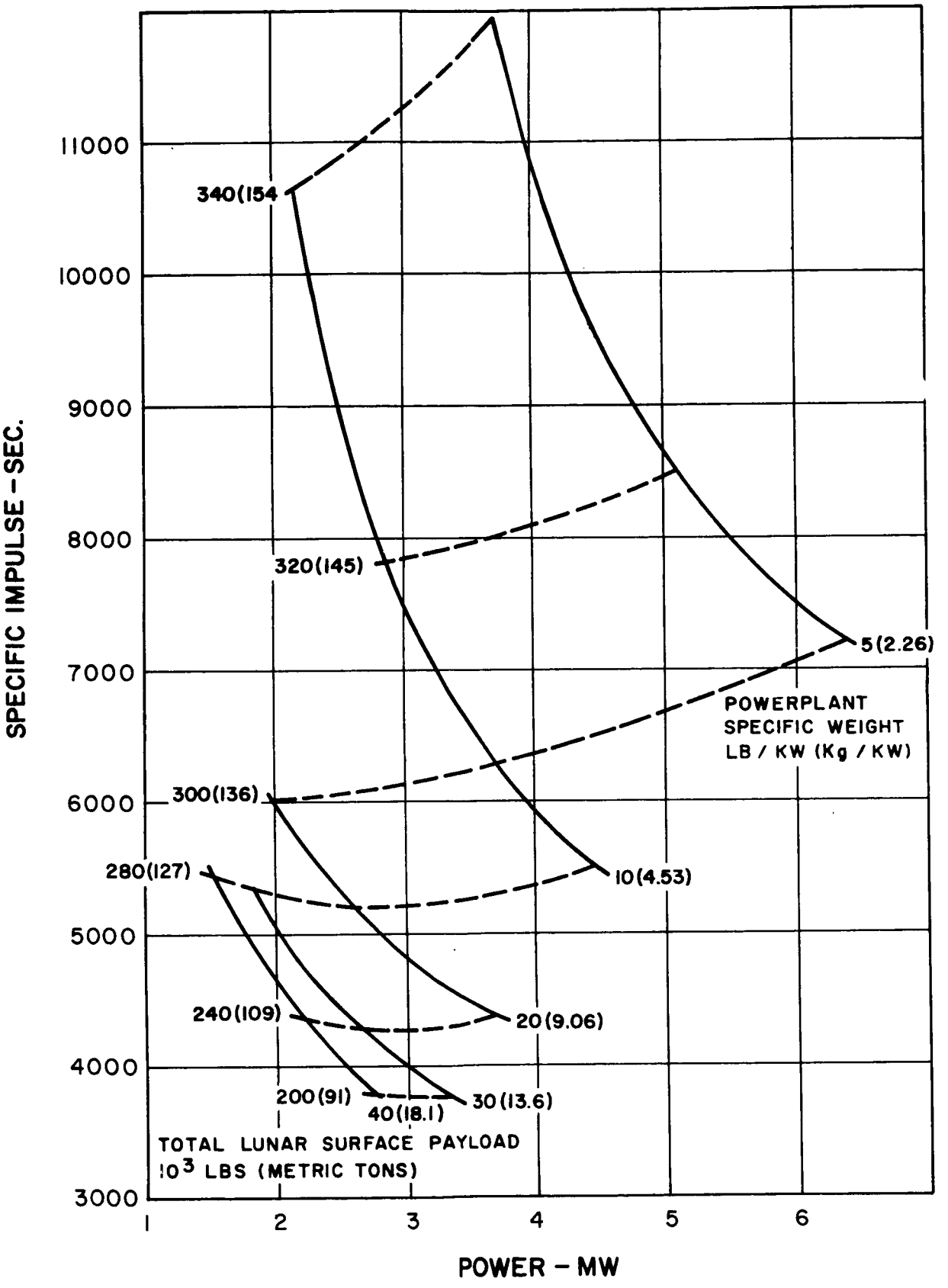

Figure 6-20. Multiple-Trip Ferry Requirements with Nominal Powerplant Design

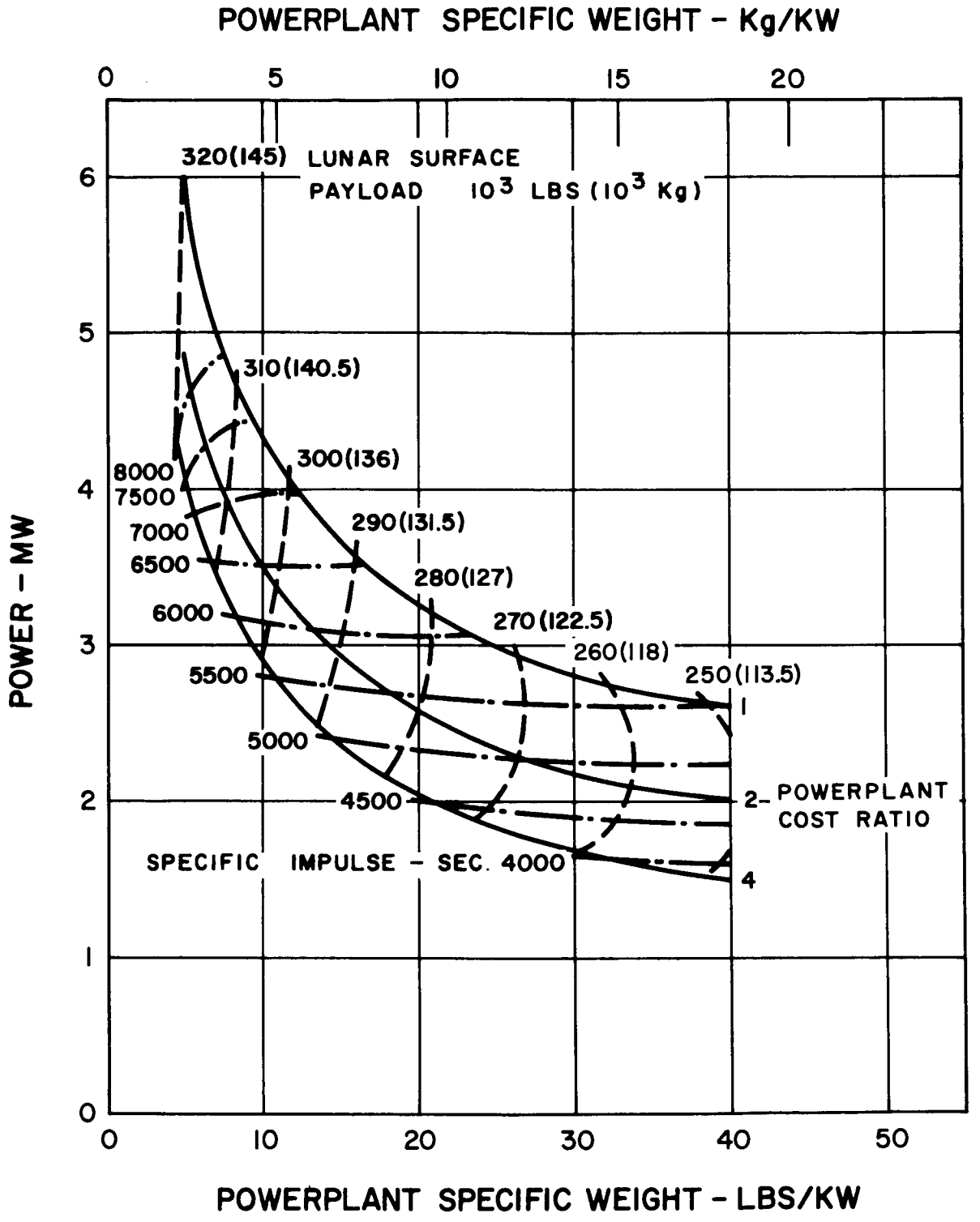

Figure 6-21. Effect of Powerplant Cost Ratio on Multiple-Trip Ferry Performance

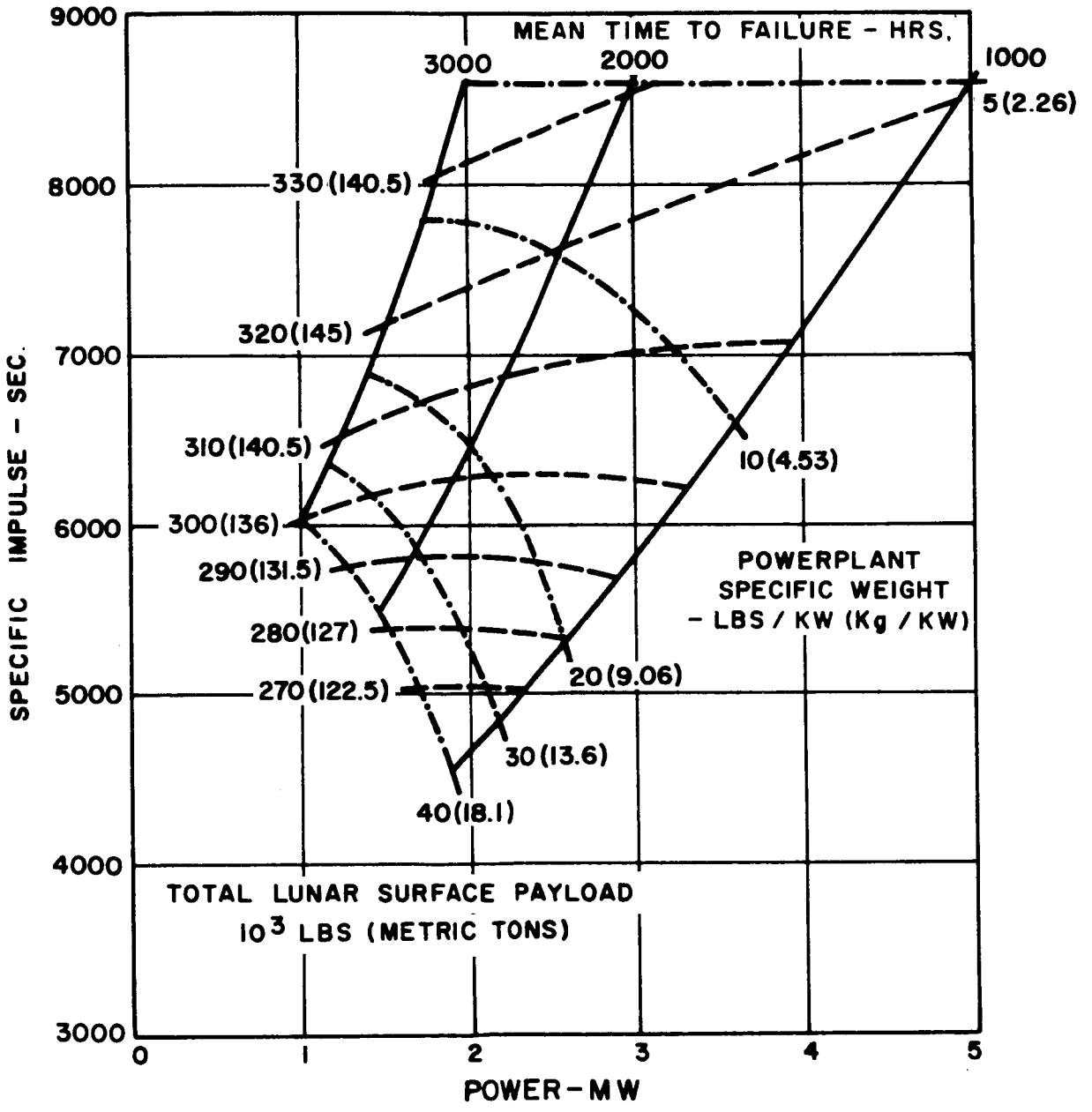

Figure 6-22. Effect of Mean Time to Failure on Multiple-Trip Ferry Performance

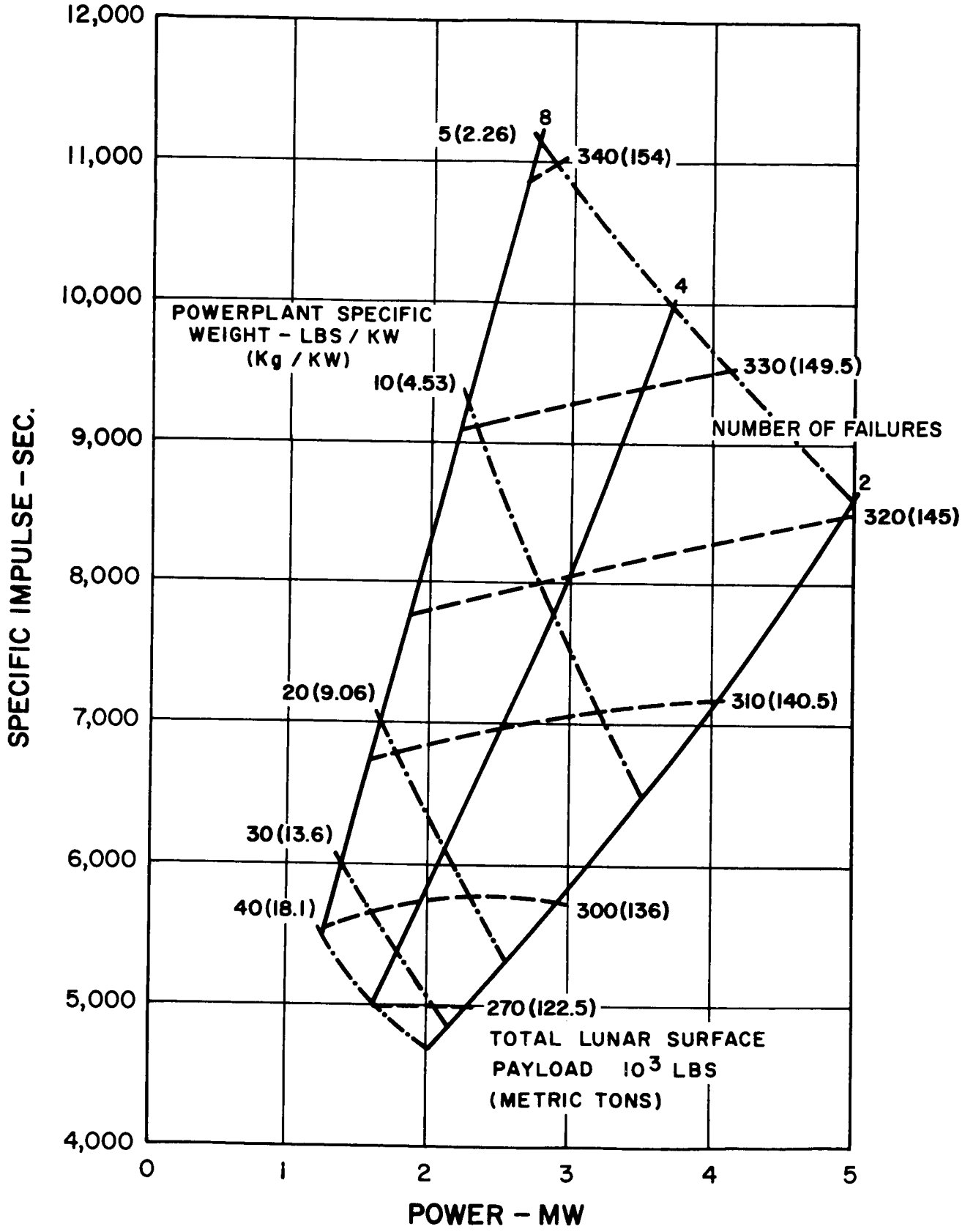

Figure 6-23. Effect of Number of Failures on Multiple-Trip Ferry Requirements

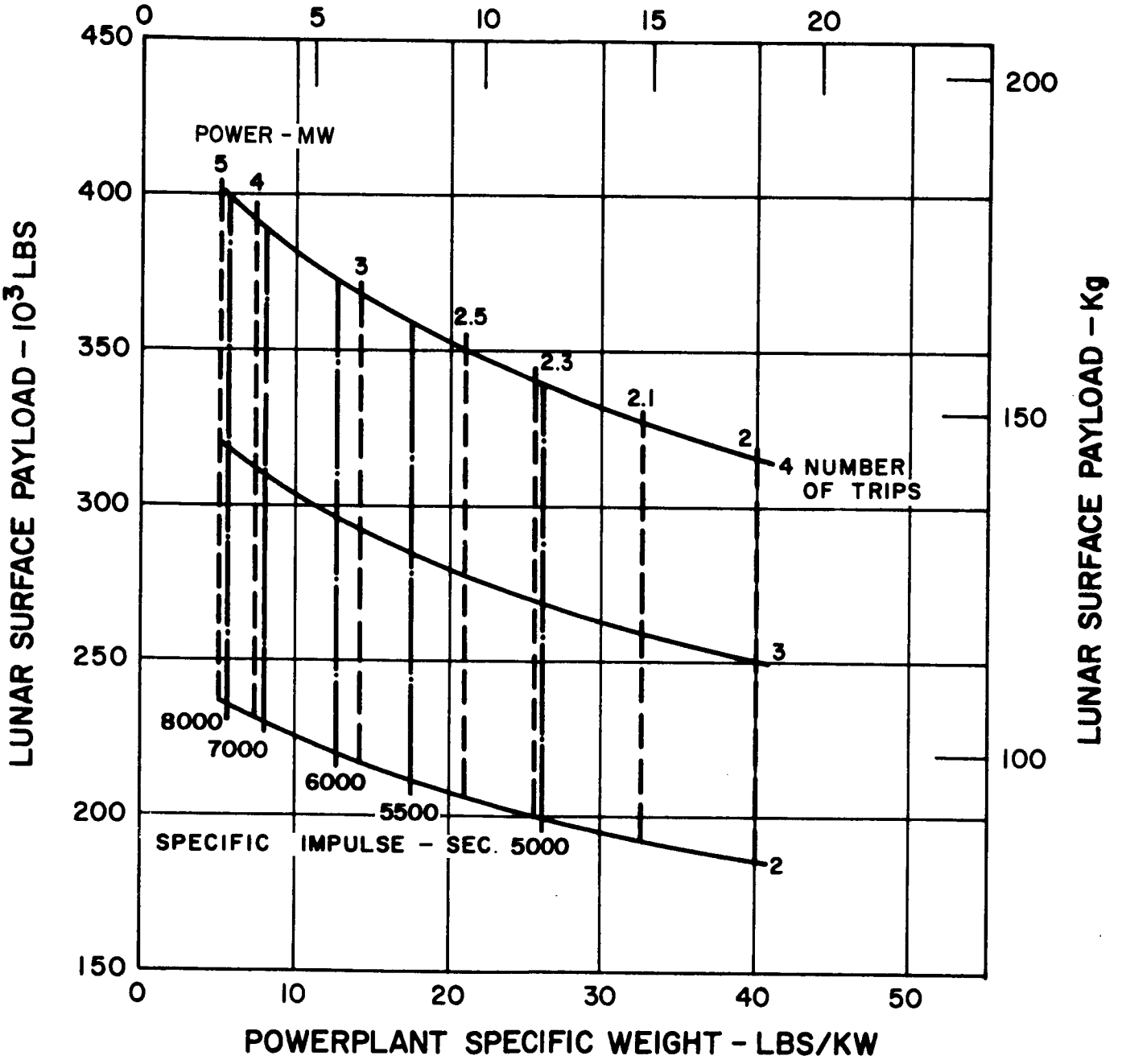

Figure 6-24. Effect of Number of Failures on Multiple-Trip Ferry Requirements

TABLE 6-1. SUMMARY OF MULTIPLE-TRIP FERRY CHARACTERISTICS

CR	Cost Ratio - Powerplant to Earth Orbital Payload
NT	Number of Trips
NF	Number of Failures (leading to aborted mission)
MTF	Mean Time to Failure - hrs.
W	Powerplant Specific Weight - lbs/kw
TT	Total Trip Time - hrs. $(TT) = (T1) + \left[(NT) - 1\right]\left[(T2) + (T3)\right]$
T1	Trip Time of Initial Outbound Leg - hrs.
T2	Trip Time of Inbound Legs - hrs.
T3	Trip Time of Subsequent Outbound Legs - hrs.
WPL1	Initial Trip Payload in Lunar Orbit - $(10)^3$ lbs.
WPL2	Middle Trip Payload in Lunar Orbit - $(10)^3$ lbs.
WPL3	Terminal Trip Payload in Lunar Orbit - $(10)^3$ lbs.
WPL	Total Payload Delivered to Lunar Surface - $(10)^3$ lbs. $(WPL) = R \left\{(WPL1) + \left[(NT) - 2\right] \quad (WPL2) + (WPL3)\right\}$
R	Ratio Lunar Surface Payload to Lunar Orbit Payload

TABLE 6-1.
SUMMARY OF MULTIPLE-TRIP FERRY CHARACTERISTICS

CR	NT	NT	MTF	W	TT	T1	T2	T3	WPL1	WPL2	WPL3	WPL
2	3	2	10,000	5	9566	3922	454	2367	373.3	203.3	209.2	314.3
					10,907	4560	470	2703	382.9	206.8	211.7	320.6
					12,816	5466	493	3182	393.3	210.9	214.8	327.6
					15,572	6773	528	3872	404.3	215.1	218.1	335.0
				10	9394	3593	597	2303	327.6	181.3	193.4	280.9
					12,895	5254	638	3183	359.5	194.8	202.3	302.7
					16,264	6843	683	4027	377.8	202.6	208.0	315.4
					21,750	9443	752	5402	396.1	210.2	213.9	328.1
				20	11,257	3963	916	2731	281.6	159.5	179.8	248.4
					13,238	4895	942	3229	306.0	170.4	186.1	265.0
					15,877	6133	979	3893	328.4	180.5	192.4	280.5
					21,142	8644	1036	5213	355.5	191.6	199.6	298.7
				30	12,822	4229	1214	3083	244.9	141.1	169.1	222.0
					15,592	5501	1264	3782	281.4	159.0	179.3	247.9
					18,411	6799	1314	4492	306.0	170.7	186.4	265.2
					23,622	9240	1391	5800	335.1	183.4	194.4	285.2
				40	13,107	3907	1489	3111	190.1	114.1	154.8	183.6
					15,835	5122	1553	3803	238.2	139.4	168.6	218.5
					20,378	7169	1655	4950	285.2	162.6	182.0	251.9
					28,170	10,780	1788	6907	327.7	181.4	193.4	281.0
2	3	2	20,000	5	16,987	7600	470	4223	402.6	210.6	213.5	330.7
				10	18,918	8158	689	4691	386.0	204.8	209.3	320.0
				20	22,422	9194	1079	5536	361.5	195.3	202.6	303.8
				30	25,674	10,158	1442	6316	343.8	188.0	197.7	291.8
				40	28,913	11,151	1788	7093	330.4	182.1	193.8	282.5
			40,000	5	24,587	11,401	470	6124	412.5	212.4	214.4	335.7
				10	26,995	12,173	670	6711	400.5	208.4	211.4	328.1
				20	32,027	13,905	1122	7939	383.3	202.2	206.9	317.0
				30	36,953	15,663	1506	9139	370.8	197.1	203.2	308.4
				40	41,545	17,288	1873	10256	361.0	193.0	200.3	301.7

TABLE 6-1.
SUMMARY OF MULTIPLE-TRIP FERRY CHARACTERISTICS (Cont'd)

CR	NT	NF	MTF	W	TT	T1	T2	T3	WPL1	WPL2	WPL3	WPL
2	3	4	10,000	5	15,761	6911	507	3918	403.5	213.6	216.6	333.5
				10	17,428	7394	698	4319	382.5	204.6	209.5	318.7
				20	20,379	8241	1046	5023	353.3	191.6	199.9	297.9
				30	23,003	8957	1378	5645	332.1	182.0	193.4	283.1
				40	25,041	9394	1704	6119	313.6	173.9	188.3	270.3
		8		5	23,032	10,454	551	5738	419.2	218.7	220.5	343.4
				10	24,436	10,757	766	6074	401.6	211.9	215.0	331.4
				20	27,391	11,588	1122	6780	375.6	200.5	206.1	312.8
				30	30,109	12,349	1454	7426	356.5	191.8	199.7	299.2
				40	32,481	12,936	1788	7985	341.0	185.1	195.1	288.5
2	2	2	10,000	5	7733	4560	470	2703	382.9	206.8	211.7	237.8
				10	9074	5254	638	3183	359.5	194.8	202.3	224.7
				20	11,005	6133	979	3893	328.4	180.5	192.4	208.3
				30	12,605	6799	1314	4492	306.0	170.7	186.4	197.0
				40	13,773	7169	1655	4950	285.2	162.6	182.0	186.9
	4			5	14,080	4560	470	2703	382.9	206.8	211.7	403.3
				10	16,716	5254	638	3183	359.5	194.8	202.3	380.6
				20	20,749	6133	979	3893	328.4	180.5	192.4	353.7
				30	24,217	6799	1314	4492	306.0	170.7	186.4	333.5
				40	26,982	7169	1655	4950	285.2	162.6	182.0	316.9
4	3	2	10,000	5	11,816	5080	439	2929	383.5	203.5	208.3	318.1
				10	14,060	5912	604	3471	360.3	191.3	198.5	300.1
				20	17,201	6935	916	4217	329.2	175.3	186.8	276.5
				30	19,534	7580	1216	4761	306.1	163.6	179.2	259.5
				40	21,697	8138	1517	5263	288.6	155.1	174.1	247.1
1				5	10,007	4067	419	2479	378.3	208.0	213.3	319.8
				10	12,126	4774	683	2993	357.0	198.2	206.0	304.5
				20	15,007	5441	1053	3681	323.8	184.5	196.8	282.1
				30	17,163	5962	1414	4187	295.7	173.8	190.5	264.0
				40	19,048	6219	1788	4627	269.3	165.0	185.9	248.1

3. Multiple Engine Ferry

The two-step graphical optimization process has also been used to determine optimum specific impulse and power requirements for the multiple engine (multiple trip) lunar ferry. The following sections describe the mission performance capabilities and associated mission requirements resulting from this optimization process.

a. Performance

Figure 6-25 contains the performance capabilities for a nominal two engine-two trip ferry mission as a function of powerplant specific weight and trip time with the survival penalty omitted. The multiple engine performance is somewhat poorer than the comparable single trip performance at the same trip time and powerplant specific weight. This performance loss is a direct result of the increased power requirement needed for completing a round trip in the same time that the single trip ferry completes its one way trip and of the increased characteristic velocity requirement for the round trip. Figure 6-26 contains the comparable data for the nominal two-engine, two-trip mission with the survival penalty included. These data have been based upon a nominal powerplant mean time to failure of 10,000 hours and a nominal powerplant to booster cost ratio of 2. The cost index minimizes at essentially the same trip time as for the single trip case but at substantially higher values.

Figures 6-27 and 6-28 illustrate the effects of variations in powerplant to booster cost ratio and mean time to failure on the multiple engine mission performance. These data indicate a substantially similar trend with respect to the corresponding variational studies in the previous sections. The cost index values are, however, 30 percent to 70 percent higher than those obtained for the single trip case. Figure 6-29 contains the performance variation with the number of engines. Data are shown for the nominal two engine -- two trip mission and for the following additional cases:

a. Three Engine - Three Trip Mission
b. Four Engine - Four Trip Mission
c. Two Engine - Four Trip Mission

Note that c) involves an engine replacement after every other trip while the other configurations shown involve a replacement after every trip. These data indicate that the payload cost increases

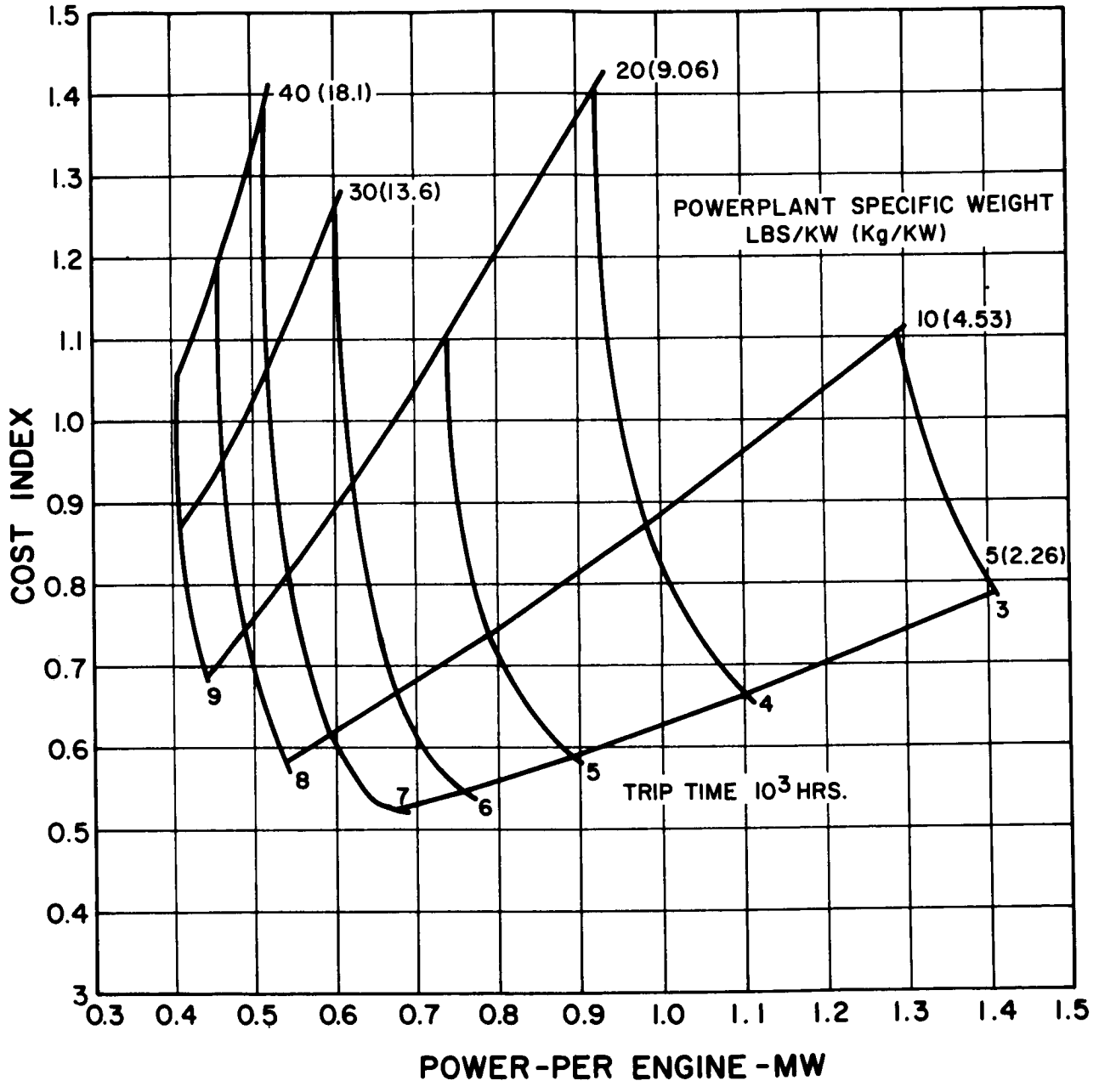

Figure 6-25. Multiple-Trip, Multiple-Engine Ferry Performance with no Survival Penalty

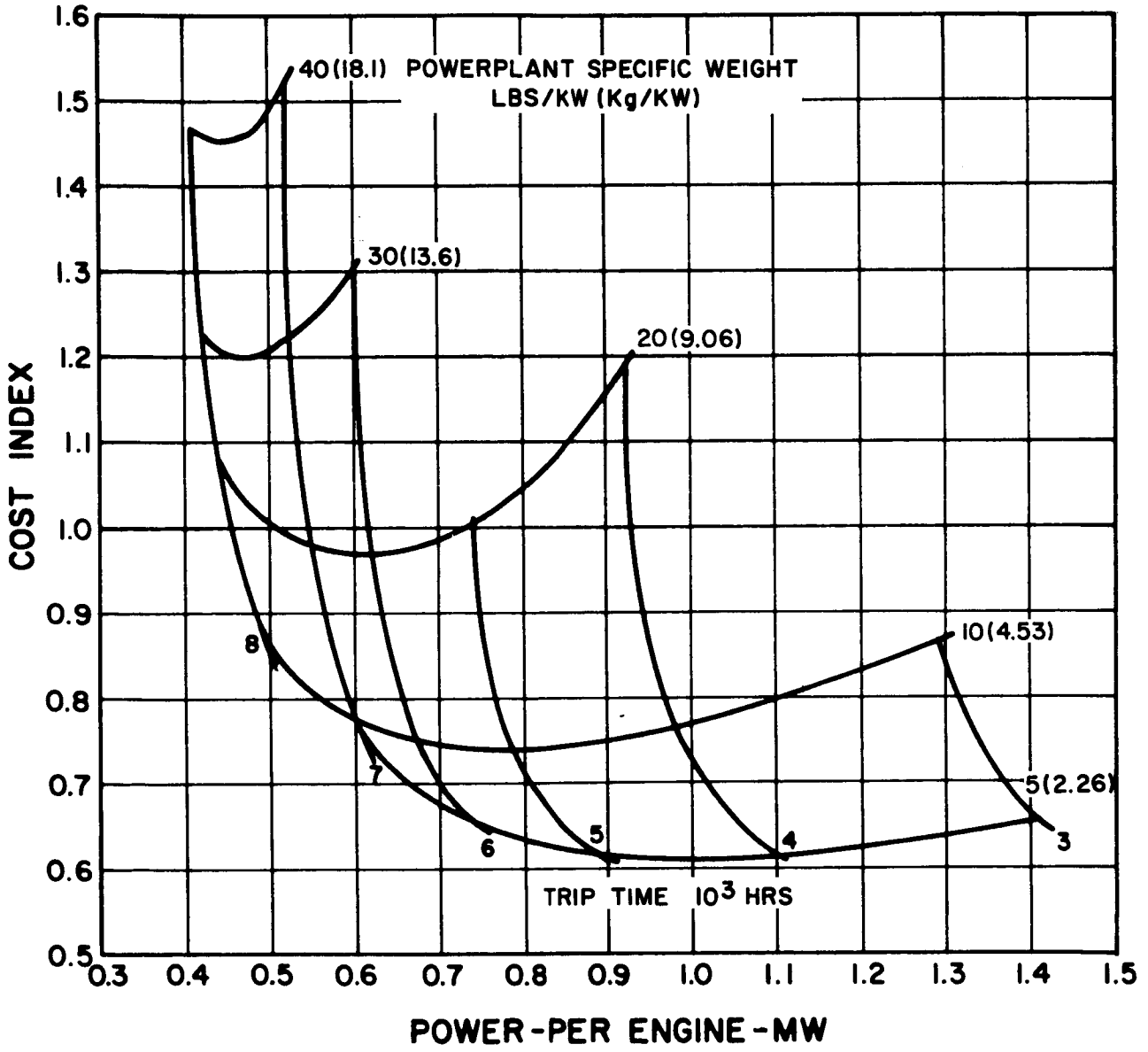

Figure 6-26. Multiple-Trip, Multiple-Engine Ferry Performance with Nominal Powerplant Design 10,000 Hrs. MTTF, Powerplant to Earth Orbit Payload Cost Ratio of 2, Two-Trip, Two-Engine Mission

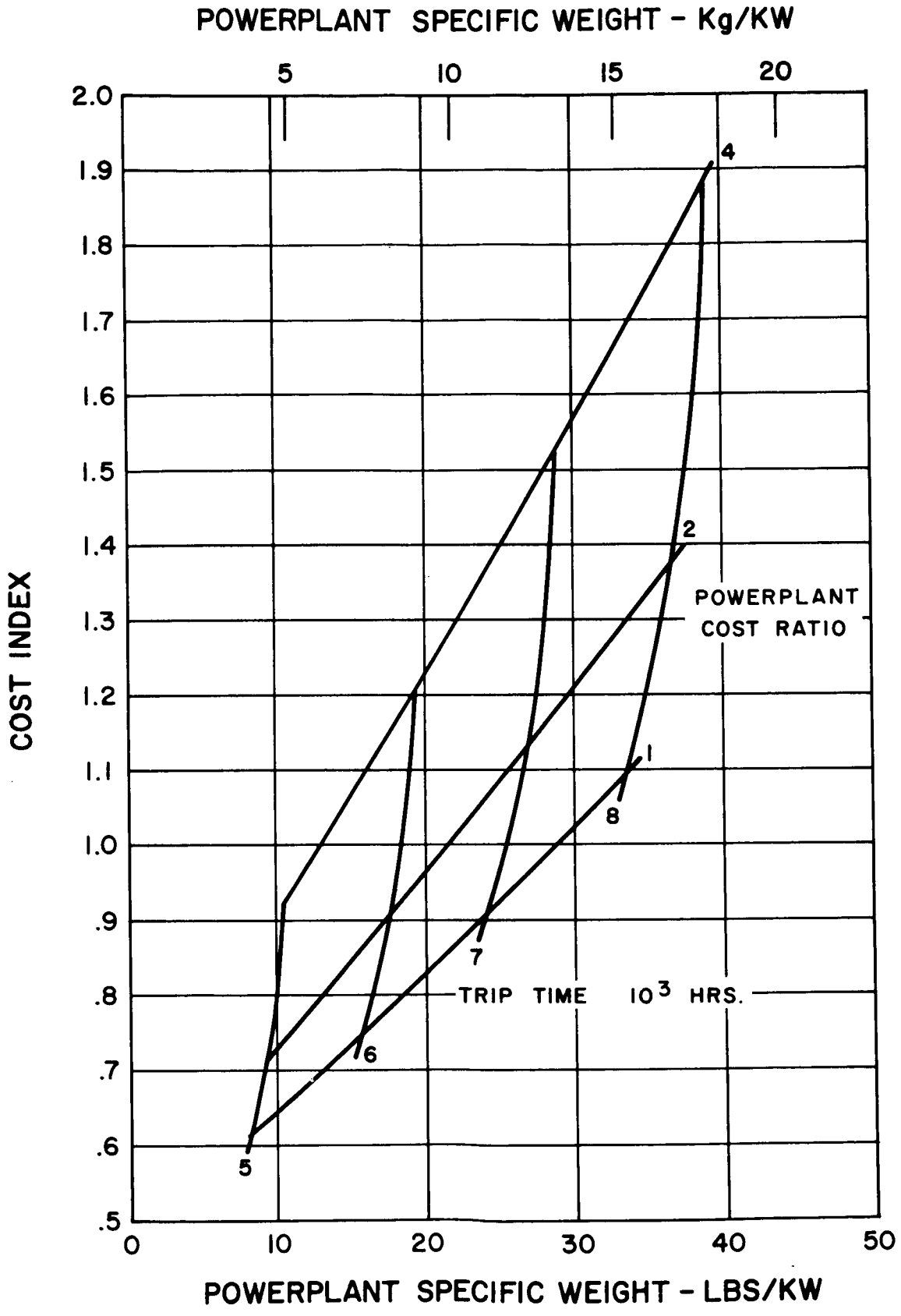

Figure 6-27. Effect of Powerplant and Boost Costs on Multiple-Trip, Multiple-Engine Ferry Performance

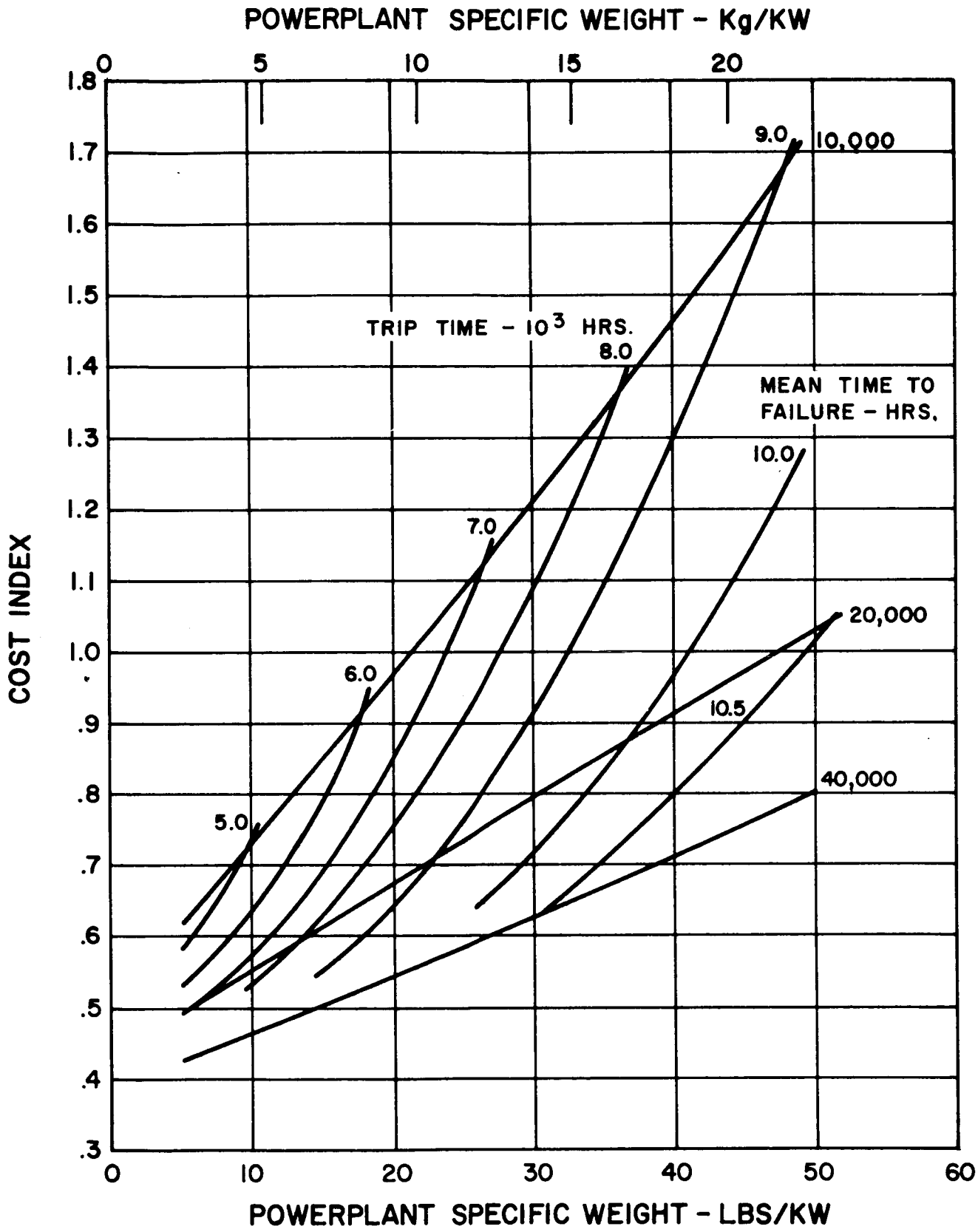

Figure 6-28. Effect of Mean Time to Failure on Multiple-Trip, Multiple-Engine Ferry Performance

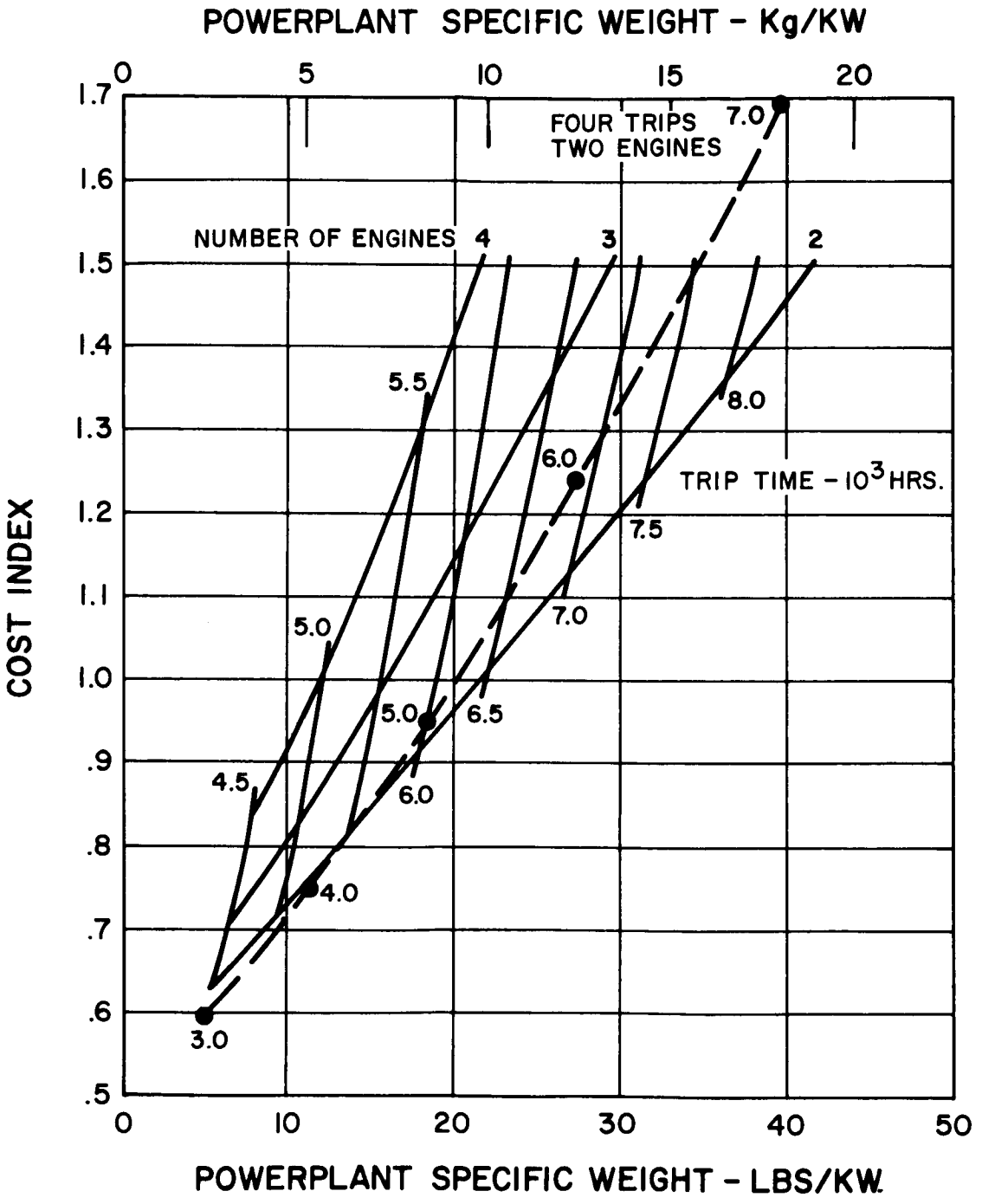

Figure 6-29. Effect of Number of Engines on Multiple-Trip, Multiple-Engine Ferry Performance

as the number of engines is increased. This trend would appear to be a consequence of the increased operating time required from each engine prior to scheduled replacement which results in an increased probability of a premature failure.

b. Mission Requirements

Figures 6-30 through 6-33 contain the corresponding mission requirements associated with the multiple engine performance data of the preceding section. These data illustrate the variations in optimum specific impulse, power, and lunar surface payload as a function of the powerplant specific weight, the powerplant specifications on mean time to failure and powerplant cost ratio, and the number of engines used per mission. Figure 6-30 contains the mission requirements variation with trip time, Figure 6-31 the variation with powerplant cost ratio, Figure 6-32 the variation with mean time to failure, and Figure 6-33 the variation with the number of engines.

4. Evaluation of Results

The performance characteristics for the single trip, multiple trip, and multiple engine ferry missions are summarized in Figure 6-34. These data have been based upon the nominal powerplant specifications of 10,000 hours mean time to failure and a powerplant to booster cost ratio of 2. The single engine data have been based upon the nominal two failures leading to mission abort. These data indicate that the cost index is reduced by about 2 percent when the mission mode is changed from single trip operation to two trip operation with a single engine. Further reductions in payload cost are obtained by increasing the number of trips to three or four. These reductions are, however, extremely small. Conversely, a substantial increase in payload cost is achieved as operation is varied to 2 trip - 2 engine, 3 trip - 3 engine, and 4 trip - 4 engine operation. The 4 trip - 2 engine case is substantially better than the 4 trip - 4 engine case but generally poorer than 2 trip - 2 engine operation. These data, therefore, indicate that the payload cost increases with increased numbers of engines and, consequently, there is no performance incentive for using more than one engine.

Figure 6-35 summarizes the variation in average lunar surface payload per trip with powerplant specific weight for each of the single engine modes of operation investigated. These data have been obtained from the data of the previous sections by dividing the total payload

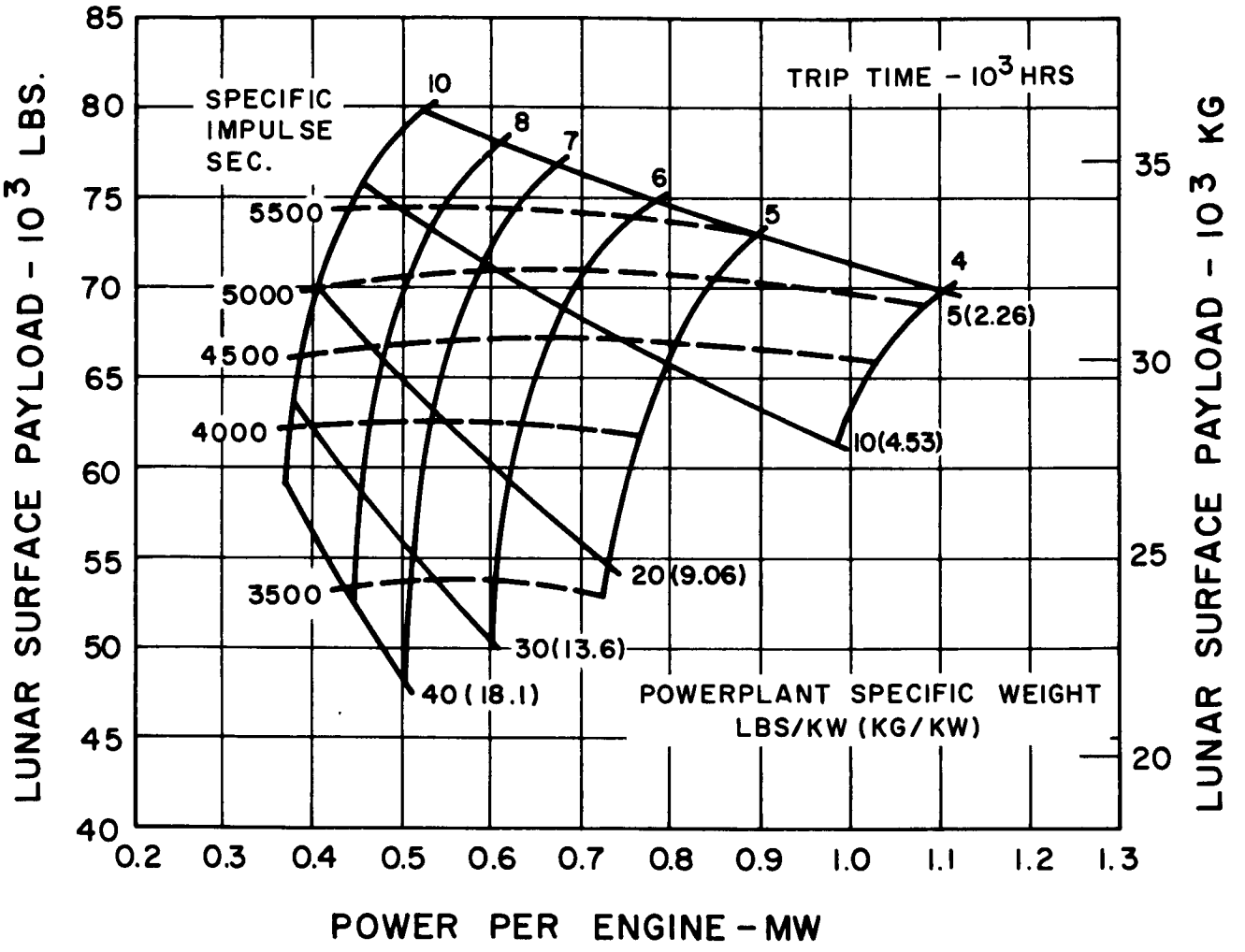

Figure 6-30. Effect of Trip Time on Multiple-Trip, Multiple-Engine Ferry Performance Nominal Powerplant, Two-Trip, Two-Engine Ferry Requirements

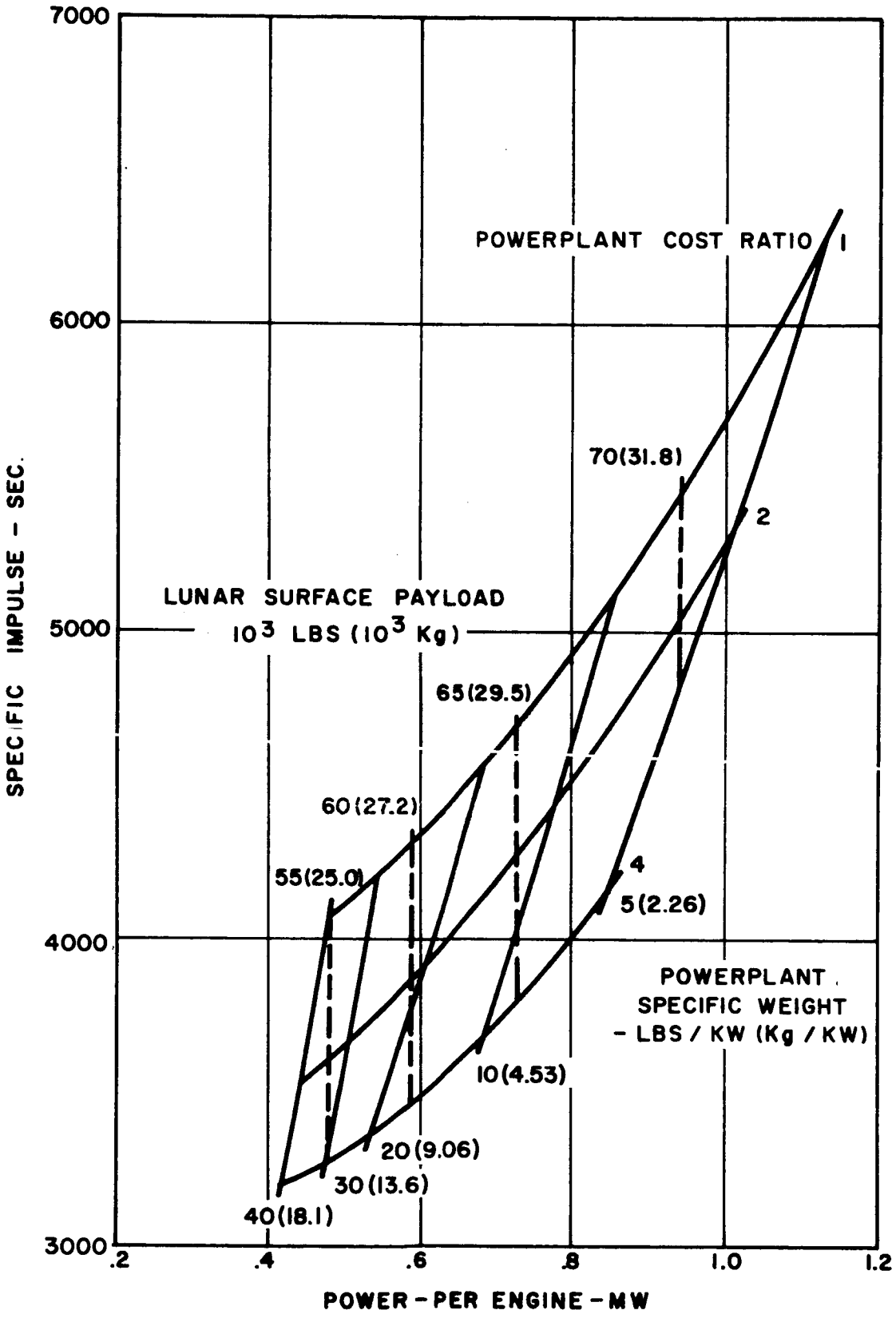

Figure 6-31. Effect of Powerplant Cost Ratio on Multiple-Trip, Multiple-Engine Ferry Requirements

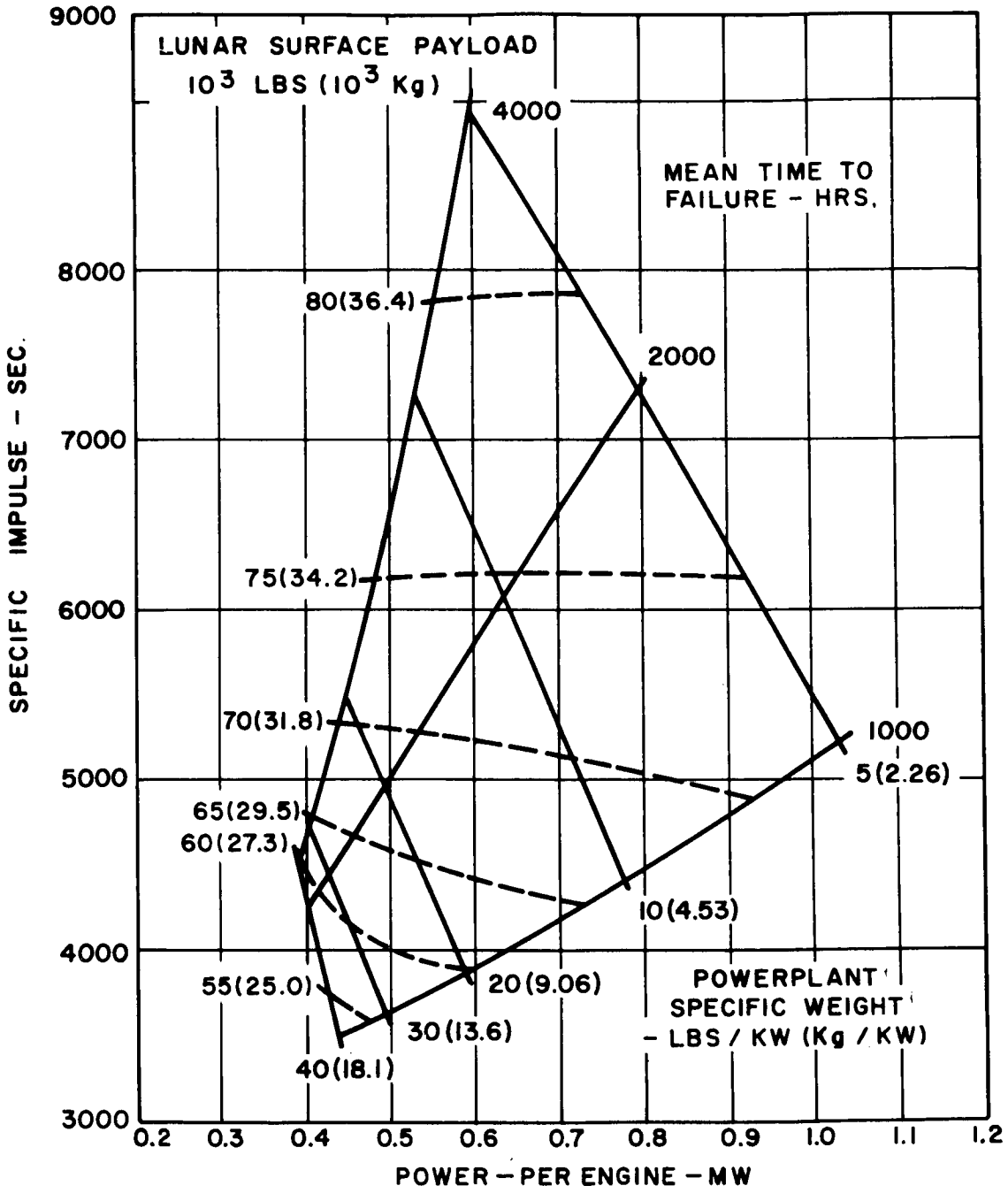

Figure 6-32. Effect of Mean Time to Failure on Multiple-Trip, Multiple-Engine Ferry Requirements

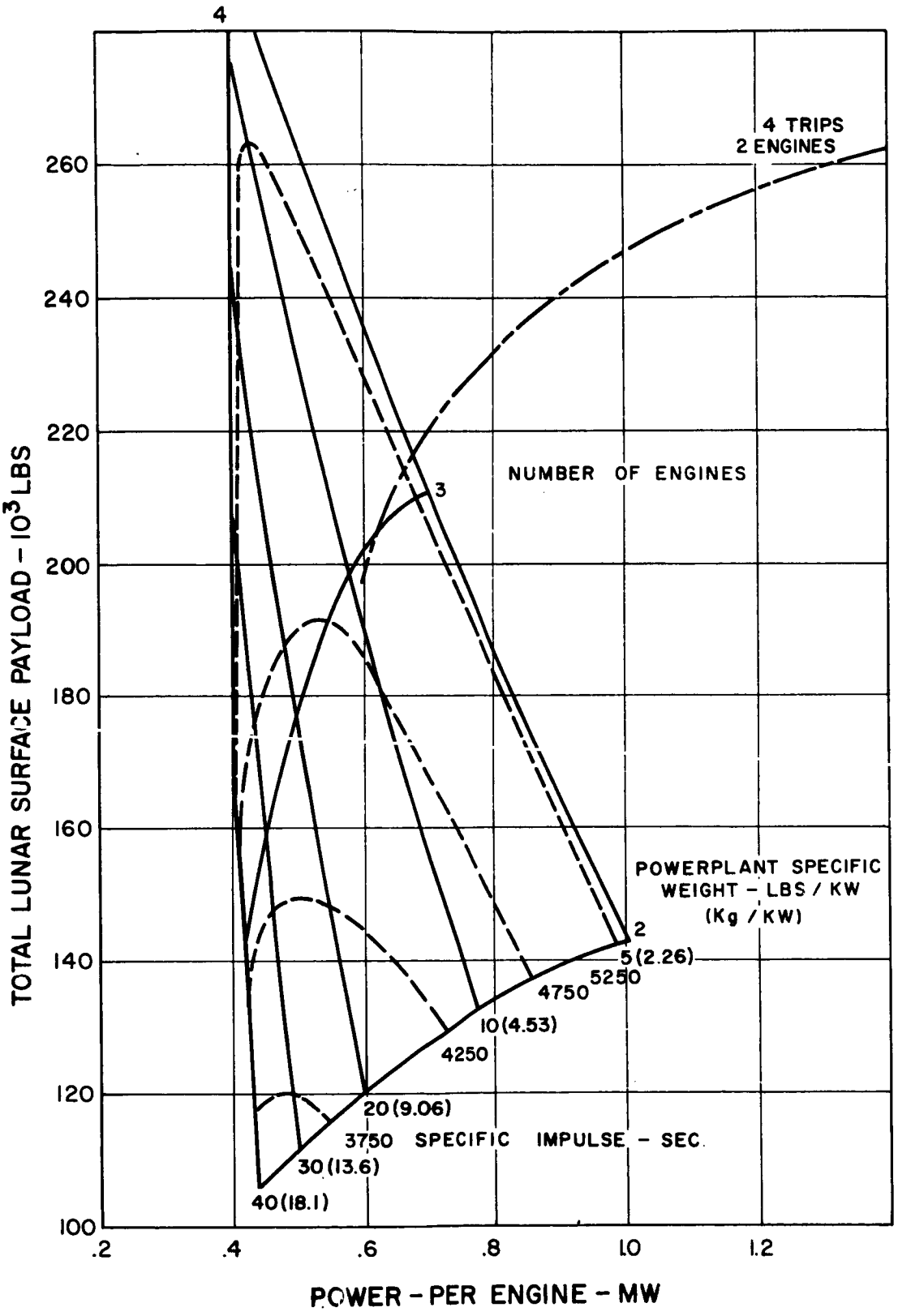

Figure 6-33. Effect of Number of Engines on Multiple-Trip, Multiple-Engine Ferry Requirements

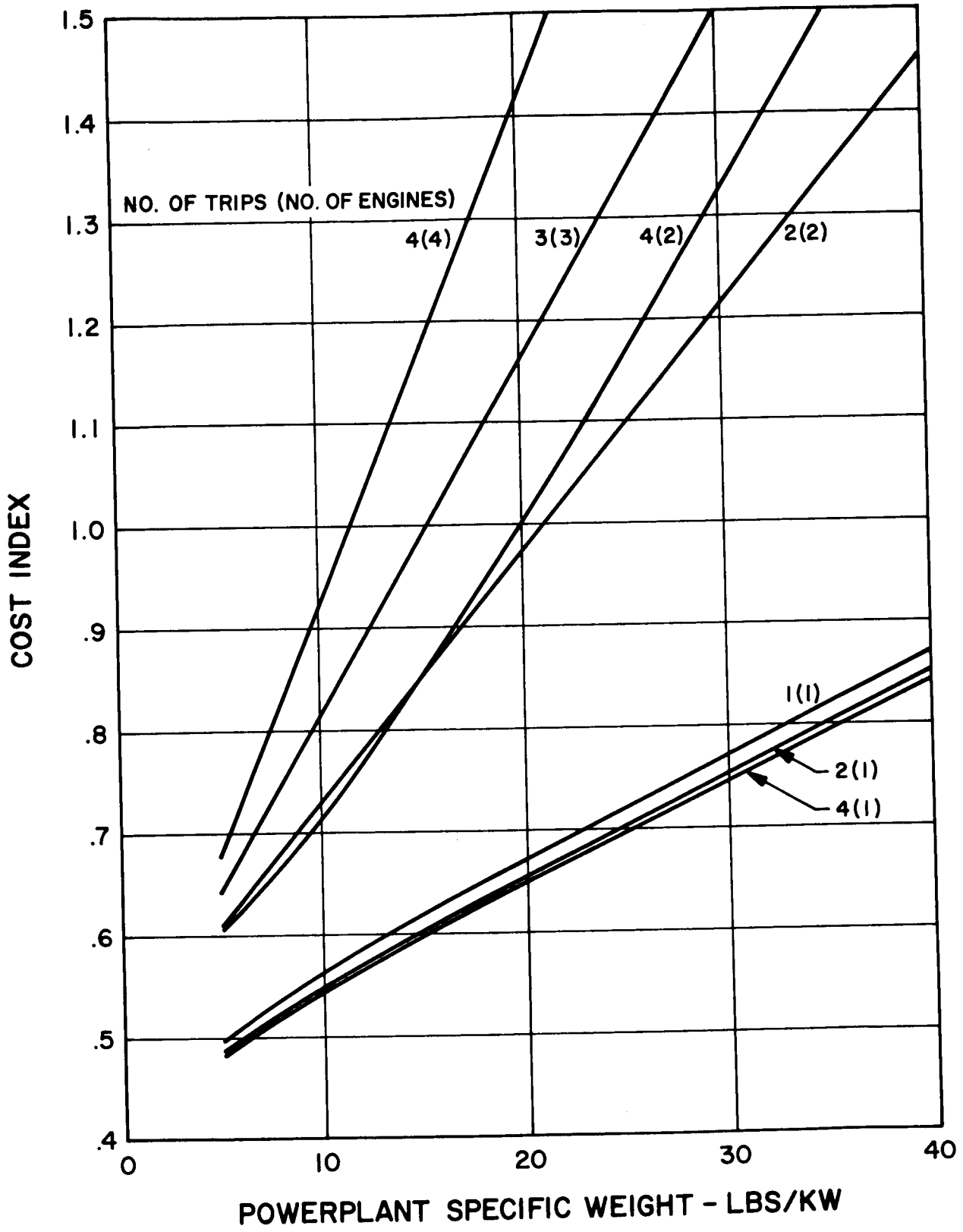

Figure 6-34. Comparison of Cost Indexes

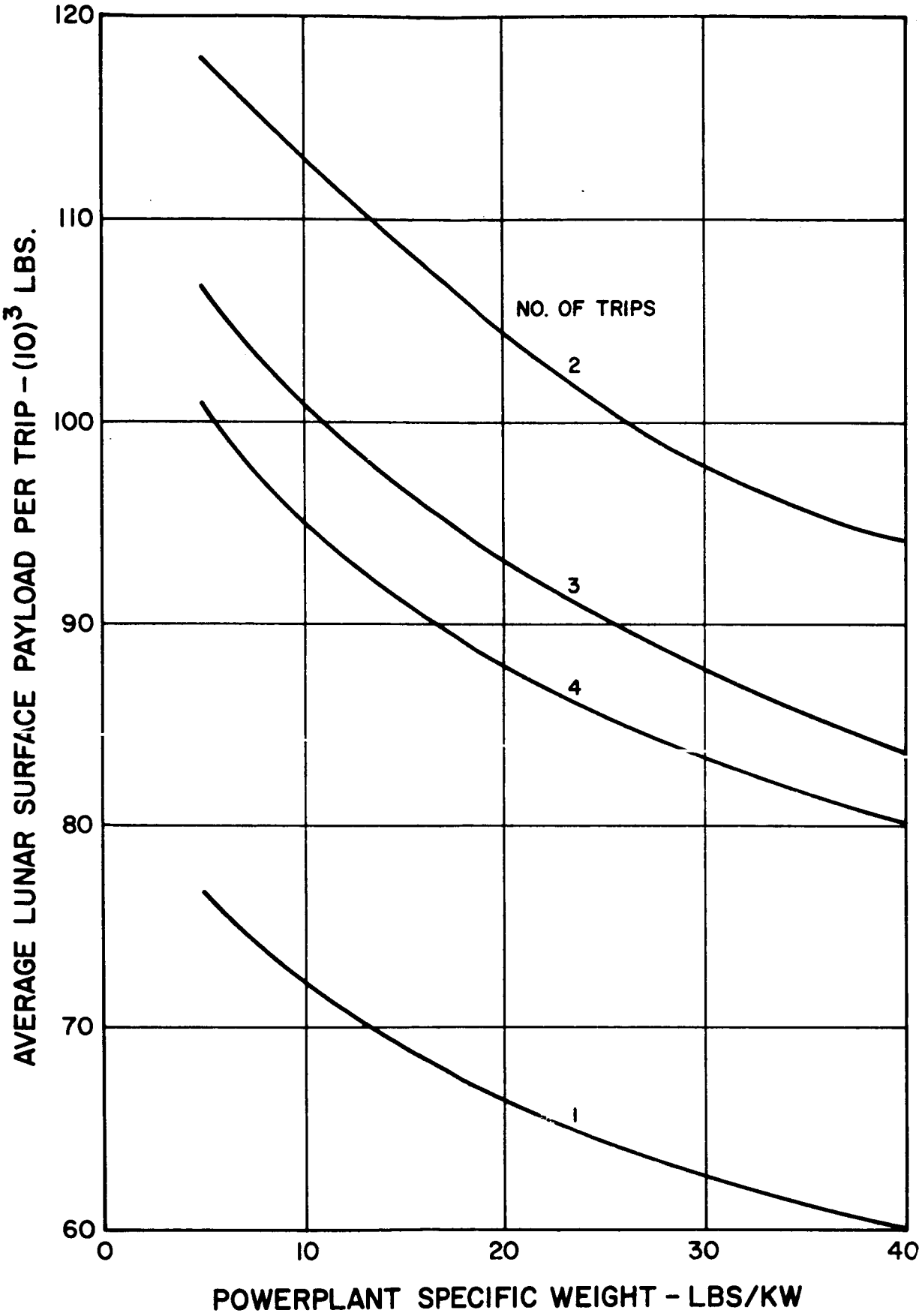

Figure 6-35. Comparison of Single Engine Payload Capabilities

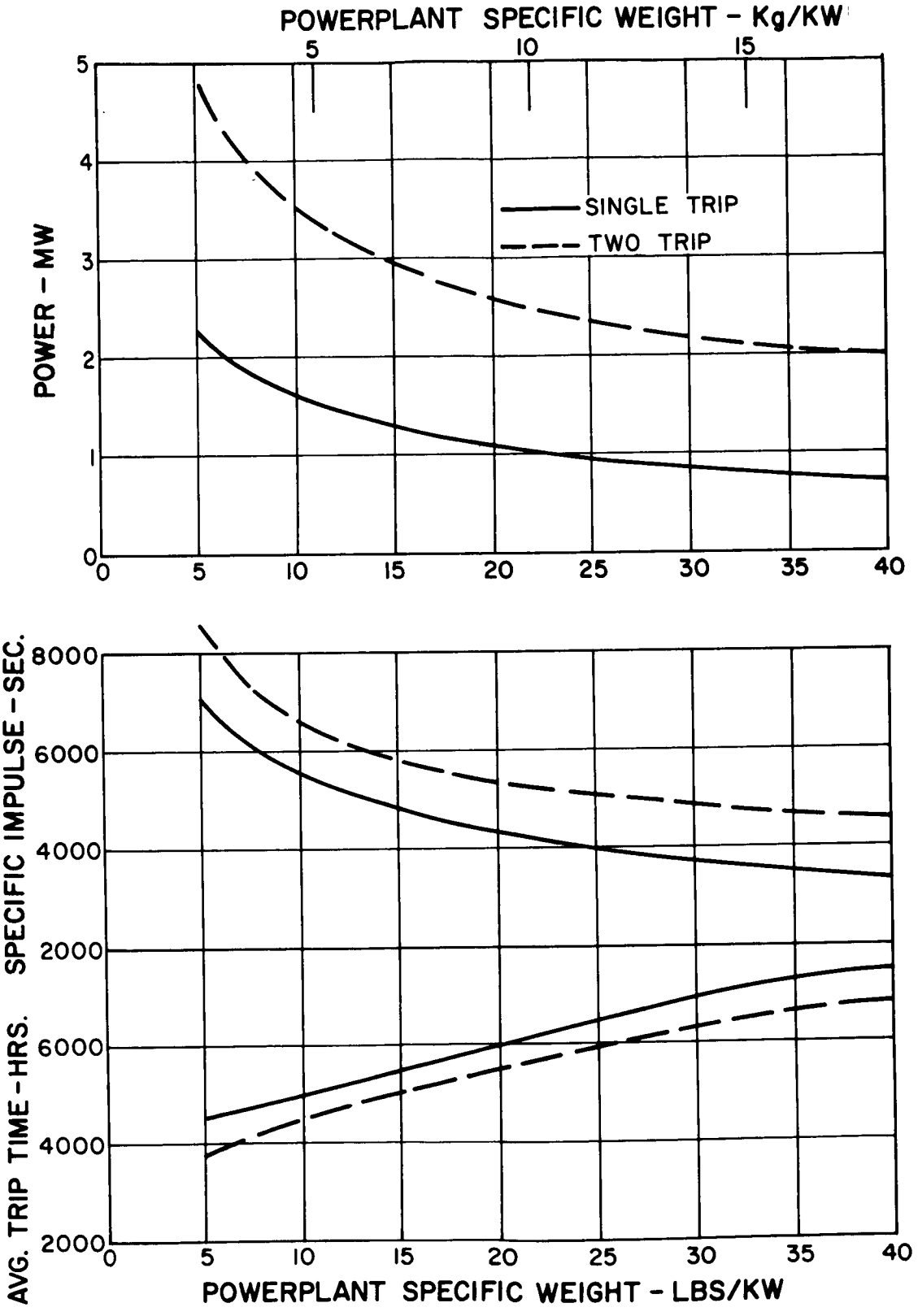

Figure 6-36. Summary of Lunar Ferry Mission Requirements

by the number of trips. These data indicate an increase in average payload per trip by 55 percent as operation is changed from single trip to two trip operation. As the number of trips is increased beyond two, however, the average payload per trip decreases by 10 to 15 percent. This decrease in payload per trip for the three and four trip cases would appear to more than offset the extremely small improvement in payload cost obtained. It has been concluded, therefore, that there is probably no incentive to go beyond two trip operation.

Figure 6-36, therefore, compares the powerplant design characteristics for the single trip and two trip modes of operation. It is anticipated that lunar ferry operation will be initiated with single trip operation and will be changed to two trip operation when the additional powerplant capability is available. These data illustrate the variation in power and specific impulse requirements and the associated average trip time per trip as a function of powerplant specific weight. The effect of the survival penalty optimization results in an average round trip time for the two trip case which is about 1000 hours shorter than the one way trip time for the single trip mode. The increased characteristic velocity requirements for the round trip result in a specific impulse increase of the order of 1000 seconds with respect to the single trip operation. These two factors result in two trip power requirements of the order of 2-1/2 times those of the single trip case. The two trip powerplant could, therefore, be developed from a two or three engine cluster of single trip powerplants.

SECTION 7

RECOMMENDATIONS FOR FURTHER STUDY

The use of an electrically-propelled space vehicle to provide logistic support of advanced lunar operations has been shown to be advantageous, within the following constraints:

1. The "equivalent" cargo requirement is sufficiently large to absorb the development cost of the electrical propulsion system.

2. Personnel are not to be directly transported in the electrically-propelled vehicle, but are to be indirectly supported by using the electrically-propelled vehicle to deliver the lunar landing craft to lunar orbit. Relative to a cargo-only system, this approach approximately doubles the "equivalent" lunar cargo market available to electrically-propelled vehicles, and it deserves serious consideration.

3. The nuclear power supply and propulsion system must perform within the regime of satisfactory performance illustrated in this study (Section 6B), with regard to specific weights, thrustor efficiency and reliability (mean time between failures). A typical set of good characteristics are:
   - 10 kg/KW_e nuclear power supply
   - 70 percent thrustor efficiency at 4000 sec.
   - 10,000 hours mean time between failures
   - 2 failures minimum to cause vehicle loss

The analysis has also shown the one-trip operating mode to be quite advantageous relative to the comparable chemical rocket system. Reuse of the power supply brings about additional cost improvements, but these further reductions are small compared to that achieved by the single-trip mode over its chemical counterpart. The single-trip mode is the logical first step in the lunar supply operation using electrical propulsion. At 10 kg/KW_e specific weight for the power supply, the power level can be selected from 1,000 to 2,000 KW_e; and the lunar landing craft, from 25 to 30 tons net lunar cargo size. A typical cargo system design is described below:

- Δ Operating Mode:

  One-way trip

- Δ Technology
  - Snap-50 Type Powerplant
  - Beryllium Radiator
  - Electron-Bombardment Thrustor
  - Saturn V Launcher

- Δ Performance
  - 3280 Hr. Trip Time
  - 4300 Sec. Specific Impulse
  - 1.9 MW_e Powerplant
  - 30.8 Tons Net Lunar Cargo

During the course of this study, several areas for new investigations were uncovered. One directly concerns the sustained lunar supply operation, where more detailed investigation into the physical characteristics of the space vehicles is required. A second area of interest is the participation of the electrically-propelled vehicle during the early lunar exploratory phase. Thirdly, during later lunar operations the power supply for the lunar surface operations can be identical to that for the supply operation. These topics for further study are discussed below.

A. SUSTAINED LUNAR SUPPLY OPERATIONS

The current study has been concentrated mainly in the area of parametric analyses. These have shown that economically attractive operations are possible with electrically-propelled spacecraft. Overall performance and cost relationships have been generated for various assumed powerplant and thrustor capabilities. This, of course, leads to a considerable range in output data. Therefore, before any judgement of the merits of electrical propulsion for lunar missions can be made, it will be necessary to narrow the assumptions on input parameters. This can be accomplished through analyses of design, operational, and development influences upon the powerplant, thrustors, and related spacecraft system. A specific statement of the scope of these tasks is outlined on the following page.

Task 1. Powerplant Definition

Prepare reference designs for turboelectric and thermionic nuclear powerplants applicable to the lunar cargo mission. Relate key technology levels in temperature, fuel burnup, materials, thermionic current densities, etc., to powerplant weights, lifetimes and dimensional envelopes. Determine effects of redundancy upon system weight, and relate component reliabilities to overall system reliabilities for different degrees of redundancy.

Task 2. Spacecraft Preliminary Design

Prepare design layouts for complete spacecraft, integrating powerplants defined in Task 1 with appropriate thrustors, tankage, shielding, radiators, power conditioning, and structures. Consider special features needed for docking and orbital assembly such as tools, fixtures, locating devices, sensors, etc. Include provisions for auxiliary component cooling, thermal insulation, electrical isolation, fault clearing, powerplant controls, and guidance equipment. Determine packaging limitations for integrating spacecraft with booster and with various lunar landing stages. Consider influence of docking and rendezvous maneuvers upon shield requirements, and relate shield weight to specific payload activation constraints.

Task 3. Operational Analysis

Define missions steps and procedures from launch to final disposal, relating powerplant and spacecraft characteristics to overall performance and cost factors. Evaluate safety and reliability aspects of the propulsion system in terms of their effect upon payload delivery cost. Parametric data generated under the present contract will provide guidelines in selecting mission profiles and power levels.

Task 4. Development Analyses

Establish areas of common requirement between the lunar cargo mission and other missions such as lunar base power, scientific space probes, and manned interplanetary spacecraft. Determine where the technologies in reactors, radiators, power conversion, thrustors, and electrical equipment can be applied to more than one mission. Identify critical thresholds in each technology and relate to present state-of-the-art. Outline potential routes of development and testing needed to achieve attractive lunar cargo costs.

B. LIMITED LUNAR EXPEDITIONS

The need for sustained lunar supply operations is somewhat speculative at this time, and a firm requirement is not apt to be established until after the initial Apollo landings. An earlier mission deserving study is the conduction of expeditions by several persons to the lunar surface with suitable equipment to establish a temporary base for the purpose of scientific study of the moon. The entire expedition can be transported by a total of two Saturn V launched spacecraft: one electrically propelled to haul the lunar landing craft via a slow trip, and the other a chemical rocket propelled to carry the crew via a fast trip, using the scheme illustrated in Figure 3- 6. This application can utilize a nuclear power supply of lower life qualified rating and system reliability than that required for sustained lunar supply.

The nuclear power supply requirements for participation in lunar exploration are 1.0 to 1.5 megawatts electrical power and 3000 hours life at a specific weight of 20 to 30 pounds per kilowatt, a modest goal by 1975. An approach to achieve this goal minimizing flight test requirements has been postulated and costs have been estimated.

The strategy for conducting a lunar expedition using electrical propulsion consists of the following steps:

1. An experimental nuclear-electric propulsion vehicle is launched by a Saturn V along with an expendable payload of lunar landing craft and expeditionary equipment and stores. This vehicle is sent to lunar orbit on a test run for the power supply and electrical propulsion system, being the first of a series of Saturn V launched vehicles.

2. Progress of the electrically-propelled vehicle is monitored, and when lunar orbit capture is assured, preparations are made to launch a second Saturn V vehicle, this time without an electrical propulsion system. Instead, the second Saturn V launches an advanced APOLLO type vehicle with a six-man crew and the remaining expedition stores for a six-month lunar stay.

3. The chemically propelled APOLLO type vehicle overtakes the electrically-propelled spacecraft and will rendezvous with it in lunar orbit. The crew transfers with the supplies to the electrically-propelled vehicle, disengages the nuclear power supply, and descends to the lunar surface in the lunar landing vehic le.

4. After the exploration period has been completed, the crew ascends to lunar orbit and meets with the APOLLO craft to return to earth.

In this approach the expeditionary crew is not committed to the lunar excursion until the lunar landing vehicle with the major portion of equipment and supplies has been satisfactorily transported to lunar orbit. The crew is launched in a space vehicle fully capable of voyaging to lunar orbit and return. The mission can be aborted at almost any time. (Apollo equivalence)

One advantage of this technique is that the crew safety is confined to success of a single Saturn V launch, whereas, several Saturn V launches are required to conduct the same mission without use of electrical propulsion. In particular, a six-man, six-month expedition using only the APOLLO type chemical propulsion system requires four Saturn V launches.

The other advantage is the booster cost reduction following from the reduced number of launches. At a cost of 100 million dollars per booster, the nuclear power supply development cost can be quickly amortized.

The nuclear systems test program costs have been estimated at approximately $500,000,000. This estimate is based on acquisition of twelve experimental powerplants and testing facilities for non-nuclear ground test, nuclear-ground test and fractional size flight test. It is estimated that the first powerplant will cost $28,000,000 and subsequent powerplant costs follow from an 85 percent learning curve. The fractional size flight test includes a nuclear powerplant model in which the main radiator is reduced in size to fit on the Titan IIIC or Saturn 1B launch vehicle. An additional cost of four manned orbital vehicles to allow examination of the flight tests are included in the cost. The resultant assumed test program runs 4-1/2 years to achieve a 3,000 hour powerplant qualification.

The first Saturn V configured nuclear powerplant model is employed in a lunar exploration mission. After successful completion of a few lunar expeditions, the powerplant reliability should prove sufficient for support of lunar bases or interplanetary missions.

The development cost for the nuclear powerplant is amortized when the need for Saturn V vehicles has been reduced by 5. Additional lunar expeditions and lunar base development can be carried out at 40 to 50 percent less cost than that required by using only chemical propulsion transportation systems.

The lunar exploration offers an opportunity to develop a nuclear power supply in the course of conducting a presently "approved" program. The powerplant life requirement of 3000 hours is a realistic goal for 1975. The cost savings in conducting a lunar mission are genuine and sufficient to underwrite the development cost. An acceleration of study in this area is required to allow timely incorporation of the nuclear power supply into the post-APOLLO program. The detailed tasks to be accomplished are listed below.

Task 1. Lunar Expedition Requirements

Conduct a preliminary investigation of the lunar expedition requirements which shall include parametric representations of the following:

1. Estimates of the equipment and supplies necessary to conduct the lunar expedition.

2. Estimates of the space vehicle performance characteristics for the earth launch, orbit transfer, lunar descent, lunar ascent and earth re-entry travel phases.

3. Comparison of expedition requirements with and without use of nuclear-electric propulsion systems.

Task 2. Systems Definition

Conduct a detailed investigation of two typical expeditions from the preliminary investigation above; this shall include the following:

1. Establishment of weights, volumes and environment constraints of equipment and supplies for lunar expedition.

2. Design description of representative transportation vehicles.

3. Design analysis of representative nuclear power supply including layout and weight estimation.

C. LUNAR SURFACE POWER

In the event that the lunar operations advance beyond the exploratory phase, the construction of semi-permanent type bases will commence, and the scale of lunar activities will be constrained by availability of surface power, as well as by transportation system cost. The current study has focused on the transportation requirements. However, in Section 5A an approach was presented whereby the nuclear power supply from the electrically-propelled cargo vehicle could be landed for continuing operation on the lunar surface. This approach yields substantially larger quantities of lunar surface power than could be provided as payload alone. For example, an electrically-propelled cargo vehicle can transport 30.8 tons of net useful cargo, as compared to 12.7 tons for the all-chemical cargo system. In both of these cargo items, a portion will be devoted to a lunar surface power supply. The landing of the nuclear power supply from the electrically propelled vehicle, with 2π shield, still yields 16.9 tons of net cargo, exclusive of power supply. The net difference between landing and not-landing the nuclear power supply, 13.9 tons, is approximately that mass required for a shielded reactor power system. However, by using the proposed approach,the power supply cost is already amortized. The availability of "cheap" lunar surface power can allow other equipment to be reduced in mass by acceptance of lower efficiency, via a systems optimization study. Utilization of lunar resources becomes more promising, which can again reduce requirements for earth-moon logistics. Early buildup of a lunar base to serve as a terminal for interplanetary expeditions can be a possibility. These concepts need further examination and task descriptions are presented below.

Task 1. Spacecraft Preliminary Design

Prepare design layouts for complete spacecraft capable of performing the dual mission, electrical propulsion and lunar surface power. Consider special problems associated with landing, such as hazards, shielding weight penalties, vehicle stability, and maintenance.

Establish general performance characteristics for the power supply to account for differences in space radiation view factor, tradeoff between power level and life, and system size scaling factors.

Task 2. Lunar Base Characteristics

Investigate lunar base equipment requirements to determine the areas where mass reductions can be realized by availability of "cheap" electric power. Such areas include mobile vehicle power supply (fuel cell), communications, excavation, repair facilities and life support. In later lunar activities lunar mining and propellant manufacture can be added to the list. Determine mass versus power tradeoff factors.

Task 3. Mission Analysis

Combine the results of the above two tasks with that for the sustained lunar supply study and perform an overall systems analysis to optimize the systems characteristics on "cost effectiveness". Compare results with the approach whereby a separate power supply is provided for lunar surface power.

APPENDIX A

GENERAL PERFORMANCE CHARACTERISTICS

The body of this report is directed towards determining the optimum operating modes of electrically propelled earth-moon shuttle vehicles. Often, it is of interest to determine the performance capability for an off-optimum selection of design parameters. Performance characteristics for various operational modes are presented in this section, without the optimization for cost being performed. The design parameters selected as independant variables are Lunar Landing Craft Size (CARGO) and Nuclear Power Supply Size, (POWER), and particular design parameters such as specific impulse on the inbound voyage has been optimized to minimize power supply life rating. These results which can be used as input to cost effectiveness optimization computer programs as presented in Appendix B, are presented in tabular form, Tables 1 to 24.

The operational modes considered are combinations of the following:

1. Single-trip mode
2a. Multiple-trip ferry with propellant tank mounted thrustors (constant lander size)
 b. Multiple-trip ferry with powerplant mounted thrustors (constant specific impulse)
3a. One-initial booster
 b. Two-initial booster
4a. Earth orbit inbound propellant tank dump (spent tanks immediately discarded)
 b. Lunar orbit inbound propellant tank dump (no replacement of inbound propellant tank)
5a. Ion jet thrustors
 b. Hybrid arc jets
6. Multiple-powerplant, multiple-trip ferry
    a. Two-powerplant, two-trip
    b. Three-powerplant, three-trip
    c. Four powerplant, four trip

The following assumed parameters are used:

Characteristic Velocity, (CHAR VEL) = 7.8 km/sec for each orbit transfer

Thrustor Jet Velocity (ETAT) = 1.1 exp $(-1690/I_{sp})$ for ion jet thrustors

= 0.7 for hybrid arc jet

Thrustor Specific Weight = $(3000/I_{sp} + 1.2$ kg/$KW_e)$ for ion jet thrustor

= 1.2 kg/KW_e for hybrid arc jet

Propellant Utilization (PROP UTIL) =0.9

Lander Cargo Fraction = 0.4

Power Supply Specific Weight = 10 kg/KW_e

Booster Net Payload = 100,000 kg

The definitions of the headings in Tables 1 to 24 are as follows:

GENERAL

CARGO = net average payload delivered to lunar surface per 100 tons of booster orbiting capacity, metric tons.

POWER = net output of nuclear power supply per 100 tons of booster orbiting capacity, metric tons.

TI = trip time for final inbound voyage, hr.

TOF = trip time for final outbound voyage, hr.

TOI = trip time for initial outbound voyage, hr.

LIFE = total operational life for nuclear power supply, hr.

Propellant Tank Mounted Thrustors

VJI = thrustor jet velocity for all inbound trips, km/sec.

VJOF = thrustor jet velocity for final outbound trip, km/sec.

VJOI = thrustor jet velocity for initial outbound trip, km/sec.

Powerplant Mounted Thrustors

VJ = thrustor jet velocity for all orbit transfers, km/sec.

WCF = Lunar cargo delivered on final voyage per 100 tons of booster payload capability, metric tons.

WCI = lunar cargo delivered on initial voyage per 100 tons of booster payload capability, metric tons.

TABLE 1. SINGLE TRIP, ELECTRIC-PROPELLED, SPACE TRANSPORT PERFORMANCE WITH ION JET THRUSTORS

SWQ = 10 KG/KWE, LANDER CARGO FRAC = .4, CHAR VEL = 7.8 KM/SEC
SWT =(3000/I + 1.2) KG/KWE, ETAT = 1.1 EXP(-1690/I), PROP UTIL = .9

CARGO	POWER	VJOI	TOI	TOF	LIFE
15.	.4	10.8	8767.	8767.	8767.
15.	.8	12.5	4307.	4307.	4307.
15.	1.2	14.4	2884.	2884.	2884.
15.	1.6	16.7	2217.	2217.	2217.
15.	2.0	19.6	1854.	1854.	1854.
15.	2.4	23.1	1650.	1650.	1650.
15.	2.8	27.7	1546.	1546.	1546.
15.	3.2	33.9	1521.	1521.	1521.
20.	.4	15.1	8702.	8702.	8702.
20.	.8	17.6	4493.	4493.	4493.
20.	1.2	20.8	3160.	3160.	3160.
20.	1.6	24.9	2560.	2560.	2560.
20.	2.0	30.2	2272.	2272.	2272.
20.	2.4	37.8	2173.	2173.	2173.
20.	2.8	49.1	2239.	2239.	2239.
25.	.4	22.5	9788.	9788.	9788.
25.	.8	27.3	5364.	5364.	5364.
25.	1.2	33.8	4047.	4047.	4047.
25.	1.4	38.1	3745.	3745.	3745.
25.	1.6	43.3	3581.	3581.	3581.
25.	1.8	50.0	3532.	3532.	3532.
30.	.4	38.8	13281.	13281.	13281.
30.	.6	44.5	9728.	9728.	9728.
30.	.8	51.7	8150.	8150.	8150.
30.	1.0	61.4	7440.	7440.	7440.
30.	1.2	74.8	7280.	7280.	7280.

TABLE 2. SINGLE TRIP, ELECTRIC-PROPELLED, SPACE TRANSPORT PERFORMANCE WITH ARC JET THRUSTORS

SWQ = 10 KG/KWE, LANDER CARGO FRAC = .4, CHAR VEL = 7.8 KM/SEC
SWT = 1.2 KG/KWE, ETAT = .7, PROP UTIL = .9

CARGO	POWER	VJOI	TOI	TOF	LIFE
15.	.4	10.5	2882.	2882.	2882.
15.	.8	11.8	1673.	1673.	1673.
15.	1.2	13.3	1298.	1298.	1298.
15.	1.6	15.0	1138.	1138.	1138.
15.	2.0	17.2	1070.	1070.	1070.
15.	2.4	19.8	1059.	1059.	1059.
15.	2.8	23.2	1090.	1090.	1090.
15.	3.2	27.6	1166.	1166.	1166.
20.	.4	14.7	4439.	4439.	4439.
20.	.8	16.8	2607.	2607.	2607.
20.	1.2	19.3	2059.	2059.	2059.
20.	1.6	22.6	1851.	1851.	1851.
20.	2.0	26.8	1804.	1804.	1804.
20.	2.4	32.6	1874.	1874.	1874.
20.	2.8	41.1	2070.	2070.	2070.
25.	.4	22.0	7189.	7189.	7189.
25.	.8	26.1	4366.	4366.	4366.
25.	1.2	31.6	3613.	3613.	3613.
25.	1.4	35.1	3488.	3488.	3488.
25.	1.6	39.5	3470.	3470.	3470.
25.	1.8	50.0	3532.	3532.	3532.
30.	.4	38.0	13311.	13311.	13311.
30.	.6	43.0	10169.	10169.	10169.
30.	.8	49.4	8862.	8862.	8862.
30.	1.0	57.9	8389.	8389.	8389.
30.	1.2	69.4	8478.	8478.	8478.

TABLE 3. MULTIPLE TRIP, ELECTRIC-PROPELLED, SPACE TRANSPORT PERFORMANCE WITH PROPELLANT TANK MOUNTED ION JETS, ONE INITIAL BOOSTER, AND EARTH ORBIT INBOUND PROPELLANT TANK DUMP

SWQ = 10 KG/KWE, LANDER CARGO FRAC = .4, CHAR VEL = 7.8 KM/SEC
SWT =(3000/I + 1.2) KG/KWE, ETAT = 1.1 EXP(-1690/I), PROP UTIL = .9

CARGO	POWER	VJI	TI	VJOI	TOI	VJOF	TOF	LIFE
TWO-TRIP FERRY MODE								
15.	0.8	26.	725.	14.6	4331.	11.4	4694.	9750.
15.	1.6	35.	768.	21.8	2411.	13.4	2497.	5676.
15.	2.0	40.	805.	26.9	2129.	14.4	2076.	5010.
15.	2.4	47.	865.	33.5	2012.	15.4	1803.	4679.
15.	2.8	56.	949.	42.6	2021.	16.4	1614.	4584.
15.	3.2	69.	1078.	55.7	2155.	17.5	1478.	4712.
20.	0.8	34.	761.	20.4	4700.	15.5	4715.	10176.
20.	1.2	39.	797.	25.6	3463.	16.7	3308.	7568.
20.	1.6	47.	865.	32.5	2960.	18.0	2617.	6442.
20.	2.0	57.	958.	42.2	2808.	19.3	2212.	5979.
20.	2.4	72.	1109.	56.6	2910.	20.6	1950.	5968.
20.	2.8	97.	1371.	80.5	3316.	21.9	1769.	6455.
25.	0.4	38.	789.	24.3	10124.	20.6	9813.	20726.
25.	0.8	46.	856.	31.6	5823.	22.3	5256.	11935.
25.	1.2	57.	958.	42.1	4676.	24.0	3755.	9390.
25.	1.4	65.	1038.	49.2	4486.	24.9	3332.	8856.
25.	1.6	75.	1140.	58.4	4471.	25.7	3019.	8630.
25.	1.8	88.	1275.	70.6	4628.	26.7	2778.	8682.
30.	0.4	58.	968.	42.1	14028.	33.2	12493.	27489.
30.	0.6	67.	1058.	50.3	10632.	34.6	8703.	20393.
30.	0.8	79.	1181.	61.2	9270.	36.0	6819.	17271.
30.	1.0	95.	1349.	76.4	8887.	37.4	5698.	15934.
30.	1.2	120.	1617.	99.0	9237.	38.9	4959.	15813.
THREE-TRIP FERRY MODE								
15.	0.8	25.	723.	14.7	4334.	11.4	4695.	15124.
15.	1.6	32.	749.	22.3	2436.	13.4	2497.	8999.
15.	2.0	36.	775.	27.9	2170.	14.3	2075.	7975.
15.	2.4	41.	813.	35.4	2082.	15.3	1802.	7439.
15.	2.8	48.	874.	45.7	2125.	16.3	1613.	7238.
15.	3.2	58.	968.	61.0	2312.	17.4	1475.	7343.
20.	0.8	32.	749.	20.6	4715.	15.5	4715.	15775.
20.	1.2	36.	775.	26.1	3492.	16.7	3308.	11829.
20.	1.6	42.	821.	33.4	3014.	18.0	2616.	10083.
20.	2.0	49.	883.	44.3	2908.	19.2	2210.	9304.
20.	2.4	60.	988.	60.8	3074.	20.5	1947.	9155.
20.	2.8	79.	1181.	88.1	3580.	21.8	1764.	9672.
25.	0.4	37.	782.	24.4	10133.	20.6	9813.	31596.
25.	0.8	43.	830.	31.9	5854.	22.3	5256.	18331.
25.	1.2	51.	901.	43.0	4748.	24.0	3754.	14385.
25.	1.4	56.	949.	50.9	4600.	24.8	3331.	13492.
25.	1.6	63.	1018.	61.1	4631.	25.7	3017.	13030.
25.	1.8	73.	1119.	74.5	4836.	26.6	2775.	12946.
30.	0.4	55.	939.	42.2	14061.	33.2	12493.	41492.
30.	0.6	61.	998.	50.7	10702.	34.6	8703.	30686.
30.	0.8	69.	1078.	62.2	9396.	36.0	6818.	25777.
30.	1.0	81.	1202.	78.3	9073.	37.4	5696.	23449.
30.	1.2	98.	1381.	102.8	9549.	38.8	4956.	22784.
FOUR-TRIP FERRY MODE								
15.	0.8	24.	723.	14.8	4338.	11.4	4695.	20500.
15.	1.6	31.	743.	22.5	2446.	13.4	2497.	12318.
15.	2.0	35.	768.	28.2	2183.	14.4	2075.	10928.
15.	2.4	39.	797.	36.2	2113.	15.4	1802.	10180.
15.	2.8	45.	847.	47.4	2181.	16.4	1613.	9857.
15.	3.2	54.	930.	63.8	2396.	17.4	1476.	9916.
20.	0.8	31.	743.	20.7	4724.	15.5	4715.	21373.
20.	1.2	35.	768.	26.2	3504.	16.7	3308.	16085.
20.	1.6	40.	805.	33.9	3042.	18.0	2617.	13714.
20.	2.0	46.	856.	45.4	2958.	19.2	2211.	12602.
20.	2.4	56.	949.	62.7	3154.	20.5	1947.	12288.
20.	2.8	72.	1109.	92.8	3742.	21.8	1765.	12789.
25.	0.4	37.	782.	24.4	10133.	20.6	9813.	42464.
25.	0.8	42.	821.	32.0	5866.	22.3	5256.	24723.
25.	1.2	49.	883.	43.4	4777.	24.0	3754.	19364.
25.	1.4	53.	920.	51.7	4650.	24.8	3331.	18099.
25.	1.6	59.	978.	62.3	4705.	25.7	3017.	17386.
25.	1.8	67.	1058.	76.8	4957.	26.6	2775.	17141.
30.	0.4	54.	930.	42.3	14073.	33.2	12493.	55493.
30.	0.6	59.	978.	50.9	10729.	34.6	8703.	40969.
30.	0.8	66.	1048.	62.6	9443.	36.0	6818.	34258.
30.	1.0	75.	1140.	79.4	9180.	37.4	5696.	30911.
30.	1.2	89.	1286.	105.1	9734.	38.8	4956.	29652.

TABLE 4. MULTIPLE TRIP, ELECTRIC-PROPELLED, SPACE TRANSPORT PERFORMANCE WITH PROPELLANT TANK MOUNTED ION JETS, TWO INITIAL BOOSTER, AND EARTH ORBIT INBOUND PROPELLANT TANK DUMP

SWQ = 10 KG/KWE, LANDER CARGO FRAC = .4, CHAR VEL = 7.8 KM/SEC
SWT =(3000/I + 1.2) KG/KWE, ETAT = 1.1 EXP(-1690/I), PROP UTIL = .9

CARGO	POWER	VJI	TI	VJOI	TOI	VJOF	TOF	LIFE
TWO-TRIP FERRY MODE								
15.	0.8	21.	731.	11.9	8645.	11.4	4695.	14071.
15.	1.6	26.	725.	14.6	4331.	13.3	2497.	7553.
15.	2.4	30.	738.	17.8	3002.	15.3	1802.	5542.
15.	3.2	35.	768.	21.8	2411.	17.3	1475.	4653.
15.	3.6	37.	782.	24.2	2246.	18.4	1373.	4401.
15.	4.0	40.	805.	26.9	2129.	19.4	1294.	4228.
20.	0.8	29.	734.	16.3	8819.	15.5	4714.	14267.
20.	1.6	34.	761.	20.4	4700.	17.9	2616.	8077.
20.	2.4	39.	797.	25.6	3463.	20.5	1947.	6207.
20.	2.8	43.	830.	28.8	3153.	21.8	1764.	5747.
20.	3.2	47.	865.	32.5	2960.	23.1	1633.	5458.
20.	3.6	51.	901.	37.0	2856.	24.5	1536.	5293.
25.	0.8	38.	789.	24.3	10124.	22.3	5255.	16169.
25.	1.2	42.	821.	27.6	7199.	24.0	3754.	11774.
25.	1.6	46.	856.	31.6	5823.	25.7	3017.	9696.
25.	1.8	49.	883.	33.8	5392.	26.6	2775.	9050.
25.	2.0	51.	901.	36.3	5080.	27.5	2585.	8567.
25.	2.2	54.	930.	39.0	4844.	28.4	2432.	8206.
30.	0.6	55.	939.	38.7	17658.	34.6	8703.	27300.
30.	0.8	58.	968.	42.1	14028.	36.0	6818.	21814.
30.	1.0	62.	1008.	45.9	11938.	37.4	5697.	18642.
30.	1.2	67.	1058.	50.3	10632.	38.8	4956.	16646.
30.	1.4	72.	1109.	55.3	9801.	40.3	4434.	15344.
30.	1.6	79.	1181.	61.2	9270.	41.8	4049.	14500.
THREE-TRIP FERRY MODE								
15.	0.8	22.	727.	11.9	8649.	11.4	4694.	19448.
15.	1.6	28.	730.	14.4	4326.	13.4	2497.	10870.
15.	2.4	32.	749.	17.6	2991.	15.4	1802.	8270.
15.	3.2	37.	782.	21.5	2397.	17.4	1476.	7151.
15.	3.6	39.	797.	23.9	2231.	18.4	1374.	6845.
15.	4.0	42.	821.	26.5	2113.	19.5	1296.	6642.
20.	0.8	30.	738.	16.3	8814.	15.5	4715.	19864.
20.	1.6	35.	769.	20.3	4693.	18.0	2617.	11700.
20.	2.4	40.	805.	25.5	3455.	20.5	1948.	9280.
20.	2.8	44.	838.	28.6	3144.	21.8	1765.	8699.
20.	3.2	47.	865.	32.5	2960.	23.2	1634.	8342.
20.	3.6	51.	901.	37.0	2856.	24.5	1536.	8146.
25.	0.8	39.	797.	24.3	10116.	22.3	5256.	22558.
25.	1.2	43.	830.	27.6	7190.	24.0	3754.	16741.
25.	1.6	47.	865.	31.5	5814.	25.7	3017.	14008.
25.	1.8	49.	883.	33.8	5392.	26.6	2776.	13165.
25.	2.0	51.	901.	36.3	5080.	27.5	2585.	12536.
25.	2.2	54.	930.	39.0	4844.	28.4	2432.	12067.
30.	0.6	54.	930.	38.7	17668.	34.6	8703.	37577.
30.	0.8	58.	968.	42.1	14028.	36.0	6818.	30276.
30.	1.0	61.	998.	46.0	11949.	37.4	5697.	26057.
30.	1.2	65.	1038.	50.4	10653.	38.8	4956.	23398.
30.	1.4	70.	1088.	55.5	9823.	40.3	4434.	21656.
30.	1.6	75.	1140.	61.5	9316.	41.8	4048.	20516.
FOUR-TRIP FERRY MODE								
15.	0.8	23.	724.	11.8	8653.	11.4	4695.	24819.
15.	1.6	28.	730.	14.4	4326.	13.4	2497.	14187.
15.	2.4	33.	755.	17.5	2987.	15.4	1802.	10996.
15.	3.2	37.	782.	21.5	2397.	17.4	1476.	9651.
15.	3.6	40.	805.	23.7	2224.	18.4	1374.	9288.
15.	4.0	42.	821.	26.5	2113.	19.5	1296.	9058.
20.	0.8	30.	738.	16.3	8814.	15.5	4715.	25460.
20.	1.6	35.	768.	20.3	4693.	18.0	2617.	15322.
20.	2.4	41.	813.	25.4	3447.	20.5	1947.	12352.
20.	2.8	44.	838.	28.6	3144.	21.8	1765.	11652.
20.	3.2	47.	865.	32.5	2960.	23.2	1634.	11228.
20.	3.6	51.	901.	37.0	2856.	24.5	1536.	11001.
25.	0.8	39.	797.	24.3	10116.	22.3	5256.	28948.
25.	1.2	43.	830.	27.6	7190.	24.0	3754.	21709.
25.	1.6	47.	865.	31.5	5814.	25.7	3017.	18322.
25.	1.8	49.	883.	33.8	5392.	26.6	2776.	17280.
25.	2.0	51.	901.	36.3	5080.	27.5	2585.	16506.
25.	2.2	53.	920.	39.2	4855.	28.4	2432.	15931.
30.	0.6	54.	930.	38.7	17668.	34.6	8703.	47853.
30.	0.8	58.	968.	42.1	14028.	36.0	6818.	38738.
30.	1.0	61.	998.	46.0	11949.	37.4	5697.	33471.
30.	1.2	65.	1038.	50.4	10653.	38.8	4956.	30149.
30.	1.4	69.	1078.	55.6	9835.	40.3	4434.	27967.
30.	1.6	73.	1119.	61.7	9341.	41.8	4048.	26529.

TABLE 5. MULTIPLE TRIP, ELECTRIC-PROPELLED, SPACE TRANSPORT PERFORMANCE WITH PROPELLANT TANK MOUNTED ION JETS, ONE INITIAL BOOSTER, AND LUNAR ORBIT INBOUND PROPELLANT TANK DUMP

SWQ = 10 KG/KWE, LANDER CARGO FRAC = .4, CHAR VEL = 7.8 KM/SEC
SWT =(3000/I + 1.2) KG/KWE, ETAT = 1.1 EXP(-1690/I), PROP UTIL = .9

CARGO	POWER	VJI	TI	VJOI	TOI	VJOF	TOF	LIFE
TWO-TRIP FERRY MODE								
15.	0.8	27.	727.	14.5	4328.	11.7	4773.	9828.
15.	1.6	36.	775.	21.6	2403.	13.9	2583.	5761.
15.	2.0	41.	813.	26.7	2120.	15.0	2162.	5096.
15.	2.4	48.	874.	33.3	2002.	16.1	1889.	4765.
15.	2.8	57.	958.	42.3	2011.	17.2	1699.	4669.
15.	3.2	70.	1088.	55.4	2145.	18.3	1561.	4795.
20.	0.8	35.	768.	20.3	4693.	15.8	4816.	10277.
20.	1.2	41.	813.	25.4	3447.	17.2	3409.	7668.
20.	1.6	48.	874.	32.3	2951.	18.6	2717.	6541.
20.	2.0	58.	968.	41.9	2799.	19.9	2309.	6076.
20.	2.4	73.	1119.	56.4	2899.	21.3	2044.	6062.
20.	2.8	97.	1371.	80.5	3316.	22.7	1860.	6546.
25.	0.4	41.	813.	24.2	10101.	20.8	9933.	20847.
25.	0.8	48.	874.	31.4	5805.	22.6	5375.	12054.
25.	1.2	59.	978.	41.8	4656.	24.5	3872.	9506.
25.	1.4	66.	1048.	49.1	4476.	25.5	3447.	8971.
25.	1.6	76.	1150.	58.2	4461.	26.4	3131.	8742.
25.	1.8	89.	1286.	70.5	4618.	27.4	2888.	8792.
30.	0.4	60.	988.	42.0	14008.	33.5	12645.	27641.
30.	0.6	69.	1078.	50.2	10611.	35.0	8852.	20542.
30.	0.8	81.	1202.	61.0	9249.	36.5	6966.	17417.
30.	1.0	97.	1371.	76.2	8865.	38.0	5841.	16077.
30.	1.2	121.	1628.	98.8	9226.	39.5	5099.	15953.
THREE-TRIP FERRY MODE								
15.	0.8	37.	809.	15.3	4357.	11.7	4772.	15798.
15.	1.6	46.	879.	24.2	2525.	13.9	2584.	9697.
15.	2.0	52.	930.	30.7	2289.	15.0	2163.	8710.
15.	2.4	60.	1006.	39.3	2231.	16.0	1889.	8235.
15.	2.8	70.	1105.	51.8	2330.	17.1	1698.	8134.
15.	3.2	86.	1269.	69.3	2562.	18.1	1558.	8397.
20.	0.8	44.	861.	21.6	4805.	15.8	4819.	16436.
20.	1.2	50.	912.	27.9	3620.	17.2	3412.	12520.
20.	1.6	58.	987.	36.6	3192.	18.5	2719.	10833.
20.	2.0	69.	1095.	49.2	3136.	19.9	2310.	10155.
20.	2.4	87.	1280.	67.6	3350.	21.2	2042.	10180.
20.	2.8	117.	1598.	98.3	3934.	22.6	1855.	11003.
25.	0.4	49.	903.	25.0	10262.	20.8	9939.	32221.
25.	0.8	57.	977.	33.6	6041.	22.7	5380.	19004.
25.	1.2	68.	1085.	46.4	5012.	24.5	3875.	15158.
25.	1.4	77.	1176.	55.1	4884.	25.5	3449.	14344.
25.	1.6	88.	1290.	66.4	4953.	26.4	3132.	13993.
25.	1.8	102.	1438.	81.8	5232.	27.3	2888.	14064.
30.	0.4	68.	1085.	43.6	14366.	33.5	12653.	42091.
30.	0.6	77.	1176.	53.0	11058.	35.0	8859.	31362.
30.	0.8	89.	1300.	65.7	9816.	36.5	6971.	26574.
30.	1.0	106.	1480.	83.6	9586.	38.0	5845.	24433.
30.	1.2	133.	1770.	110.1	10145.	39.5	5100.	24060.
FOUR-TRIP FERRY MODE								
15.	0.8	46.	905.	15.9	4388.	11.7	4774.	22183.
15.	1.6	55.	981.	26.7	2651.	13.9	2587.	14057.
15.	2.0	62.	1046.	34.7	2468.	15.0	2166.	12757.
15.	2.4	71.	1134.	45.8	2482.	16.1	1891.	12163.
15.	2.8	85.	1275.	60.3	2620.	17.1	1699.	12092.
15.	3.2	104.	1474.	82.5	2963.	18.2	1559.	12559.
20.	0.8	53.	963.	22.6	4902.	15.8	4822.	23013.
20.	1.2	60.	1027.	30.0	3767.	17.2	3414.	17793.
20.	1.6	69.	1114.	40.4	3410.	18.6	2721.	15561.
20.	2.0	82.	1245.	55.7	3445.	19.9	2312.	14700.
20.	2.4	103.	1464.	78.4	3783.	21.3	2044.	14824.
20.	2.8	138.	1838.	116.5	4570.	22.6	1857.	16105.
25.	0.4	58.	1008.	25.7	10391.	20.8	9944.	44014.
25.	0.8	66.	1084.	35.5	6259.	22.7	5385.	26377.
25.	1.2	79.	1214.	50.5	5331.	24.5	3879.	21248.
25.	1.4	88.	1306.	61.2	5298.	25.5	3453.	20175.
25.	1.6	101.	1442.	74.6	5443.	26.4	3135.	19731.
25.	1.8	118.	1623.	92.6	5815.	27.3	2890.	19867.
30.	0.4	77.	1194.	44.9	14681.	33.5	12659.	56962.
30.	0.6	86.	1286.	55.6	11478.	35.0	8866.	42610.
30.	0.8	99.	1421.	70.2	10357.	36.5	6977.	36174.
30.	1.0	119.	1634.	90.4	10251.	38.0	5850.	33262.
30.	1.2	148.	1946.	121.2	11052.	39.5	5103.	32702.

TABLE 6. MULTIPLE TRIP, ELECTRIC-PROPELLED, SPACE TRANSPORT PERFORMANCE WITH PROPELLANT TANK MOUNTED ION JETS, TWO INITIAL BOOSTER, AND LUNAR ORBIT INBOUND PROPELLANT TANK DUMP

SWQ = 10 KG/KWE, LANDER CARGO FRAC = .4, CHAR VEL = 7.8 KM/SEC
SWT =(3000/I + 1.2) KG/KWE, ETAT = 1.1 EXP(-1690/I), PROP UTIL = .9

CARGO	POWER	VJI	TI	VJOI	TOI	VJOF	TOF	LIFE
TWO-TRIP FERRY MODE								
15.	0.8	22.	727.	11.9	8649.	11.8	4785.	14161.
15.	1.6	28.	730.	14.4	4326.	14.0	2596.	7652.
15.	2.4	32.	749.	17.6	2991.	16.2	1907.	5647.
15.	3.2	37.	782.	21.5	2397.	18.4	1584.	4762.
15.	3.6	39.	797.	23.9	2231.	19.5	1483.	4511.
15.	4.0	42.	821.	26.5	2113.	20.7	1406.	4340.
20.	0.8	31.	743.	16.3	8810.	15.8	4822.	14376.
20.	1.6	36.	775.	20.2	4687.	18.6	2730.	8192.
20.	2.4	41.	813.	25.4	3447.	21.4	2066.	6325.
20.	2.8	45.	847.	28.5	3136.	22.9	1884.	5867.
20.	3.2	48.	874.	32.3	2951.	24.3	1754.	5579.
20.	3.6	53.	920.	36.6	2837.	25.8	1657.	5414.
25.	0.8	41.	813.	24.2	10101.	22.7	5384.	16298.
25.	1.2	44.	838.	27.5	7182.	24.6	3885.	11905.
25.	1.6	48.	874.	31.4	5805.	26.5	3150.	9829.
25.	1.8	51.	901.	33.6	5374.	27.5	2909.	9184.
25.	2.0	53.	920.	36.1	5061.	28.5	2720.	8701.
25.	2.2	56.	949.	38.8	4825.	29.5	2567.	8341.
30.	0.6	57.	958.	38.6	17640.	35.0	8862.	27460.
30.	0.8	61.	998.	42.0	13999.	36.5	6979.	21975.
30.	1.0	65.	1038.	45.8	11908.	38.1	5858.	18804.
30.	1.2	69.	1078.	50.2	10611.	39.6	5120.	16809.
30.	1.4	75.	1140.	55.1	9770.	41.2	4598.	15507.
30.	1.6	81.	1202.	61.0	9249.	42.8	4213.	14665.
THREE-TRIP FERRY MODE								
15.	0.8	32.	780.	12.2	8630.	11.7	4781.	20077.
15.	1.6	38.	815.	15.2	4353.	14.0	2595.	11471.
15.	2.4	42.	845.	19.1	3063.	16.2	1908.	8855.
15.	3.2	47.	886.	24.0	2514.	18.4	1586.	7729.
15.	3.6	50.	912.	26.9	2365.	19.5	1484.	7422.
15.	4.0	53.	940.	30.4	2276.	20.7	1407.	7225.
20.	0.8	40.	830.	16.8	8866.	15.8	4825.	20472.
20.	1.6	45.	869.	21.5	4795.	18.6	2734.	12284.
20.	2.4	51.	921.	27.7	3607.	21.5	2069.	9854.
20.	2.8	55.	958.	31.6	3329.	22.9	1887.	9277.
20.	3.2	59.	996.	36.3	3177.	24.3	1756.	8930.
20.	3.6	64.	1045.	42.0	3110.	25.8	1659.	8756.
25.	0.8	49.	903.	25.0	10262.	22.7	5390.	23131.
25.	1.2	53.	940.	28.9	7372.	24.6	3891.	17304.
25.	1.6	57.	977.	33.6	6041.	26.5	3155.	14569.
25.	1.8	60.	1006.	36.2	5631.	27.5	2914.	13727.
25.	2.0	63.	1035.	39.1	5335.	28.5	2724.	13103.
25.	2.2	66.	1065.	42.4	5129.	29.5	2571.	12644.
30.	0.6	65.	1055.	39.7	17956.	35.0	8871.	38071.
30.	0.8	68.	1085.	43.6	14366.	36.6	6988.	30771.
30.	1.0	72.	1125.	48.0	12318.	38.1	5867.	26555.
30.	1.2	77.	1176.	53.0	11058.	39.7	5127.	23909.
30.	1.4	83.	1238.	58.8	10268.	41.2	4605.	22189.
30.	1.6	90.	1311.	65.5	9797.	42.8	4219.	21083.
FOUR-TRIP FERRY MODE								
15.	0.8	42.	875.	12.4	8621.	11.7	4779.	26416.
15.	1.6	47.	913.	15.8	4382.	14.0	2597.	15720.
15.	2.4	52.	955.	20.2	3124.	16.2	1909.	12494.
15.	3.2	57.	999.	26.1	2621.	18.4	1588.	11133.
15.	3.6	60.	1027.	29.8	2502.	19.6	1487.	10777.
15.	4.0	63.	1055.	34.3	2448.	20.7	1410.	10562.
20.	0.8	49.	929.	17.1	8912.	15.9	4827.	26992.
20.	1.6	54.	972.	22.5	4890.	18.7	2737.	16806.
20.	2.4	61.	1036.	29.8	3751.	21.5	2072.	13819.
20.	2.8	65.	1075.	34.5	3512.	22.9	1891.	13129.
20.	3.2	70.	1124.	40.1	3390.	24.4	1759.	12733.
20.	3.6	76.	1184.	46.8	3361.	25.8	1662.	12562.
25.	0.8	58.	1008.	25.7	10391.	22.7	5395.	30390.
25.	1.2	62.	1046.	30.0	7539.	24.6	3896.	23132.
25.	1.6	67.	1094.	35.3	6241.	26.6	3160.	19742.
25.	1.8	70.	1124.	38.4	5857.	27.5	2919.	18707.
25.	2.0	73.	1153.	41.9	5591.	28.5	2729.	17946.
25.	2.2	76.	1184.	45.9	5420.	29.5	2576.	17395.
30.	0.6	73.	1153.	40.6	18247.	35.1	8879.	49109.
30.	0.8	77.	1194.	44.9	14681.	36.6	6995.	39994.
30.	1.0	82.	1245.	49.8	12661.	38.1	5874.	34737.
30.	1.2	87.	1296.	55.5	11455.	39.7	5134.	31445.
30.	1.4	93.	1358.	62.1	10727.	41.3	4611.	29315.
30.	1.6	100.	1432.	70.0	10330.	42.9	4225.	27956.

TABLE 7. MULTIPLE TRIP, ELECTRIC-PROPELLED, SPACE TRANSPORT PERFORMANCE WITH PROPELLANT TANK MOUNTED ARC JETS, ONE INITIAL BOOSTER, AND EARTH ORBIT INBOUND PROPELLANT TANK DUMP

SWQ = 10 KG/KWE, LANDER CARGO FRAC = .4, CHAR VEL = 7.8 KM/SEC
SWT = 1.2 KG/KWE, ETAT = .7, PROP UTIL = .9

CARGO	POWER	VJI	TI	VJOI	TOI	VJOF	TOF	LIFE
TWO-TRIP FERRY MODE								
15.	0.8	22.	481.	13.7	2029.	10.8	1617.	4126.
15.	1.6	28.	581.	19.9	1593.	12.3	1021.	3195.
15.	2.0	32.	648.	24.2	1602.	13.0	910.	3159.
15.	2.4	37.	733.	29.9	1695.	13.8	840.	3269.
15.	2.8	45.	870.	37.1	1853.	14.5	794.	3517.
15.	3.2	55.	1042.	48.1	2146.	15.3	764.	3952.
20.	0.8	27.	564.	19.5	3112.	14.8	2414.	6090.
20.	1.2	32.	648.	24.0	2639.	15.8	1798.	5085.
20.	1.6	38.	750.	29.9	2548.	16.7	1498.	4797.
20.	2.0	46.	887.	38.2	2677.	17.7	1326.	4891.
20.	2.4	58.	1094.	50.6	3026.	18.6	1218.	5338.
20.	2.8	78.	1439.	70.9	3714.	19.6	1146.	6299.
25.	0.4	32.	648.	23.7	7829.	20.2	6744.	15222.
25.	0.8	38.	750.	30.3	5161.	21.5	3765.	9676.
25.	1.2	47.	905.	39.6	4636.	22.8	2790.	8331.
25.	1.4	54.	1025.	45.8	4662.	23.5	2517.	8204.
25.	1.6	62.	1163.	54.0	4863.	24.1	2316.	8342.
25.	1.8	72.	1336.	64.9	5259.	24.8	2163.	8758.
30.	0.4	49.	939.	41.2	14528.	32.7	11713.	27180.
30.	0.6	56.	1060.	48.8	11627.	33.8	8252.	20939.
30.	0.8	66.	1232.	58.8	10648.	34.9	6535.	18415.
30.	1.0	80.	1474.	72.7	10666.	36.0	5515.	17654.
30.	1.2	101.	1837.	93.3	11550.	37.2	4844.	18231.
THREE-TRIP FERRY MODE								
15.	0.8	21.	464.	13.8	2048.	10.8	1617.	6526.
15.	1.6	26.	547.	20.3	1633.	12.3	1021.	5096.
15.	2.0	29.	597.	25.0	1665.	13.0	910.	5009.
15.	2.4	33.	665.	31.3	1785.	13.8	840.	5121.
15.	2.8	39.	768.	39.6	1987.	14.5	794.	5420.
15.	3.2	47.	905.	52.0	2335.	15.3	764.	5962.
20.	0.8	26.	547.	19.6	3132.	14.8	2414.	9460.
20.	1.2	29.	597.	24.5	2701.	15.8	1798.	7910.
20.	1.6	34.	682.	30.8	2631.	16.7	1498.	7402.
20.	2.0	40.	785.	39.9	2809.	17.7	1326.	7431.
20.	2.4	49.	939.	53.8	3233.	18.6	1218.	7925.
20.	2.8	64.	1197.	77.0	4052.	19.6	1146.	9082.
25.	0.4	31.	631.	23.8	7848.	20.2	6744.	23140.
25.	0.8	35.	699.	30.6	5221.	21.5	3765.	14716.
25.	1.2	42.	819.	40.4	4742.	22.8	2790.	12519.
25.	1.4	46.	887.	47.4	4835.	23.5	2517.	12201.
25.	1.6	52.	991.	56.3	5086.	24.1	2316.	12239.
25.	1.8	60.	1128.	68.1	5536.	24.8	2163.	12637.
30.	0.4	46.	887.	41.4	14586.	32.7	11713.	40692.
30.	0.6	51.	973.	49.2	11729.	33.8	8252.	31095.
30.	0.8	58.	1094.	59.6	10817.	34.9	6535.	26981.
30.	1.0	68.	1267.	74.3	10927.	36.0	5515.	25373.
30.	1.2	82.	1508.	96.7	11982.	37.2	4844.	25536.
FOUR-TRIP FERRY MODE								
15.	0.8	21.	464.	13.8	2048.	10.8	1617.	8924.
15.	1.6	25.	530.	20.6	1657.	12.3	1021.	6995.
15.	2.0	28.	581.	25.4	1691.	13.0	910.	6848.
15.	2.4	31.	631.	32.2	1844.	13.8	840.	6954.
15.	2.8	36.	716.	41.3	2082.	14.5	794.	7284.
15.	3.2	43.	836.	54.9	2475.	15.3	764.	7905.
20.	0.8	26.	547.	19.6	3132.	14.8	2414.	12827.
20.	1.2	29.	597.	24.5	2701.	15.8	1798.	10724.
20.	1.6	32.	648.	31.3	2683.	16.7	1498.	9995.
20.	2.0	37.	733.	41.1	2899.	17.7	1326.	9940.
20.	2.4	45.	870.	55.9	3367.	18.6	1218.	10447.
20.	2.8	58.	1094.	81.1	4278.	19.6	1146.	11740.
25.	0.4	30.	614.	23.8	7868.	20.2	6744.	31059.
25.	0.8	34.	682.	30.7	5245.	21.5	3765.	19749.
25.	1.2	40.	785.	40.8	4794.	22.8	2790.	16686.
25.	1.4	44.	853.	47.9	4892.	23.5	2517.	16159.
25.	1.6	48.	922.	57.6	5211.	24.1	2316.	16079.
25.	1.8	58.	1042.	70.0	5702.	24.8	2163.	16426.
30.	0.4	45.	870.	41.4	14608.	32.7	11713.	54200.
30.	0.6	49.	939.	49.3	11777.	33.8	8252.	41236.
30.	0.8	55.	1042.	60.0	10896.	34.9	6535.	35513.
30.	1.0	63.	1180.	75.3	11073.	36.0	5515.	33020.
30.	1.2	74.	1370.	98.7	12250.	37.2	4844.	32706.

TABLE 8. MULTIPLE TRIP, ELECTRIC-PROPELLED, SPACE TRANSPORT PERFORMANCE WITH PROPELLANT TANK MOUNTED ARC JETS, TWO INITIAL BOOSTER, AND EARTH ORBIT INBOUND PROPELLANT TANK DUMP

SWQ = 10 KG/KWE, LANDER CARGO FRAC = .4, CHAR VEL = 7.8 KM/SEC
SWT = 1.2 KG/KWE, ETAT = .7, PROP UTIL = .9

CARGO	POWER	VJI	TI	VJOI	TOI	VJOF	TOF	LIFE
TWO-TRIP FERRY MODE								
15.	0.8	20.	448.	11.4	3198.	10.8	1617.	5263.
15.	1.6	22.	481.	13.7	2029.	12.3	1021.	3530.
15.	2.0	23.	497.	15.1	1825.	13.0	910.	3232.
15.	2.4	24.	514.	16.6	1711.	13.8	840.	3064.
15.	2.8	26.	547.	18.2	1633.	14.6	794.	2974.
15.	3.2	28.	581.	19.9	1593.	15.3	764.	2938.
20.	0.8	24.	514.	15.9	4871.	14.8	2414.	7798.
20.	1.2	25.	530.	17.6	3678.	15.8	1798.	6006.
20.	1.6	27.	564.	19.5	3112.	16.7	1498.	5174.
20.	2.0	29.	597.	21.6	2813.	17.7	1326.	4737.
20.	2.4	32.	648.	24.0	2639.	18.6	1218.	4506.
20.	2.8	34.	682.	26.8	2577.	19.6	1146.	4405.
25.	0.4	29.	597.	21.2	13719.	20.2	6744.	21060.
25.	0.8	32.	648.	23.7	7829.	21.5	3765.	12242.
25.	1.2	35.	699.	26.7	5976.	22.8	2790.	9465.
25.	1.4	36.	716.	28.4	5501.	23.5	2517.	8734.
25.	1.6	38.	750.	30.3	5161.	24.1	2316.	8227.
25.	1.8	40.	785.	32.3	4928.	24.8	2163.	7876.
30.	0.4	43.	836.	35.3	24538.	32.7	11713.	37086.
30.	0.6	46.	887.	38.1	17774.	33.8	8252.	26914.
30.	0.8	49.	939.	41.2	14528.	34.9	6535.	22002.
30.	1.0	52.	991.	44.7	12715.	36.0	5515.	19220.
30.	1.2	56.	1080.	48.6	11627.	37.2	4844.	17531.
THREE-TRIP FERRY MODE								
15.	0.8	20.	448.	11.4	3198.	10.8	1617.	7663.
15.	1.6	23.	497.	13.6	2012.	12.3	1021.	5425.
15.	2.0	24.	514.	15.0	1807.	13.0	910.	5066.
15.	2.4	26.	547.	16.3	1676.	13.8	840.	4877.
15.	2.8	27.	564.	18.0	1615.	14.5	794.	4797.
15.	3.2	29.	597.	19.7	1576.	15.3	764.	4784.
20.	0.8	24.	514.	15.9	4871.	14.8	2414.	11168.
20.	1.2	26.	547.	17.6	3660.	15.8	1798.	8820.
20.	1.6	28.	581.	19.4	3094.	16.7	1498.	7755.
20.	2.0	30.	614.	21.5	2795.	17.7	1326.	7215.
20.	2.4	32.	665.	23.8	2622.	18.6	1219.	6946.
20.	2.8	35.	699.	26.7	2558.	19.6	1146.	6849.
25.	0.4	29.	597.	21.2	13719.	20.2	6744.	28978.
25.	0.8	32.	648.	23.7	7829.	21.5	3765.	17272.
25.	1.2	35.	699.	26.7	5976.	22.8	2790.	13616.
25.	1.4	36.	716.	28.4	5501.	23.5	2517.	12565.
25.	1.6	38.	750.	30.3	5161.	24.1	2316.	12009.
25.	1.8	40.	785.	32.3	4928.	24.8	2163.	11559.
30.	0.4	43.	836.	35.3	24538.	32.7	11713.	50591.
30.	0.6	46.	887.	38.1	17774.	33.8	8252.	37045.
30.	0.8	48.	922.	41.2	14547.	34.9	6535.	30509.
30.	1.0	51.	973.	44.8	12734.	36.0	5515.	26804.
30.	1.2	55.	1042.	48.8	11646.	37.2	4844.	24545.
FOUR-TRIP FERRY MODE								
15.	0.8	20.	448.	11.4	3198.	10.8	1617.	10063.
15.	1.6	23.	497.	13.6	2012.	12.3	1021.	7321.
15.	2.0	24.	514.	15.0	1807.	13.0	910.	6901.
15.	2.4	26.	547.	16.3	1676.	13.8	840.	6692.
15.	2.8	28.	581.	17.8	1599.	14.5	794.	6615.
15.	3.2	29.	597.	19.7	1576.	15.3	764.	6631.
20.	0.8	25.	530.	15.9	4853.	14.8	2414.	14533.
20.	1.2	26.	547.	17.6	3660.	15.8	1798.	11637.
20.	1.6	28.	581.	19.4	3094.	16.7	1498.	10338.
20.	2.0	31.	631.	21.4	2778.	17.7	1326.	9689.
20.	2.4	33.	665.	23.8	2622.	18.6	1218.	9386.
20.	2.8	35.	699.	26.7	2558.	19.6	1146.	9294.
25.	0.4	29.	597.	21.2	13719.	20.2	6744.	36896.
25.	0.8	32.	648.	23.7	7829.	21.5	3765.	22301.
25.	1.2	35.	699.	26.7	5976.	22.8	2790.	17768.
25.	1.4	37.	733.	28.4	5483.	23.5	2517.	16592.
25.	1.6	38.	750.	30.3	5161.	24.1	2316.	15791.
25.	1.8	40.	785.	32.3	4928.	24.8	2163.	15241.
30.	0.4	43.	836.	35.3	24538.	32.7	11713.	64095.
30.	0.6	45.	870.	38.1	17793.	33.8	8252.	47178.
30.	0.8	48.	922.	41.2	14547.	34.9	6535.	39014.
30.	1.0	51.	973.	44.8	12734.	36.0	5515.	34385.
30.	1.2	54.	1025.	48.9	11665.	37.2	4844.	31558.

TABLE 9. MULTIPLE TRIP, ELECTRIC-PROPELLED, SPACE TRANSPORT PERFORMANCE WITH PROPELLANT TANK MOUNTED ARC JETS, ONE INITIAL BOOSTER, AND LUNAR ORBIT INBOUND PROPELLANT TANK DUMP

SWQ = 10 KG/KWE, LANDER CARGO FRAC = .4, CHAR VEL = 7.8 KM/SEC
SWT = 1.2 KG/KWE, ETAT = .7, PROP UTIL = .9

CARGO	POWER	VJI	TI	VJOI	TOI	VJOF	TOF	LIFE
TWO-TRIP FERRY MODE								
15.	0.8	22.	481.	13.7	2029.	11.1	1679.	4188.
15.	1.6	28.	581.	19.9	1593.	12.7	1085.	3259.
15.	2.0	32.	648.	24.2	1602.	13.5	975.	3225.
15.	2.4	38.	750.	29.6	1677.	14.3	907.	3334.
15.	2.8	45.	870.	37.1	1853.	15.1	862.	3585.
15.	3.2	56.	1060.	47.7	2128.	15.9	832.	4020.
20.	0.8	28.	581.	19.4	3094.	15.1	2490.	6165.
20.	1.2	32.	648.	24.0	2639.	16.1	1876.	5163.
20.	1.6	38.	750.	29.9	2548.	17.1	1578.	4876.
20.	2.0	46.	887.	38.2	2677.	18.2	1407.	4972.
20.	2.4	58.	1094.	50.6	3026.	19.3	1300.	5420.
20.	2.8	78.	1439.	70.9	3714.	20.3	1230.	6383.
25.	0.4	32.	648.	23.7	7829.	20.3	6843.	15321.
25.	0.8	38.	750.	30.3	5161.	21.8	3866.	9777.
25.	1.2	48.	922.	39.5	4618.	23.2	2892.	8432.
25.	1.4	54.	1025.	45.8	4662.	23.9	2620.	8307.
25.	1.6	62.	1163.	54.0	4863.	24.7	2421.	8447.
25.	1.8	73.	1353.	64.7	5241.	25.4	2268.	8863.
30.	0.4	50.	956.	41.2	14511.	32.9	11857.	27324.
30.	0.6	57.	1077.	48.7	11609.	34.1	8398.	21085.
30.	0.8	67.	1249.	58.7	10631.	35.3	6683.	18562.
30.	1.0	81.	1491.	72.5	10648.	36.5	5664.	17804.
30.	1.2	101.	1837.	93.3	11550.	37.7	4995.	18382.
THREE-TRIP FERRY MODE								
15.	0.8	31.	659.	14.8	2223.	11.1	1690.	7236.
15.	1.6	38.	775.	23.0	1888.	12.7	1096.	5919.
15.	2.0	43.	859.	28.9	1963.	13.5	985.	5925.
15.	2.4	50.	978.	36.6	2125.	14.4	915.	6168.
15.	2.8	60.	1149.	46.7	2380.	15.2	869.	6654.
15.	3.2	74.	1389.	61.6	2797.	16.0	838.	7472.
20.	0.8	37.	758.	21.0	3386.	15.1	2504.	10223.
20.	1.2	42.	842.	26.8	3001.	16.2	1888.	8758.
20.	1.6	49.	961.	34.7	3007.	17.2	1589.	8383.
20.	2.0	60.	1149.	45.3	3225.	18.2	1416.	8608.
20.	2.4	75.	1407.	61.9	3753.	19.3	1307.	9412.
20.	2.8	102.	1872.	88.1	4662.	20.4	1235.	11084.
25.	0.4	41.	826.	24.7	8190.	20.4	6859.	23891.
25.	0.8	48.	944.	32.7	5628.	21.8	3880.	15585.
25.	1.2	59.	1132.	44.3	5239.	23.3	2904.	13591.
25.	1.4	67.	1269.	52.2	5357.	24.0	2631.	13421.
25.	1.6	77.	1441.	62.3	5667.	24.7	2430.	13658.
25.	1.8	90.	1665.	75.9	6205.	25.5	2276.	14322.
30.	0.4	59.	1132.	42.9	15174.	32.9	11875.	41516.
30.	0.6	67.	1269.	51.8	12398.	34.1	8414.	32074.
30.	0.8	79.	1476.	63.5	11555.	35.3	6696.	28183.
30.	1.0	95.	1752.	79.9	11786.	36.5	5576.	26902.
30.	1.2	119.	2166.	104.5	12985.	37.8	5004.	27564.
FOUR-TRIP FERRY MODE								
15.	0.8	39.	824.	15.7	2389.	11.1	1699.	10868.
15.	1.6	47.	955.	26.0	2171.	12.8	1104.	9188.
15.	2.0	54.	1072.	33.1	2282.	13.6	991.	9258.
15.	2.4	63.	1224.	42.6	2510.	14.4	920.	9677.
15.	2.8	75.	1429.	55.9	2883.	15.2	873.	10473.
15.	3.2	93.	1737.	74.4	3419.	16.0	841.	11787.
20.	0.8	45.	922.	22.4	3651.	15.2	2514.	14874.
20.	1.2	51.	1022.	29.5	3343.	16.2	1897.	12962.
20.	1.6	60.	1173.	39.0	3422.	17.2	1596.	12529.
20.	2.0	73.	1394.	52.3	3765.	18.3	1422.	12945.
20.	2.4	92.	1720.	72.7	4449.	19.3	1312.	14210.
20.	2.8	124.	2272.	106.1	5659.	20.4	1238.	16789.
25.	0.4	49.	988.	25.5	8507.	20.4	6872.	33054.
25.	0.8	57.	1123.	35.0	6062.	21.8	3892.	22002.
25.	1.2	70.	1343.	48.8	5816.	23.3	2913.	19398.
25.	1.4	79.	1497.	58.4	6044.	24.0	2639.	19221.
25.	1.6	91.	1703.	70.6	6466.	24.8	2437.	19607.
25.	1.8	107.	1978.	86.8	7138.	25.5	2282.	20596.
30.	0.4	68.	1309.	44.4	15764.	33.0	11890.	56317.
30.	0.6	77.	1463.	54.6	13121.	34.1	8428.	43689.
30.	0.8	90.	1686.	68.1	12454.	35.3	6708.	38465.
30.	1.0	108.	1996.	87.2	12916.	36.6	5685.	36722.
30.	1.2	136.	2479.	115.5	14408.	37.8	5012.	37572.

TABLE 10. MULTIPLE TRIP, ELECTRIC-PROPELLED, SPACE TRANSPORT PERFORMANCE WITH PROPELLANT TANK MOUNTED ARC JETS, TWO INITIAL BOOSTER, AND LUNAR ORBIT INBOUND PROPELLANT TANK DUMP

SWQ = 10 KG/KWE, LANDER CARGO FRAC = .4, CHAR VEL = 7.8 KM/SEC
SWT = 1.2 KG/KWE, ETAT = .7, PROP UTIL = .9

CARGO	POWER	VJI	TI	VJOI	TOI	VJOF	TOF	LIFE
TWO-TRIP FERRY MODE								
15.	0.8	20.	448.	11.4	3195.	11.1	1681.	5327.
15.	1.6	22.	481.	13.7	2039.	12.7	1091.	3600.
15.	2.0	24.	514.	15.0	1807.	13.5	982.	3303.
15.	2.4	25.	530.	16.5	1692.	14.4	915.	3138.
15.	2.8	26.	547.	18.2	1633.	15.2	872.	3052.
15.	3.2	28.	581.	19.9	1593.	16.1	844.	3018.
20.	0.8	24.	514.	15.9	4871.	15.1	2494.	7879.
20.	1.2	25.	547.	17.6	3660.	16.1	1881.	6088.
20.	1.6	28.	581.	19.4	3094.	17.2	1585.	5259.
20.	2.0	30.	614.	21.5	2795.	18.2	1416.	4825.
20.	2.4	32.	648.	24.0	2639.	19.3	1311.	4598.
20.	2.8	35.	699.	26.7	2558.	20.4	1242.	4499.
25.	0.4	30.	614.	21.2	13701.	20.3	6845.	21160.
25.	0.8	32.	648.	23.7	7822.	21.8	3870.	12348.
25.	1.2	35.	699.	26.7	5976.	23.2	2899.	9574.
25.	1.4	37.	733.	28.4	5483.	24.0	2628.	8844.
25.	1.6	39.	760.	30.2	5143.	24.7	2429.	8340.
25.	1.8	41.	802.	32.1	4911.	25.5	2278.	7991.
30.	0.4	44.	853.	35.3	24520.	32.9	11860.	37234.
30.	0.6	47.	905.	38.1	17757.	34.1	8403.	27065.
30.	0.8	50.	956.	41.2	14511.	35.3	6689.	22155.
30.	1.0	53.	1008.	44.7	12697.	36.5	5673.	19378.
30.	1.2	57.	1077.	48.7	11609.	37.8	5005.	17692.
THREE-TRIP FERRY MODE								
15.	0.8	28.	610.	11.9	3370.	11.1	1695.	8321.
15.	1.6	31.	659.	14.8	2243.	12.8	1104.	6083.
15.	2.0	33.	692.	16.4	2022.	13.6	995.	5723.
15.	2.4	34.	709.	18.4	1940.	14.5	929.	5544.
15.	2.8	36.	742.	20.6	1892.	15.3	885.	5476.
15.	3.2	39.	792.	22.7	1860.	16.2	856.	5469.
20.	0.8	33.	692.	16.5	5007.	15.1	2509.	11839.
20.	1.2	35.	725.	18.6	3916.	16.2	1896.	9494.
20.	1.6	37.	758.	21.0	3386.	17.3	1600.	8435.
20.	2.0	40.	809.	23.5	3103.	18.3	1430.	7905.
20.	2.4	42.	842.	26.8	3001.	19.4	1325.	7659.
20.	2.8	46.	910.	30.2	2946.	20.5	1255.	7587.
25.	0.4	38.	775.	21.6	14033.	20.4	6863.	29659.
25.	0.8	41.	826.	24.7	8100.	21.9	3887.	17959.
25.	1.2	45.	893.	28.2	6367.	23.3	2915.	14316.
25.	1.4	46.	910.	30.4	5933.	24.1	2645.	13377.
25.	1.6	49.	961.	32.5	5599.	24.9	2445.	12735.
25.	1.8	51.	995.	35.1	5406.	25.6	2294.	12305.
30.	0.4	53.	1029.	36.0	25070.	32.9	11880.	51243.
30.	0.6	56.	1081.	39.2	18358.	34.1	8423.	37711.
30.	0.8	59.	1132.	42.9	15174.	35.4	6708.	31195.
30.	1.0	63.	1200.	47.0	13406.	36.6	5691.	27521.
30.	1.2	68.	1286.	51.6	12367.	37.9	5022.	25307.
FOUR-TRIP FERRY MODE								
15.	0.8	36.	776.	12.2	3491.	11.1	1704.	11901.
15.	1.6	39.	824.	15.7	2389.	12.8	1114.	9167.
15.	2.0	41.	856.	17.7	2214.	13.7	1005.	8750.
15.	2.4	43.	889.	20.0	2137.	14.5	938.	8569.
15.	2.8	46.	938.	22.4	2092.	15.4	893.	8505.
15.	3.2	48.	972.	25.6	2132.	16.3	865.	8553.
20.	0.8	41.	856.	17.0	5294.	15.2	2521.	16395.
20.	1.2	43.	889.	19.5	4138.	16.2	1908.	13502.
20.	1.6	46.	938.	22.2	3617.	17.3	1611.	12217.
20.	2.0	49.	988.	25.4	3379.	18.4	1441.	11601.
20.	2.4	52.	1038.	29.2	3304.	19.5	1335.	11345.
20.	2.8	56.	1106.	33.5	3310.	20.6	1265.	11319.
25.	0.4	46.	938.	21.9	14296.	20.4	6877.	38754.
25.	0.8	50.	1006.	25.4	8473.	21.9	3900.	24172.
25.	1.2	53.	1056.	29.7	6747.	23.3	2929.	19674.
25.	1.4	56.	1106.	32.0	6284.	24.1	2657.	18524.
25.	1.6	58.	1139.	34.7	6023.	24.9	2458.	17757.
25.	1.8	61.	1190.	37.6	5841.	25.6	2306.	17253.
30.	0.4	61.	1190.	36.7	25567.	33.0	11898.	65862.
30.	0.6	65.	1258.	40.2	18376.	34.2	8439.	48971.
30.	0.8	68.	1309.	44.4	15764.	35.4	6724.	40857.
30.	1.0	73.	1394.	49.0	14032.	36.6	5706.	36295.
30.	1.2	78.	1480.	54.4	13077.	37.9	5037.	33565.

TABLE 11. MULTIPLE TRIP, ELECTRIC-PROPELLED, SPACE TRANSPORT PERFORMANCE WITH POWERPLANT MOUNTED ION JETS, ONE INITIAL BOOSTER, AND EARTH ORBIT INBOUND PROPELLANT TANK DUMP

SWQ = 10 KG/KWE, LANDER CARGO FRAC = .4, CHAR VEL = 7.8 KM/SEC
SWT =(3000/I + 1.2) KG/KWE, ETAT = 1.1 EXP(-1690/I), PROP UTIL = .9

CARGO	POWER	VJ	TI	WCI	TOI	WCF	TOF	LIFE
TWO-TRIP FERRY MODE								
15.	0.8	13.3	911.	11.8	4305.	18.2	4767.	9982.
15.	1.6	17.0	778.	9.7	2225.	20.3	2686.	5688.
15.	2.4	21.1	731.	7.9	1588.	22.1	2068.	4387.
15.	3.2	25.8	724.	6.2	1303.	23.8	1817.	3844.
15.	3.6	28.5	732.	5.3	1219.	24.7	1756.	3707.
15.	4.0	31.4	745.	4.5	1159.	25.5	1722.	3627.
20.	0.8	17.8	764.	17.4	4499.	22.6	4961.	10224.
20.	1.6	22.9	724.	15.4	2463.	24.6	2954.	6141.
20.	2.4	28.9	734.	13.6	1845.	26.4	2386.	4964.
20.	2.8	32.4	751.	12.7	1690.	27.3	2263.	4705.
20.	3.2	36.4	778.	11.9	1590.	28.1	2201.	4569.
20.	3.6	40.9	812.	11.0	1528.	29.0	2184.	4525.
25.	0.8	25.7	724.	22.8	5199.	27.2	5712.	11635.
25.	1.2	29.6	736.	21.8	3736.	28.2	4283.	8756.
25.	1.6	34.3	761.	20.9	3043.	29.1	3601.	7435.
25.	1.8	36.4	778.	20.4	2827.	29.6	3438.	7042.
25.	2.0	39.0	797.	20.0	2664.	30.0	3301.	6762.
25.	2.2	41.9	820.	19.5	2541.	30.5	3206.	6567.
30.	0.6	39.7	803.	28.5	8982.	31.5	9625.	19409.
30.	0.8	43.3	832.	28.0	7154.	32.0	7834.	15821.
30.	1.0	47.3	867.	27.6	6098.	32.4	6819.	13785.
30.	1.2	51.8	908.	27.1	5463.	32.9	6200.	12542.
30.	1.4	56.8	956.	26.6	4998.	33.4	5817.	11771.
30.	1.6	62.5	1012.	26.2	4713.	33.8	5593.	11319.
THREE-TRIP FERRY MODE								
15.	0.8	13.5	898.	12.2	4307.	18.4	4768.	15639.
15.	1.2	15.3	821.	11.0	2906.	19.5	3364.	11276.
15.	1.6	17.2	775.	9.8	2229.	20.4	2689.	9158.
15.	2.0	19.0	748.	8.7	1885.	21.2	2302.	7935.
15.	2.4	20.8	732.	7.6	1579.	21.9	2057.	7159.
15.	2.8	22.6	725.	6.3	1398.	22.5	1888.	6623.
20.	0.8	17.8	764.	17.4	4501.	22.6	4964.	15956.
20.	1.6	22.6	725.	15.1	2444.	24.4	2934.	9762.
20.	2.4	27.5	729.	12.8	1797.	25.8	2325.	7905.
20.	2.8	30.3	740.	11.7	1623.	26.5	2176.	7454.
20.	3.2	33.1	756.	10.5	1499.	27.1	2078.	7167.
20.	3.6	36.0	778.	9.3	1403.	27.6	2010.	6971.
25.	0.8	25.3	724.	22.6	5158.	27.0	5669.	17941.
25.	1.2	28.6	733.	21.4	3670.	27.9	4208.	13551.
25.	1.6	32.2	750.	20.3	2946.	28.6	3517.	11480.
25.	1.8	34.1	762.	19.7	2712.	28.9	3300.	10836.
25.	2.0	36.1	775.	19.1	2529.	29.3	3136.	10352.
25.	2.2	38.1	790.	18.5	2383.	29.6	3011.	9986.
30.	0.6	38.4	793.	28.2	8790.	31.3	9421.	29218.
30.	0.8	41.3	816.	27.6	6985.	31.6	7585.	23727.
30.	1.0	44.4	842.	27.1	5824.	32.0	6315.	20538.
30.	1.2	47.6	870.	26.6	5109.	32.3	5532.	18513.
30.	1.4	51.1	902.	26.9	4613.	32.7	5373.	17164.
30.	1.6	54.8	937.	25.3	4257.	33.0	5056.	16245.
FOUR-TRIP FERRY MODE								
15.	0.8	13.6	893.	12.3	4308.	18.6	4769.	21292.
15.	1.2	15.4	818.	11.1	2909.	19.6	3367.	15463.
15.	1.6	17.2	774.	9.9	2230.	20.4	2691.	12627.
15.	2.0	18.9	748.	8.7	1834.	21.2	2301.	10982.
15.	2.4	20.4	735.	7.1	1567.	21.8	2043.	9900.
20.	0.8	17.8	764.	17.5	4502.	22.6	4965.	21688.
20.	1.6	22.3	726.	15.0	2437.	24.3	2925.	13388.
20.	2.0	24.6	723.	13.7	2037.	24.9	2542.	11833.
20.	2.4	27.0	727.	12.5	1777.	25.5	2301.	10861.
20.	2.8	29.4	736.	11.2	1598.	26.1	2140.	10221.
20.	3.2	31.2	744.	9.5	1444.	26.3	2005.	9692.
25.	0.8	25.1	723.	24.8	5139.	26.0	5648.	24252.
25.	1.2	28.2	731.	21.2	3641.	27.7	4175.	18360.
25.	1.6	31.8	746.	20.0	2905.	28.3	3459.	15549.
25.	1.8	33.1	756.	19.3	2664.	28.7	3244.	14663.
25.	2.0	34.9	767.	18.7	2479.	29.0	3071.	13987.
25.	2.2	36.6	779.	18.1	2342.	29.2	2959.	13465.
30.	0.6	37.9	788.	28.1	8703.	31.1	9328.	39052.
30.	0.8	40.4	809.	27.5	6823.	31.5	7474.	31671.
30.	1.0	43.1	831.	26.8	5706.	31.8	6334.	27352.
30.	1.2	45.9	855.	26.2	4973.	32.1	5679.	24576.
30.	1.4	48.9	881.	25.6	4468.	32.4	5195.	22686.
30.	1.6	51.9	909.	24.9	4081.	32.6	4850.	21360.

TABLE 12. MULTIPLE TRIP, ELECTRIC-PROPELLED, SPACE TRANSPORT PERFORMANCE WITH POWERPLANT MOUNTED ION JETS, TWO INITIAL BOOSTER, AND EARTH ORBIT INBOUND PROPELLANT TANK DUMP

SWO = 10 KG/KWE, LANDER CARGO FRAC = .4, CHAR VEL = 7.8 KM/SEC
SWT =(3000/I + 1.2) KG/KWE, ETAT = 1.1 EXP(-1690/I), PROP UTIL = .9

CARGO	POWER	VJ	TI	WCI	TOI	WCF	TOF	LIFE
TWO-TRIP FERRY MODE								
15.	0.8	12.1	999.	14.2	8636.	16.5	4789.	14424.
15.	1.6	14.5	850.	13.7	4329.	17.6	2622.	7802.
15.	2.4	17.0	778.	13.2	2967.	18.6	1944.	5688.
15.	3.2	19.7	741.	12.7	2322.	19.6	1633.	4695.
15.	3.6	21.1	731.	12.5	2117.	20.1	1539.	4387.
15.	4.0	22.6	725.	12.2	1959.	20.5	1470.	4154.
20.	0.8	16.2	797.	19.4	8801.	21.2	4859.	14457.
20.	1.6	19.4	743.	18.9	4620.	22.3	2780.	8144.
20.	2.4	22.9	724.	18.3	3283.	23.3	2134.	6141.
20.	2.8	24.8	723.	18.1	2919.	23.8	1965.	5607.
20.	3.2	26.8	726.	17.8	2655.	24.3	1850.	5232.
20.	3.6	28.9	734.	17.6	2460.	24.9	1771.	4964.
25.	0.8	23.3	724.	24.4	9931.	26.1	5461.	16115.
25.	1.2	25.7	724.	24.2	6932.	26.6	3979.	11635.
25.	1.6	28.2	731.	23.9	5461.	27.2	3266.	9458.
25.	1.8	29.6	736.	23.8	4982.	27.4	3038.	8756.
25.	2.0	31.0	743.	23.6	4605.	27.7	2862.	8210.
25.	2.2	32.4	752.	23.5	4303.	28.0	2725.	7779.
30.	0.6	36.4	778.	29.6	16962.	30.8	9092.	26831.
30.	0.8	38.6	794.	29.5	13213.	31.1	7239.	21246.
30.	1.0	40.9	812.	29.3	10993.	31.4	6152.	17956.
30.	1.2	43.3	832.	29.2	9539.	31.6	5449.	15821.
30.	1.4	45.9	855.	29.0	8526.	31.9	4970.	14351.
30.	1.6	48.7	880.	28.9	7791.	32.2	4631.	13303.
THREE-TRIP FERRY MODE								
15.	0.8	12.6	958.	15.0	8614.	17.3	4773.	20077.
15.	1.6	15.3	821.	14.8	4360.	18.6	2637.	11276.
15.	2.4	18.1	760.	14.3	3012.	19.6	1970.	8472.
15.	3.2	20.8	732.	13.8	2369.	20.5	1663.	7159.
15.	3.6	22.2	726.	13.4	2159.	20.9	1566.	6744.
20.	0.8	16.6	786.	19.8	8854.	21.7	4886.	20197.
20.	1.6	20.1	737.	19.4	4679.	22.8	2813.	11780.
20.	2.4	23.7	723.	18.9	3336.	23.8	2166.	9115.
20.	2.8	25.6	724.	18.6	2966.	24.3	1996.	8405.
20.	3.2	27.5	729.	18.2	2695.	24.7	1877.	7905.
20.	3.6	29.6	736.	17.9	2491.	25.2	1792.	7549.
25.	0.8	23.7	723.	24.6	9995.	26.3	5497.	22437.
25.	1.2	26.1	725.	24.4	6988.	26.8	4011.	16459.
25.	1.6	28.6	733.	24.1	5505.	27.3	3291.	13551.
25.	1.8	29.9	738.	23.9	5018.	27.6	3059.	12613.
25.	2.0	31.3	745.	23.8	4633.	27.8	2879.	11881.
25.	2.2	32.7	753.	23.6	4322.	28.1	2736.	11301.
30.	0.6	36.4	777.	29.6	16953.	30.8	9087.	36683.
30.	0.8	38.4	793.	29.4	13185.	31.1	7224.	29218.
30.	1.0	40.6	810.	29.3	10944.	31.3	6124.	24812.
30.	1.2	42.8	828.	29.1	9467.	31.5	5408.	21940.
30.	1.4	45.2	849.	28.9	8427.	31.8	4912.	19949.
30.	1.6	47.5	870.	28.7	7662.	32.0	4555.	18513.
FOUR-TRIP FERRY MODE								
15.	0.8	12.9	938.	15.5	8609.	17.6	4769.	25729.
15.	1.2	14.4	858.	15.4	5765.	18.4	3341.	19360.
15.	1.6	15.8	807.	15.3	4380.	19.1	2648.	14746.
15.	2.0	17.2	774.	15.1	3569.	19.6	2245.	12627.
15.	2.4	18.6	752.	14.9	3039.	20.1	1985.	11252.
15.	2.8	19.9	739.	14.8	2664.	20.5	1805.	10294.
20.	0.8	16.9	780.	20.1	8885.	21.9	4902.	26933.
20.	1.6	20.5	734.	19.7	4713.	23.1	2833.	15413.
20.	2.4	24.2	723.	19.1	3365.	24.1	2184.	12086.
20.	2.8	26.0	725.	18.8	2991.	24.5	2012.	11199.
20.	3.2	27.9	730.	18.4	2715.	24.9	1890.	10575.
20.	3.6	29.8	738.	18.0	2503.	25.3	1800.	10116.
25.	0.8	23.9	723.	24.7	10036.	26.4	5517.	28756.
25.	1.2	26.3	725.	24.5	7019.	26.9	4028.	21281.
25.	1.6	28.9	733.	24.2	5528.	27.4	3305.	17643.
25.	1.8	30.2	739.	24.0	5037.	27.6	3071.	16467.
25.	2.0	31.5	746.	23.8	4648.	27.9	2888.	15549.
25.	2.2	32.8	754.	23.6	4332.	28.1	2743.	14821.
30.	0.6	36.4	777.	29.6	16949.	30.8	9085.	46535.
30.	0.8	38.4	792.	29.4	13170.	31.0	7215.	37193.
30.	1.0	40.4	809.	29.2	10917.	31.3	6109.	31671.
30.	1.2	42.6	826.	29.1	9426.	31.5	5386.	28062.
30.	1.4	44.8	845.	28.9	8374.	31.7	4882.	25554.
30.	1.6	47.1	865.	28.7	7594.	31.9	4516.	23737.

TABLE 13. MULTIPLE TRIP, ELECTRIC-PROPELLED, SPACE TRANSPORT PERFORMANCE WITH POWERPLANT MOUNTED ION JETS, ONE INITIAL BOOSTER, AND LUNAR ORBIT INBOUND PROPELLANT TANK DUMP

SWQ = 10 KG/KWE, LANDER CARGO FRAC = .4, CHAR VEL = 7.8 KM/SEC
SWT =(3000/I + 1.2) KG/KWE, ETAT = 1.1 EXP(-1690/I), PROP UTIL = .9

CARGO	POWER	VJ	TI	WCI	TOI	WCF	TOF	LIFE
TWO-TRIP FERRY MODE								
15.	0.8	13.4	906.	11.9	4306.	18.1	4812.	10024.
15.	1.6	17.1	775.	9.8	2229.	20.2	2721.	5725.
15.	2.4	21.2	730.	8.0	1592.	22.0	2097.	4419.
15.	3.2	25.9	725.	6.3	1306.	23.7	1843.	3874.
15.	3.6	28.6	732.	5.4	1222.	24.6	1780.	3735.
15.	4.0	31.5	746.	4.6	1162.	25.4	1744.	3652.
20.	0.8	17.8	763.	17.5	4503.	22.5	4996.	10262.
20.	1.6	23.0	724.	15.5	2467.	24.5	2983.	6174.
20.	2.4	29.0	734.	13.6	1849.	26.4	2410.	4993.
20.	2.8	32.6	752.	12.8	1694.	27.2	2286.	4733.
20.	3.2	36.5	779.	11.9	1594.	28.1	2223.	4595.
20.	3.6	41.1	814.	11.1	1532.	28.9	2205.	4550.
25.	0.8	25.7	724.	22.8	5204.	27.2	5739.	11667.
25.	1.2	29.6	737.	21.8	3741.	28.2	4308.	8786.
25.	1.6	34.0	761.	20.9	3048.	29.1	3653.	7463.
25.	1.8	36.5	778.	20.6	2831.	29.5	3460.	7069.
25.	2.0	39.1	798.	20.0	2668.	30.0	3322.	6788.
25.	2.2	42.0	821.	19.6	2545.	30.4	3227.	6593.
30.	0.6	39.7	803.	28.5	8987.	31.5	9647.	19436.
30.	0.8	43.4	833.	28.0	7160.	32.0	7855.	15847.
30.	1.0	47.4	868.	27.6	6103.	32.4	6839.	13810.
30.	1.2	51.8	909.	27.1	5438.	32.9	6220.	12567.
30.	1.4	56.8	957.	26.6	5002.	33.4	5836.	11795.
30.	1.6	62.5	1013.	26.2	4718.	33.8	5612.	11342.
THREE-TRIP FERRY MODE								
15.	0.8	15.0	963.	7.1	4347.	19.6	4921.	17159.
20.	0.4	16.3	899.	16.5	8817.	22.1	9375.	30257.
20.	0.8	19.1	821.	14.3	4593.	23.3	5138.	17200.
20.	1.2	21.6	785.	12.8	3207.	24.2	3754.	12864.
20.	1.6	24.2	770.	10.9	2525.	25.0	3083.	10737.
20.	2.0	26.7	766.	9.4	2122.	25.7	2694.	9497.
25.	0.8	26.3	766.	20.7	5258.	27.3	5828.	18908.
25.	1.2	29.9	772.	19.1	3759.	28.2	4354.	14420.
25.	1.6	33.7	789.	17.7	3027.	28.9	3653.	12278.
25.	1.8	35.7	800.	17.0	2789.	29.3	3432.	11606.
25.	2.0	37.7	813.	16.3	2603.	29.6	3264.	11097.
25.	2.2	39.8	828.	15.7	2455.	29.9	3136.	10710.
30.	0.6	39.1	823.	27.4	8888.	31.3	9562.	29989.
30.	0.8	42.1	846.	26.7	7017.	31.7	7720.	24462.
30.	1.0	45.3	872.	26.0	5911.	32.1	6645.	21247.
30.	1.2	48.7	901.	25.3	5190.	32.4	5958.	19196.
30.	1.4	52.3	933.	24.6	4691.	32.8	5494.	17824.
30.	1.6	56.1	968.	24.0	4332.	33.1	5175.	16888.
FOUR-TRIP FERRY MODE								
20.	0.4	17.8	1031.	13.2	8996.	23.0	9660.	44389.
25.	0.8	27.4	825.	18.8	5380.	27.7	6001.	27439.
25.	1.2	31.1	823.	16.0	3848.	28.5	4488.	21152.
25.	1.6	34.7	834.	14.1	3086.	29.1	3752.	18070.
25.	1.8	36.4	841.	13.2	2827.	29.4	3506.	17046.
25.	2.0	37.5	847.	11.9	2696.	29.5	3284.	16135.
30.	0.6	39.4	859.	26.3	8931.	31.4	9635.	41510.
30.	0.8	42.3	877.	25.3	7034.	31.7	7764.	33999.
30.	1.0	45.2	899.	24.4	5904.	32.1	6661.	29577.
30.	1.2	48.3	923.	23.5	5158.	32.4	5944.	26710.
30.	1.4	51.4	949.	22.6	4633.	32.6	5449.	24744.
30.	1.6	54.7	978.	21.8	4247.	32.9	5095.	23351.

TABLE 14. MULTIPLE TRIP, ELECTRIC-PROPELLED, SPACE TRANSPORT PERFORMANCE WITH POWERPLANT MOUNTED ION JETS, TWO INITIAL BOOSTER, AND LUNAR ORBIT INBOUND PROPELLANT TANK DUMP

SWQ = 10 KG/KWE, LANDER CARGO FRAC = .4, CHAR VEL = 7.8 KM/SEC
SWT =(3000/I + 1.2) KG/KWE, ETAT = 1.1 EXP(-1690/I), PROP UTIL = .9

CARGO	POWER	VJ	TI	WCI	TOI	WCF	TOF	LIFE
TWO-TRIP FERRY MODE								
15.	0.8	12.1	994.	14.3	8632.	16.4	4839.	14466.
15.	1.6	14.6	847.	13.8	4332.	17.4	2663.	7841.
15.	2.4	17.1	775.	13.3	2971.	18.4	1978.	5725.
15.	3.2	19.8	740.	12.8	2327.	19.3	1662.	4729.
15.	3.6	21.2	730.	12.6	2122.	19.8	1567.	4419.
15.	4.0	22.7	725.	12.3	1964.	20.3	1496.	4185.
20.	0.8	16.2	796.	19.4	8806.	21.1	4895.	14497.
20.	1.6	19.5	743.	18.9	4626.	22.2	2811.	8179.
20.	2.4	23.0	724.	18.4	3289.	23.2	2160.	6174.
20.	2.8	24.9	723.	18.1	2924.	23.7	1991.	5638.
20.	3.2	26.9	727.	17.9	2661.	24.2	1874.	5262.
20.	3.6	29.0	734.	17.6	2465.	24.8	1794.	4993.
25.	0.8	23.4	724.	24.5	9938.	26.1	5487.	16149.
25.	1.2	25.7	724.	24.2	6939.	26.6	4004.	11667.
25.	1.6	28.3	731.	23.9	5468.	27.1	3289.	9488.
25.	1.8	29.6	737.	23.8	4989.	27.4	3061.	8786.
25.	2.0	31.0	744.	23.7	4611.	27.6	2884.	8239.
25.	2.2	32.5	752.	23.5	4309.	27.9	2746.	7807.
30.	0.6	36.4	778.	29.6	16969.	30.8	9112.	26859.
30.	0.8	38.6	794.	29.5	13220.	31.1	7259.	21273.
30.	1.0	40.9	812.	29.3	11000.	31.3	6171.	17983.
30.	1.2	43.4	833.	29.2	9546.	31.6	5469.	15847.
30.	1.4	46.0	856.	29.1	8533.	31.9	4989.	14377.
30.	1.6	48.8	881.	28.9	7798.	32.2	4650.	13328.
THREE-TRIP FERRY MODE								
15.	0.8	14.0	1039.	12.6	8629.	18.4	4909.	21745.
15.	1.2	15.5	939.	11.7	5821.	19.0	3478.	15639.
20.	0.8	17.7	852.	18.3	8990.	22.2	5044.	21556.
20.	1.6	21.6	785.	17.2	4810.	23.3	2952.	12864.
20.	2.4	25.5	767.	16.2	3452.	24.4	2291.	10045.
20.	2.8	27.3	767.	15.6	3065.	24.8	2109.	9260.
25.	0.8	24.5	769.	23.7	10158.	26.5	5639.	23471.
25.	1.2	27.2	767.	23.2	7134.	27.1	4142.	17398.
25.	1.6	29.9	772.	22.7	5639.	27.6	3415.	14420.
25.	1.8	31.3	777.	22.4	5147.	27.9	3180.	13453.
25.	2.0	32.7	784.	22.2	4758.	28.1	2996.	12695.
25.	2.2	34.2	791.	22.0	4442.	28.4	2851.	12092.
30.	0.6	36.9	808.	29.2	17107.	30.9	9207.	37481.
30.	0.8	39.1	823.	28.9	13332.	31.1	7340.	29989.
30.	1.0	41.3	840.	28.7	11083.	31.4	6237.	25556.
30.	1.2	43.7	858.	28.5	9600.	31.6	5518.	22661.
30.	1.4	46.1	879.	28.2	8555.	31.9	5020.	20650.
30.	1.6	48.7	901.	28.0	7785.	32.1	4660.	19196.
FOUR-TRIP FERRY MODE								
20.	0.4	17.1	1080.	17.6	17808.	22.4	9588.	53470.
20.	0.8	19.3	952.	16.0	9230.	23.2	5251.	30597.
25.	0.8	25.9	832.	22.7	10450.	27.1	5841.	32168.
25.	1.2	28.9	822.	21.9	7381.	27.7	4318.	24287.
25.	1.6	31.8	824.	21.1	5851.	28.2	3571.	20374.
25.	1.8	33.3	828.	20.8	5344.	28.4	3327.	19088.
25.	2.0	34.7	834.	20.5	4938.	28.6	3135.	18070.
25.	2.2	36.1	840.	20.1	4601.	28.8	2977.	17236.
30.	0.6	37.6	848.	28.7	17333.	31.0	9356.	49086.
30.	0.8	39.9	862.	28.4	13530.	31.3	7474.	39624.
30.	1.0	42.3	877.	28.0	11255.	31.5	6357.	33999.
30.	1.2	44.6	894.	27.7	9747.	31.8	5624.	30306.
30.	1.4	47.1	913.	27.3	8677.	32.0	5112.	27721.
30.	1.6	49.5	933.	27.0	7884.	32.2	4740.	25839.

TABLE 15. MULTIPLE TRIP, ELECTRIC-PROPELLED, SPACE TRANSPORT PERFORMANCE WITH POWERPLANT MOUNTED ARC JETS, ONE INITIAL BOOSTER, AND EARTH ORBIT INBOUND PROPELLANT TANK DUMP

SWQ = 10 KG/KWE, LANDER CARGO FRAC = .4, CHAR VEL = 7.8 KM/SEC
SWT = 1.2 KG/KWE, ETAT = .7, PROP UTIL = .9

CARGO	POWER	VJ	TI	WCI	TOI	WCF	TOF	LIFE
15.	0.8	12.7	335.	12.3	1832.	17.7	1996.	4164.
15.	1.6	16.0	384.	10.3	1222.	19.7	1441.	3047.
15.	2.4	19.6	442.	8.5	1044.	21.5	1325.	2811.
15.	3.2	23.9	511.	6.8	985.	23.2	1338.	2834.
15.	3.6	26.3	552.	6.0	978.	24.0	1372.	2902.
15.	4.0	28.9	597.	5.2	982.	24.8	1422.	3000.
20.	0.8	17.1	402.	17.7	2664.	22.3	2903.	5968.
20.	1.6	21.7	476.	15.8	1766.	24.2	2082.	4325.
20.	2.4	27.2	567.	14.1	1526.	25.9	1936.	4030.
20.	2.8	30.4	622.	13.2	1484.	26.8	1950.	4056.
20.	3.2	34.1	683.	12.4	1474.	27.6	2002.	4159.
20.	3.6	38.2	754.	11.5	1487.	28.5	2087.	4329.
25.	0.8	25.0	530.	23.0	4155.	27.0	4527.	9213.
25.	1.2	28.5	590.	22.1	3223.	27.9	3656.	7469.
25.	1.6	32.6	658.	21.2	2805.	28.8	3308.	6771.
25.	1.8	34.8	697.	20.7	2686.	29.3	3227.	6609.
25.	2.0	37.3	738.	20.3	2604.	29.7	3187.	6529.
25.	2.2	39.9	783.	19.8	2561.	30.2	3180.	6515.
30.	0.6	39.1	760.	28.6	9134.	31.4	9748.	19951.
30.	0.8	42.4	826.	28.1	7902.	31.9	8174.	16502.
30.	1.0	46.2	891.	27.7	6880.	32.3	7317.	14787.
30.	1.2	50.4	963.	27.2	6023.	32.8	6832.	13818.
30.	1.4	55.1	1044.	26.8	5683.	33.2	6574.	13302.
30.	1.6	60.5	1137.	26.3	5491.	33.7	6475.	13103.
THREE-TRIP FERRY MODE								
15.	0.8	12.9	338.	12.8	1873.	18.0	2040.	6631.
15.	1.6	16.1	387.	10.6	1239.	19.9	1460.	4933.
15.	2.4	19.5	440.	8.4	1037.	21.4	1316.	4549.
15.	3.2	23.1	499.	6.2	950.	22.7	1290.	4528.
15.	3.6	25.0	531.	5.1	924.	23.3	1297.	4579.
15.	4.0	26.7	558.	3.8	895.	23.7	1296.	4605.
20.	0.8	17.2	403.	17.6	2675.	22.3	2914.	9310.
20.	1.6	21.8	472.	15.6	1741.	24.0	2053.	6790.
20.	2.4	26.1	549.	13.4	1456.	25.4	1848.	6250.
20.	2.8	28.7	592.	12.3	1387.	26.1	1822.	6214.
20.	3.2	31.4	637.	11.2	1343.	26.7	1825.	6267.
20.	3.6	34.3	687.	10.1	1318.	27.3	1849.	6390.
25.	0.8	24.7	525.	22.8	4090.	26.9	4457.	14052.
25.	1.2	27.7	576.	21.7	3121.	27.6	3540.	11384.
25.	1.6	31.1	632.	20.6	2659.	28.4	3135.	10194.
25.	1.8	32.8	662.	20.1	2514.	28.7	3021.	9880.
25.	2.0	34.7	694.	19.5	2403.	29.0	2942.	9674.
25.	2.2	36.6	726.	18.9	2319.	29.4	2891.	9554.
30.	0.6	37.9	749.	28.3	8839.	31.2	9433.	29203.
30.	0.8	40.6	795.	27.8	7152.	31.5	7792.	24327.
30.	1.0	43.5	845.	27.2	6166.	31.9	6835.	21568.
30.	1.2	46.6	897.	26.7	5533.	32.2	6277.	19881.
30.	1.4	49.9	954.	26.1	5105.	32.6	5906.	18824.
30.	1.6	53.4	1015.	25.5	4808.	32.9	5670.	18178.
FOUR-TRIP FERRY MODE								
15.	0.8	13.0	340.	12.8	1892.	18.1	2061.	9095.
15.	1.6	16.2	388.	10.6	1246.	20.0	1469.	6817.
15.	2.0	17.8	413.	9.5	1118.	20.7	1368.	6461.
15.	2.4	19.5	439.	8.3	1034.	21.4	1312.	6288.
15.	2.8	21.1	466.	7.2	976.	22.0	1282.	6219.
15.	3.2	22.6	491.	5.8	926.	22.4	1257.	6171.
20.	0.8	17.2	403.	17.8	2680.	22.4	2920.	12651.
20.	1.6	21.3	470.	15.5	1730.	24.0	2039.	9257.
20.	2.4	25.7	541.	13.2	1427.	25.2	1811.	8485.
20.	2.8	27.9	580.	12.0	1348.	25.8	1771.	8399.
20.	3.2	30.3	620.	10.7	1293.	26.3	1756.	8421.
20.	3.6	32.7	661.	9.5	1252.	26.8	1757.	8505.
25.	0.8	24.5	522.	22.7	4060.	26.8	4423.	18896.
25.	1.2	27.4	570.	21.6	3075.	27.5	3489.	15252.
25.	1.6	30.4	621.	20.4	2596.	28.1	3062.	13646.
25.	1.8	32.0	648.	19.8	2442.	28.4	2934.	13190.
25.	2.0	33.6	676.	19.2	2322.	28.7	2842.	12875.
25.	2.2	35.3	704.	18.6	2227.	29.0	2776.	12668.
30.	0.6	37.4	740.	28.2	8703.	31.1	9288.	38785.
30.	0.8	39.8	781.	27.6	6995.	31.4	7622.	32203.
30.	1.0	42.3	825.	27.0	5986.	31.7	6656.	28427.
30.	1.2	45.0	870.	26.4	5328.	32.0	6044.	26069.
30.	1.4	47.8	918.	25.8	4872.	32.3	5636.	24532.
30.	1.6	50.7	968.	25.1	4543.	32.5	5357.	23517.

TABLE 16. MULTIPLE TRIP, ELECTRIC-PROPELLED, SPACE TRANSPORT PERFORMANCE WITH POWERPLANT MOUNTED ARC JETS, TWO INITIAL BOOSTER, AND EARTH ORBIT INBOUND PROPELLANT TANK DUMP

SWQ = 10 KG/KWE, LANDER CARGO FRAC = .4, CHAR VEL = 7.8 KM/SEC
SWT = 1.2 KG/KWE, ETAT = .7, PROP UTIL = .9

CARGO	POWER	VJ	TI	WCI	TOI	WCF	TOF	LIFE
TWO-TRIP FERRY MODE								
15.	0.8	11.6	321.	14.3	3275.	16.3	1784.	5380.
15.	1.6	13.7	351.	13.8	2030.	17.3	1197.	3578.
15.	2.4	16.0	384.	13.4	1629.	18.2	1034.	3047.
15.	3.2	18.3	421.	13.0	1446.	19.1	982.	2849.
15.	3.6	19.6	442.	12.7	1392.	19.6	977.	2811.
15.	4.0	21.0	463.	12.5	1354.	20.0	981.	2799.
20.	0.8	18.7	380.	19.6	4803.	21.1	2617.	7800.
20.	1.6	18.6	425.	19.0	2038.	22.0	1732.	5095.
20.	2.4	21.7	476.	18.5	2359.	23.0	1494.	4325.
20.	2.8	23.4	504.	18.3	2204.	23.5	1448.	4156.
20.	3.2	25.3	535.	18.0	2103.	24.0	1428.	4065.
20.	3.6	27.2	567.	17.8	2035.	24.5	1428.	4030.
25.	0.8	22.8	493.	24.5	7491.	26.0	4081.	12066.
25.	1.2	25.0	530.	24.3	5540.	26.5	3142.	9213.
25.	1.6	27.3	569.	24.0	4599.	27.0	2711.	7879.
25.	1.8	28.5	590.	23.9	4297.	27.2	2582.	7469.
25.	2.0	29.8	612.	23.8	4065.	27.5	2488.	7164.
25.	2.2	31.2	634.	23.6	3883.	27.7	2420.	6937.
30.	0.6	36.0	716.	29.6	16694.	30.8	8908.	26317.
30.	0.8	38.0	750.	29.5	13295.	31.0	7243.	21288.
30.	1.0	40.1	787.	29.4	11296.	31.3	6281.	18364.
30.	1.2	42.4	826.	29.2	10002.	31.5	5673.	16502.
30.	1.4	44.9	868.	29.1	9114.	31.8	5272.	15254.
30.	1.6	47.6	914.	29.0	8484.	32.1	5002.	14400.
THREE-TRIP FERRY MODE								
15.	0.8	12.1	327.	15.1	3443.	17.0	1876.	7850.
15.	1.6	14.5	362.	14.9	2173.	18.2	1281.	5460.
15.	2.4	17.0	399.	14.5	1755.	19.2	1113.	4779.
15.	3.2	19.5	440.	14.0	1556.	20.1	1057.	4549.
15.	3.6	20.8	461.	13.8	1494.	20.5	1048.	4514.
15.	4.0	22.2	484.	13.5	1448.	20.9	1049.	4513.
20.	0.8	16.2	387.	19.9	4962.	21.8	2703.	11142.
20.	1.6	19.3	436.	19.0	3070.	22.6	1810.	7564.
20.	2.4	22.6	490.	19.1	2463.	23.5	1562.	6568.
20.	2.8	24.3	519.	18.8	2300.	24.0	1510.	6358.
20.	3.2	26.1	549.	18.5	2184.	24.4	1484.	6250.
20.	3.6	28.0	581.	18.1	2102.	24.8	1475.	6213.
25.	0.8	23.2	500.	24.7	7617.	26.2	4150.	16916.
25.	1.2	25.4	537.	24.4	5645.	26.7	3202.	13124.
25.	1.6	27.7	576.	24.2	4681.	27.2	2760.	11354.
25.	1.8	29.0	597.	24.0	4368.	27.4	2624.	10811.
25.	2.0	30.2	618.	23.9	4123.	27.6	2523.	10406.
25.	2.2	31.6	640.	23.7	3928.	27.9	2448.	10104.
30.	0.6	36.0	716.	29.6	16687.	30.8	8904.	35928.
30.	0.8	37.9	749.	29.5	13259.	31.0	7223.	29203.
30.	1.0	39.9	783.	29.3	11228.	31.2	6243.	25281.
30.	1.2	42.0	819.	29.2	9900.	31.5	5615.	22770.
30.	1.4	44.3	857.	29.0	8974.	31.7	5190.	21069.
30.	1.6	46.6	897.	28.8	8300.	31.9	4893.	19881.
FOUR-TRIP FERRY MODE								
15.	0.8	12.3	331.	15.4	3539.	17.3	1928.	10315.
15.	1.6	14.9	368.	15.4	2252.	18.7	1328.	7341.
15.	2.4	17.5	408.	15.1	1822.	19.7	1156.	6514.
15.	3.2	20.1	450.	14.6	1614.	20.6	1096.	6251.
15.	3.6	21.4	471.	14.2	1545.	21.0	1084.	6212.
15.	4.0	22.6	491.	13.8	1481.	21.2	1072.	6171.
20.	0.8	16.4	391.	20.1	5053.	21.7	2753.	14483.
20.	1.6	19.7	445.	19.8	3144.	22.8	1854.	10033.
20.	2.4	23.0	498.	19.3	2521.	23.9	1599.	8812.
20.	2.8	24.8	527.	19.0	2350.	24.2	1544.	8560.
20.	3.2	26.6	556.	18.7	2227.	24.6	1513.	8434.
20.	3.6	28.4	587.	18.3	2137.	25.0	1499.	8396.
25.	0.8	23.4	503.	24.8	7689.	26.3	4189.	21766.
25.	1.2	25.6	541.	24.5	5704.	26.8	3236.	17034.
25.	1.6	28.0	580.	24.3	4727.	27.3	2787.	14828.
25.	1.8	29.2	601.	24.1	4407.	27.5	2648.	14151.
25.	2.0	30.4	621.	24.0	4154.	27.7	2542.	13646.
25.	2.2	31.7	643.	23.8	3952.	27.9	2463.	13268.
30.	0.6	36.0	716.	29.6	16682.	30.8	8902.	45534.
30.	0.8	37.8	748.	29.5	13238.	31.0	7212.	37118.
30.	1.0	39.8	781.	29.3	11192.	31.2	6223.	32203.
30.	1.2	41.8	816.	29.1	9844.	31.4	5584.	29043.
30.	1.4	43.9	852.	28.9	8897.	31.6	5146.	26839.
30.	1.6	46.1	889.	28.7	8202.	31.8	4836.	25377.

TABLE 17. MULTIPLE TRIP, ELECTRIC-PROPELLED, SPACE TRANSPORT PERFORMANCE WITH POWERPLANT MOUNTED ARC JETS, ONE INITIAL BOOSTER, AND LUNAR ORBIT INBOUND PROPELLANT TANK DUMP

SWQ = 10 KG/KWE, LANDER CARGO FRAC = .4, CHAR VEL = 7.8 KM/SEC
SWT = 1.2 KG/KWE, ETAT = .7, PROP UTIL = .9

CARGO	POWER	VJ	TI	WCI	TOI	WCF	TOF	LIFE
TWO-TRIP FERRY MODE								
15.	0.8	12.7	336.	12.4	1844.	17.6	2027.	4207.
15.	1.6	16.1	385.	10.4	1231.	19.6	1469.	3085.
15.	2.4	19.7	444.	8.6	1052.	21.4	1351.	2847.
15.	3.2	24.0	514.	6.9	992.	23.1	1363.	2868.
15.	3.6	26.4	554.	6.1	984.	23.9	1397.	2936.
15.	4.0	29.1	599.	5.3	988.	24.7	1447.	3034.
20.	0.8	17.2	403.	17.8	2675.	22.2	2930.	6008.
20.	1.6	21.8	478.	15.9	1775.	24.1	2109.	4361.
20.	2.4	27.3	569.	14.1	1534.	25.9	1962.	4065.
20.	2.8	30.6	624.	13.3	1491.	26.7	1975.	4090.
20.	3.2	34.2	686.	12.4	1480.	27.6	2026.	4192.
20.	3.6	38.4	757.	11.6	1494.	28.4	2111.	4362.
25.	0.8	25.0	531.	23.0	4165.	27.0	4554.	9249.
25.	1.2	28.5	591.	22.1	3231.	27.9	3681.	7504.
25.	1.6	32.7	660.	21.2	2813.	28.8	3333.	6805.
25.	1.8	34.9	698.	20.7	2693.	29.3	3252.	6643.
25.	2.0	37.4	740.	20.3	2611.	29.7	3212.	6563.
25.	2.2	40.0	785.	19.9	2559.	30.1	3204.	6548.
30.	0.6	39.1	769.	28.6	9143.	31.4	9773.	19685.
30.	0.8	42.5	827.	28.1	7510.	31.9	8198.	16535.
30.	1.0	46.2	892.	27.7	6588.	32.3	7341.	14820.
30.	1.2	50.4	964.	27.2	6030.	32.8	6856.	13850.
30.	1.4	55.2	1045.	26.8	5691.	33.2	6598.	13335.
30.	1.6	60.6	1138.	26.3	5498.	33.7	6499.	13135.
THREE-TRIP FERRY MODE								
15.	0.8	14.4	423.	7.9	2154.	19.3	2401.	8284.
15.	1.2	16.3	441.	6.0	1666.	20.3	1939.	6865.
20.	0.8	18.4	466.	14.8	2901.	23.0	3206.	10653.
20.	1.2	20.8	499.	13.1	2234.	23.9	2577.	8770.
20.	1.6	23.2	535.	11.5	1902.	24.7	2284.	7906.
20.	2.0	25.6	572.	10.1	1708.	25.4	2130.	7466.
20.	2.4	28.1	612.	8.8	1584.	26.1	2047.	7247.
20.	2.8	30.6	652.	7.4	1493.	26.6	1999.	7131.
25.	0.8	25.6	572.	21.1	4272.	27.2	4604.	15159.
25.	1.2	29.0	626.	19.5	3278.	28.0	3756.	12385.
25.	1.6	32.5	684.	18.1	2798.	28.7	3336.	11171.
25.	1.8	34.4	715.	17.4	2646.	29.0	3216.	10834.
25.	2.0	36.3	747.	16.8	2530.	29.4	3132.	10611.
25.	2.2	38.3	780.	16.1	2440.	29.7	3076.	10473.
30.	0.6	38.5	784.	27.6	8997.	31.3	9637.	30158.
30.	0.8	41.4	832.	26.9	7300.	31.6	7989.	25258.
30.	1.0	44.4	883.	26.2	6305.	32.0	7046.	22475.
30.	1.2	47.6	937.	25.5	5666.	32.3	6462.	20772.
30.	1.4	51.0	995.	24.8	5232.	32.7	6086.	19701.
30.	1.6	54.7	1057.	24.2	4923.	33.0	5845.	19037.
FOUR-TRIP FERRY MODE								
20.	0.4	17.3	556.	13.7	5392.	22.8	5747.	26152.
20.	0.8	20.0	563.	10.3	3206.	23.9	3587.	17222.
25.	0.8	26.8	638.	18.6	4496.	27.6	4973.	22589.
25.	1.2	30.2	687.	16.5	3439.	28.3	3971.	18594.
25.	1.6	33.7	740.	14.7	2912.	29.0	3499.	16755.
25.	1.8	35.5	767.	13.8	2738.	29.2	3353.	16205.
25.	2.0	37.2	795.	13.0	2598.	29.5	3243.	15798.
25.	2.2	38.9	822.	12.1	2478.	29.7	3150.	15462.
30.	0.6	38.8	821.	26.5	9073.	31.3	9745.	41840.
30.	0.8	41.6	866.	25.5	7337.	31.7	8055.	35147.
30.	1.0	44.4	912.	24.6	6305.	32.0	7070.	31278.
30.	1.2	47.3	960.	23.8	5627.	32.3	6442.	28844.
30.	1.4	50.3	1010.	22.9	5155.	32.5	6020.	27242.
30.	1.6	53.4	1062.	22.1	4811.	32.8	5729.	26169.

TABLE 18. MULTIPLE TRIP, ELECTRIC-PROPELLED, SPACE TRANSPORT PERFORMANCE WITH POWERPLANT MOUNTED ARC JETS, TWO INITIAL BOOSTER, AND LUNAR ORBIT INBOUND PROPELLANT TANK DUMP

SWQ = 10 KG/KWE, LANDER CARGO FRAC = .4, CHAR VEL = 7.8 KM/SEC
SWT = 1.2 KG/KWE, ETAT = .7, PROP UTIL = .9

CARGO	POWER	VJ	TI	WCI	TOI	WCF	TOF	LIFE
TWO-TRIP FERRY MODE								
15.	0.8	11.7	322.	14.4	3293.	16.2	1812.	5426.
15.	1.6	13.8	352.	14.0	2045.	17.1	1222.	3619.
15.	2.4	16.1	385.	13.5	1642.	18.0	1058.	3085.
15.	3.2	18.5	423.	13.1	1457.	18.9	1006.	2886.
15.	3.6	19.7	444.	12.8	1403.	19.3	1000.	2847.
15.	4.0	21.1	466.	12.6	1365.	19.8	1004.	2834.
20.	0.8	15.8	381.	19.5	4818.	21.0	2642.	7841.
20.	1.6	18.7	426.	19.0	2951.	21.9	1756.	5133.
20.	2.4	21.8	478.	18.6	2366.	22.9	1517.	4361.
20.	2.8	23.6	506.	18.3	2215.	23.3	1471.	4192.
20.	3.2	25.4	536.	18.1	2113.	23.8	1451.	4100.
20.	3.6	27.3	569.	17.8	2045.	24.3	1450.	4065.
25.	0.8	22.9	495.	24.5	7504.	26.0	4104.	12103.
25.	1.2	25.0	531.	24.3	5553.	26.4	3165.	9249.
25.	1.6	27.4	570.	24.0	4610.	26.9	2734.	7914.
25.	1.8	28.6	591.	23.9	4309.	27.2	2604.	7504.
25.	2.0	29.9	613.	23.8	4076.	27.4	2510.	7199.
25.	2.2	31.3	636.	23.7	3894.	27.7	2442.	6972.
30.	0.6	36.0	716.	29.6	16706.	30.7	8930.	26352.
30.	0.8	38.0	751.	29.5	13307.	31.0	7265.	21322.
30.	1.0	40.2	788.	29.4	11308.	31.3	6302.	18398.
30.	1.2	42.5	827.	29.2	10013.	31.5	5695.	16535.
30.	1.4	44.9	869.	29.1	9125.	31.8	5293.	15287.
30.	1.6	47.6	915.	29.0	8494.	32.1	5024.	14433.
THREE-TRIP FERRY MODE								
15.	0.0	13.4	412.	12.8	3939.	18.1	2203.	9694.
15.	1.2	14.9	427.	12.2	2922.	18.8	1749.	7812.
15.	1.6	16.3	441.	11.7	2500.	19.4	1523.	6865.
15.	2.0	17.3	453.	10.7	2158.	19.6	1368.	6222.
20.	0.8	17.2	451.	18.5	5344.	22.0	2958.	12587.
20.	1.6	20.8	499.	17.4	3351.	23.2	2019.	8770.
20.	2.4	24.4	553.	16.5	2690.	24.2	1746.	7649.
20.	2.8	26.2	582.	16.1	2508.	24.6	1686.	7395.
20.	3.2	28.1	612.	15.6	2375.	25.0	1652.	7247.
20.	3.6	30.0	643.	15.1	2272.	25.4	1632.	7168.
25.	0.8	24.0	547.	23.8	7914.	26.4	4352.	18073.
25.	1.2	26.4	586.	23.3	5907.	27.0	3390.	14208.
25.	1.6	29.0	626.	22.8	4917.	27.5	2937.	12385.
25.	1.8	30.3	647.	22.6	4593.	27.7	2797.	11819.
25.	2.0	31.6	669.	22.4	4338.	27.9	2692.	11394.
25.	2.2	33.0	692.	22.2	4134.	28.2	2613.	11075.
30.	0.6	36.5	749.	29.2	16935.	30.8	9072.	36901.
30.	0.8	38.5	784.	29.0	13495.	31.1	7338.	30158.
30.	1.0	40.7	820.	28.8	11455.	31.3	6404.	26219.
30.	1.2	42.9	857.	28.5	10115.	31.6	5772.	23688.
30.	1.4	45.2	896.	28.3	9180.	31.8	5344.	21971.
30.	1.6	47.6	937.	28.1	8499.	32.0	5045.	20772.
FOUR-TRIP FERRY MODE								
20.	0.4	16.7	560.	17.8	10297.	22.3	5499.	30426.
20.	0.8	19.1	588.	16.7	6053.	23.2	3397.	19565.
25.	0.8	25.4	619.	22.8	8453.	27.0	4682.	25656.
25.	1.2	28.2	657.	22.0	6350.	27.6	3573.	20566.
25.	1.6	30.9	698.	21.4	5291.	28.1	3188.	18117.
25.	1.8	32.3	719.	21.0	4939.	28.3	3034.	17345.
25.	2.0	33.7	740.	20.7	4659.	28.5	2917.	16755.
25.	2.2	35.1	762.	20.4	4431.	28.7	2825.	16302.
30.	0.6	37.2	795.	28.8	17307.	31.0	9298.	48670.
30.	0.8	39.4	830.	28.4	13821.	31.2	7591.	40149.
30.	1.0	41.6	866.	28.1	11740.	31.5	6588.	35147.
30.	1.2	43.8	903.	27.8	10361.	31.7	5936.	31909.
30.	1.4	46.1	941.	27.5	9389.	31.9	5489.	29696.
30.	1.6	48.5	980.	27.2	8670.	32.1	5169.	28123.

TABLE 19. TWO-POWERPLANT, TWO-TRIP, ELECTRIC-PROPELLED, SPACE TRANSPORT PERFORMANCE WITH PROPELLANT TANK MOUNTED ION JETS, AND EARTH ORBIT INBOUND PROPELLANT TANK DUMP

SWQ = 10 KG/KWE, LANDER CARGO FRAC = .4, CHAR VEL = 7.8 KM/SEC
SWT =(3000/I + 1.2) KG/KWE, ETAT = 1.1 EXP(-1690/I), PROP UTIL = .9

CARGO	POWER	VJI	TI	VJOI	TOI	TOF	LIFE
15.	0.4	23.	724.	12.9	4476.	4476.	9677.
15.	0.6	26.	725.	14.8	3067.	3067.	6858.
15.	0.8	29.	734.	16.9	2399.	2399.	5533.
15.	1.0	32.	749.	19.2	2027.	2027.	4802.
15.	1.2	35.	768.	21.8	1801.	1801.	4370.
15.	1.4	38.	789.	24.7	1662.	1662.	4114.
15.	1.6	41.	813.	28.1	1581.	1581.	3974.
15.	1.8	45.	847.	31.9	1536.	1536.	3920.
15.	2.0	49.	883	36.4	1526.	1526.	3935.
20.	0.2	27.	727.	15.3	8887.	8887.	18502.
20.	0.4	30.	738.	17.7	4676.	4676.	10090.
20.	0.6	34.	761.	20.4	3325.	3325.	7412.
20.	0.8	37.	782.	23.6	2696.	2696.	6174.
20.	1.0	41.	813.	27.2	2355.	2355.	5524.
20.	1.2	45.	847.	31.4	2167.	2167.	5181.
20.	1.4	50.	892.	36.4	2070.	2070.	5032.
20.	1.6	56.	949.	42.3	2040.	2040.	5028.
20.	1.8	63.	1018.	49.5	2066.	2066.	5150.
25.	0.2	36.	775.	22.3	9941.	9941.	20656.
25.	0.4	40.	805.	26.3	5470.	5470.	11746.
25.	0.6	45.	847.	31.0	4067.	4067.	8982.
25.	0.7	48.	874.	33.6	3699.	3699.	8272.
25.	0.8	51.	901.	36.6	3447.	3447.	7796.
25.	0.9	54.	930.	39.9	3277.	3277.	7483.
25.	1.0	58.	968.	43.6	3162.	3162.	7291.
25.	1.1	62.	1008.	47.7	3096.	3096.	7199.
30.	0.2	63.	920.	37.2	13165.	13165.	27249.
30.	0.3	57.	958.	41.2	9489.	9489.	19934.
30.	0.4	62.	1008.	45.7	7731.	7731.	16469.
30.	0.5	67.	1058.	50.9	6761.	6761.	14580.
30.	0.6	74.	1129.	56.9	6193.	6193.	13515.
30.	0.7	81.	1202.	64.1	5881.	5881.	12965.
30.	0.8	90.	1296.	72.5	5747.	5747.	12790.

TABLE 20. THREE-POWERPLANT, THREE-TRIP, ELECTRIC-PROPELLED, SPACE TRANSPORT PERFORMANCE WITH PROPELLANT TANK MOUNTED ION JETS, AND EARTH ORBIT INBOUND PROPELLANT TANK DUMP

SWQ = 10 KG/KWE, LANDER CARGO FRAC = .4, CHAR VEL = 7.8 KM/SEC
SWT =(3000/I + 1.2) KG/KWE, ETAT = 1.1 EXP(-1690/I), PROP UTIL = .9

CARGO	POWER	VJI	TI	VJOI	TOI	TOF	LIFE
15.	0.4	26.	725.	15.0	3128.	3128.	10834.
15.	0.6	30.	738.	18.1	2251.	2251.	8231.
15.	0.8	34.	761.	21.7	1860.	1860.	7103.
15.	1.0	38.	789.	25.7	1665.	1665.	6575.
15.	1.2	43.	830.	30.4	1568.	1568.	6363.
15.	1.4	48.	874.	35.9	1537.	1537.	6358.
15.	1.6	55.	939.	42.1	1544.	1544.	6511.
15.	1.8	62.	1008.	49.9	1598.	1598.	6810.
15.	2.0	71.	1099.	59.2	1688.	1688.	7260.
20.	0.2	29.	734.	16.5	6126.	6126.	19845.
20.	0.4	33.	755.	20.4	3386.	3386.	11669.
20.	0.6	38.	789.	24.9	2550.	2550.	9228.
20.	0.8	44.	838.	30.2	2192.	2192.	8251.
20.	1.0	50.	892.	36.6	2041.	2041.	7907.
20.	1.2	58.	969.	44.2	2000.	2000.	7935.
20.	1.4	67.	1058.	53.8	2045.	2045.	8252.
20.	1.6	79.	1181.	65.8	2162.	2162.	8849.
20.	1.8	95.	1349.	81.4	2360.	2360.	9779.
25.	0.2	38.	789.	24.1	6986.	6986.	22535.
25.	0.4	44.	838.	30.3	4090.	4090.	13948.
25.	0.6	52.	911.	37.9	3252.	3252.	11576.
25.	0.7	57.	958.	42.4	3061.	3061.	11100.
25.	0.8	62.	1008.	47.6	2959.	2959.	10891.
25.	0.9	68.	1068.	53.4	2917.	2917.	10836.
25.	1.0	75.	1140.	60.1	2926.	2926.	11056.
25.	1.1	83.	1228.	67.9	2982.	2982.	11390.
30.	0.2	56.	949.	40.3	9432.	9432.	30195.
30.	0.3	62.	1008.	46.3	7070.	7070.	23224.
30.	0.4	70.	1088.	53.3	5998.	5998.	20172.
30.	0.5	79.	1181.	61.7	5474.	5474.	18785.
30.	0.6	89.	1286.	71.0	5258.	5258.	18346.
30.	0.7	103.	1435.	84.3	5241.	5241.	18591.
30.	0.8	119.	1636.	100.2	5415.	5415.	19458.

TABLE 21. FOUR-POWERPLANT, FOUR-TRIP, ELECTRIC-PROPELLED, SPACE TRANSPORT PERFORMANCE WITH PROPELLANT TANK MOUNTED ION JETS, AND EARTH ORBIT INBOUND PROPELLANT TANK DUMP

SWQ = 10 KG/KWE, LANDER CARGO FRAC = .4, CHAR VEL = 7.8 KM/SEC
SWT = (3000/I + 1.2) KG/KWE, ETAT = 1.1 EXP(-1690/I), PROP UTIL = .9

CARGO	POWER	VJI	TI	VJOI	TOI	TOF	LIFE
15.	0.4	29.	734.	17.0	2492.	2492.	12170.
15.	0.6	34.	761.	21.5	1888.	1888.	9836.
15.	0.8	39.	797.	26.8	1648.	1648.	8983.
15.	1.0	46.	856.	32.8	1548.	1548.	8759.
15.	1.2	53.	920.	40.1	1538.	1538.	8911.
15.	1.4	61.	998.	49.1	1589.	1589.	9349.
15.	1.6	72.	1109.	59.7	1683.	1683.	10060.
15.	1.8	85.	1244.	73.3	1837.	1837.	11080.
15.	2.0	102.	1424.	90.7	2056.	2056.	12497.
20.	0.2	30.	738.	17.8	4768.	4768.	21287.
20.	0.4	36.	775.	23.2	2776.	2776.	13428.
20.	0.6	43.	830.	29.7	2210.	2210.	11329.
20.	0.8	51.	901.	37.6	2014.	2014.	10761.
20.	1.0	61.	998.	47.4	1984.	1984.	10930.
20.	1.2	73.	1119.	59.9	2068.	2068.	11630.
20.	1.4	90.	1296.	75.9	2243.	2243.	12860.
20.	1.6	112.	1531.	98.1	2543.	2543.	14766.
20.	1.8	144.	1877.	129.8	3016.	3016.	17693.
25.	0.2	40.	805.	23.8	5528.	5528.	24527.
25.	0.4	49.	883.	34.5	3440.	3440.	16409.
25.	0.6	60.	988.	45.6	2921.	2921.	14649.
25.	0.7	67.	1058.	52.5	2846.	2846.	14559.
25.	0.8	75.	1140.	60.4	2847.	2847.	14809.
25.	0.9	85.	1244.	69.7	2907.	2907.	15359.
25.	1.0	96.	1360.	81.0	3033.	3033.	16214.
25.	1.1	110.	1510.	94.5	3220.	3220.	17408.
30.	0.2	59.	978.	43.5	7605.	7605.	33353.
30.	0.3	68.	1068.	51.8	5921.	5921.	26887.
30.	0.4	79.	1181.	61.7	5231.	5231.	24469.
30.	0.5	92.	1318.	74.2	4986.	4986.	23896.
30.	0.6	108.	1488.	90.0	5018.	5018.	24537.
30.	0.7	130.	1725.	110.4	5273.	5273.	26267.
30.	0.8	160.	2051.	138.2	5781.	5781.	29279.

TABLE 22. TWO-POWERPLANT, TWO-TRIP, ELECTRIC-PROPELLED, SPACE TRANSPORT PERFORMANCE WITH PROPELLANT TANK MOUNTED ARC JETS, AND EARTH ORBIT INBOUND PROPELLANT TANK DUMP

SWQ = 10 KG/KWE, LANDER CARGO FRAC = .4, CHAR VEL = 7.8 KM/SEC
SWT = (3000/I + 1.2) KG/KWE, ETAT = 1.1 EXP(-1690/I), PROP UTIL = .9

CARGO	POWER	VJI	TI	VJOI	TOI	TOF	LIFE
15.	0.4	20.	448.	12.2	1816.	1816.	4080.
15.	0.6	22.	481.	13.7	1434.	1434.	3349.
15.	0.8	23.	497.	15.5	1275.	1275.	3046.
15.	1.0	25.	530.	17.4	1194.	1194.	2919.
15.	1.2	27.	564.	19.5	1163.	1163.	2890.
15.	1.4	30.	614.	21.8	1155.	1155.	2924.
15.	1.6	32.	648.	24.6	1181.	1181.	3010.
15.	1.8	35.	699.	27.6	1221.	1221.	3140.
15.	2.0	39.	768.	31.0	1274.	1274.	3315.
20.	0.2	23.	497.	14.9	4573.	4573.	9644.
20.	0.4	25.	530.	16.9	2730.	2730.	5991.
20.	0.6	27.	564.	19.2	2164.	2164.	4892.
20.	0.8	30.	614.	21.8	1918.	1918.	4449.
20.	1.0	33.	665.	24.8	1812.	1812.	4289.
20.	1.2	36.	716.	28.3	1788.	1788.	4292.
20.	1.4	40.	785.	32.4	1814.	1814.	4412.
20.	1.6	45.	870.	37.2	1882.	1882.	4635.
20.	1.8	51.	973.	43.0	1996.	1996.	4965.
25.	0.2	30.	614.	21.9	7257.	7257.	15129.
25.	0.4	33.	665.	25.3	4375.	4375.	9416.
25.	0.6	37.	733.	29.3	3516.	3516.	7765.
25.	0.7	39.	768.	31.6	3314.	3314.	7395.
25.	0.8	42.	819.	34.1	3185.	3185.	7188.
25.	0.9	45.	870.	36.9	3115.	3115.	7101.
25.	1.0	48.	922.	40.0	3093.	3093.	7109.
25.	1.1	51.	973.	43.5	3113.	3113.	7199.
30.	0.2	44.	853.	36.5	12989.	12989.	26831.
30.	0.3	48.	922.	40.1	9675.	9675.	20271.
30.	0.4	52.	991.	44.1	8132.	8132.	17254.
30.	0.5	56.	1060.	48.7	7321.	7321.	15702.
30.	0.6	62.	1163.	54.1	6885.	6885.	14933.
30.	0.7	68.	1267.	60.4	6703.	6703.	14673.
30.	0.8	76.	1405.	67.9	6699.	6699.	14802.

TABLE 23. THREE-POWERPLANT, THREE-TRIP, ELECTRIC-PROPELLED, SPACE TRANSPORT PERFORMANCE WITH PROPELLANT TANK MOUNTED ARC JETS, AND EARTH ORBIT INBOUND PROPELLANT TANK DUMP

SWQ = 10 KG/KWE, LANDER CARGO FRAC = .4, CHAR VEL = 7.8 KM/SEC
SWT =(3000/I + 1.2) KG/KWE, ETAT = 1.1 EXP(-1690/I), PROP UTIL = .9

CARGO	POWER	VJI	TI	VJOI	TOI	TOF	LIFE
15.	0.4	22.	481.	13.9	1476.	1476.	5391.
15.	0.6	24.	514.	16.5	1265.	1265.	4823.
15.	0.8	27.	564.	19.3	1191.	1191.	4701.
15.	1.0	30.	614.	22.6	1186.	1186.	4787.
15.	1.2	34.	682.	26.3	1213.	1213.	5004.
15.	1.4	38.	750.	30.7	1277.	1277.	5332.
15.	1.6	43.	836.	35.7	1365.	1365.	5766.
15.	1.8	49.	939.	41.6	1480.	1480.	6319.
15.	2.0	56.	1060.	48.9	1633.	1633.	7018.
20.	0.2	24.	514.	15.9	3372.	3372.	11145.
20.	0.4	27.	564.	19.2	2193.	2193.	7706.
20.	0.6	31.	631.	22.9	1865.	1865.	6858.
20.	0.8	35.	699.	27.2	1773.	1773.	6717.
20.	1.0	40.	785.	32.4	1785.	1785.	6923.
20.	1.2	46.	887.	38.7	1868.	1868.	7378.
20.	1.4	54.	1025.	46.2	2006.	2006.	8069.
20.	1.6	63.	1180.	56.0	2225.	2225.	9036.
20.	1.8	76.	1405.	68.3	2518.	2518.	10365.
25.	0.2	31.	631.	23.3	5324.	5324.	17235.
25.	0.4	36.	716.	28.6	3491.	3491.	11905.
25.	0.6	43.	836.	35.0	3022.	3022.	10738.
25.	0.7	46.	887.	38.9	2963.	2963.	10663.
25.	0.8	51.	973.	43.1	2948.	2948.	10792.
25.	0.9	56.	1060.	47.9	2992.	2992.	11095.
25.	1.0	61.	1146.	53.6	3090.	3090.	11562.
25.	1.1	68.	1267.	60.0	3220.	3220.	12193.
30.	0.2	47.	905.	39.1	9521.	9521.	30372.
30.	0.3	52.	991.	44.4	7428.	7428.	24264.
30.	0.4	58.	1094.	50.6	6534.	6534.	21789.
30.	0.5	66.	1232.	57.8	6145.	6145.	20898.
30.	0.6	74.	1370.	66.8	6071.	6071.	20955.
30.	0.7	85.	1560.	77.6	6208.	6208.	21745.
30.	0.8	99.	1803.	91.3	6549.	6549.	23253.

TABLE 24. FOUR-POWERPLANT, FOUR-TRIP, ELECTRIC-PROPELLED, SPACE TRANSPORT PERFORMANCE WITH PROPELLANT TANK MOUNTED ARC JETS, AND EARTH ORBIT INBOUND PROPELLANT TANK DUMP

SWQ = 10 KG/KWE, LANDER CARGO FRAC = .4, CHAR VEL = 7.8 KM/SEC
SWT =(3000/I + 1.2) KG/KWE, ETAT = 1.1 EXP(-1690/I), PROP UTIL = .9

CARGO	POWER	VJI	TI	VJOI	TOI	TOF	LIFE
15.	0.4	23.	497.	15.7	1336.	1336.	6837.
15.	0.6	27.	564.	19.3	1205.	1205.	6513.
15.	0.8	31.	631.	23.6	1198.	1198.	6686.
15.	1.0	36.	716.	28.3	1244.	1244.	7123.
15.	1.2	42.	819.	33.9	1328.	1328.	7769.
15.	1.4	48.	922.	41.0	1466.	1466.	8629.
15.	1.6	57.	1077.	49.1	1625.	1625.	9732.
15.	1.8	67.	1249.	59.7	1852.	1852.	11157.
15.	2.0	80.	1474.	73.2	2151.	2151.	13024.
20.	0.2	25.	530.	16.9	2784.	2784.	12727.
20.	0.4	29.	597.	21.5	1954.	1954.	9608.
20.	0.6	34.	682.	26.9	1777.	1777.	9153.
20.	0.8	41.	802.	33.2	1773.	1773.	9498.
20.	1.0	49.	939.	41.0	1878.	1878.	10329.
20.	1.2	58.	1094.	51.2	2082.	2082.	11609.
20.	1.4	71.	1318.	64.0	2367.	2367.	13424.
20.	1.6	89.	1630.	81.4	2778.	2778.	16000.
20.	1.8	114.	2062.	106.5	3401.	3401.	19790.
25.	0.2	33.	665.	24.8	4368.	4368.	19467.
25.	0.4	40.	795.	32.1	3088.	3088.	14707.
25.	0.6	49.	939.	41.4	2872.	2872.	14304.
25.	0.7	55.	1042.	47.0	2896.	2896.	14710.
25.	0.8	61.	1146.	53.6	2996.	2996.	15420.
25.	0.9	69.	1284.	61.3	3143.	3143.	16423.
25.	1.0	78.	1439.	70.5	3359.	3359.	17752.
25.	1.1	89.	1630.	81.7	3645.	3645.	19471.
30.	0.2	50.	956.	41.8	7829.	7829.	34184.
30.	0.3	57.	1077.	49.0	6376.	6376.	28733.
30.	0.4	65.	1215.	57.8	5860.	5860.	27086.
30.	0.5	76.	1405.	68.5	5761.	5761.	27259.
30.	0.6	90.	1647.	81.9	5946.	5946.	28725.
30.	0.7	107.	1941.	99.6	6410.	6410.	31461.
30.	0.8	131.	2357.	123.5	7178.	7178.	35782.

APPENDIX B.

REFINED COST EFFECTIVENESS OPTIMIZATION PROCEDURE

During the course of this study various approaches were developed for optimization of the mission parameters accounting for power supply costs. The first approach, used at the inception of the study, consisted of defining a Powerplant/Booster Cost Ratio, whereby the cost per unit gross mass of nuclear power supply was divided by the cost per unit gross mass (wet) of earth launch vehicle. At about the halfway point through the study, this cost ratio parameter was redefined by the substitution of cost per unit net mass orbited by the booster in place of the cost per unit gross mass (wet) of earth launch vehicle. This change did not affect the results of the optimization analysis, since a constant of proportionality can be applied to convert from one approach to the other. Results from this second method were presented in parametric form in Section 6.

As work proceeded on analysis of the lunar cargo vehicle, a third approach with more refinement was derived, which included development as well as manufacture cost, and this method is described in this section. Unfortunately, it required much additional information and was derived too late to be used for the general parametric study presented in Section 6. However, some results were attained using the General Performance Characteristics from Appendix B, and these were used to illustrate effects of mission requirements and operational modes in Sections 3 and 5. The results were not very different, but added more breadth to the understanding of the mission characteristics. This approach can be further refined for use in future studies.

The normalization of electrical propulsion system parameters to the chemical propulsion system characteristics provides the simplest approach to cost analysis. The particular parameter of interest is the cost index, which is the cost of cargo delivery using electrical propulsion divided by that for a system using only chemical propulsion. Cost index can be calculated by use of the fo llowing equation:

$$C_I = \frac{W_C}{W_N}\left(1 + \frac{C_M}{N\,C_B}\right) + \frac{C_D\,W_C}{C_B\,W_T}$$

where

C_B = booster cost to launch
C_D = nuclear electric system development cost
C_I = cost index
C_M = nuclear powerplant manufacture cost
N = number of lunar landers delivered per powerplant
W_C = cargo mass delivered by reference chemical system
W_N = cargo mass delivered by selected electric system
W_T = total lunar cargo to be delivered

The nuclear powerplant manufacture cost, C_M, and development cost, C_D, influence the selection of powerplant size insofar as they vary with the powerplant size. The many variables in the above equation can be better evaluated by separating it into parts.

The function,

$$M_I = 1 + \frac{C_M}{N C_B},$$

is defined as "manufacture index" and describes the influence of the powerplant manufacture cost. The powerplant manufacture cost parameter, C_M, is estimated in the range of $15,000,000 per megawatt electric powerplant size. The variation of manufacture index with powerplant size, booster cost and number of trips is presented in Figure B-1. The Saturn V booster cost is not presently defined, but is judged to be about $100,000,000. The power rating for single trip operating modes ranges between one and two megawatts. Thus, the manufacture index can be on the order of 1.3.

The portion of the cost index not related to development cost,

$$C_{1M} = \frac{W_c}{W_N}\left(1 + \frac{C_M}{NC_B}\right) = \frac{W_C M_I}{W_N},$$

is described in Figure B-2 as a function of the manufacture index described above and the lunar cargo per landing vehicle. The influence of powerplant manufacture cost is readily apparent from this graph. Values of lunar cargo between 25 and 30 tons are necessary to establish a clear advantage over a chemical rocket system.

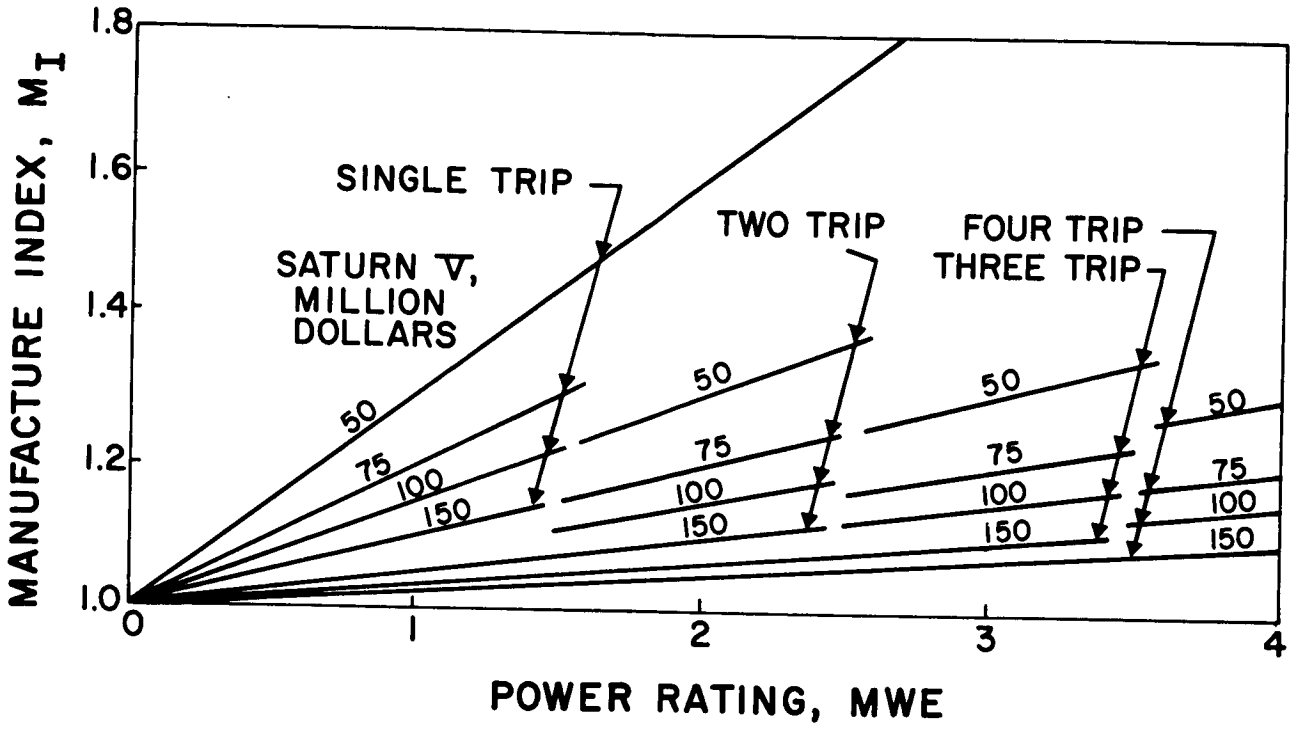

Figure B-1. Manufacture Index

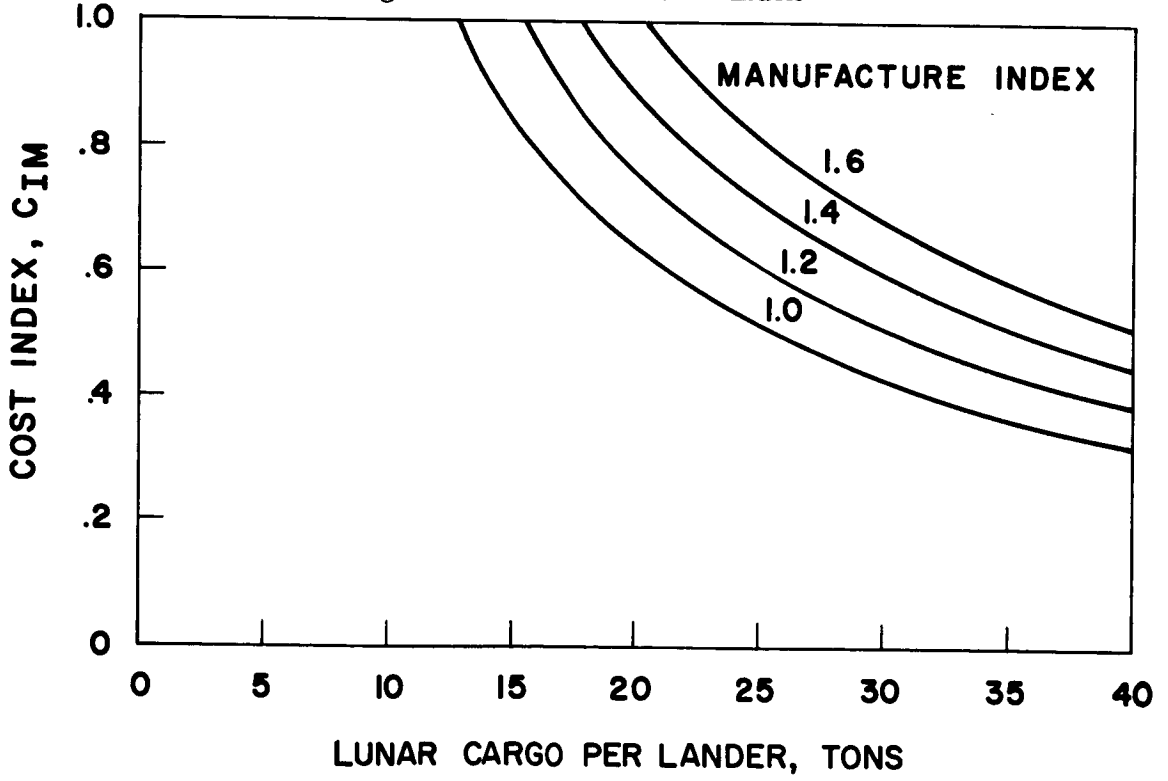

Figure B-2. Cost Index Based on Manufacture Alone

The powerplant development cost has to be amortized by the delivery cost savings resulting from Figure B-2, and this is clearly a function of the total cargo delivery requirement over the life of the developed transportation system. The powerplant development is also a function of powerplant size.

An estimate of this development cost is:

$$C_D = 300\ (1 + P) \text{ million dollars,}$$

where P = power supply output, MW_e.

Using this relationship a development index, D_I, is defined whereby:

$$D_I = C_D / C_B.$$

This relationship is plotted in Figure B-3 and interpreted in Figure B-4 as an incremented addition to the cost index:

$$C_{ID} = \frac{C_D\ W_C}{C_B\ W_T}$$

the effective cost index,

$$C_I = C_{IM} + C_{ID}.$$

It is readily apparent that the larger the cumulative lunar cargo delivered, the greater the development cost that can be accommodated.

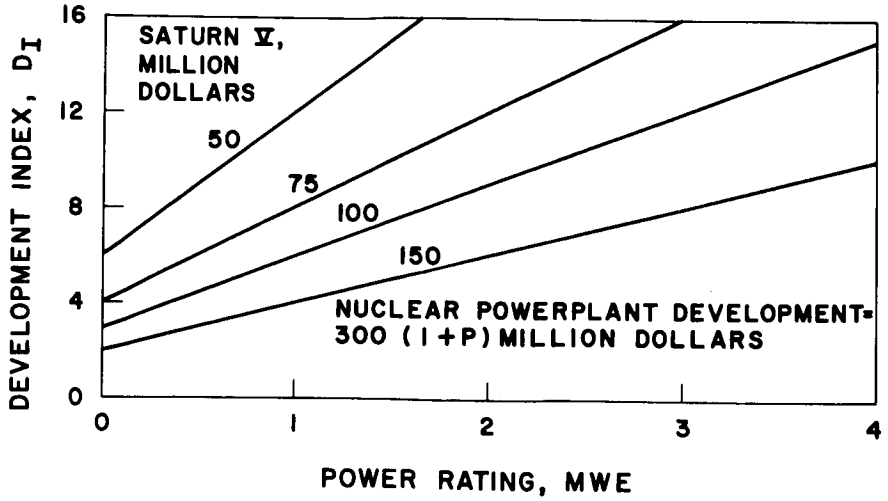

Figure B-3. Development Index

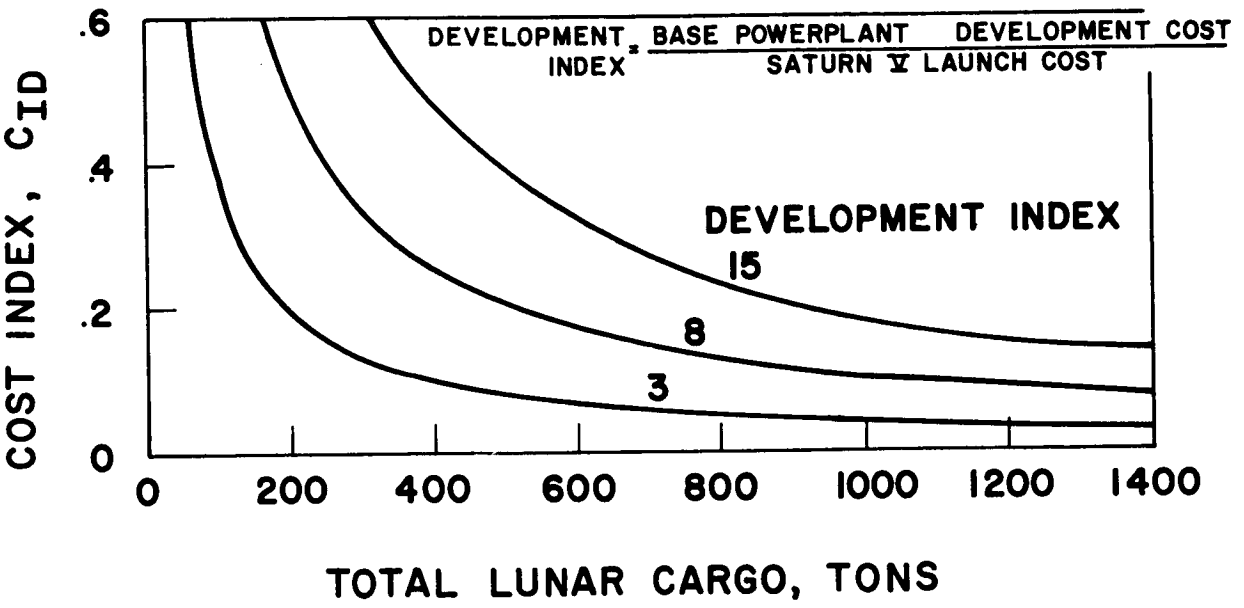

Figure B-4. Cost Index Increment Due to Development Amortization

These graphs aid in understanding the effects that cost of development and manufacture would have on performance of the lunar cargo vehicle, if these costs were better known. To use this approach properly, supporting studies on development planning are necessary.

A second refinement in this cost effectiveness optimization procedure is to allow variation of the power supply specific weight and lunar lander cargo fraction with size. A large variation in neither of these items is anticipated, but their consideration can modify slightly the optimum selection of design parameters.

The characteristics of the nuclear power supply were presented in Section 5A, based on a SNAP-50 type system. The specific weight of this power supply varies with power level, operating life, and mean time to radiator puncture by meteoroids, to name but a few influences. An approximate empirical equation can be derived into the form:

$$S = \frac{a}{P} + b + c\,(PT)^{d}$$

Where

S = specific weight

P = net output power

T = mean time to radiator puncture

a, b, c, d = empirical constants

The lander cargo fraction has been calculated in detail to allow bias towards lower values of trip time. The weight of insulation has been estimated for a particular selection of requirements and the following empirical equation developed to allow for variation of the design requirements.

$$W_I = \left(\frac{2.7\,\theta\,T}{10^6\,R_B}\right)^{1/2} \left(\frac{W_P^{\,2}\,N_T}{5400}\right)^{1/3}$$

where

W_I = insulation weight, tons (metric)

θ = tank outer skin temperature, ^{o}R

T = trip time earth to moon, hours

R_B = ratio of propellant boiloff to insulation mass

W_P = mass of lander propellant at earth departure, tons (metric)

N_T = number of hydrogen tanks.

This equation applies to the case of a hydrogen-oxygen chemical propulsion system to descend the lunar cargo from orbit to the surface. The heating of the cryogenic propellants is retarded by insulation and dissipated by boiloff. An optimization study was conducted yielding the conclusion that the ratio of boiloff to insulation should be 1.8.

The lunar cargo fraction is calculated by use of the following additional assumptions:

1. Propellant mass fraction is 0.4 at start of lunar descent
2. Propellant tank utilization is 0.9
3. Landing structure mass fraction 0.1 of lander gross weight at start of descent.

The computer program using the above approach can be prepared in a straightforward manner. To aid in this understanding, a sample calculation is presented below, which contains many of the assumptions used in preparing the Cost Index graphs in Sections 3 and 5.

TABLE 1. SAMPLE CALCULATION AND COMPUTER PROGRAM

```
C     LUNAR CARGO COST STUDY ' 4/8/65  ' J. W. LARSON
   1  READ 3,WC,WCC,SCQ,CB,CR,XND,RCC
C        WC = 2000., METRIC TONS CUMULATIVE LUNAR CARGO REQUIREMENT
C        WCC = 12.7, METRIC TONS CARGO DELIVERED PER CHEMICAL SATURN V
C        SCQ = 15., MILLION DOLLARS TO MANUFACTURE EACH MWE OF POWER SUPPLY
C        CB = 100., MILLION DOLLARS COST PER SATURN V
C        CR = 300., MILLION DOLLARS BASIC POWER SUPPLY RESEARCH COST
C        XND = 20., RATIO TOTAL DEVELOPMENT COST TO COST OF MANUFACTURING
C          SINGLE UNIT POWER SUPPLY
C        RCC = 1.09, HUNDRED TONS OF NET ORBITED PAYLOAD PER BOOSTER
   3  FORMAT (F10.0,F10.1,F10.0,F10.0,F1 .0,F10.0,F10.2)
      PUNCH 3,WC,WCC,SCQ,CB,CR,XND,RCC
      READ 7,FP,FT,RB,FS,CBT,TEMP,XNT
C        FP = .4, LUNAR CARGO FRACTION OF LANDER
C        FT = .05, TANK MASS FRACTION FOR LANDER
C        RB = 1.8, PROPELLANT BOILOFF TO INSULATION MASS FOR LANDER
C        FS = .1, LANDING STRUCTURE FRACTION OF LANDER
C        CBT = 2.7, EMPIRICAL CONSTANT FOR INSULATION MASS OF LANDER
C        TEMP = 552., DEG. F ENVIRONMENT TEMPERATURE FOR LANDER TANKS
C        XNT = 1., NO. OF EQUIVALENT LIQUID HYDROGEN TANKS PER LANDER
   7  FORMAT (F10.2,F10.2,F10.2,F10.2,F1 .2,F10.0,F10.0)
      PUNCH 7,FP,FT,RB,FS,CBT,TEMP,XNT
      READ 8,TMF,XF
C        TMF = 100000., MEAN TIME BETWEEN SPACECRAFT FAILURES
C        XF = 2., NO. OF FAILURES TO LOSE LANDER
   8  FORMAT (F20.0,F10.0)
      PUNCH 8,TMF,XF
   4  READ 19,CO,WLC,PMW,VJI,TI,VJOI,TOI,VJO,TO,TT
C        CO = 211., CODE TO IDENTIFY MISSION PROFILE, MEANS 2-TRIPS AND
C          2-INITIAL BOOSTERS
C        WLC = 25., METRIC TONS NOMINAL LUNAR CARGO PER HUNDRED TONS ORBITED
C        PMW = 1.2, MWE POWER SUPPLY PER HUNDRED TONS ORBITED
C        VJI  = NOT USED IN THIS PROGRAM
C        TI = 958., HOURS PROPULSION TIME FOR INBOUND VOYAGE
C        VJOI = NOT USED IN THIS PROGRAM
C        TOI = 4676., HOURS PROPULSION TIME FOR FIRST OUTBOUND VOYAGE
C        VJO  = NOT USED IN THIS PROGRAM
C        TO = 3755., HOURS PROPULSION TIME FOR LAST OUTBOUND VOYAGE
C        TT = 9399., HOURS POWER SUPPLY LIFE RATING REQUIREMENT
  19  FORMAT(F5.0,F5.0,F6.1,F7.0,F7.0,F8.1,F8.0,F8.1,F8.0,F9.0)
      W = WC
C        W = 2000.
      P=PMW*RCC
C        P = 1.308, ACTUAL POWER SUPPLY SIZE
      WLLC=WLC*2.5*RCC
C        WLLC = 68.125 , REFERENCE LANDER GROSS MASS
      WB=RB*WLLC*.05
C        WB = 6.1312, BOILOFF MASS FIRST GUESS
      WBI=WB
C        WBI = 6.1312
```

```
      WL=WLLC-WB
C        WL = 61.994, LANDER GROSS MASS IN LUNAR ORBIT
      WP=FP*WL
C        WP = 24.797, PROPELLANT MASS IN LANDER
      WPI=WP+WB
C        WPI = 30.929, PROPELLANT TANK SIZE
      S = (WPI*WPI*XNT/5400.)**(1./3.)
C        S = .56162
      WI=SQRTF(CBT*TOI*TEMP/RB/1.E6)*S
C        WI = 1.1050, INSULATION MASS
      WB=RB*WI
C        WB = 1.9891
      WI=WI*(1.+2./3.*(WB-WBI)/WPI)
C        WI = 1.0064
      WB=RB*WI
C        WB = 1.8115
      WL=WLLC-WB
C        WL = 66.314
      WP=FP*WL
C        WP = 26.525
      WT=FT*(WP+WB)
C        WT = 1.4168, TANKAGE MASS FOR LANDER
      WS=FS*WL
C        WS = 6.6314, LANDING GEAR FRACTION
      WCN=WL-WP-WT-WI-WS
C        WCN = 30.734, NET LUNAR CARGO
      FC=WCN/WLLC
C        FC = .45113, LANDER CARGO FRACTION
      COC=CO
C        COC = 211.
      YNQ = 0.
      YIPS = 0.
      CIA=0.
      CIB=0.
      CIC=0.
   21 YNQ = YNQ + 1.
C        YNQ = 1., 2.
      CO = CO - 100.
C        CO = 111., 11.
      IF(CO-100.)22,21,21
   22 IF(CO-10.)24,23,23
   23 YIPS = 1. + YIPS
C        YIPS = 1.
      CO = CO - 10.
C        CO = 1.
      GO TO 22
   24 XNB = CO
C        XNB = 1.
      ZNB=1.-(TOI+T1*YNQ/2.+TO*(YNQ-2.)/2.)/TMF
C        ZNB = .94366
      XN =XNB+(YNQ-1.)*ZNB
C        XN = 1.9437, NO. OF BOOSTERS PER POWER SUPPLY
```

```
      XC=XNB*(1.-(TCI/TMF)**XF)+(YNQ-1.)*ZNB*(1.-(TO/TMF)**XF)
C        XC = 1.9401, NO. OF LANDERS DELIVERED PER POWER SUPPLY
      CIM=XN/XC
C        CIM = 1.0016
      DO 2 IWC = 1,4
      CI = WCC/WCN*(1.+SCQ*P/CB/XN)*CIM (CR+XND*SCQ*P)/W/CB*WCC
C        CI = .49973 , COST INDEX
      CID=CIC
      CIC=CIB
      CIB=CIA
      CIA=CI
    2 W = W * 2.
      PUNCH 6, COC,WLC,PMW,CID,CIC,CIB,CIA,FC,TT
    6 FORMAT(F5.0,F5.0,F6.1,F10.4,F10.4,F10.4,F10.4,F8.4,F8.0)
      GO TO 4
      END
```